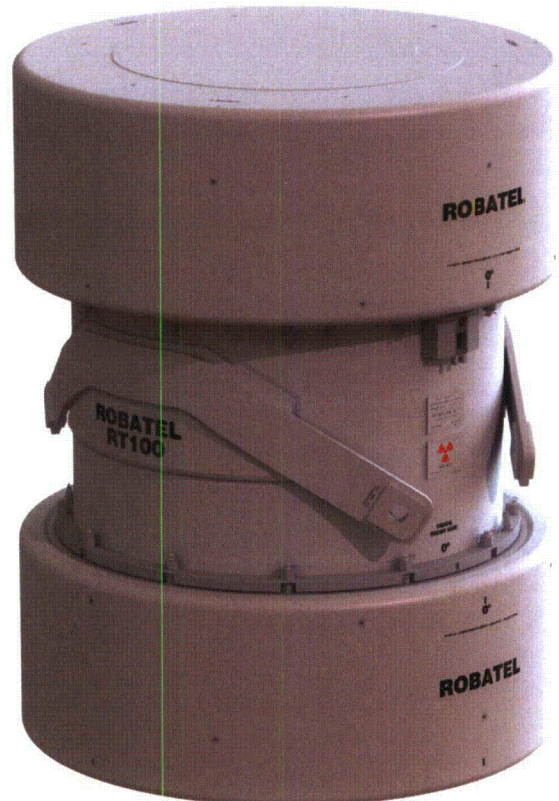


ROBATEL
technologies

**RT-100 Type B Cask
Safety Analysis Report
Docket Number 71-9365
TAC Number L24686
Revision 5
January 30, 2015**



This Part 71 Application for Approval of RT-100 Type B Cask Package for Radioactive Material represents Robatel Technologies, LLC approach to its business as applied to the specifications of this submittal. This Application requests that the Nuclear Regulatory Commission respects the proprietary information and withholds it from public disclosure subject to the provisions of 10 CFR 2.390. All detailed drawings are considered proprietary information.

TABLE OF CONTENTS

1. GENERAL INFORMATION..... 1-1

1.1 Introduction..... 1-1

1.2 Package Description..... 1-3

 1.2.1 Packaging..... 1-3

 1.2.1.1 Overall Dimensions 1-3

 1.2.1.2 Weight 1-4

 1.2.1.3 Containment Features 1-4

 1.2.1.4 Neutron and Gamma Shielding Features 1-4

 1.2.1.5 Shielding Features for Personnel Barriers 1-4

 1.2.1.6 Criticality Control Features..... 1-4

 1.2.1.7 Structural Features – Lifting and Tie-Down Devices 1-4

 1.2.1.8 Structural Features – Impact Limiters..... 1-5

 1.2.1.9 Structural Features – Internal Supporting or Positioning Features..... 1-5

 1.2.1.10 Structural Features – Outer Shell or Outer Packaging..... 1-5

 1.2.1.11 Structural Features – Packaging Closure Device..... 1-6

 1.2.1.12 Structural Features – Heat Transfer Features 1-6

 1.2.1.13 Structural Features – Packaging Markings 1-6

 1.2.1.14 Additional Information 1-6

 1.2.2 Contents 1-6

 1.2.2.1 Identification and Maximum Quantity of Radioactive Material 1-7

 1.2.2.2 Identification and Maximum Quantity of Fissile Material 1-7

 1.2.2.3 Physical and Chemical Form – Density, Moisture Content and Moderators 1-7

 1.2.2.3.1 Ion-Exchange Resins 1-7

 1.2.2.3.2 Filters..... 1-8

 1.2.2.3.3 Secondary Containers..... 1-8

 1.2.2.4 Location and Configuration 1-8

 1.2.2.5 Use of Non-Fissile Materials as Neutron Absorbers/Moderators 1-8

 1.2.2.6 Chemical/Galvanic/Gas Generation 1-8

 1.2.2.7 Maximum Weight of Contents and Payload 1-9

 1.2.2.8 Maximum Decay Heat..... 1-9

 1.2.2.9 Loading Restrictions..... 1-10

 1.2.2.10 Contents for the Certificate of Compliance 1-10

1.2.3 Special Requirements for Plutonium	1-10
1.2.4 Operational Features	1-10
1.3 Engineering Drawings and Additional Information	1-11
1.3.1 Engineering Drawings	1-11
1.3.2 Conformance to Approved Design	1-11
1.3.3 Referenced Pages	1-11
1.3.4 Special Fabrication Procedures	1-11
1.3.5 Package Category	1-11
1.3.6 Supplemental Information.....	1-11
1.4 Appendix.....	1-12
1.5 References.....	1-27
2. STRUCTURAL EVALUATION	2-1
2.1 Description of Structural Design	2-1
2.1.1 Discussion	2-3
2.1.1.1 Containment Boundary	2-4
2.1.2 Design Criteria	2-4
2.1.2.1 Cask Body Criteria (except Bolts and O-Rings)	2-5
2.1.2.2 Bolts.....	2-5
2.1.2.3 Lead.....	2-6
2.1.2.4 Foam.....	2-6
2.1.3 Weights and Centers of Gravity	2-6
2.1.4 Identification of Codes and Standards for Package Design	2-7
2.2 Materials.....	2-8
2.2.1 Material Properties and Specifications	2-8
2.2.2 Chemical, Galvanic, or Other Reactions.....	2-10
2.2.2.1 Component Material Categories.....	2-10
2.2.2.1.1 Stainless/Nickel Alloy Steels.....	2-11
2.2.2.1.2 Nonferrous Metals.....	2-11
2.2.2.1.3 Shielding Materials	2-11
2.2.2.1.4 Criticality Control Material.....	2-12
2.2.2.1.5 Energy Absorbing Material	2-12
2.2.2.1.6 Cellular Foam and Insulation.....	2-12
2.2.2.1.7 Lubricant and Grease.....	2-12

2.2.2.1.8 O-Rings.....	2-12
2.2.2.1.9 Secondary Containers and Shoring	2-12
2.2.2.1.10 Filters.....	2-12
2.2.2.2 General Effects of Identified Reactions.....	2-12
2.2.2.3 Adequacy of the Cask Operating Procedures.....	2-13
2.2.2.4 Effects of Reaction Products.....	2-13
2.2.3 Effects of Radiation on Materials	2-13
2.3 Fabrication and Examination.....	2-13
2.3.1 Fabrication	2-13
2.3.2 Examination	2-13
2.4 General Requirements for All Packages.....	2-14
2.4.1 Minimum Package Size	2-14
2.4.2 Tamper-Indicating Feature.....	2-14
2.4.3 Positive Closure.....	2-14
2.5 Lifting and Tie-Down Standards for All Packages	2-14
2.5.1 Lifting Devices.....	2-14
2.5.1.1 Lifting Design Criteria.....	2-15
2.5.1.2 Lifting Device Descriptions	2-15
2.5.1.3 Lifting Device Evaluations	2-15
2.5.1.3.1 Cask Body Lifting Evaluation.....	2-15
2.5.1.3.1.1 Lifting Pocket Design Features	2-16
2.5.1.3.1.2 Lifting Pocket Tear-out Stresses	2-17
2.5.1.3.1.3 Lifting Pocket Bearing Stresses	2-18
2.5.1.3.1.4 Lifting Pocket Weld Stresses	2-18
2.5.1.3.1.5 Lifting Pocket Average Pure Shear	2-20
2.5.1.3.1.6 Summary of Results	2-20
2.5.1.3.2 Primary Lid Lifting Evaluation.....	2-21
2.5.1.3.2.1 Primary Lid Lifting Ring Working Loads	2-21
2.5.1.3.2.2 Primary Lid Thread Engagement	2-22
2.5.1.3.3 Secondary Lid Lifting Evaluation	2-23
2.5.1.3.3.1 Lifting Ring Working Load	2-23
2.5.1.3.3.2 Secondary Lid Thread Engagement	2-23
2.5.1.3.4 Upper Impact Limiter Lifting Evaluation.....	2-24

2.5.1.3.4.1 Lifting Ring Working Load	2-24
2.5.1.3.4.2 Impact Limiter Thread Engagement	2-25
2.5.1.3.5 Lower Impact Limiter Lifting Evaluation	2-26
2.5.1.3.5.1 Attachment Bolt Stresses	2-26
2.5.1.3.5.2 Lower Impact Limiter Thread Engagement	2-27
2.5.2 Tie-down Devices.....	2-28
2.5.2.1 Tie-down Load Calculation	2-28
2.5.2.2 Tie-down Force Calculation.....	2-29
2.5.2.3 Tie-Down Arm Evaluation	2-33
2.5.2.4 Tie-down Arm & Plate Weld Evaluation.....	2-34
2.5.2.4.1 Tie Down Arm-to-Plate Weld Stress	2-35
2.5.2.4.2 Tie Down Plate-to-Outer Shell Weld Stress	2-35
2.5.2.5 Tie-Down Evaluation Summary.....	2-36
2.6 Normal Conditions of Transport.....	2-36
2.6.1 Heat	2-37
2.6.1.1 Summary of Pressures and Temperatures.....	2-37
2.6.1.2 Differential Thermal Expansion.....	2-38
2.6.1.3 Stress Calculations	2-38
2.6.1.4 Comparison with Allowable Stresses	2-38
2.6.2 Cold	2-38
2.6.3 Reduced External Pressure.....	2-39
2.6.4 Increased External Pressure	2-39
2.6.5 Vibration	2-39
2.6.5.1 Vibration Evaluation of the RT-100 Cask Primary Lid Bolts.....	2-39
2.6.5.2 Vibration Evaluation of the RT-100 Cask Secondary Lid Bolts	2-41
2.6.6 Water Spray.....	2-42
2.6.7 Free Drop	2-42
2.6.7.1 Methodology	2-42
2.6.7.2 Finite Element Analysis.....	2-42
2.6.7.2.1 Model Description.....	2-43
2.6.7.2.2 Boundary Conditions.....	2-48
2.6.7.3 Side Drop	2-53
2.6.7.4 End Drop.....	2-61
2.6.8 Corner Drop	2-69

2.6.9 Compression.....	2-69
2.6.10 Penetration	2-69
2.7 Hypothetical Accident Conditions.....	2-69
2.7.1 Free Drop	2-69
2.7.1.1 End Drop.....	2-71
2.7.1.1.1 End Drop Evaluation	2-71
2.7.1.1.2 Lead Slump Evaluation	2-71
2.7.1.1.2.1 Elastic Deformation.....	2-71
2.7.1.1.2.2 Plastic Deformation with Maximum Gap	2-71
2.7.1.2 Side Drop	2-82
2.7.1.3 Corner Drop	2-90
2.7.1.4 Oblique Drops	2-92
2.7.1.5 Summary of Results	2-94
2.7.2 Crush.....	2-94
2.7.3 Puncture	2-94
2.7.3.1 Lid Puncture.....	2-94
2.7.3.1.1 Lid Puncture Boundary Conditions	2-94
2.7.3.1.2 Lid Puncture Results	2-95
2.7.3.2 Cask Side Puncture.....	2-97
2.7.3.2.1 Cask Side Puncture Minimum Wall Thickness.....	2-97
2.7.3.2.2 Cask Sidewall Bending Stresses	2-97
2.7.3.3 Lead Deformation during Side Puncture	2-98
2.7.3.3.1 Outer Shell Stiffness.....	2-98
2.7.3.3.2 Lead Stiffness.....	2-99
2.7.3.3.3 Inner Shell Stiffness	2-99
2.7.3.3.4 Lead Deformation due to Puncture Load.....	2-99
2.7.4 Thermal.....	2-102
2.7.4.1 Summary of Pressures and Temperatures.....	2-102
2.7.4.2 Differential Thermal Expansion.....	2-102
2.7.4.3 Stress Calculations	2-102
2.7.4.3.1 Bolt stresses during fire accident	2-102
2.7.4.3.2 Pressure stress during fire accident	2-102
2.7.4.4 Comparison with Allowable Stresses	2-102
2.7.5 Immersion – Fissile Material.....	2-104

2.7.6 Immersion – All Package.....	2-104
2.7.7 Deep Water Immersion Test (for Type B Packages Containing More than 10^5 A2).....	2-104
2.7.8 Summary of Damage	2-104
2.8 Accident Conditions for Air Transport of Plutonium.....	2-104
2.9 Accident Conditions for Fissile Material Packages for Air Transport	2-104
2.10 Special Form	2-104
2.11 Fuel Rods	2-104
2.12 Appendix – Impact Limiter Analysis.....	2-105
2.12.1 Assumptions.....	2-105
2.12.2 Analysis Inputs.....	2-105
2.12.2.1 Cask Assembly.....	2-105
2.12.2.2 Foam Material Properties.....	2-107
2.12.2.2.1 Density.....	2-107
2.12.2.2.2 Crush Strength.....	2-107
2.12.2.3 Temperatures.....	2-107
2.12.3 Methodology	2-108
2.12.3.1 Numerical Integration.....	2-109
2.12.3.2 Crush Strength.....	2-110
2.12.3.3 Crush Force.....	2-113
2.12.3.3.1 End-Drop Case.....	2-114
2.12.3.3.2 Side-Drop Case	2-116
2.12.3.3.3 Corner-Drop Case	2-119
2.12.4 Calculations.....	2-123
2.12.4.1 RT-100 Cask Drop Analysis	2-123
2.12.4.1.1 Calculation for Drop Height of 9.0 m.....	2-123
2.12.4.1.1.1 HAC End-Drop Case.....	2-124
2.12.4.1.1.2 HAC Side-Drop Case	2-127
2.12.4.1.1.3 HAC Corner-Drop Case.....	2-130
2.12.4.1.2 Calculation for Drop Height of 0.3 m.....	2-134
2.12.4.1.2.1 NCT End-Drop Case	2-134
2.12.4.1.2.2 NCT Side-Drop Case.....	2-137
2.12.4.1.2.3 NCT Corner-Drop Case.....	2-140
2.12.4.2 Pin Puncture	2-143

2.12.4.3 Confirmatory Testing - 3/10 Scale Cask.....	2-144
2.12.4.3.1 End-Drop	2-146
2.12.4.3.2 Corner-Drop.....	2-148
2.12.4.3.3 Side-Drop.....	2-150
2.12.5 Discussion of Test Results	2-152
2.12.6 Summary of Accelerations.....	2-152
2.13 Appendix – Closure Bolt Evaluation	2-161
2.13.1 Methodology	2-161
2.13.2 Loads	2-161
2.13.2.1 Internal Pressure Loads.....	2-161
2.13.2.1.1 Internal Pressure Loads for Primary Lid Closure Bolts.....	2-161
2.13.2.1.2 Internal Pressure Load for Secondary Lid Closure Bolts	2-163
2.13.2.2 Temperature Loads.....	2-164
2.13.2.2.1 Temperature Loads for Primary Lid Closure Bolts.....	2-164
2.13.2.2.2 Temperature Loads for Secondary Lid Closure Bolts	2-165
2.13.2.3 Bolt Preloads.....	2-165
2.13.2.3.1 Bolt Preload for Primary Lid Closure Bolts.....	2-165
2.13.2.3.2 Bolt Preload for Secondary Lid Closure Bolts.....	2-166
2.13.2.4 Impact Loads.....	2-167
2.13.2.4.1 Dynamic Load Factors.....	2-167
2.13.2.4.2 End Drop Loads	2-170
2.13.2.4.2.1 Primary Lid Bolts	2-170
2.13.2.4.2.2 Secondary Lid Bolts	2-174
2.13.2.4.3 Corner Drop Evaluations	2-177
2.13.2.4.4 Side Drop Evaluations	2-178
2.13.2.5 Puncture Loads.....	2-178
2.13.2.5.1 End Puncture.....	2-178
2.13.2.5.1.1 Primary Lid Bolts	2-178
2.13.2.5.1.2 Secondary Lid Bolts	2-182
2.13.2.5.2 Side Puncture	2-185
2.13.2.6 External Pressure.....	2-185
2.13.2.6.1 Primary Lid Bolts.....	2-186
2.13.2.6.2 Secondary Lid Bolts	2-187
2.13.2.7 Gasket Seating Load.....	2-188

2.13.3 Load Combinations.....	2-188
2.13.3.1 Primary Lid Closure Bolt Evaluation under Normal Conditions of Transport	2-189
2.13.3.2 Secondary Lid Closure Bolt Evaluation under Normal Conditions of Transport	2-194
2.13.3.3 Primary Lid Closure Bolt Evaluation under Hypothetical Accident Conditions	2-198
2.13.3.4 Secondary Lid Closure Bolt Evaluation under Hypothetical Accident Conditions.....	2-202
2.13.4 Seal Integrity	2-206
2.13.4.1 Primary Lid Seals	2-206
2.13.4.2 Secondary Lid Seals	2-206
2.13.5 Vent Port Cover Plate O-Ring and Bolt Evaluation	2-207
2.13.5.1 Vent Port Cover Plate O-Ring Evaluation	2-207
2.13.5.1.1 O-ring Sealing Force	2-207
2.13.5.1.2 Vent Port Cover Plate Preload	2-208
2.13.5.1.3 Factor of Safety to Maintain a Tight Seal.....	2-208
2.13.5.2 Bolt Evaluation.....	2-209
2.13.5.2.1 Thread Engagement.....	2-209
2.13.5.2.2 Thread Shear Evaluation.....	2-209
2.13.5.2.3 Load to Break Bolt	2-210
2.14 Appendix – Fabrication Stress Evaluation	2-210
2.14.1 Lead Pour	2-211
2.14.1.1 Cask Shell Geometry	2-211
2.14.1.2 Stresses Resulting from Lead Pour.....	2-211
2.14.2 Cool-down.....	2-212
2.14.2.1 Hoop (Circumferential) Stresses	2-212
2.14.2.2 Axial Stress	2-213
2.14.2.3 Effects of Temperature Differential during Cool-down	2-214
2.14.3 Lead Creep	2-215
2.15 Appendix – Seal Region Stress Evaluation	2-215
2.15.1 Seal Region Post-Processing Methodology	2-215
2.15.2 Stress Concentration Factors.....	2-215
2.15.3 Seal Region Stress Results	2-216
2.15.4 Displacement Results.....	2-216
2.16 References	2-228
3. THERMAL EVALUATION	3-1

3.1 Description of Thermal Design	3-3
3.1.1 Design Features	3-3
3.1.1.1 RT-100 Description	3-3
3.1.1.2 RT-100 Dimensions.....	3-4
3.1.2 Content’s Decay Heat	3-4
3.1.3 Summary Tables of Temperatures.....	3-5
3.1.4 Summary Tables of Maximum Pressures	3-7
3.2 Material Properties and Component Specifications	3-7
3.2.1 Material Properties	3-8
3.2.2 Component Specifications	3-11
3.2.3 Content Properties	3-12
3.3 Thermal Evaluation under Normal Conditions of Transport	3-13
3.3.1 Heat and Cold.....	3-14
3.3.1.1 Load Cases.....	3-14
3.3.1.2 Analytical Model.....	3-16
3.3.1.3 Analysis Results	3-19
3.3.2 Maximum Normal Operating Pressure	3-29
3.3.2.1 Calculation Method	3-29
3.3.2.2 Pressure Due to the Initially Sealed Air in the Cavity	3-29
3.3.2.3 Pressure Due to the Water Vapor in the Cask.....	3-29
3.3.2.4 Pressure Due to Generation of Gas	3-30
3.3.2.5 Total Pressure.....	3-30
3.4 Thermal Evaluation under Hypothetical Accident Conditions	3-31
3.4.1 HAC Fire Analysis—Pin Puncture Damage to Top Impact Limiter	3-31
3.4.1.1 Initial Conditions—Pin Puncture Damage to Top Impact Limiter.....	3-31
3.4.1.2 HAC Fire and Cool-down Analysis—Pin Puncture Damage to Top Impact Limiter	3-31
3.4.1.3 HAC Fire Analysis Results—Pin Puncture Damage to Top Impact Limiter.....	3-32
3.4.2 HAC Fire Evaluation—Pin Puncture Damage to the Side of the Cask Body	3-43
3.4.2.1 Initial Condition—Pin Puncture Damage to the Side of the Cask Body	3-43
3.4.2.2 HAC Fire Analysis—Pin Puncture Damage to the Side of the Cask Body	3-44
3.4.2.3 HAC Fire and Cool-down Analysis—Pin Puncture Damage to the Side of the Cask Body.....	3-44

3.4.3 Maximum Temperatures and Pressure.....	3-57
3.4.3.1 Maximum Temperatures.....	3-57
3.4.3.2 Maximum Accident Condition Pressure.....	3-57
3.4.3.2.1 Calculation Method.....	3-58
3.4.3.2.2 Pressure Due to the Initially Sealed Air in the Cavity.....	3-58
3.4.3.2.3 Pressure Due to the Water Vapor in the Cask.....	3-58
3.4.3.2.4 Pressure Due to Generation of Gas.....	3-58
3.4.3.2.5 Total Pressure.....	3-59
3.4.3.2.6 Total Pressure Accounting for Combustion of Contents.....	3-59
3.4.4 Maximum Thermal Stress.....	3-60
3.4.5 Accident Conditions for Fissile Material Packages for Air Transport.....	3-60
3.5 Appendix.....	3-61
3.6 References.....	3-70
4. CONTAINMENT.....	4-1
4.1 Description of Containment System.....	4-1
4.1.1 Containment Vessel.....	4-1
4.1.2 Containment Penetration.....	4-3
4.1.3 Welds and Seals.....	4-5
4.1.4 Closure.....	4-5
4.1.5 Cavity Volume, Conditions, and Contents.....	4-6
4.2 Allowable Leakage Rates at Test Conditions.....	4-7
4.3 Leakage Rate Test for Type B Packages.....	4-8
4.3.1 Determination of Equivalent Reference Leakage Rate for Helium Gas.....	4-9
4.4 Hydrogen Gas Generation.....	4-15
4.4.1 Determination of Bounding G Values.....	4-16
4.4.1.1 G Values for Waste and Secondary Container Materials.....	4-17
4.4.1.2 Calculation of Effective G Values.....	4-18
4.4.1.3 Operating Temperature G Value Adjustment.....	4-19
4.4.2 Hydrogen Gas Generation by Radiolysis.....	4-21
4.4.3 Hydrogen Generation – Radiolysis in Waste, Water and Polyethylene Container.....	4-23
4.4.4 Hydrogen Gas Generation – Simplified Model used to develop Loading Curve.....	4-30
4.4.5 Hydrogen Gas Generation – Analytical Model used for Detailed Analysis.....	4-33
4.5 Appendix.....	4-36

4.6 References	4-47
5. SHIELDING EVALUATION	5-1
5.1 Description of Shielding Design	5-5
5.1.1 Design Features	5-5
5.1.2 Summary Table of Maximum Radiation Levels	5-5
5.2 Source Specification	5-6
5.2.1 Gamma Source	5-6
5.2.2 Neutron Source.....	5-7
5.3 Shielding Model	5-8
5.3.1 Configuration of Source and Shielding.....	5-8
5.3.1.1 Source Term.....	5-9
5.3.1.2 NCT Model	5-9
5.3.1.3 HAC Model.....	5-9
5.3.2 Material Properties	5-17
5.4 Shielding Evaluation	5-19
5.4.1 Methods	5-19
5.4.1.1 MCNP6 Analysis.....	5-19
5.4.1.2 Dose Rate Response Calculation.....	5-19
5.4.1.3 Maximum allowed source strength density	5-23
5.4.1.4 Variance Reduction	5-24
5.4.2 Input and Output Data	5-24
5.4.3 Flux-to-Dose Rate Conversion.....	5-24
5.4.4 External Radiation Levels.....	5-26
5.4.4.1 MCNP6 Statistics Evaluation.....	5-27
5.4.4.1.1 Tally Statistics Diagnostics.....	5-27
5.4.4.1.2 Fractional Standard Deviation of Individual Tally Segments.....	5-27
5.4.4.2 Media Composition and Density	5-29
5.4.4.2.1 Effect of Media Composition.....	5-29
5.4.4.2.2 Effect of Media Density	5-30
5.4.4.3 Shielding Evaluation Uncertainty	5-31
5.4.4.3.1 Calculation of Dose Rates	5-31
5.4.4.3.1.1 Radiation Source Generation	5-31
5.4.4.3.1.2 Cross Section Data	5-32

5.4.4.3.1.3 Radiation Transport Codes	5-32
5.4.4.3.2 Attenuation from other material (i.e. secondary containers) not included in shielding analysis.....	5-32
5.4.4.3.3 Nominal Media Bulk Density	5-33
5.4.4.4 Loading Table	5-33
5.4.4.5 Dose Rates for Maximum Radionuclide Loading	5-34
5.5 Appendix.....	5-51
5.5.1 List of Gamma Radionuclides with Greater than 1 Day Half Life.....	5-51
5.5.2 Gamma Radionuclide Responses	5-53
5.5.3 Radionuclide Maximum Ci/g Loading Limits	5-69
5.5.4 Process Description for Calculating Maximum Allowed Source Strength Density	5-77
5.6 References.....	5-78
6. CRITICALITY EVALUATION.....	6-1
7. PACKAGE OPERATIONS.....	7-1
7.1 Package Loading	7-3
7.1.1 Preparation for Loading.....	7-3
7.1.1.1 Upper Impact Limiter Removal	7-5
7.1.1.2 Optional Loading Steps	7-5
7.1.1.3 Removal of Quick-Disconnect Valve Cover Plate.....	7-5
7.1.1.4 Removal of the Primary Lid.....	7-6
7.1.1.5 Removal of the Secondary Lid.....	7-6
7.1.2 Loading of the RT-100	7-7
7.1.2.1 Content Loading.....	7-7
7.1.2.2 Primary Lid Replacement	7-8
7.1.2.3 Secondary Lid Replacement	7-8
7.1.2.4 Quick-Disconnect Valve Cover Plate Replacement	7-9
7.1.3 Preparation for Transport.....	7-9
7.1.3.1 Replacement of Upper Impact Limiter.....	7-10
7.1.3.2 Verification for Transport.....	7-11
7.2 Package Unloading	7-11
7.2.1 Receipt of Package from Carrier	7-11
7.2.2 Removal of Contents	7-12
7.3 Preparation of Empty Package for Transport	7-13

7.4 Other Operations.....	7-13
7.4.1 Lower Impact Limiter Removal.....	7-13
7.4.2 Package Removal from Trailer.....	7-14
7.4.3 Replacement of Lower Impact Limiter.....	7-16
7.4.4 Reloading the Package onto the Trailer.....	7-16
7.4.5 Tightening of Components.....	7-18
7.4.5.1 Tightening Torques.....	7-18
7.4.5.2 Threaded Bolts – Tightening Methods and Equipment.....	7-19
7.4.5.3 Replacement of the Impact Limiter Threaded Studs.....	7-19
7.5 Hydrogen Buildup in RT-100 Transport Cask.....	7-20
7.5.1 Hydrogen Gas Generation – Simplified Model used to develop Loading Curve.....	7-20
7.5.2 Hydrogen Gas Generation – Analytical Model used for Detailed Analysis.....	7-23
7.5.3 Hydrogen Gas Generation – Analytical Model Example.....	7-26
7.6 Appendix.....	7-27
7.6.1 RT-100 Loading Table Discussion.....	7-28
7.6.1.1 RT-100 Loading Table Procedure.....	7-33
7.6.1.2 Turkey Point Source Term Example Evaluation.....	7-33
7.6.1.3 St. Lucie Loading Table.....	7-35
7.6.1.4 Additional Examples.....	7-37
7.7 References.....	7-46
8. ACCEPTANCE TESTS AND MAINTENANCE PROGRAM.....	8-1
8.1 Acceptance Tests.....	8-2
8.1.1 Visual Inspections and Measurements.....	8-3
8.1.2 Weld Examinations.....	8-3
8.1.3 Structural and Pressure Tests.....	8-3
8.1.4 Leakage Tests.....	8-4
8.1.4.1 Cask Containment Boundary.....	8-5
8.1.4.1.1 Cask Body Leak Testing – Prior to Lead Pouring.....	8-5
8.1.4.1.2 Primary Lid Assembly Including Secondary Lid and Cover Plate – Prior to Final Assembly.....	8-6
8.1.4.2 Primary and Secondary Lid Containment O-Rings Helium Leak Testing.....	8-7
8.1.4.3 Quick Disconnect Valve Helium Leak Testing.....	8-8
8.1.4.4 Quick Disconnect Valve Cover Plate Containment O-Rings Helium Leak Testing.....	8-10

8.1.5 Component and Material Tests.....	8-12
8.1.5.1 Foam.....	8-13
8.1.5.2 O-Ring.....	8-13
8.1.5.3 Ceramic Paper.....	8-14
8.1.5.4 Fusible Plugs.....	8-14
8.1.5.5 Carbon Steel and Alloy Steel Fasteners.....	8-15
8.1.5.6 Stainless Steel Fasteners.....	8-17
8.1.5.7 Thread Inserts.....	8-19
8.1.5.8 Quick Disconnect Valve.....	8-20
8.1.6 Shielding Tests.....	8-20
8.1.7 Thermal Tests.....	8-21
8.1.8 Miscellaneous Tests.....	8-21
8.2 Maintenance Program.....	8-21
8.2.1 Structural and Pressure Tests.....	8-21
8.2.2 Leakage Tests.....	8-22
8.2.2.1 Periodic and Maintenance Leak Test.....	8-22
8.2.2.2 Pre-Shipment Leak Test – Gas Pressure Rise Option.....	8-22
8.2.2.3 Pre-Shipment Leak Test – Gas Pressure Drop Option.....	8-24
8.2.3 Component and Material Tests.....	8-27
8.2.3.1 Routine Component Inspection.....	8-27
8.2.3.2 Annual Component Inspection.....	8-27
8.2.4 Thermal Tests.....	8-28
8.2.5 Miscellaneous Tests.....	8-28
8.3 Appendix.....	8-29
8.3.1 Summary of Leak Test Requirements.....	8-29
8.3.2 Minimum Lead Thickness and Gap Determination.....	8-30
8.3.2.1 Explanation of the Gap Between Lead and the External Shell.....	8-30
8.3.2.2 Conclusion.....	8-35
8.4 References.....	8-36

List of Figures

Figure 1-1	Information Flow for General Information	1-2
Figure 1.2.1-1	RT-100 Cask Package Artist Concept	1-3
Figure 2-1	Information Flow for the Structural Review	2-2
Figure 2.5.1-1	RT-100 Lifting Pocket Dimensions	2-17
Figure 2.5.1-2	Weld Geometry	2-19
Figure 2.5.2-1	RT-100 Tie-Down Arm Geometry	2-31
Figure 2.5.2-2	RT-100 Tie-Down Free Body Diagrams	2-32
Figure 2.6.7-1	RT-100 Solid Model	2-45
Figure 2.6.7-2	RT-100 Finite Element Model	2-46
Figure 2.6.7-3	Gap Elements Used to Represent the Impact Limiters for Side and End Drop Configurations	2-47
Figure 2.6.7-4	Bolt Pre-load Using ANSYS Pre-Tension Elements (PRETS179)	2-51
Figure 2.6.7-5	Pressure Distribution Used to Simulate the Contents	2-52
Figure 2.6.7-6	RT-100 NCT Side Drop Stress Intensity Results	2-55
Figure 2.6.7-7	RT-100 Inner Shell NCT Side Drop Stress Intensity Results	2-56
Figure 2.6.7-8	RT-100 Outer Shell NCT Side Drop Stress Intensity Results	2-57
Figure 2.6.7-9	RT-100 Flange NCT Side Drop Stress Intensity Results	2-58
Figure 2.6.7-10	RT-100 Outer Lid NCT Side Drop Stress Intensity Results	2-59
Figure 2.6.7-11	RT-100 Inner Lid NCT Side Drop Stress Intensity Results	2-60
Figure 2.6.7-12	RT-100 NCT Bottom Drop Stress Intensity Results	2-63
Figure 2.6.7-13	RT-100 Inner Shell NCT End Drop Stress Intensity Results	2-64
Figure 2.6.7-14	RT-100 Outer Shell NCT End Drop Stress Intensity Results	2-65
Figure 2.6.7-15	RT-100 Flange NCT End Drop Stress Intensity Results	2-66
Figure 2.6.7-16	RT-100 Outer Lid NCT End Drop Stress Intensity Results	2-67
Figure 2.6.7-17	RT-100 Inner Lid NCT End Drop Stress Intensity Results	2-68
Figure 2.7.1-1	RT-100 HAC End Drop Stress Intensity Results	2-75
Figure 2.7.1-2	RT-100 Inner Shell HAC End Drop Stress Intensity Results	2-76
Figure 2.7.1-3	RT-100 Outer Shell HAC End Drop Stress Intensity Results	2-77
Figure 2.7.1-4	RT-100 Flange HAC End Drop Stress Intensity Results	2-78
Figure 2.7.1-5	RT-100 Outer Lid HAC End Drop Stress Intensity Results	2-79
Figure 2.7.1-6	RT-100 Inner Lid HAC End Drop Stress Intensity Results	2-80
Figure 2.7.1-7	RT-100 Lead Slump	2-81
Figure 2.7.1-8	RT-100 HAC Side Drop Stress Intensity Results	2-84

Figure 2.7.1-9	RT-100 Inner Shell HAC Side Drop Stress Intensity Results.....	2-85
Figure 2.7.1-10	RT-100 Outer Shell HAC Side Drop Stress Intensity Results	2-86
Figure 2.7.1-11	RT-100 Flange HAC Side Drop Stress Intensity Results	2-87
Figure 2.7.1-12	RT-100 Outer Lid HAC Side Drop Stress Intensity Results.....	2-88
Figure 2.7.1-13	RT-100 Inner Lid HAC Side Drop Stress Intensity Results	2-89
Figure 2.7.3-1	RT-100 ANSYS Puncture Model.....	2-96
Figure 2.7.3-2	RT-100 Pin Puncture Stress Intensity Results	2-96
Figure 2.7.3-3	RT-100 Side Puncture Details.....	2-101
Figure 2.12.2-1	Schematic of the RT100 impact limiters	2-106
Figure 2.12.3-1	Example Crush Strength-Strain Curve	2-113
Figure 2.12.3-2	Cask configuration at impact (End-Drop).....	2-114
Figure 2.12.3-3	Cask configuration when velocity becomes zero (End-Drop)	2-115
Figure 2.12.3-4	Diagram for contact area calculation (End-Drop)	2-115
Figure 2.12.3-5	Cask configuration at impact (Side-Drop).....	2-117
Figure 2.12.3-6	Cask configuration when velocity becomes zero (Side-Drop).....	2-117
Figure 2.12.3-7	Diagram of Contact Zones	2-118
Figure 2.12.3-8	Cask Configuration at Impact (Corner-Drop)	2-119
Figure 2.12.3-9	Cask configuration when velocity becomes zero (Corner-Drop).....	2-120
Figure 2.12.3-10	Typical Unit Cell Configuration	2-121
Figure 2.12.3-11	Crush sequence of two foam cell	2-122

Proprietary Information Content Withheld Under 10 CFR 2.390

Proprietary Information Content Withheld Under 10 CFR 2.390

Figure 2.13.4-1	Compression Set vs. Temperature	2-207
Figure 2.15.4-1	Stress Intensity Contour Plot of Primary Lid Following End Drop.	2-219
Figure 2.15.4-2	Stress Intensity Contour Plot of the Primary Seal Region.....	2-220
Figure 2.15.4-3	Lid Seal Geometry	2-221
Figure 2.15.4-4	Primary Lid Sealing Surface Displacement during Side drop	2-222
Figure 2.15.4-5	Secondary Lid Sealing Surface Displacement during Side drop.....	2-223
Figure 2.15.4-6	Primary Lid Sealing Surface Displacement during End drop	2-224
Figure 2.15.4-7	Secondary Lid Sealing Surface Displacement during End drop	2-225
Figure 2.15.4-8	Primary Lid Sealing Surface Displacement during Puncture.....	2-226
Figure 2.15.4-9	Secondary Lid Sealing Surface Displacement during Puncture.....	2-227
Figure 3-1	Information Flow for the Thermal Review	3-2
Figure 3.3.1-1	RT-100 ANSYS Finite Element Model Volumes.....	3-17
Figure 3.3.1-2	RT-100 ANSYS Normal Condition Finite Element Mesh.....	3-18
Figure 3.3.1-3	Temperature Contour Plot of Package—Hot Case 1	3-19
Figure 3.3.1-4	Temperature Contour Plot of Cask Body—Hot Case 1	3-20
Figure 3.3.1-5	Temperature Contour Plot of Inner Shell Surface—Hot Case 1	3-21
Figure 3.3.1-6	Temperature Contour Plot of Lead Shielding—Hot Case 1	3-22
Figure 3.3.1-7	Temperature Contour Plot of Package—Hot Case 2.....	3-23

Figure 3.3.1-8	Temperature Contour Plot of Cask Body—Hot Case 2.....	3-24
Figure 3.3.1-9	Temperature Contour Plot of Package—Cold Case 1	3-25
Figure 3.3.1-10	Temperature Contour Plot of Cask Body—Cold Case 1	3-26
Figure 3.3.1-11	Temperature Contour Plot of Package—Cold Case 2	3-27
Figure 3.3.1-12	Temperature Contour Plot of Cask Body Cold Case 2.....	3-28
Figure 3.4.1-1	Temperature Contour Plot of Package Pre-Fire Fire Condition—HAC Pin Damage on Top Impact Limiter	3-33
Figure 3.4.1-2	Temperature Contour Plot of Cask Body Pre-Fire Condition—HAC Pin Damage on Top Impact Limiter	3-34
Figure 3.4.1-3	Temperature Contour Plot of Inner Shell Pre-Fire Condition—HAC Pin Damage on Top Impact Limiter	3-35
Figure 3.4.1-4	Temperature Contour Plot of Package at the End of Fire—HAC Pin Damage on Top Impact Limiter.....	3-36
Figure 3.4.1-5	Temperature Contour Plot of Cask Body at the End of Fire—HAC Pin Damage on Top Impact Limiter	3-37
Figure 3.4.1-6	Temperature Contour Plot of Package after Cool-Down—HAC Pin Damage on Top Impact Limiter.....	3-38
Figure 3.4.1-7	Temperature Contour Plot of Cask Body after Cool-Down—HAC Pin Damage on Top Impact Limiter	3-39
Figure 3.4.1-8	Time-History Plot of Critical Package Components—HAC Pin Damage on Top Impact Limiter	3-40
Figure 3.4.1-9	Time-History Enhanced View Plot of Critical Package Components—HAC Pin Damage on Top Impact Limiter.....	3-41
Figure 3.4.1-10	Maximum Temperature of the Inner Shell—HAC Pin Damage on Top Impact Limiter	3-42
Figure 3.4.1-11	Maximum Temperature of Lead Shielding—HAC Pin Damage on Top Impact Limiter	3-43
Figure 3.4.2-1	Cask Model-HAC Pin Damage on Cask Body Side.....	3-45
Figure 3.4.2-2	Temperature Contour Plot of Package Pre-Fire Condition—HAC Pin Damage on Cask Body Side	3-46
Figure 3.4.2-3	Temperature Contour Plot of Cask Body Pre-Fire Condition—HAC Pin Damage on Cask Body Side	3-47
Figure 3.4.2-4	Temperature Contour Plot of Inner Shell Pre-Fire Condition—HAC Pin Damage on Cask Body Side	3-48

Figure 3.4.2-5	Temperature Contour Plot of Package at the End of Fire—HAC Pin Damage on Cask Body Side	3-49
Figure 3.4.2-6	Temperature Contour Plot of Cask Body at the End of Fire—HAC Pin Damage on Cask Body Side	3-50
Figure 3.4.2-7	Temperature Contour Plot of Package after Cool-Down—HAC Pin Damage on Cask Body Side	3-51
Figure 3.4.2-8	Temperature Contour Plot of Cask Body After Cool-Down—HAC Pin Damage on Cask Body Side	3-52
Figure 3.4.2-9	Time-History Plot of Critical Package Components—HAC Pin Damage on Cask Body Side	3-53
Figure 3.4.2-10	Time-History Enhanced View Plot of Critical Package Components—HAC Pin Damage on Cask Body Side	3-54
Figure 3.4.2-11	Maximum Temperature of the Inner Shell—HAC Pin Damage on Cask Body Side	3-55
Figure 3.4.2-12	Maximum Temperature of Lead Shielding—HAC Pin Damage on Cask Body Side	3-56
Figure 4-1	Information Flow for the Containment Review	4-2
Figure 4.1.2-1	Illustration of Containment Boundary	4-4
Figure 4.3.1-1	Allowable Air/Helium Mixture Test Leakage Rates	4-12
Figure 4.3.1-2	Allowable Helium Test Leakage Rates	4-13
Figure 4.4.4-1	Package Loading Curve for Hydrogen Generation – Decay Heat Limit Versus Waste Volume	4-31
Figure 5-1	Information Flow for the Shielding Evaluation	5-4
Figure 5.3.1-1	NCT Model 1 & 2	5-11
Figure 5.3.1-2	NCT Model Tally Surfaces for Dose Rate Response Estimation	5-12
Figure 5.3.1-3	HAC Model 1	5-13
Figure 5.3.1-4	HAC Model 2	5-14
Figure 5.3.1-5	HAC Model General Tally Surfaces	5-15
Figure 5.3.1-6	HAC Model Surface Tally	5-16
Figure 5.4.1-1	Fe-59 Spectrum Grouped into Generic Energy Lines	5-21
Figure 5.4.4-1	Fluctuation in Radial Dose Rates (Cs-137)	5-28
Figure 5.4.4-2	Summary of Calculated Dose Rate Margins	5-31
Figure 5.4.4-3	Example of Media Density Effect	5-33
Figure 5.4.4-4	NCT Maximum Gamma Dose Rates for Co-60 Content at 1.00 g/cc	5-36

Figure 7-1	Information Flow for the Operating Procedures Review.....	7-2
Figure 7.1.1-1	Preparation for Loading Process Flowchart.....	7-4
Figure 7.1.2-1	Loading of the RT-100 Process Flowchart	7-7
Figure 7.1.3-1	Preparation for Transport Process Flowchart.....	7-10
Figure 7.4.2-1	Lifting Yoke Arm Positioned on Cask	7-15
Figure 7.4.2-2	Lifting Yoke Connections.....	7-15
Figure 7.4.2-3	Lifting Yoke Secured with Locking Pin.....	7-15
Figure 7.4.2-4	Assembled Cask Ready to Lift.....	7-15
Figure 7.4.4-1	Example Trailer Illustration.....	7-17
Figure 7.4.4-2	Loading of the RT-100 on Transportation Trailer.....	7-17
Figure 7.5-1	Package Loading Curve for Hydrogen Generation – Decay Heat Limit Versus Waste Volume.....	7-21
Figure 8-1	Information Flow for the Acceptance Tests and Maintenance Program Review	8-1
Figure 8.1.4-1	Cask Body Containment Boundary Test Apparatus.....	8-5
Figure 8.1.4-2	Primary Lid Assembly Containment Boundary Test Apparatus.....	8-6
Figure 8.1.4-3	Test Apparatus for Measuring the Helium Leak Rate through the Quick Disconnect Valve	8-9
Figure 8.1.4-4	Alternate Test Apparatus for Measuring the Helium Leak Rate through the Quick Disconnect Valve	8-9
Figure 8.1.4-5	Test Apparatus for Measuring the Helium Leak Rate through the Quick Disconnect Valve Cover Plate	8-11
Figure 8.1.4-6	Alternate Test Apparatus for Measuring the Helium Leak Rate through the Quick Disconnect Valve Cover Plate	8-11
Figure 8.3.2-1	Lead Solidification Diagram.....	8-31
Figure 8.3.2-2	Effect of temperature on the physical properties of AISI 301 stainless steel.....	8-33

List of Tables

Table 2.1.2-1	Load Combinations for RT-100 Cask Body Analyses	2-5
Table 2.1.2-2	Structural Design Criteria for RT-100.....	2-5
Table 2.1.3-1	Assembly Weights and Center of Gravity Locations.....	2-7
Table 2.2.1-1	Cask Temperature-Dependent Material Properties	2-9
Table 2.2.1-2	Cask Temperature-Independent Material Properties	2-10
Table 2.2.1-3	Allowable Stresses for Cask Body Materials.....	2-10
Table 2.5.1-1	Summary of Results for Lifting Assembled Cask.....	2-21
Table 2.5.2-1	Tie-down Arms Horizontal Angles	2-29
Table 2.5.2-2	Calculated Values for Tie-Down Arms	2-33
Table 2.5.2-3	Calculated Forces for Tie-Down Arms.....	2-33
Table 2.6.7-1	NCT Side Drop Stress Summary	2-54
Table 2.6.7-2	NCT End Drop Stress Summary	2-62
Table 2.7.1-1	Deceleration Loadings in RT-100 Cask Body Finite Element Analyses.....	2-70
Table 2.7.1-2	HAC End Drop Stress Summary.....	2-74
Table 2.7.1-3	HAC Side Drop Stress Summary	2-83
Table 2.7.1-4	Corner Drop Component Accelerations	2-90
Table 2.7.1-5	HAC Corner Drop Stress Summary	2-91
Table 2.7.3-1	HAC Pin Puncture Stress Summary	2-95
Table 2.7.4-1	HAC Pressure Stress Summary.....	2-103
Table 2.12.3-1	Foam Crush Strength Coefficients	2-112
Table 2.12.4-1	Maximum Decelerations Summary for 9.0 m End-Drop Case	2-127
Table 2.12.4-2	Maximum Crush Depths for 9.0 m End-Drop Case	2-127
Table 2.12.4-3	Maximum Decelerations Summary for 9.0 m Side-Drop Case.....	2-130
Table 2.12.4-4	Maximum Crush Depths for 9.0 m Side-Drop Case	2-130
Table 2.12.4-5	Maximum Decelerations for 9.0 m Corner-Drop Case.....	2-133
Table 2.12.4-6	Maximum Crush Depths for 9.0 m Corner-Drop Case.....	2-133
Table 2.12.4-7	Maximum Decelerations for 0.3 m End-drop Case.....	2-137
Table 2.12.4-8	Maximum Crush Depths for 0.3 m End-drop Case.....	2-137
Table 2.12.4-9	Maximum Decelerations for 0.3 m Side-drop Case	2-140
Table 2.12.4-10	Maximum Crush Depths for 0.3 m Side-Drop Case	2-140
Table 2.12.4-11	Maximum Decelerations for 0.3 m Corner-Drop Case.....	2-143
Table 2.12.4-12	Maximum Crush Depths for 0.3 m Corner-Drop Case.....	2-143
Table 2.12.4-13	Actual Test Conditions - 3/10 Scale Cask Drop Tests.....	2-145

Table 2.12.4-14	Foam Densities - 3/10 Scale Cask Drop Tests	2-145
Table 2.12.4-15	Predicted and Actual Deceleration and Crush Depth - 3/10 Scale Cask End-Drop.....	2-146
Table 2.12.4-16	Predicted and Actual Deceleration and Crush Depth - 3/10 Scale Cask Corner-Drop.....	2-148
Table 2.12.4-17	Predicted and Actual Deceleration and Crush Depth - 3/10 Scale Cask Side-Drop.....	2-150
Table 2.12.5-1	Comparison of 3/10th Scale Drop Test Results and Analytical Method	2-152
Table 2.12.6-1	Design Decelerations for Subsequent Cask Body Analysis.....	2-153
Table 2.13.2-1	Closure Bolt Loads for 9.0 m Corner-Drop	2-178
Table 2.13.3-1	Primary Lid Bolt Load Summary.....	2-189
Table 2.13.3-2	Secondary Lid Bolt Load Summary	2-189
Table 2.15.4-1	Stress Concentration Factors.....	2-216
Table 2.15.4-2	Sealing Surface Stress Summary.....	2-217
Table 2.15.4-3	Lid Seal Groove Region Stresses	2-217
Table 2.15.4-4	HAC Seal Region Displacement	2-218
Table 3.1.3-1	RT-100 Maximum Normal Condition Temperature Summary	3-6
Table 3.1.3-2	RT-100 Maximum Calculated Temperature of Cask under HAC with Pin Puncture Damage on Top Impact Limiter	3-6
Table 3.1.3-3	RT-100 Maximum Calculated Temperature of Cask under HAC with Pin Puncture Damage at the Side of the Cask Body.....	3-7
Table 3.1.4-1	RT-100 Summary of Maximum Normal and Hypothetical Accident Condition Pressures	3-7
Table 3.2.1-1	Temperature-Independent Material Properties	3-9
Table 3.2.1-2	Temperature-Dependent Material Properties—Stainless Steel 304	3-10
Table 3.2.1-3	Temperature-dependent Material Properties—Lead.....	3-11
Table 3.2.1-4	Temperature-dependent Material Properties—Ceramic Paper	3-11
Table 3.2.2-1	Component Specifications – Minimum and Maximum Temperatures.....	3-12
Table 3.2.3-1	Maximum Temperature Limits for RT-100 Content Materials.....	3-13
Table 4.1.4-1	Bolt Torque Requirements.....	4-6
Table 4.1.5-1	Cask Cavity Dimensions.....	4-6
Table 4.1.5-2	Cask Cavity Volume.....	4-6
Table 4.1.5-3	Parameters for Normal Transport and Accident Conditions.....	4-7
Table 4.3-1	Leakage Tests of the RT-100 Package	4-9

Table 4.3.1-1	Helium and Air Viscosity	4-11
Table 4.3.1-2	Allowable Helium Test Leakage Rates, cm ³ /sec.....	4-14
Table 4.4-1	G Values (Molecules/100eV) for Potential Content Materials	4-17
Table 4.4-2	Effective G Values (Molecules/100eV) for Potential Content Materials	4-18
Table 4.4-3	Activation Energy	4-19
Table 4.4-4	Bounding G Values for Contents at Maximum NCT Temperature.....	4-20
Table 4.4-5	Effective G Values and Corresponding α Values for Contents.....	4-25
Table 4.4.3-6	Secondary Container Volumes and Allowable Shoring Volume	4-29
Table 4.4.4-1	Conditions and Justifications for using Package Loading Curve (Figure 4.4.4-1)	4-32
Table 4.4.5-1	Conditions for Shipper to use the Detailed Analysis.....	4-34
Table 4.4.5-2	G-values and α -Fractions for a Range of Alpha/Gamma Decay Heat Distributions.....	4-35
Table 5.1.2-1	Summary Table of External Radiation Levels (Exclusive Use).....	5-6
Table 5.2.1-1	One Curie Co-60 Gamma Source Term	5-7
Table 5.3-1	Model Shielding Thicknesses	5-8
Table 5.3.2-1	RT-100 Material Composition Summary	5-18
Table 5.4.3-1	ANSI/ANS 6.1.1-1977 – Gamma Flux-to-Dose Conversion Factors	5-25
Table 5.4.4-1	Maximum Dose Rates and Responsible Radionuclides	5-26
Table 5.4.4-2	Media Composition Comparison	5-29
Table 5.4.4-3	Media Density Comparison	5-30
Table 5.4.4-4	NCT Dose Rate Responses Due to Bremsstrahlung.....	5-32
Table 5.4.4-5	NCT Gamma Dose Rates for the Maximum Radionuclide Loading.....	5-37
Table 5.4.4-6	HAC Gamma Dose Rates for the Maximum Radionuclide Loading	5-44
Table 5.5.1-1	List of Gamma Radionuclides with Greater Than 1 Day Half Life.....	5-51
Table 5.5.2-1	NCT Gamma Dose Rate Responses (mrem/hr/Ci).....	5-53
Table 5.5.2-2	HAC Gamma Dose Rate Responses (mrem/hr/Ci)	5-61
Table 5.5.3-1	Radionuclide Maximum Ci/g Loading Limits based on Gamma Response	5-69
Table 7.4.5-1	Lid Bolt Tightening Torques.....	7-18
Table 7.4.5-2	Tightening Torques - Other Parts.....	7-18
Table 7.5.1-1	Conditions for using Package Loading Curve (Excerpt from Table 4.4.4-1)	7-21
Table 7.5.1-2	Secondary Container and Allowable Shoring Volumes (Excerpt from Table 4.4.3-6)	7-22
Table 7.5.2-1	Conditions for Shipper to use the Detailed Analysis (From Table 4.4.5-1).....	7-24

Table 7.5.2-2	G-values and α -Fractions for a Range of Alpha/Gamma Decay Heat Distributions (Excerpt from Table 4.4.5-2)	7-25
Table 7.6.1-1	RT-100 Loading Table Illustration.....	7-31
Table 7.6.1-2	Turkey Point Loading Table Example.....	7-34
Table 7.6.1-3	St. Lucie Loading Table Example.....	7-36
Table 7.6.1-4	Maximum Co-60 Loading Table Example	7-37
Table 7.6.1-5	Failed Loading Table Example	7-37
Table 7.6.1-6	Radionuclide Activity Concentration Limits	7-38
Table 8.1.5-1	Material Specifications for O-Rings.....	8-13
Table 8.1.5-2	Basic Requirements for O-Rings.....	8-13
Table 8.1.5-3	Supplementary Requirements for O-Rings	8-14
Table 8.1.5-4	Critical Characteristics of Ceramic Paper.....	8-14
Table 8.1.5-5	Materials and Reference Standards for Carbon Steel and Alloy Steel Fasteners	8-15
Table 8.1.5-6	Chemical Composition for Carbon Steel and Alloy Steel Fasteners.....	8-16
Table 8.1.5-7	Mechanical Properties of Carbon Steel and Alloy Steel Fasteners	8-17
Table 8.1.5-8	Materials and Reference Standards for Stainless Steel Fasteners	8-18
Table 8.1.5-9	Chemical Composition for Stainless Steel Fasteners	8-18
Table 8.1.5-10	Mechanical Properties of Stainless Steel Fasteners.....	8-18
Table 8.1.5-11	Chemical Composition for Stainless Steel Bars.....	8-19
Table 8.1.5-12	Mechanical Properties of Stainless Steel Bars	8-19
Table 8.1.5-13	Chemical Composition for Threaded Inserts	8-20
Table 8.1.5-14	Mechanical Properties of Threaded Inserts.....	8-20
Table 8.3-1	RT-100 Leakage Test Types	8-29
Table 8.3-2	Allowable Helium Leakage Rates.....	8-29

List of Attachments

Attachment 1.4-1	RT100 NM 1000 Rev. F — Bill of Material.....	1-13
Attachment 1.4-2	RT100 PE 1001-1 Rev. H — Robatel Transport Package RT-100 General Assembly Sheet 1/2	1-19
Attachment 1.4-3	RT100 PE 1001-2 Rev. H — Robatel Transport Package RT-100 General Assembly Sheet 2/2	1-20
Attachment 1.4-4	RT100 PRS 1011 Rev. E — Robatel Transport Package RT-100 Cask Sub Assembly Weld Map Cask Body	1-21
Attachment 1.4-5	RT100 PRS 1013 Rev. C — Robatel Transport Package RT-100 Cask Sub Assembly Weld Map Secondary Lid.....	1-22
Attachment 1.4-6	RT100 PRS 1031 Rev. D — Robatel Transport Package RT-100 Cask Sub Assembly Weld Map Lower Impact Limiter	1-23
Attachment 1.4-7	RT100 PRS 1032 Rev. D — Robatel Transport Package RT-100 Cask Sub Assembly Weld Map Upper Impact Limiter.....	1-24
Attachment 1.4-8	102885 MD 1031-06 Rev. F — Robatel Transport Package RT-100 Sub Assembly Fabrication Drawing Impact Limiter Foam	1-25
Attachment 2.12-1	General Plastics Foam Product Information Sheets	2-154
Attachment 3.5-1	EPDM Temperature Specifications	3-61
Attachment 3.5-2	Seal Material EPDM Working Temperature.....	3-62
Attachment 3.5-3	Water Vapor Pressure Reference (80°C).....	3-63
Attachment 3.5-4	Water Vapor Pressure Reference (150°C).....	3-66
Attachment 4.5-1	EPDM Temperature Specifications	4-36
Attachment 4.5-2	Seal Material EPDM Working Temperature.....	4-37
Attachment 4.5-3	Seal Material EPDM Helium gas permeation rate	4-38
Attachment 4.5-4	Seal Material EPDM Characteristics With Respect to Damage by Radiation and Hardness Concerns	4-40
Attachment 4.5-5	Additional Support Information about EPDM Resistance to Radiation Up to 5x10 ⁸ Rads While Retaining Reasonable Flexibility and Strength, Hardness and Very Good Compression Set Resistance	4-44

1. GENERAL INFORMATION

ROBATEL Technologies, LLC (RT) submitted its Application and Safety Analysis Report (SAR), Revision 3, to the Nuclear Regulatory Commission (NRC) on 14 January 2014 [Ref. 3] for the Model RT-100 Type B(U) Cask Package (RT-100). Revision 3 addressed the Request for Additional Information (RAI) received from the NRC on 26 November 2013 [Ref. 4].

After further review, RT submits this Revision 4 of our Application and SAR in accordance with its NRC-approved RT Quality Assurance Program [Ref. 1]. Revision 4 includes editorial changes for clarification, and replaces the previous submittal (Revision 3) in its entirety.

Chapter 1 of the SAR provides General Information that feeds information to later sections in this application according to Figure 1-1 on the following page. The RT-100 meets the following general requirements for all packages:

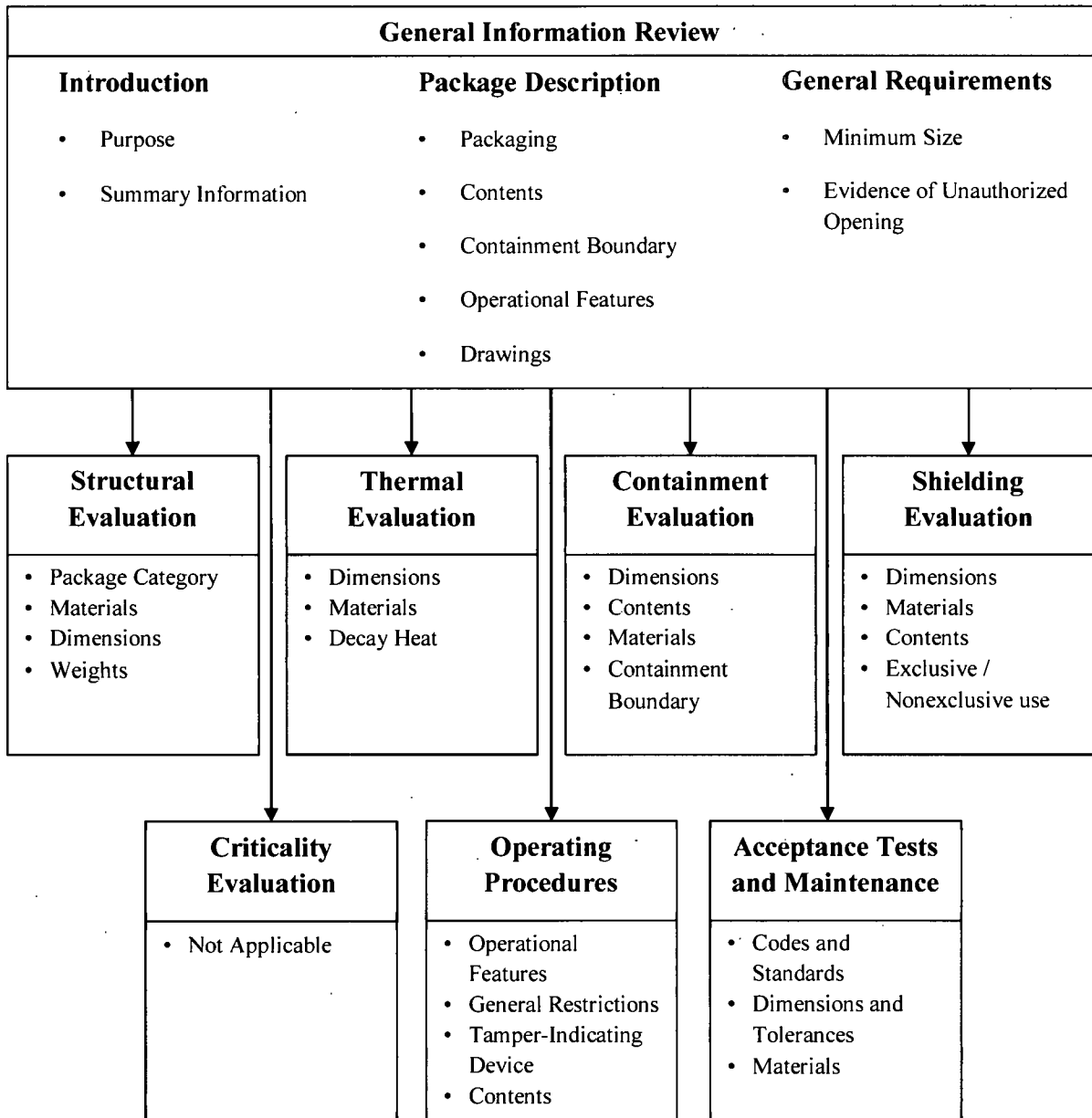
- The smallest overall dimension of the RT-100 is not less than 10 cm (4 in.).
- The outside of the RT-100 incorporates a feature that, while intact, is evidence that the package has not been opened by unauthorized persons.

1.1 Introduction

The purpose of this application is for the approval of a new type B(U) cask design. The “RT-100” is the proposed cask model number. The RT-100 is proposed to package and transport contaminated spent resins and spent filters.

This application does not request the packaging and/or transport of fissile material in quantities exceeding those exempted from consideration in accordance with 10 CFR 71.15 [Ref. 2] and thus, the Criticality Safety Index (CSI) is non-applicable.

Figure 1-1 Information Flow for General Information



1.2 Package Description

Section 1.2 provides a summary of all design aspects of the RT-100. A general arrangement of the RT-100 cask is included in Appendix 1.4. The general arrangement depicts the package dimensions and the materials of construction. Figure 1.2.1-1 shows the major components of the RT-100 as an exploded artist view with the various components labeled.

1.2.1 Packaging

Section 1.2.1 provides details regarding overall dimensions, weight, containment, shielding, criticality, structural features, heat transfer features and package markings.

1.2.1.1 Overall Dimensions

The package consists of a stainless-steel and lead cylindrical shipping cask with a pair of cylindrical foam-filled impact limiters installed on each end. The package configuration is shown in Figure 1.2.1-1.

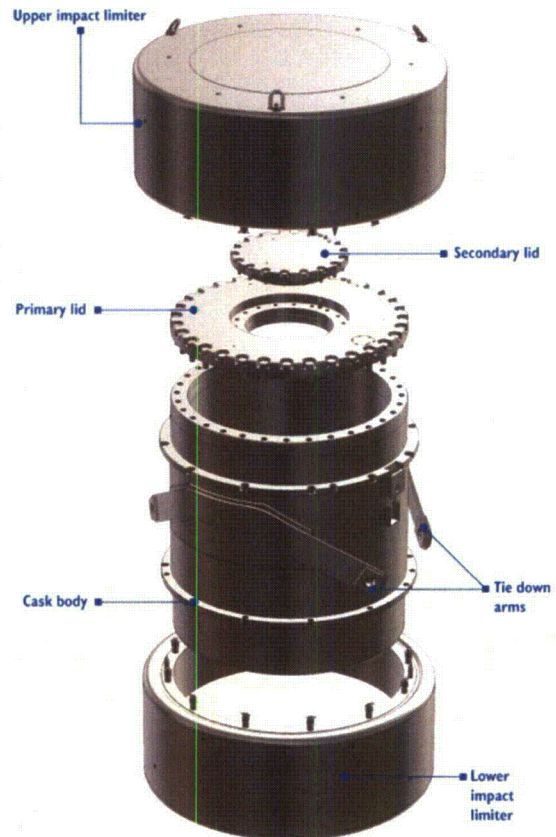


Figure 1.2.1-1 RT-100 Cask Package Artist Concept

The internal cavity dimensions are 1730 mm in diameter and 1956 mm high. The cylindrical cask body is comprised of a 35 mm thick outer stainless-steel shell and a 30 mm thick inner stainless-steel plate. The annular space between the shells is filled with 90 mm thick lead.

The base of the cask consists of a 30 mm thick stainless steel outer bottom plate, a 75 mm thick gamma shield of poured lead, and a 50 mm thick stainless steel inner bottom forging.

The primary lid consists of a 210 mm thick stainless steel forging. The primary lid is fastened to the cask body with thirty-two (32) M48 hex head bolts.

The secondary lid is made of 100 mm thick stainless steel plate, a 60 mm thick lead gamma shield and a 10 mm thick stainless steel plate. The secondary lid is attached to the primary lid with eighteen (18) M36 hex head bolts.

1.2.1.2 Weight

The maximum gross weight of the RT-100 including impact limiters is 41,500 kg (including the maximum payload weight of 6,804 kg). The maximum (empty) weight of the RT-100 including impact limiters is 34,696 kg.

1.2.1.3 Containment Features

The containment vessel of the RT-100 cask consists of the inner shell, the bottom forging, the top flange, the primary lid, the primary lid inner O-ring, the stainless steel vent port cover plate and its inner O-ring, the secondary lid and the secondary lid inner O-ring. The containment system prevents leakage of radioactive material from the cask cavity and allows pre-shipment leakage testing of the assembled cask configuration.

1.2.1.4 Neutron and Gamma Shielding Features

The RT-100 is not designed to carry fissile material or neutron sources (except typical small quantities consistent with contaminated resins and filters as discussed in Chapter 5) and thus, provision of neutron shielding is not required for the RT-100.

In regards to gamma shielding, the RT-100 cask walls provide a shield thickness of 90 mm of lead and 70 mm of stainless steel including the thermal shield plate of 5 mm thickness (65 mm used for HAC analysis). The cask bottom end provides a shield thickness of 75 mm of lead and 80 mm of stainless steel. The top end provides a shield thickness of 210 mm of stainless steel for the primary lid and a shield thickness of 60 mm of lead and 110 mm of stainless steel for the secondary lid. Contents are limited such that the radiological shielding provided assures compliance with U.S. Department of Transportation (DOT) regulatory requirements.

1.2.1.5 Shielding Features for Personnel Barriers

The RT-100 does not require the use of personnel barriers to meet 10 CFR 71 dose rate limits.

1.2.1.6 Criticality Control Features

The RT-100 contents are resins and filters from commercial nuclear power plants that contain only trace quantities of fissile radionuclides. As such, the contents meet the requirements of 10 CFR 71.15 [Ref. 2] and are exempt from classification as fissile material. As a result, the RT-100 does not require any criticality control features.

1.2.1.7 Structural Features – Lifting and Tie-Down Devices

The RT-100 cask employs lifting devices that are a structural part of the package. Two lifting pockets are welded to the cylindrical cask body as shown in Drawing RT100 PE 1001-02, Rev. H (Chapter 1, Appendix 1.4, Attachment 1.4-3). The pockets engage the arms of a separate lifting yoke used to lift the package. When not in use for package lifting, the pockets are rendered inoperable so they cannot be inadvertently used as cask tie-downs. Removable lifting lugs are

utilized for removal and handling of the primary and secondary lids, as well as the impact limiters. Refer to Chapter 2, Section 2.5.1 for a detailed analysis of the structural integrity of the lifting devices.

Two tie-down arms are welded to the external cask shell and are considered a structural part of the package. When not in use for package tie-down, the arms' holes are rendered inoperable preventing the tie-down arms from being used to lift the packaging. Refer to Chapter 2, Section 2.5.2 for a detailed analysis of the structural integrity of the tie-down arms.

1.2.1.8 Structural Features – Impact Limiters

The impact limiters have an outside diameter of 2587 mm. The lower impact limiter extends 494 mm beyond the base of the cask. The upper impact limiter extends 498 mm beyond the cask primary lid. The impact limiter external shells are stainless-steel, allowing them to withstand large plastic deformation without fracturing. The volume inside the shell is filled with crushable shock-absorbing and thermal-insulating polyurethane foam. The polyurethane is preformed and inserted into the shell to the void space. The use of preformed foam ensures homogeneous density. Several different foam densities are used to customize the shock absorbing performance of the impact limiters during hypothetical accident conditions. The rationale for use of preformed foam blocks and the use of different foam densities is presented in detail in Chapter 2, Section 2.2.

The impact limiters are attached to the cask via two stainless-steel bolt ring flanges located on the exterior cask body. The flanges are welded along the cask circumference and considered a structural part of the package. Each impact limiter is equipped with twelve (12) M36 studs and attached to the bolt ring using twelve (12) M36 stainless steel hex head nuts. The purpose of the bolt rings and bolts are to ensure the impact limiters remain attached to the cask body for all Normal Conditions of Transport (NCT) and Hypothetical Accident Conditions (HAC) events. Additionally, use of bolt rings facilitates removal of the impact limiters during loading and unloading operations.

1.2.1.9 Structural Features – Internal Supporting or Positioning Features

The RT-100 cask interior has no supporting or positioning features. The waste contents shall be pre-packaged in liners and placed into the cask cavity. Waste liners may require appropriate shoring to prevent movement during transit. It is the responsibility of the shipper to provide shoring that meets DOT requirements.

1.2.1.10 Structural Features – Outer Shell or Outer Packaging

The external surface of the cylindrical cask body is comprised of a 35 mm thick stainless-steel outer shell.

1.2.1.11 Structural Features – Packaging Closure Device

The chief packaging closure device is the primary lid that consists of a 210 mm thick stainless steel forging as described in Section 1.2.1.1. The primary lid is fastened to the cask body with thirty-two (32) M48 hex head bolts.

The secondary lid also represents a closure device for the cask and is made of 100 mm thick stainless steel plate with lead shielding and another stainless steel plate as described in Section 1.2.1.1. The secondary lid is attached to the primary lid with eighteen (18) M36 hex head bolts.

1.2.1.12 Structural Features – Heat Transfer Features

The RT-100 relies on the insulating properties of the impact limiter polyurethane foam and the cask body ceramic fiber thermal shield to minimize heat input during the hypothetical fire accident event. See Chapter 3, Section 3.4 for details.

There are no special features designed to dissipate heat from the cask.

1.2.1.13 Structural Features – Packaging Markings

The side of the cask body is marked with the Model Number of the cask “RT-100”, the Certificate of Compliance No., Empty Weight, Type B(U)-96, UN 2916 and other required data.

1.2.1.14 Additional Information

- RT-100 cask has one configuration as depicted in the engineering drawings provided in Appendix 1.4, Attachments 1.4-1 thru 1.4-8.
- The RT-100 has no receptacles.
- Pressure test ports are provided between the twin O-rings for the primary lid, between the O-rings for the secondary lid, and between the O-rings for the vent port cover plate. These ports facilitate leak testing of the package in accordance with ANSI N14.5-1997 [Ref. 4].
- The vent port is provided for venting pressures within the containment cavity which may be generated during transport and prior to lid removal. Each port is sealed with an EPDM O-ring. Specification information for all O-rings is contained in Chapter 4, Section 4.1.3.
- The RT-100 does not rely on any coolants to perform its function of providing safe transportation of its radioactive contents.
- There are no external/internal protrusions other than the tie-down arms previously described.

1.2.2 Contents

The authorized contents of the RT-100 are generally described in Section 1.2.2. The radioactive contents are described to the extent required to demonstrate compliance with 10 CFR 71

requirements relating to the structural, thermal and shielding performance of the cask.

1.2.2.1 Identification and Maximum Quantity of Radioactive Material

The contents of the RT-100 cask are limited to contaminated resins and filters containing byproduct or otherwise radioactive nuclear material.

The maximum quantity of material is defined as a Type B quantity of radioactive materials not to exceed 3000 A₂. The activity of beta, gamma and neutron emitting radionuclides will not exceed the limits established in the shielding evaluation provided in Chapter 5 and using the procedure presented in Chapter 7.

1.2.2.2 Identification and Maximum Quantity of Fissile Material

The RT-100 will not transport fissile material exceeding the quantities exempt in 10 CFR 71.15 [Ref. 2]. Thus, Section 1.2.2.2 is non-applicable.

1.2.2.3 Physical and Chemical Form – Density, Moisture Content and Moderators

The type/form of material is defined as byproduct, source, or special nuclear material in the form of resins, filters, and mixtures of resins/filters. These materials are contained within secondary container(s). The chemical form of the contents is resins and filter media containing radioactive materials. The radioactive content of the resins and filters is considered to be in the form of dispersible solids. There are no contents in powdered form. The contents may include the metal housings associated with the media.

1.2.2.3.1 Ion-Exchange Resins

Single or mixed bed ion exchange resins are used in deep bed filter demineralizers for reduction of particulate matter and dissolved contaminants in utility power plant condensates. Radioactive waste systems in nuclear power plants include ion exchange systems for the removal of trace quantities of radioactive nuclides from water that will be released to the environment. The primary resin system used is the mixed bed.

Conventional ion exchange resins consist of a cross-linked polymer matrix with a relatively uniform distribution of ion-active sites throughout the structure. Ion exchange resin materials are sold as spheres or sometimes granules with a specific size and uniformity to meet the needs of a particular application. Ion exchange resins can contain up to 66% water when delivered from the manufacturer. This is essentially the same moisture content within the resin when delivered for disposal. The majority are prepared in spherical (bead) form, either as conventional resin with a polydispersed particle size distribution from about 0.3 mm to 1.2 mm (50-16 mesh) or as uniform particle sized (UPS) resin with all beads in a narrow particle size range. In the water swollen state, ion exchange resins typically show a specific gravity of 1.1-1.5. The bulk density as installed in a column includes a normal 35-40 percent voids volume for a spherical

conventional resin product. Bulk densities in the range of 560-960 g/l (35-60 lb/ft³) are typical for wet resinous products [Ref. 8].

The contents are limited by the maximum overall weight limit of 6,804 kg as described in Section 1.2.1.2. The radioactive inventory of the contents are limited as a function of the activity concentration as described in Chapter 5.

1.2.2.3.2 Filters

Filters packaged in the secondary liner are designed for use in a nuclear power plant's primary water chemistry; therefore, the housings are a non-corrosive and non-reactive material. Filter housings may be stainless steel or a thermoplastic such as polyethylene or polypropylene. They are designed to filter radioactive material from the water, and thus are acceptable for use in a radiation environment. The filter housings do not interact with the secondary container and therefore do not interact with the RT-100 metal cavity.

1.2.2.3.3 Secondary Containers

Secondary containers may be constructed of carbon steel or stainless steel, or a thermoplastic such as polyethylene or polypropylene. The secondary containers are used to package resins or filters generated by nuclear power plants. There is a long history of transportation of these resins and filters via typical polyethylene or metal liners in metal casks by the nuclear power industry and other low-level waste generators. Secondary containers are required to be passively vented within the cask cavity during shipment. The RT-100 stainless steel inner cavity does not interact with polyethylene or metal liners typically used in the nuclear industry for the shipment of resins and filters. Secondary containers may be positioned or braced within the cavity using shoring. This shoring may be constructed of carbon steel or stainless steel, wood, or a thermoplastic material or any combination thereof.

1.2.2.4 Location and Configuration

The contents shall be packaged in secondary containers. Except for close fitting contents, shoring is placed between the secondary containers and the cask cavity liner to prevent movement during accident conditions. Providing appropriate shoring is the responsibility of the shipper.

1.2.2.5 Use of Non-Fissile Materials as Neutron Absorbers/Moderators

The RT-100 does not contain non-fissile materials as neutron absorbers/moderators.

1.2.2.6 Chemical/Galvanic/Gas Generation

Chemical Reaction and Galvanic Reactions

The contents do not include materials that may cause any significant chemical, galvanic, or other reaction.

Gas Generation

Secondary packages containing water and/or organic substances may generate combustible gases via radioanalytical reactions. A maximum molar quantity of 5% hydrogen by volume at standard temperature and pressure is allowed. The time duration is calculated as twice the expected shipment time.

Determination of hydrogen generation is made using the methods in NUREG/CR-6673 [Ref. 6], "*Hydrogen Generation in TRU Waste Transportation Packages*", and supplemented with data from EPRI NP-5977 [Ref. 7], "*Radwaste Radiolytic Gas Generation Literature Review*". NUREG/CR-6673 provides equations that allow prediction of the hydrogen concentration as a function of time for simple nested enclosures and for packages containing multiple contents packaged within multiple nested confinement layers. The inputs to these equations include the bounding effective $G(H_2)$ -value for the contents, the $G(H_2)$ -values for the packaging material(s), the void volume in the containment vessel and in the confinement layers (when applicable), the temperature when the package was sealed, the temperature of the package during transport, and the contents decay heat. EPRI NP-5799 provides G-Values for a wide range of ion exchange resins [Ref. 7].

For any package delivered to a carrier for transport, the secondary container is prepared for shipment in the same manner in which the determination for gas generation is made. Shipment period begins when the package is prepared (sealed) and is completed within a time period that is one half the time used in the hydrogen generation calculation. It is the shipper's responsibility to ensure that hydrogen generation in the cavity will be below 5% by volume, representing the lower flammability limit for hydrogen. The maximum allowable shipping time is not restricted for any other reason. Detailed discussion of the hydrogen generation calculations are provided in Chapter 4, Section 4.4, and Chapter 7, Section 7.5.

Secondary packages with radioactive contents less than Low Specific Activity (LSA) and shipped within 10 days of preparation (or within 10 days of venting the secondary container) do not require a determination of hydrogen gas generation or a restriction on shipping time.

1.2.2.7 Maximum Weight of Contents and Payload

All contents shall be packaged in a secondary container (liner). The maximum gross weight of payload is 6,804 kg including the secondary container (liner).

1.2.2.8 Maximum Decay Heat

The maximum decay heat of the RT-100 contents is 200 watts.

1.2.2.9 Loading Restrictions

Contents that are prohibited include explosives, non-radioactive pyrophoric materials, and corrosives (pH less than 2 or greater than 12.5). Pyrophoric radionuclides may be present only in residual amounts less than 1% by weight. Materials that may auto-ignite or undergo phase transformation at temperatures less than 140 °C, with the exception of water, are not included in the contents. As required by 10 CFR 71.43(d) [Ref. 2], the contents do not include materials that may cause any significant chemical, galvanic, or other reactions.

1.2.2.10 Contents for the Certificate of Compliance

The type and form of material is defined as byproduct, source, or special nuclear material in the form of dewatered or grossly dewatered resins, spent filters, or mixtures of resins/filters, contained within secondary container(s). Secondary containers are required to be passively vented within the cask cavity during shipment. The maximum bulk density of the contents may not exceed 1.0 g/cm³. The maximum quantity of payload material including contents, secondary containers, and shoring is limited to 6,804 kg. The maximum quantity of material is defined as a Type B quantity of radioactive materials not to exceed 3000 A₂. The activity of alpha, beta, gamma and neutron emitting radionuclides does not exceed the limits established in the shielding evaluation provided in Chapter 5 and using the loading table provided in Appendix 7.6, Section 7.6.1. The contents may include fissile materials provided at least one of the paragraphs (a) through (f) of 10 CFR 71.15 [Ref. 2] is met.

1.2.3 Special Requirements for Plutonium

The RT-100 will not contain plutonium in solid form. Therefore, the requirements of 10 CFR 71.63 [Ref. 2] specifying that more than 0.74 TBq (20 Ci) of plutonium must be in solid form do not apply.

1.2.4 Operational Features

The RT-100 has no complex operational requirements. The various valves, connections, openings, seals and containment boundaries are depicted in the drawings provided in Appendix 1.4, Attachments 1.4-1 through 1.4-8. There are no piping systems associated with the RT-100 cask.

1.3 Engineering Drawings and Additional Information

Appendix 1.4 contains the engineering drawings (Attachments 1.4-1 thru 1.4-8) and additional information associated with the RT-100.

1.3.1 Engineering Drawings

The RT-100 drawings are enclosed in Appendix 1.4, Attachments 1.4-1 thru 1.4-8, and contain the following information:

- Safety features (primary and secondary lids, seals, bolts, containment boundary, and shielding)
- Materials list, dimensions, vent and leak test ports and weld inspection requirements
- Weld joint requirements
- Details of gasket joints

Appendix 1.4 does not include detailed construction drawings.

1.3.2 Conformance to Approved Design

The RT-100 cask will be fabricated in accordance with the drawings referenced in the CoC.

1.3.3 Referenced Pages

All referenced pages are generally available to the public.

1.3.4 Special Fabrication Procedures

Fabrication of the RT-100 involves standard cask fabrication techniques.

1.3.5 Package Category

The RT-100 is categorized as a Type B(U)-96 Package.

1.3.6 Supplemental Information

This application contains no supplemental information.

1.4 Appendix

Appendix 1.4 contains Proprietary Information that Robatel requests be withheld from public disclosure under 10 CFR 2.390. This request is in accordance with the Robatel Affidavit and as requested in 10 CFR 2.390.

Attachment 1.4-1 RT100 NM 1000 Rev. F — Bill of Material

**Attachment 1.4-2 RT100 PE 1001-1 Rev. H — Robatel Transport Package RT-100
General Assembly Sheet 1/2**

**Attachment 1.4-3 RT100 PE 1001-2 Rev. H — Robatel Transport Package RT-100
General Assembly Sheet 2/2**

**Attachment 1.4-4 RT100 PRS 1011 Rev. E — Robatel Transport Package RT-100
Cask Sub Assembly Weld Map Cask Body**

**Attachment 1.4-5 RT100 PRS 1013 Rev. C — Robatel Transport Package RT-100
Cask Sub Assembly Weld Map Secondary Lid**

**Attachment 1.4-6 RT100 PRS 1031 Rev. D — Robatel Transport Package RT-100
Cask Sub Assembly Weld Map Lower Impact Limiter**

**Attachment 1.4-7 RT100 PRS 1032 Rev. D — Robatel Transport Package RT-100
Cask Sub Assembly Weld Map Upper Impact Limiter**

**Attachment 1.4-8 102885 MD 1031-06 Rev. F — Robatel Transport Package RT-100
Sub Assembly Fabrication Drawing Impact Limiter Foam**

**WITHHELD PER 10
CFR 2.390**

1.5 References

1. Robatel Technologies, LLC, Quality Assurance Program for Packaging and Transportation of Radioactive Material, 10 CFR 71 Subpart H, Dated January 31, 2012 and NRC Approved on March 21, 2012
2. U.S. Nuclear Regulatory Commission, 10 CFR Part 71--PACKAGING AND TRANSPORTATION OF RADIOACTIVE MATERIAL

71.15	71.43(d)	71.63
-------	----------	-------
3. Robatel Technologies, LLC Application and Safety Analysis Report, Revision 3, for the Model RT-100 Cask Package, dated January 14, 2014.
4. USNRC Request for Additional Information, dated November 26, 2013.
5. ANSI N14.5-1997, "American National Standard for Radioactive Materials – Leakage Tests on Packages for Shipment," American National Standards Institute, Inc., 11 West 42nd Street, New York, NY, www.ansi.org.
6. NUREG/CR-6673, "Hydrogen Generation in TRU Waste Transportation Packages," Anderson, B., Sheaffer, M., & Fischer, L., Lawrence Livermore National Laboratory, Livermore, CA, May 2000.
7. EPRI NP-5977, "Radwaste Radiolytic Gas Generation Literature Review", Electric Power Research Institute, September 1988.
8. Resin and Filter Handbook – Primers and Product Information

This page is intentionally left blank.

2. STRUCTURAL EVALUATION

Chapter 2 describes the structural evaluation for the RT-100 under the RT Quality Assurance Program [Ref. 1] and summarizes the results to demonstrate compliance with the structural requirements of 10 CFR Part 71 [Ref. 2]. These evaluations follow nuclear industry standards [Refs. 3 – 20]. Chapter 1 General Information and Chapter 3 Thermal Evaluation provide input to the Chapter 2 Structural Evaluation; furthermore, these three chapters feed information to later Chapters of the SAR as demonstrated in Figure 2-1 on the following page.

The RT-100 structural performance under 10 CFR Part 71 [Ref. 2] Normal Conditions of Transport (NCT) and Hypothetical Accident Conditions (HAC) significantly affects the package ability to meet the thermal, containment, shielding and subcriticality requirements. Consequently, results from the structural evaluation are used in the thermal, containment, and shielding evaluations (Note: criticality issues are not applicable to the RT-100).

The foremost structural requirement of the RT-100 is to withstand NCT and HAC loadings with sufficient structural integrity to maintain shielded containment. Evaluations in the following sections demonstrate the RT-100 package design satisfies these requirements. Before presenting these detailed evaluations, a general description of the RT-100 cask design is provided and includes complete specifications for the containment boundary.

2.1 Description of Structural Design

Major design features that govern the structural performance of the RT-100 under NCT and HAC conditions are the impact limiters (upper and lower) and the cask body including the impact limiter attachment rings, bolting ring, primary and secondary lids, lifting pockets and tie-down arms. These features are sufficiently designed so that the structural response of the RT-100 exceeds all 10 CFR 71 [Ref. 2] requirements.

Appendix 1.4 (Attachment 1.4-2 thru 1.4-8) shows the general assembly drawings of the RT-100 Cask Package. The major components are identified and include the impact limiters and cask body. As subsequently discussed in Section 2.1.1.1, the package containment boundary is defined by the inner surfaces of the cask body, and the primary and secondary lids. Shielding is provided by the following features:

- Cask bottom and sidewall that contain 75 and 90 mm lead layers, respectively
- 210 mm thick stainless steel primary lid
- 170 mm (nominally) stainless steel secondary lid with embedded 60 mm thick lead layer

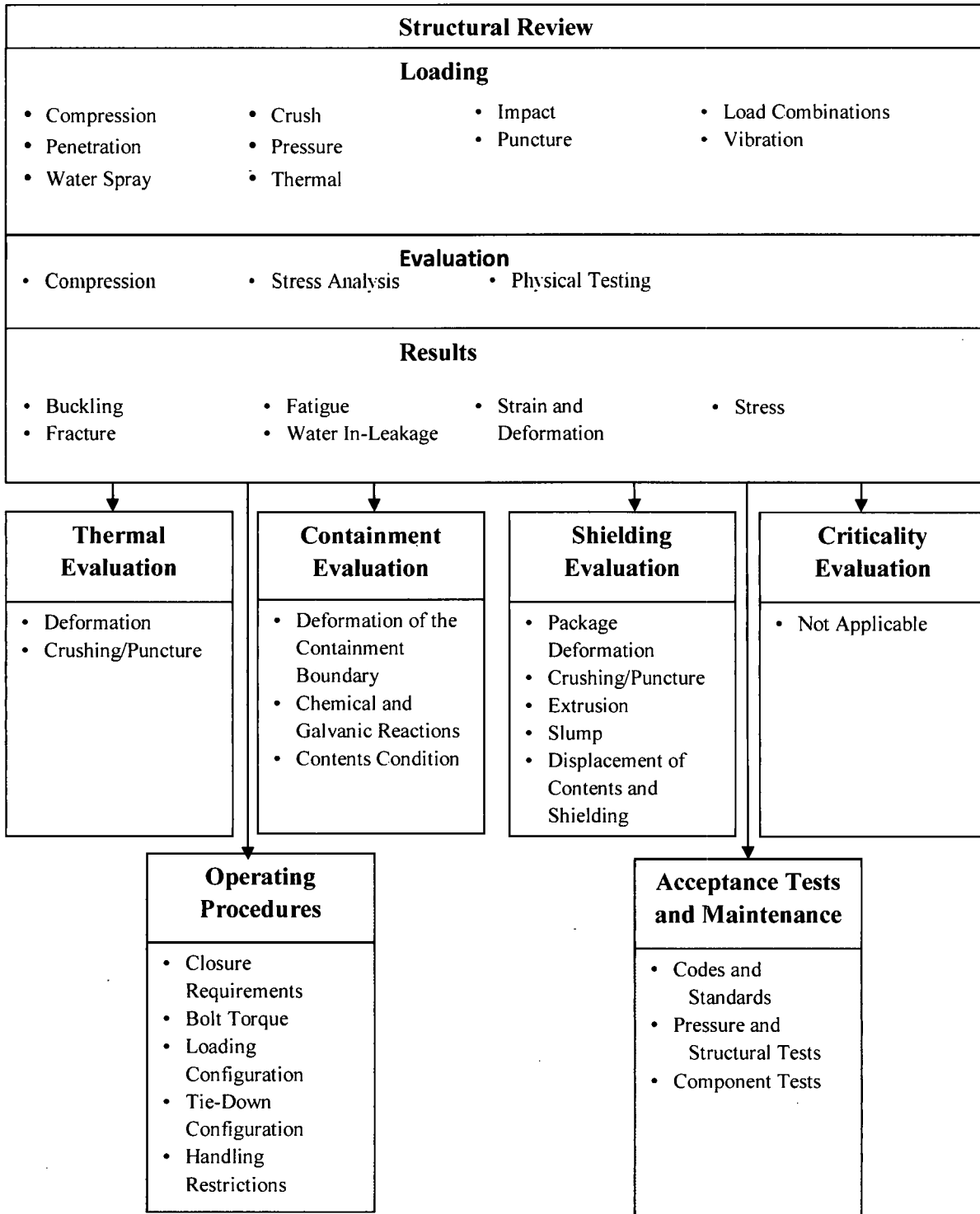


Figure 2-1 Information Flow for the Structural Review

2.1.1 Discussion

The RT-100 cask body is a cylindrical container with an outside diameter of 2060 mm and an overall height of 2321 mm (including lids). The sidewalls are nominally 165 mm thick, consist of a 90 mm thick lead layer encased by 30 mm thick internal and 35 mm thick external (ASTM A240, Type 304) stainless steel shells, have a 5 mm thick ceramic insulation layer, and have an outer 5 mm thick protective shell (ASTM A240, Type 304L stainless steel). The cask sidewall design varies from the above description in the following areas:

- Regions of the cask body encompassed by the impact limiters
- Impact limiter attachment rings
- Lifting pocket locations
- Tie-down arm attachment pads.

The specific sidewall configuration at each of these locations is further described and fully considered in all subsequent evaluations.

The bottom end of the cask body consists of a 75 mm thick lead layer encased by a 50 mm thick (ASTM A240, Type 304L) stainless steel bottom forging on top, and a 30 mm thick external stainless steel bottom plate underneath. The bottom forging is connected to the inner shell with full penetration welds. The bottom plate is connected to the outer shell with a full penetration weld.

The top end of the cask body consists of an upper forging (ASTM A240, Type 304L), and two lids (primary and secondary, both ASTM A240, Type 304L). The upper forging is connected to the inner shell with full penetration welds. The upper forging is connected to the cask outer shell with full penetration welds. Thirty-two (32) M48×2d threaded holes for securing the primary lid are equally spaced along the upper forging top surface. The upper forging top surface also provides a seating surface for the primary lid seals. The primary lid is nominally 210 mm thick.

The primary lid has thirty-two (32) clearance holes near its outer periphery for the M48 bolts (ASTM A354 Gr. BD or equivalent), which secure it to the bolting ring. These clearance holes are sufficiently counter-bored to preclude direct impact to the M48 bolts during a drop. Additionally, the primary lid has a central 737 mm diameter through-hole with a 2016 mm OD × 82 mm deep counter-bore. The counter-bore surface has eighteen (18) M36×2d equally spaced threaded holes for securing the secondary lid and also provides a seating surface for the secondary lid seals. The secondary lid is nominally 170 mm thick with an embedded 60 mm thick lead layer. The secondary lid has eighteen (18) clearance holes near its outer periphery for the M36 bolts (ASTM A354 Gr. BD or equivalent) used to attach it to the primary lid. The primary and secondary lids have one vent port each which allows for leakage monitoring.

The impact limiters are cylindrically-shaped components that surround the top and bottom ends of the cask as shown in Chapter 1, Figure 1.2.1-1. Each impact limiter has twelve (12) M36 studs. The impact limiters are attached to the cask with these studs that pass through clearance holes in the top and bottom impact limiter attachment rings, and accept M36 stainless steel nuts. The

impact limiters are comprised of segmented polyurethane foam blocks encased in relatively thin stainless steel outer coverings. The outer coverings are 4 mm thick except near the cask surface where the thickness is 10 mm. During NCT and HAC tests, the impact limiters are designed to protect the cask by absorbing energy and for providing thermal insulation.

2.1.1.1 Containment Boundary

As shown in Chapter 4, Figure 4.1.2-1 (“Illustration of Containment Boundary”), the containment boundary of the RT-100 cask is defined by the following specific features of the cask body and the primary and secondary lid.

- Bottom forging at the bottom end of the cask
- Inner shell that forms the wall of the cask with a full penetration weld
- Full penetration weld between the inner bottom forging and the inner shell bottom
- Top forging at the top of the cask
- Full penetration weld between the upper forging and inner shell top
- Primary lid and inner O-ring
- Vent port cover plate and inner O-ring
- Secondary lid and inner O-ring

2.1.2 Design Criteria

The RT-100 design satisfies the NCT requirements of 10 CFR 71.71 [Ref. 2], and HAC requirements of 10 CFR 71.73 [Ref. 2]. Furthermore, the design complies with “General Standards for All Packages” as specified in 10 CFR 71.43 [Ref. 2], and the “Lifting and Tie-Down Standards” specified in 10 CFR 71.45 [Ref. 2]. These criteria are demonstrated in Sections 2.5.1 and 2.5.2.

The design criteria used in the qualification of the RT-100 were selected based on guidance provided in Regulatory Guide 7.6 [Ref. 4]. Regulatory Guide 7.6 provides design criteria based on the ASME B&PV Code, Section III [Ref.7], and is intended for Type B packages used to transport irradiated fuel assemblies. Therefore, allowable stresses values for NCT Service Level A Limits and HAC Service Level D Limits are conservatively adopted from Regulatory Guide 7.6 [Ref. 4] for the qualification of the RT-100 cask body.

Allowable stresses are derived from the Stress Intensity values appropriate to ASME B&PV Code, Section III, Subsection ND [Ref. 7]. Stress Intensity values based on Subsection ND are presented in Table 2.2.1-1.

The load combinations used in performing the structural evaluations of the RT-100 cask are in accordance with Regulatory Guide 7.8 [Ref. 3]. Load combinations for the RT-100 cask body analysis are summarized in Table 2.1.2-1.

Table 2.1.2-1 Load Combinations for RT-100 Cask Body Analyses

LOAD		NORMAL		ACCIDENT			
Reg. Guide 7.8 Load Combinations		A		D			
		1	2	1	2	3	4
Dead Weight	With maximum contents	X	X	X	X	X	X
Thermal Stresses	Hot	X		X		X	
	Cold		X		X		X
Internal Pressure	Normal	X	X	X	X		
	Accident (fire)					X	X
Drop/Impact	0.3 Meters	X	X				
Drop/Impact	9 Meters			X	X		

2.1.2.1 Cask Body Criteria (except Bolts and O-Rings)

The criteria for the cask shells and lids are developed per Regulatory Guide 7.6 Regulatory Position 2 [Ref. 4]. (The tie-down arms are also fabricated from stainless steel but their criteria are developed separately in Section 2.5.2). Table 2.1.2-2 provides a summary of the allowable stress limits defined in Regulatory Guide 7.6.

Table 2.1.2-2 Structural Design Criteria for RT-100

Reg. Guide 7.6 Service Level	Stress Criteria	Notes
Normal conditions: Service Level A	$P_m \leq S_m$	(1)(2)
	$P_m + P_b \leq 1.5 S_m$	(2)
	$P_m + P_b + Q \leq 3 S_m$	(3)
Accident conditions: Service Level D	$P_m \leq 2.4 S_m$ or $0.7 S_u$ (whichever is less)	(4)
	$P_m + P_b \leq 3.6 S_m$ or $1.0 S_u$ (whichever is less)	(4)
	Total Stress $< 2 S_u$	(5)

1. Regulatory Guide 7.6 [Ref. 4], Regulatory Position 1
2. Regulatory Guide 7.6, Regulatory Position 2
3. Regulatory Guide 7.6, Regulatory Position 4
4. Regulatory Guide 7.6, Regulatory Position 6
5. Regulatory Guide 7.6, Regulatory Position 7

2.1.2.2 Bolts

The allowable stresses under NCT (per NUREG/CR-6007 [Ref. 10]) are:

$$f_t < S_m$$

$$f_t^{\max} < 3S_m \text{ if } S_u < 689 \text{ MPa}$$

$$< 2.7S_m \text{ if } S_u > 689 \text{ MPa}$$

$$P_m + P_b + \text{residual torsion} < S_m$$

where

$$f_t = \text{average tensile stress}$$

f_t^{\max} = maximum tensile stress under combined tension and bending, and all other terms are as previously defined.

The allowable stresses under NCT (per NUREG/CR-6007 [Ref. 10]) are:

$$\begin{aligned} f_t &< F_{tb} \\ f_v &< F_{vb} \\ \left(\frac{f_t}{F_{tb}}\right)^2 + \left(\frac{f_v}{F_{vb}}\right)^2 &< 1.0 \end{aligned}$$

where

f_v = average shear stress
 F_{tb} = allowable average tensile stress
= Min (0.7Su, Sy) at temperature
 F_{vb} = allowable average shear stress
= Min (0.42Su, 0.6Sy) at temperature and all other terms are as previously defined.

2.1.2.3 Lead

The structural integrity of the RT-100 cask does not depend on lead strength and thus, no lead strength criteria are specified. Mechanical and thermal properties which are important to the RT-100 cask structural performance are discussed in Sections 2.2, 2.14, and 3.2

2.1.2.4 Foam

Criteria of the polyurethane foam used in the impact limiters are provided in Appendix 2.12 Impact Limiter Evaluation.

2.1.3 Weights and Centers of Gravity

The nominal RT-100 weights and centers of gravity are shown in Table 2.1.3-1. Refer to RT100 PE 1001-1 Rev. H – Robatel Transport Package RT-100 General Assembly Sheet 1/2 (Chapter 1, Appendix 1.4, Attachment 1.4-2) for identification of assemblies and centers of gravity data. These weights are utilized in the structural evaluation presented in this chapter.

With the exception of the impact limiter, all analyses are performed with no less than a minimum gross weight of 41,500 kg. The impact limiter calculation is performed using 41,000 kg. The reason for this is that the max crush is obtained by using the minimum density of the foam. The calculation package RTL-001-CALC-ST-0401 Rev. 6 [Ref. 40] calculates the maximum g-load using both 41,500 kg and 41,000 kg. It is shown that max g-load is obtained using a gross weight of 41,000 kg. Thus, the impact limiter calculation is performed using a gross weight of 41,000 kg.

Table 2.1.3-1 Assembly Weights and Center of Gravity Locations

Assembly ³	Nominal Weight (kg)	Center of Gravity ³ (mm)
Lower Impact Limiter	2,450	516
Cask Body	24,500	1,446
Primary Lid w/ bolts	3,670	2,716
Secondary Lid w/ bolts	870	2,737
Upper Impact Limiter	2,550	2,812
Total Assembly Empty	34,040	1,650
Payload	6,805 ¹	1,434 min. ³ 1,826 max. ³
Total Assembly with payload	40,845 ²	1,620 min. ³ 1,676 max. ³

Notes: 1. Maximum.

2. A minimum weight of 41,000 kg was used in all structural evaluations.

3. Value determined using payload center of gravity at 10% of cask interior height below or above the cask interior geometric centerline.

As shown in Table 2.1.3-1, the center of gravity of the empty RT-100 cask is approximately 1650 mm above the bottom of the cask. This location is just 20 mm lower than the 1630 mm elevation of the center of the inner cavity. Further, the maximum payload weight is less than 17% (= 6,805/40,845 × 100%) of the loaded cask weight. Thus, payload weight and/or center of gravity variations will not result in large changes to the loaded RT-100 cask center of gravity. Indeed, locating the payload center of gravity within 10% of the cavity internal height above or below the cavity centerline elevation moves the loaded RT-100 cask center of gravity by no more than +/- 28 mm. Such minor variations are insignificant during either NCT or HAC.

2.1.4 Identification of Codes and Standards for Package Design

Since the package is used to transport contents with 3,000 A₂ (as defined in 10 CFR 71.4 [Ref. 2]), the RT-100 cask is a Type B Category II package per Regulatory Guide 7.11 [Ref. 5]. The codes and standards used in the design of the RT-100 cask are selected based on guidance provided in Regulatory Guide 7.6 [Ref. 4 and NUREG/CR-3854 [Ref. 6] for packages transporting Category II contents.

Per NUREG/CR-3854 [Ref. 6], the package containment system is fabricated in accordance with the ASME Code, Section III, Subsection ND [Ref. 7], and the tie-downs are fabricated in accordance with Subsection NF [Ref. 8]. These codes are applicable to the RT-100 cask design as they were developed for components of similar material as well as, for similar loading operations and potential package failures.

Several regulatory guides and NUREGs are used to design and evaluate the RT-100 package. Regulatory Guide 7.8 [Ref. 3] is used in identifying the load combinations to be used in package design evaluation. Regulatory Guide 7.6 [Ref. 4] is used to determine the design criteria. NUREG/CR-4554 [Ref. 9] is used in evaluating buckling of the containment vessel.

NUREG/CR-6007 [Ref. 10] is followed for the bolt evaluations.

2.2 Materials

Material properties used in the RT-100 cask structural analyses are shown in Tables 2.2.1-1, 2.2.1-2, and 2.2.1-3. Material properties for the structural analyses of the polyurethane foam used in the impact limiter evaluations are provided in Appendix 2.12. Properties of both cask materials and foam used in the thermal analyses are provided in Section 3.2.1.

2.2.1 Material Properties and Specifications

Structural components of the cask body are specified to be ASME A240 Type 304/304L steel, with the exception of the tie-down straps, which are ASME A240 UNS No. S31803 (Type 318) stainless steel. The primary and secondary lids are ASME A240 Type 304/304L steel, and the M36 and M48 bolts used to secure the lids are fabricated to meet the critical characteristics given in Chapter 8. These materials meet the requirements of ASME Section III, Subsection ND [Ref. 7]. Strength properties for these materials are presented in Table 2.2.1-1 using material information taken from ASME Section II-D [Ref. 31]. Table 2.2.1-2 provides density and Poisson's ratio values also from ASME Section II-D.

The shielding is specified to be ASTM B-29 lead. The lead properties are provided in NUREG/CR-0481 [Ref. 11] and are presented in Table 2.2.1-2.

EPDM (material designation per ASTM D1418) is used for all O-rings as part of the containment boundary. They serve as one of the boundaries for the cask. These O-rings have a usable temperature range going from -50°C up to 150°C; this temperature range meets or exceeds both NCT and HAC requirements.

RT verifies that all the materials of structural components have sufficient fracture toughness to preclude brittle fracture under NCT and HAC. Regulatory Guides 7.11 [Ref. 5] and 7.12 [Ref. 16] are used to provide criteria for fracture toughness. RT shall procure all materials under the RT Quality Assurance Program [Ref. 1] with the specifications for each material. Regulatory Guides 7.11 and 7.12 do not apply to the RT-100; use of Stainless Steel ASTM A-240 type 304, ASTM A-240 type 304L, and ASTM A-240 UNS S31803 precludes brittle fracture under both NCT and HAC.

RT verifies that all material properties are appropriate for the load conditions specified in Regulatory Guide 7.6 [Ref. 4] and temperatures at which allowable stress limits are defined are consistent with minimum and maximum service temperatures. Allowable stresses based on Regulatory Guide 7.6 [Ref. 4] at the bounding NCT temperature of 100°C are provided in Table 2.2.1-3. Allowable stress intensities at other temperatures considered to be the bounding condition for a specific case are defined as needed in the section where that analysis is presented.

RT verifies that all the force-deformation properties for impact limiters are based on appropriate test conditions and temperature. Test parameters for qualifying the foam material are identified in Chapter 2, Appendix 2.13.

Table 2.2.1-1 Cask Temperature-Dependent Material Properties

Material	Temperature (°C)	Yield Strength (S _y)	Tensile Strength (S _u)	Design Stress Intensity (S _m)	Young's Modulus (GPa)	Coefficient of Thermal Expansion (10 ⁻⁶ /°C)
		(MPa)				
ASME SA-240 Type 304/304L (Dual Certified)	-30	207	517	138	198	—
	20	207	517	138	195	15.3
	65	184	496	138	192	15.8
	100	170	485	138	189	16.2
	150	154	456	138	186	16.6
	200	144	442	129	183	17.0
	250	135	437	122	179	17.4
ASME SA-240 Type 304L	-30	172	483	115	198	—
	20	172	483	115	195	15.3
	65	157	463	115	192	15.8
	100	146	452	115	189	16.2
	150	132	421	115	186	16.6
	200	121	406	110	183	17.0
	250	114	398	103	179	17.4
ASME SA-240 Type 316L	-30	172	483	115	198	—
	20	172	483	115	195	15.3
	65	157	471	106	192	15.8
	100	145	467	96.3	189	16.2
	150	131	441	87.4	186	16.6
	200	121	429	81.2	183	17.0
	250	114	426	76.0	179	17.4
ASME SA-240 UNS No. S31803	-30	448	621	207 = S _y /3	211	—
	20	448	621	207	205	15.3
	65	418	620	207	200	15.8
	100	395	619	206	194	16.2
	150	370	598	199	190	16.6
	200	354	577	193	186	17.0
	250	344	564	188	183	17.4
ASME SA-354 Grade BD (Bolting material)	-30	896	1030	343 = S _y /3	199	—
	20	896	1030	343	202	11.5
	65	855	1030	343	199	11.8
	100	816	1030	343	197	12.1
	150	792	1030	343	194	12.4
	200	768	1030	343	191	12.7
	250	737	1030	343	188	13.0
ASME SA-479, ER308	-30 to 40	205	515	—	—	—
ASTM B-29 Lead	-29	—	—	—	16.75	28.2
	20	—	—	—	15.67	28.9
	50	—	—	—	14.94	29.4
	100	—	—	—	13.73	30.2
	150	—	—	—	12.74	31.2
	200	—	—	—	11.80	32.6
	250	—	—	—	10.70	34.1

**Table 2.2.1-2 Cask Temperature-Independent Material Properties
ASME [Ref. 31]**

Material	Density (kg/m ³)	Poisson's Ratio
ASME SA-240 Type 304/304L (Dual Certified)	8030	0.31
ASME SA-240 UNS No. S31803	8030	0.31
ASME SA-354 Grade BD (Bolting material)	7750	0.30
ASTM B-29 Lead	11300	0.40

Table 2.2.1-3 Allowable Stresses for Cask Body Materials

Design Criteria		Material				
		ASME SA-240 Type 304/304L (Dual Certified)	ASME SA-240 Type 304L	ASME SA-240 Type 316L	ASME SA-240 UNS No. S31803	ASME SA-354 Grade BD
		MPa	MPa	MPa	MPa	MPa
Yield Stress, S_y		170	146	145	395	816
Tensile Strength, S_u		485	452	467	619	1030
Design Stress Intensity, S_m		138	115	96.3	206	299
Normal Conditions	P_m	138	115	96.3	206	299
	$P_m + P_b$	207	173	144	309	449
	$P_m + P_b + Q$	414	345	289	618	897
Hypothetical Accident Conditions	P_m	331	276	231	433	718
	$P_m + P_b$	485	414	347	619	1030
	Total Stress	970	904	934	1238	2060

2.2.2 Chemical, Galvanic, or Other Reactions

The materials used in the fabrication and operation of the RT-100, including coatings, lubricants, and cleaning agents, are evaluated to determine whether chemical, galvanic, or other reactions among the materials, contents, and environments can occur. All phases of operation, loading, unloading, handling, storage, and transportation, are considered (in conjunction with the procedures described in Chapter 7) for the environments that may be encountered under normal, off-normal, or accident conditions. Based on the evaluation, there are no potential reactions that could adversely affect the overall integrity of the cask or the structural integrity and retrievability of the contents from the cask. The evaluation conforms to the guidelines of NRC Bulletin 96-04, "Chemical, Galvanic, or Other Reactions in spent Fuel Storage and Transportation Casks," dated July 5, 1996 [Ref. 52], and demonstrates that the RT-100 cask meets the requirements of 10 CFR 71.43(d) [Ref. 2].

2.2.2.1 Component Material Categories

The component materials evaluated are categorized based on similarity of physical and chemical properties and/or on similarity of component functions. The categories of materials that are considered are as follows:

- Stainless/nickel alloy steels
- Nonferrous metals
- Shielding materials
- Criticality control materials
- Energy absorbing materials
- Cellular foams and insulations
- Lubricants and greases
- O-rings
- Secondary Containers and Shoring
- Filters

These categories are evaluated based on the environment to which they could be exposed during operation or use of the RT-100.

The RT-100 component materials are not reactive among themselves, with the cask's contents, nor with the cask's operating environments during any phase of normal, or accident condition loading, unloading, handling, storage or transportation operations. No reactions occur, and no gases or other corrosion byproducts are generated.

2.2.2.1.1 Stainless/Nickel Alloy Steels

No reaction of the cask components (stainless or nickel alloy) is expected in any environment. During the fabrication process of the RT-100 ridges and crevices on the external surfaces are reduced through the finishing process and the external surface is passivated to prevent corrosion.

Galvanic corrosion between the stainless steels and nickel alloy steels does not occur due to the lack of effective electrochemical potential difference between these metals. No coatings are applied to the stainless steel or nickel alloy steels.

There is no potential for a reaction between stainless steel and any silicone products, fluorocarbon elastomers, dry film lubricants, blended polytetrafluoroethylene (PTFE), or ethylene glycol.

Based on the foregoing discussion, there are no potential reactions expected with the stainless steel cask components.

2.2.2.1.2 Nonferrous Metals

There are no nonferrous metals used in the RT-100. Therefore, no electrochemical driving potential exists.

2.2.2.1.3 Shielding Materials

The primary shielding materials used in the RT-100 is lead which is completely enclosed and sealed in stainless steel. Therefore, there are no potential reactions associated with the cask shielding materials.

2.2.2.1.4 Criticality Control Material

The RT-100 does not contain materials for criticality control. Therefore, no potential reactions associated with these materials exist.

2.2.2.1.5 Energy Absorbing Material

The RT-100 utilizes polyurethane foam for energy absorption in the impact limiters. The foam is completely enclosed (sealed) in stainless steel and there are no potential reactions between the foam and the stainless steel shells. The foam is cured, cut, and machined prior to installation. During fabrication the machined foam blocks are inserted into the impact limiter stainless steel shell. During the welding process backing strips, high temperature heat tape, and rock wool are used to protect the foam. Therefore, no potential reactions associated with the energy absorbing material exists.

2.2.2.1.6 Cellular Foam and Insulation

The RT-100 does not utilize cellular foam or insulation. Therefore, no potential reactions associated with the cellular foam or insulation exists.

2.2.2.1.7 Lubricant and Grease

The dry film lubricants used with the RT-100 meet the performance and general compositional requirements of the nuclear power industry. These lubricants are used primarily on threaded/mechanical connection surfaces. These lubricants are insoluble in most solutions. There are no potential reactions associated with these lubricants or grease.

2.2.2.1.8 O-Rings

The RT-100 utilizes seals formed from EPDM. EPDM is a synthetic rubber elastomer. Elastomer O-rings are used for transport cask applications because of their excellent short-term sealing capabilities, ease of handling, and more economical cost. Seal and gasket materials have stable, non-reactive compositions. There are no potential reactions associated with the RT-100 seal materials.

2.2.2.1.9 Secondary Containers and Shoring

Secondary containers and shoring features may be constructed of carbon steel, stainless steel, wood, or a thermoplastic such as polyethylene or polypropylene.

2.2.2.1.10 Filters

Filters shipped for disposal may be constructed from stainless steel or thermoplastic such as polyethylene or polypropylene.

2.2.2.2 General Effects of Identified Reactions

No significant potential galvanic or other reactions have been identified for the RT-100. Therefore, no adverse conditions can result during any phase of cask operations for NCT or HAC.

2.2.2.3 Adequacy of the Cask Operating Procedures

Based on the results of this evaluation, it is concluded that the RT-100 operating controls and procedures presented in Chapter 7 are adequate to minimize occurrence of hazardous conditions.

2.2.2.4 Effects of Reaction Products

No significant potential chemical, galvanic, or other reactions are identified for the RT-100. Therefore, the overall integrity of the cask and the structural integrity and retrievability of the contents are not adversely affected for any cask operations throughout the design basis life of the cask. Based on the evaluation, no significant reactions are identified and thus, there is no change in cask properties, no binding of mechanical surface, and no degradation of any safety components either directly or indirectly.

2.2.3 Effects of Radiation on Materials

Gamma radiation has no significant effect on metal and therefore, the radiation produced by the contained radioactivity does not cause any measurable damage to the cask metallic components (stainless steel, carbon steel and lead).

For seals, the absorbed dose in a year is expected to be below 350 rad which is significantly below the polymer damage threshold of 1×10^5 rad. Additional support information about EPDM resistance to radiation up to 5×10^8 rads while retaining reasonable flexibility and strength, hardness and very good compression set resistance is provided by an IEEE paper [Ref. 54].

For the ceramic thermal shield, the absorbed dose is expected to be below 350 rad. However, ceramic materials are insensitive to gamma radiation damage and thus, the ceramic thermal shield is expected to be unaffected by radiation.

2.3 Fabrication and Examination

The following subsections provide a summary description of fabrication and examination of the RT-100. A more detailed description is provided in subsequent sections of the SAR.

2.3.1 Fabrication

The RT-100 packaging is designed as a category II container, as mentioned in Section 2.1.4. Fabrication and procurement of the containment components is based on ASME B&PV code, section III, Subsection ND [Ref. 7]. The other components (non-containment) are fabricated based on ASME B&PV code, Section III, subsection NF [Ref.8]. See Sections 2.1.2 and 2.1.4 for additional information.

2.3.2 Examination

Examination of the RT-100 during and after fabrication is conducted in accordance with the requirements of the ASME B&PV code, Section III, Subsection ND-5000 [Ref. 7]. The non-containment components examination is conducted in accordance with the requirements of ASME B&PV Code, Section III, Subsection ND-5000 or NF5000 [Ref. 8]. See Chapter 8, Sections 8.1 and 8.2 for additional information.

2.4 General Requirements for All Packages

The RT-100 meets or exceeds all the requirements in 10 CFR 71.43 [Ref 2]. Also, the RT-100 meets the general package requirements Regulatory Guide 7.9 [Ref. 49] as listed below:

- Smallest overall dimension is greater than 10 cm (4 in).
- Outside of the cask incorporates a feature, such as a seal, that is not readily breakable and that, while intact, would be evidence that the package has not been opened by unauthorized persons.
- Cask includes a containment system closed by a positive fastening device that cannot be opened unintentionally or by a pressure that may arise within the package.

The following sections describe compliance of the RT-100 with these requirements.

2.4.1 Minimum Package Size

This section is not applicable since the RT-100 has dimensions larger than 10 cm (4 inches). The smallest overall dimension of the cask body is the outer diameter, which is over 200 cm.

2.4.2 Tamper-Indicating Feature

The RT-100 upper impact limiter covers the upper end of the cask including the primary and secondary lids, which prevents access to the cask lids. Therefore, tamper-indicating devices are attached to the impact limiter aligning pin. Impact limiters are installed on the cask body following the lid closure operation. Once the impact limiters are installed on the cask body, the attachment nuts are threaded on the attaching studs and hand-tightened (drop testing has shown that torquing of the attachment bolts is not necessary). A tamper-indicating seal is installed on the aligning pin of the upper impact limiter to ensure that removal of the impact limiter by unauthorized individuals can be detected.

2.4.3 Positive Closure

The RT-100 design includes a containment system that is bounded by the inner shell, primary lid, secondary lid, and vent port cover plate. Each lid and the cover plate are secured to the cask body by multiple bolts. These bolts are tightened during the loading process to a set torque value that cannot be inadvertently loosened. Additionally, the stress analysis of the bolts presented in Section 2.6.7 demonstrates that the bolts can maintain positive closure during operation.

2.5 Lifting and Tie-Down Standards for All Packages

The RT-100 lifting and tie-down components are evaluated structurally in the following sections. The lifting and tie-down requirements are as specified in 10 CFR 71.45 [Ref. 2].

2.5.1 Lifting Devices

The primary lifting device for the RT-100 is the set of two lifting pockets that are welded to the outer shell of the cask. After removal of the impact limiters, the lifting pockets are designed to allow the loaded cask to be lifted using a lifting yoke. The primary and secondary lids and the upper/lower impact limiters are fitted with threaded bolt holes; these bolt holes provide for attachment of lifting rings that are used in lifting each component.

2.5.1.1 Lifting Design Criteria

Lifting attachments that are a structural part of the RT-100 cask are designed with a minimum safety factor of three against yielding when used to lift the package. The lifting devices are also designed so that any failure of the lifting device under excessive load would not impair the ability of the RT-100 to meet other requirements of 10 CFR 71.45 [Ref. 2]. The design weights used in the lifting evaluation are as follows:

- Fully loaded RT-100 with maximum contents and the lower impact limiter is 41,500 kg
- Primary lid with secondary lid in place is 4,505 kg
- Secondary lid is 857 kg
- Upper impact limiter is 2,541 kg
- Lower impact limiter is 2,448 kg

2.5.1.2 Lifting Device Descriptions

In this section, the following RT-100 components are evaluated for lifting:

- Lifting Pockets
- Primary Lid
- Secondary Lid
- Lower Impact Limiter
- Upper Impact Limiter

The lifting pockets are utilized to lift the assembled cask; the bounding configuration is the cask loaded with the maximum payload weight and the lower impact limiter attached. Additionally, the primary and secondary lids and the upper and lower impact limiters are evaluated for lifts using removable lifting rings.

2.5.1.3 Lifting Device Evaluations

In the following sections, each device used for lifting is evaluated for stress. The details of each evaluation are presented including the worst-case stress results and safety factors. Additional details supporting these calculations are provided in Calculation Package RTL-001-CALC-ST-0201, Rev. 5 [Ref. 33].

2.5.1.3.1 Cask Body Lifting Evaluation

The cask is lifted by using the two lifting pockets that are welded to the cask exterior sidewall on opposite sides of the cask body. The assembled and loaded cask is lifted with the upper impact limiter removed to accommodate the connection between the lift yoke and the lifting pockets. The cask lifting load is the total weight of the fully assembled cask, including the payload, but with the upper impact limiter load removed. The upper impact limiter is lifted separately. The lifting pockets are evaluated for the tear-out stress, bearing stress, and weld stress due to the required lifting activities. The lifting pockets are also evaluated for pure shear stress as described in ASME Section III Subsection NF [Ref. 8].

A Dynamic Load Factor (DLF) of 1.35 is applied to the lift forces that act on the cask components during movement. ANSI N14.6 [Ref. 56] requires additional safety features for handling of critical loads. One option identified is to apply increased stress design factors on the load-bearing members; however, the standard does not recommend a value for the stress design factor. The German Nuclear Safety Standards Commission provides standard KTA-3905 for lifting loads in nuclear power plants. [Ref. 57] This standard requires a live load factor of 1.35 for dead weight lifts. This calculation uses the KTA-3905 live load factor value as the dynamic load factor. The dynamic load factor is applied to all load bearing members.

2.5.1.3.1.1 Lifting Pocket Design Features

The lifting pockets are manufactured from blocks of ASTM A240 Dual Certified Type 304/304L stainless steel that are welded to opposite sides of the outer shell of the cask body, also manufactured from ASTM A240 Type 304/304L stainless steel. The weld material is SA-279 Grade ER308 UNS S30880. The welds extend down both sides and along the bottom of the lifting pockets, forming a “U” shape. The lifting pockets have a cutout that allows the lifting yoke to pass downward and through the lifting pocket. The connection is completed with a rectangular shaped retaining pin that is inserted through cutouts in both the lifting pocket and the lifting yoke. Figure 2.5.1-1 provides the configuration and dimensions of the lifting pockets and shows the cutouts for the lifting yoke and retaining pin. The design loads and material strengths of the lifting pocket base metal and weld materials are as follows:

Total Lifted Cask Weight	$W = 41,500 - 2,541 \text{ kg} = 38,959 \rightarrow \text{use } 39,500 \text{ kg}$
Dynamic Load Factor	$DLF = 1.35$
Number of Lifting Pockets	$n_p = 2$
Gravitational Acceleration	$g = 9.81 \text{ m/s}^2$
Vertical Shear Load	$PV = \frac{W \times DLF \times g}{n_p} = \frac{39500 \times 1.35 \times 9.81}{2} \times \frac{1 \text{ kN}}{1000 \text{ N}}$ $= 261.6 \text{ kN pocket}$
Lifting Pocket Yield Strength	$S_y = 199 \text{ MPa}$
Lifting Pocket Tensile Strength	$S_u = 511 \text{ MPa}$
Factor of Safety on Yield Strength	$F_{sy} = 3$
Factor of Safety on Tensile Strength	$F_{su} = 5$

The critical dimensions for the weld evaluation are as follows. These dimensions ignore the dimensions of the welds.

Lifting Pocket Length	$L_p = 191 \text{ mm} = 0.191 \text{ m}$
Lifting Pocket Edge Distance	$d_p = 55 \text{ mm} = 0.055 \text{ m}$
Lifting Pocket Eye Length	$L_e = 84 \text{ mm} = 0.084 \text{ m}$
Retaining Pin Dimensions	$W_p = 60 \text{ mm} = 0.060 \text{ m}$ $H_p = 80 \text{ mm} = 0.080 \text{ m}$

The “eye” refers to the rectangular cutout in the lifting pocket for the retaining pin and the eye length is the vertical height of the eye. The lifting pocket length is the distance from the horizontal centerline of the retaining pin eye to the top of the lifting pocket. The lifting pocket edge distance refers to the vertical height of the recessed cap on the lifting pocket.

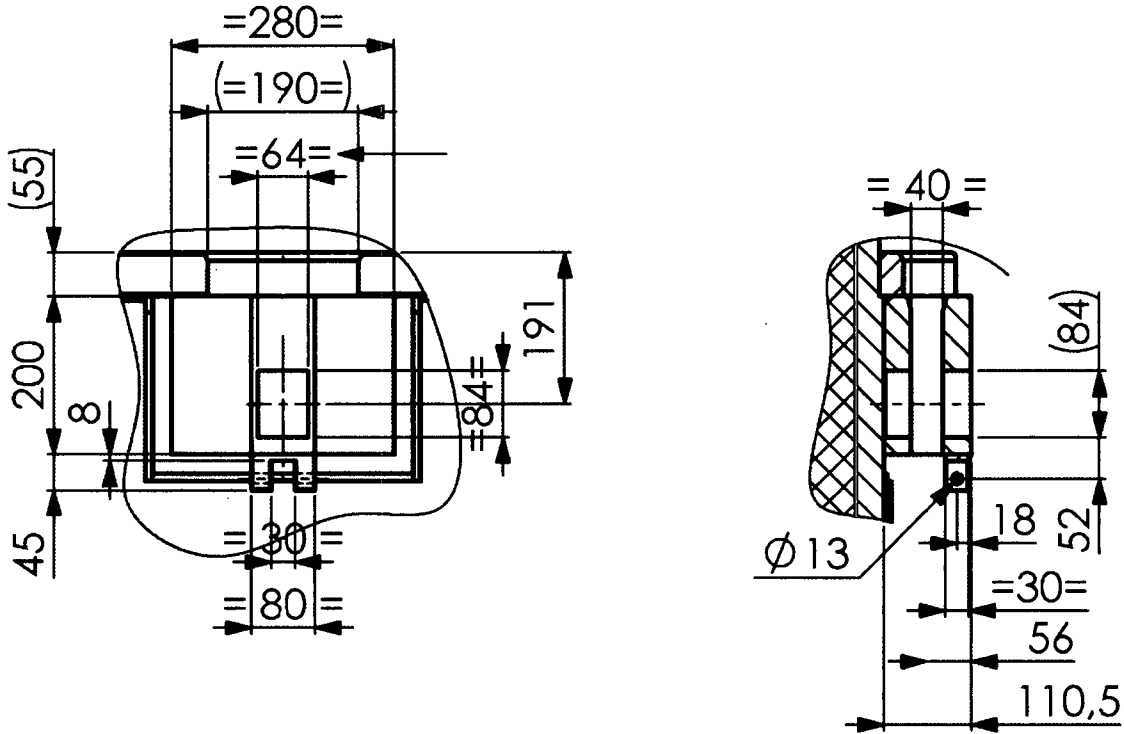


Figure 2.5.1-1 RT-100 Lifting Pocket Dimensions

2.5.1.3.1.2 Lifting Pocket Tear-out Stresses

The lifting pockets are used for lifting the assembled and loaded cask body, without the upper impact limiter, and are rendered inoperable by removing the lifting attachment from the lifting pocket during transport. The lifting pockets are considered to be a structural part of the package with respect to lifting and shall be designed for the factor of safety against yielding and ultimate stresses. A lifting yoke is used to lift the assembled cask body and to ensure that the lifting straps or cables remain parallel to the body of the cask during lifting operations. The tear-out stresses for the lifting pocket retaining pin hole are as follows:

$$\text{Lifting Eye Tear-out distance } d_{to} = L_p - d_p - \frac{L_e}{2} = 0.191 - 0.055 - \frac{0.084}{2} = 0.094 \text{ m}$$

$$\text{Lifting Pocket Thickness } t_p = 110.5 - 40 = 70.5 \text{ mm} = 0.071 \text{ m}$$

$$\text{Lifting eye Tear-out Area } A_{to} = d_{to} \times t_p = 0.094 \times 0.071 = 0.00663 \text{ m}^2$$

The tear-out stresses for the lifting pocket are calculated:

$$\text{Nominal Tear-out Stress } \tau_{to} = \frac{P_V}{2 \times A_{to}} = \frac{261.6}{2 \times 0.00663} = 19734 \frac{kN}{m^2} = 19.7 \text{ MPa}$$

Allowable Yield Stress

$$\sigma_y = 0.6 \times S_{yL} = 119 \text{ MPa}$$

Allowable Ultimate Stress

$$\sigma_u = 0.6 \times S_{uL} = 307 \text{ MPa}$$

Factor of Safety on Yield Strength

$$FS = \frac{\sigma_y}{\tau_{to}} = \frac{119}{19.7} = 6.05 > 3.0$$

Factor of Safety on Tensile Strength

$$FS = \frac{\sigma_u}{\tau_{to}} = \frac{307}{19.7} = 15.54 > 5.0$$

2.5.1.3.1.3 Lifting Pocket Bearing Stresses

The bearing stress in the lifting pocket from the lift yoke retaining pin is calculated as follows. The acceptance criterion for the pocket bearing stress are the yield strength of the material.

Lifting Pocket Bearing Area

$$A_b = W_p \times t_p = 0.06 \times 0.071 = 0.00423 \text{ m}^2$$

Nominal Bearing Stress

$$\tau_b = \frac{P_V}{A_b} = \frac{261.6}{0.00423} = 61834 \frac{kN}{m^2} = 61.8 \text{ MPa}$$

Factor of Safety on Yield Strength

$$FS = \frac{S_y}{\tau_b} = \frac{199}{61.8} = 3.22 > 1.0$$

2.5.1.3.1.4 Lifting Pocket Weld Stresses

The stresses in the welds (attaching the lifting pocket to the cask outer shell) are found by applying the shear load from the lifting pockets to the weld around the perimeter of the plate. Based on the safety factors for the lifting pocket, yielding controls the weld evaluation. The stresses and allowables are determined as described in "Design of Welded Structures" [Ref. 25] and Calculation Package RTL-001-CALC-ST-0201, Rev. 5 [Ref. 33]

Conservatively, the upper section of the pocket is considered to take the full lifting load. The lifting pocket is seal welded to and bears upon the cask bolting ring. The lifting load is therefore shared between the lifting pocket weld and the bolting ring. Conservatively, the full load is considered to be taken by the lifting pocket weld only.

The stresses in the welds attaching the lifting pocket to the cask outer shell are found by applying the shear load from the lifting pockets to the weld around the perimeter of the lifting pocket. Based on the safety factors for the lifting pocket, yielding controls the weld evaluation. The welds on the lifting pockets are evaluated as a line force on the weld as described in “Design of Welded Structures” [Ref. 25] (Refer to pages 7.4-6 and 7, Tables 4 and 5). Since the cask is lifted using a yoke that maintains the force in a vertical direction, there are no bending or twisting loads, so the section Modulus and the polar moment of inertia are zero and can be ignored. The weld geometry is provided in Figure 2.5.1-2

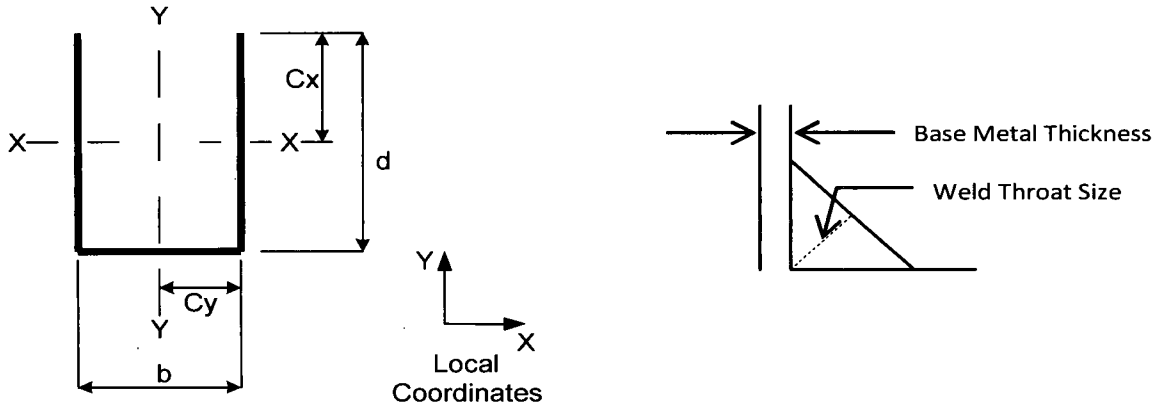


Figure 2.5.1-2 Weld Geometry

Weld properties are as follows:

Length of horizontal weld	$b = 0.28 \text{ m}$
Length of vertical weld	$d = 0.20 \text{ m}$
Weld Length	$A_w = b + 2d = 0.68 \text{ m}$
Weld Throat Size	$T_w = 0.015 \text{ m}$
Base Metal (Cask Wall) Thickness	$T_c = 0.035 \text{ m}$

The force acting on the weld is:

$$f_{vy} = \frac{F_y}{A_w} = \frac{261.6}{0.68} = 384.71 \frac{\text{kN}}{\text{m}}$$

Yield Weld Allowable

$$\tau_{wya} = 0.6 \times S_{wy} \times T_w \times 1000$$

$$= 0.6 \times 205 \times 0.015 \times 1000 = 1845 \text{ kN/m}$$

Tensile Weld Allowable

$$\tau_{wya} = 0.6 \times S_{wu} \times T_w \times 1000$$

$$= 0.6 \times 515 \times 0.015 \times 1000 = 4635 \text{ kN/m}$$

Yield Cask Allowable

$$\tau_{cya} = \frac{0.6 \times S_{cy} \times T_c \times 1000}{0.7071} = \frac{0.6 \times 199 \times 0.035 \times 1000}{0.7071}$$

$$= 5910 \text{ kN/m}$$

Tensile Cask Allowable

$$\tau_{cua} = \frac{0.6 \times S_{cu} \times T_c \times 1000}{0.7071} = \frac{0.6 \times 511 \times 0.036 \times 1000}{0.7071}$$

$$= 15176 \text{ kN/m}$$

Weld Yield FS

$$= \frac{\tau_{wya}}{f_w} = \frac{1845}{384.71} = 4.80 > 3.0$$

Weld Tensile FS

$$= \frac{\tau_{wua}}{f_w} = \frac{4635}{384.71} = 12.05 > 5.0$$

Cask Yield FS

$$= \frac{\tau_{cya}}{f_w} = \frac{5910}{384.71} = 15.36 > 3.0$$

Cask Ultimate FS

$$= \frac{\tau_{cua}}{f_w} = \frac{15176}{384.71} = 39.45 > 5.0$$

2.5.1.3.1.5 Lifting Pocket Average Pure Shear

The lifting pocket average pure shear is evaluated in accordance with ASME Section III Subsection NF [Ref. 8] Subparagraph 3223.2 and is limited to 0.6 S_m . The factor of safety is determined by comparing the pure shear to the lifting pocket tear out stress. For the lifting pocket weld evaluation, the average pure shear is evaluated as follows.

Cask Membrane Strength

$$S_m = 115 \text{ MPa}$$

Cask Allowable Pure Shear

$$S_{ap} = 0.6 \times S_m = 0.6 \times 115 = 69.0 \text{ MPa}$$

FS for Cask Pure Shear

$$= \frac{S_{ap}}{\tau_{to}} = \frac{69.0}{19.7} = 3.50 > 1.0 \text{ cask pure shear is OK}$$

2.5.1.3.1.6 Summary of Results

Table 2.5.1-1 provides a summary of the Factors of Safety for each of the lifting conditions that are evaluated for the assembled RT-100. The table shows that all of the lifting conditions meet the required factor of safety greater than 3.0 against yield and the factor of safety greater than 5.0 against ultimate stress for the tear out and weld stress and a greater than 1.0 for the bearing stresses and average pure shear.

Table 2.5.1-1 Summary of Results for Lifting Assembled Cask

Lifting Condition Evaluated	Factor of Safety	
	Yield (> 3)	Ultimate (>5)
Lifting Pocket Tear-out Stresses	6.05	15.54
Lifting Pocket Weld Stresses: Weld	4.80	12.05
Lifting Pocket Weld Stresses: Cask	15.36	39.45
	Factor of Safety (>1)	
Lifting Pocket Bearing Stresses	3.22	N/A
Lifting Pocket Average Pure Shear	3.50	

2.5.1.3.2 Primary Lid Lifting Evaluation

The primary lid is evaluated for the working load limit in the lifting rings and for the tear-out stresses in the lid from the lifting activities. The lifting rings for the primary lid can only be used when the cask lid is separated from the cask body. The secondary cask lid is also removable, so the primary lid may be lifted with the secondary lid attached or separated from the primary lid. Conservatively, the combined primary and secondary lid is used for the lifting evaluation. The primary lid design information is:

- Primary Lid Weight $W_{PL} = 3648 \text{ kg, assume } 3700 \text{ kg}$
- Secondary Lid Weight $W_{SL} = 857 \text{ kg, assume } 900 \text{ kg}$
- Total Lid Lifting Weight $W_L = 3700 + 900 = 4600 \text{ kg}$
- Number of Lifting Rings $n_r = 3$
- Dynamic Load Factor $DLF = 1.35$

2.5.1.3.2.1 Primary Lid Lifting Ring Working Loads

The lifting rings on the primary lid are only used for lifting when the lid is detached from the cask body, and are rendered inoperable by removing the rings from the lid when the cask is assembled. The rings are therefore not considered to be a structural part of the package and do not need to be designed for the factor of safety against yielding.

- Lifting Ring Load $P_r = \frac{W_L \times DLF}{n_r} = \frac{4600 \times 1.35}{3} = 2070 \text{ kg}$
- Ring Working Load Limit $P_{r,max} = 3000 \text{ kg}$
- Factor of Safety $FS = \frac{P_{r,max}}{P_r} = \frac{3000}{2070} = 1.45 > 1.0$

2.5.1.3.2.2 Primary Lid Thread Engagement

The minimum required thread engagement length is determined in accordance with “Machinery’s Handbook [Ref. 27]. The primary lid is manufactured from ASTM A240 Type 304L SS material. This material is weaker than the M20 lifting ring material (ASTM A-354 Gr. BD), so failure will occur at the root of the primary lid material threads. The minimum required thread engagement length that prevents primary lid material failure is:

$$\text{Minimum Engagement Length } L_e = \frac{S_{bt} \times 2 \times A_b}{S_{ct} \times \pi \times n \times D_{s,\min} \times \left[\frac{1}{2 \times n} + 0.57735 \times (D_{s,\min} - E_{n,\max}) \right]}$$

Where

S_{bt} = Bolt External Thread Tensile Strength, MPa

A_b = Stress Area of Bolt External Threads, mm²

S_{ct} = Cask Internal Thread Tensile Strength, MPa n = Number of threads per millimeter

$D_{s,\min}$ = Minimum Major Bolt Diameter, mm

$E_{n,\max}$ = Maximum Pitch Diameter of Internal Thread, mm

Solving the equation for Minimum Engagement Length, L_e :

$$\begin{aligned} \text{Minimum Engagement Length} \\ L_e &= \frac{150,000 \times 2 \times 0.38}{69,000 \times \pi \times 10.16 \times 0.773 \times \left[\frac{1}{2 \times 10.16} + 0.57735 \times (0.773 - 0.699) \right]} \\ &= 0.73 \text{ in} = 18.5 \text{ mm} \end{aligned}$$

Where

S_{bt} = 1030 MPa = 150,000 psi

A_b = 245.0 mm² = 0.38 in²

S_{L_t} = 470 MPa = 69,000 psi

p = Thread Pitch = 2.5 mm = 0.098 in

$n = \frac{1}{p} = \frac{1}{0.098} = 10.16$ Threads/inch

$D_{s,\min} = 19.623 \text{ mm} = 0.773 \text{ in}$

$E_{n,\max} = 17.744 \text{ mm} = 0.699 \text{ in}$

The available thread engagement, L_{ep} , is 32 mm. Therefore, the factor of safety is:

$$FS = \frac{L_{ep}}{L_e} = \frac{32.0}{18.5} = 1.73 > 1.0$$

The lifting ring configuration is acceptable for the applied loads. In the unlikely event that failure does occur in the lid threads, no adverse effects on the RT-100 will occur since the threads are outside the cask containment boundary.

2.5.1.3.3 Secondary Lid Lifting Evaluation

The secondary lid is lifted using a set of three lifting rings that attach to threaded holes in the top surface of the lid. Although the maximum evaluated weight of the secondary lid lift includes only the secondary lid, the hardware is the same as that used for the primary lid. The combined primary and secondary lid are evaluated for lifting in Section 2.5.1.3.2. This section evaluates the working load limit in the lifting rings and for the minimum thread engagement in the lid during lifting activities. The secondary lid design information is:

Secondary Lid Weight	$W_{SL} = 857 \text{ kg, assume } 900 \text{ kg}$
Number of Lifting Rings	$n_r = 3$
Dynamic Load Factor	$DLF = 1.35$

2.5.1.3.3.1 Lifting Ring Working Load

The lifting rings on the secondary lid are only used for lifting when the lid is detached from the cask and are rendered inoperable by removing the rings from the lid when the cask is assembled. The rings are therefore not considered to be a structural part of the package and do not need to be designed for the factor of safety against yielding.

Lifting Ring Load

$$P_r = \frac{W_{SL} \times DLF}{n_r} = \frac{900 \times 1.35}{3} = 405 \text{ kg}$$

Ring Working Load Limit

$$P_{r,max} = 3000 \text{ kg}$$

Factor of Safety

$$FS = \frac{P_{r,max}}{P_r} = \frac{3000}{405} = 7.4 > 1.0$$

2.5.1.3.3.2 Secondary Lid Thread Engagement

The minimum required thread engagement length is determined in accordance with "Machinery's Handbook" [Ref. 27]. The secondary lid is manufactured from ASTM A240 Type 304L SS material. This material is weaker than the M20 lifting ring material (ASTM A-354 Gr. BD), so failure will occur at the root of the secondary lid material threads. The minimum required thread engagement length that prevents secondary lid material failure is:

$$\text{Minimum Engagement Length } L_e = \frac{S_{bt} \times 2 \times A_b}{S_{ct} \times \pi \times n \times D_{s,min} \times \left[\frac{1}{2 \times n} + 0.57735 \times (D_{s,min} - E_{n,max}) \right]}$$

S_{bt} = Bolt External Thread Tensile Strength, MPa

A_b = Stress Area of Bolt External Threads, mm²

S_{ct} = Cask Internal Thread Tensile Strength, MPa n = Number of threads per millimeter

$D_{s,min}$ = Minimum Major Bolt Diameter, mm

$E_{n,max}$ = Maximum Pitch Diameter of Internal Thread, mm

Solving the equation for Minimum Engagement Length, L_e :

Minimum Engagement Length

$$L_e = \frac{150,000 \times 2 \times 0.38}{69,000 \times \pi \times 10.16 \times 0.773 \times \left[\frac{1}{2 \times 10.16} + 0.57735 \times (0.773 - 0.699) \right]}$$
$$= 0.73 \text{ in} = 18.5 \text{ mm}$$

Where

$$\begin{aligned} S_{bt} &= 1030 \text{ MPa} = 150,000 \text{ psi} \\ A_b &= 245.0 \text{ mm}^2 = 0.38 \text{ in}^2 \\ S_{Lt} &= 470 \text{ MPa} = 69,000 \text{ psi} \\ p &= \text{Thread Pitch} = 2.5 \text{ mm} = 0.098 \text{ in} \\ n &= \frac{1}{p} = \frac{1}{0.098} = 10.16 \text{ Threads/inch} \\ D_{s,\min} &= 19.623 \text{ mm} = 0.773 \text{ in} \\ E_{n,\max} &= 17.744 \text{ mm} = 0.699 \text{ in} \end{aligned}$$

The available thread engagement, L_{ep} , is 32 mm. Therefore, the factor of safety is:

$$FS = \frac{L_{ep}}{L_e} = \frac{32.0}{18.5} = 1.73 > 1.0$$

Therefore, the secondary lid lifting ring configuration is acceptable for the required loads.

2.5.1.3.4 Upper Impact Limiter Lifting Evaluation

The upper impact limiter is lifted using a set of three lifting rings that attach to threaded holes in the top surface of the limiter. The lifting rings are designed to remove the impact limiter from the cask body and not to lift the cask body while still attached. In the following sections, the impact limiter is evaluated for the working load limit in the lifting ring and the lifting ring thread engagement. The upper impact limiter design information is:

Secondary Lid Weight	$W_{UL} = 2541 \text{ kg}$, assume 2700 kg
Number of Lifting Rings	$n_r = 3$
Dynamic Load Factor	DLF = 1.35

2.5.1.3.4.1 Lifting Ring Working Load

The lifting rings on the upper impact limiter are used only for lifting when the impact limiter is detached from the cask body; the rings are rendered inoperable by removing the rings from the impact limiter when the cask is assembled. Since the rings are not considered a structural part of the package, they do not need to be designed for the factor of safety against yielding.

Lifting Ring Load

$$P_r = \frac{W_{UL} \times DLF}{n_r} = \frac{2700 \times 1.35}{3} = 1215 \text{ kg}$$

Ring Working Load Limit

$$P_{r,max} = 3000 \text{ kg}$$

Factor of Safety

$$FS = \frac{P_{r,max}}{P_r} = \frac{3000}{1215} = 2.47 > 1.0$$

2.5.1.3.4.2 Impact Limiter Thread Engagement

The minimum required thread engagement length to prevent impact limiter material failure is determined in accordance with “Machinery’s Handbook” [Ref. 27]. The upper impact limiter is manufactured from ASTM A240 Dual Certified Type 304/304L material. This material is weaker than the M20 lifting ring material (ASTM A-354 Gr. BD), so failure will occur at the root of the upper impact limiter material threads. The minimum required thread engagement length that prevents upper impact limiter material failure is:

$$\text{Minimum Engagement Length } L_e = \frac{S_{bt} \times 2 \times A_b}{S_{ct} \times \pi \times n \times D_{s,min} \times \left[\frac{1}{2 \times n} + 0.57735 \times (D_{s,min} - E_{n,max}) \right]}$$

S_{bt} = Bolt External Thread Tensile Strength, MPa

A_b = Stress Area of Bolt External Threads, mm²

S_{ct} = Cask Internal Thread Tensile Strength, MPa n = Number of threads per millimeter

$D_{s,min}$ = Minimum Major Bolt Diameter, mm

$E_{n,max}$ = Maximum Pitch Diameter of Internal Thread, mm

Solving the equation for Minimum Engagement Length, L_e :

Minimum Engagement Length

$$L_e = \frac{150,000 \times 2 \times 0.38}{69,000 \times \pi \times 10.16 \times 0.773 \times \left[\frac{1}{2 \times 10.16} + 0.57735 \times (0.773 - 0.699) \right]}$$

$$= 0.73 \text{ in} = 18.5 \text{ mm}$$

Where

$$S_{bt} = 1030 \text{ MPa} = 150,000 \text{ psi}$$

$$A_b = 245.0 \text{ mm}^2 = 0.38 \text{ in}^2$$

$$\begin{aligned}
 S_{Lt} &= 470 \text{ MPa} = 69,000 \text{ psi} \\
 p &= \text{Thread Pitch} = 2.5 \text{ mm} = 0.098 \text{ in} \\
 n &= \frac{1}{p} = \frac{1}{0.098} = 10.16 \text{ Threads/inch} \\
 D_{s,\min} &= 19.623 \text{ mm} = 0.773 \text{ in} \\
 E_{n,\max} &= 17.744 \text{ mm} = 0.699 \text{ in}
 \end{aligned}$$

The available thread engagement, L_{ep} , is 32 mm. Therefore, the factor of safety is:

$$FS = \frac{L_{ep}}{L_e} = \frac{32.0}{18.5} = 1.73 > 1.0$$

Therefore, the upper impact limiter lifting ring configuration is acceptable for the required loads.

2.5.1.3.5 Lower Impact Limiter Lifting Evaluation

The lower impact limiter is lifted using three of the threaded bolt studs that are utilized to attach the lower limiter to the cask body. As such, it cannot be lifted while attached to the cask body. The lower impact limiter is evaluated for the bolt stresses and for minimum thread engagement in the lower impact limiter during lifting activities. The lower impact limiter design information is:

Lower Impact Limiter Weight	$W_{LL} = 2448 \text{ kg, assume } 2600 \text{ kg}$
Number of Lifting Rings	$n_r = 3$
Dynamic Load Factor	$DLF = 1.35$
Gravitational Acceleration	$g = 9.81 \text{ m/s}^2$

2.5.1.3.5.1 Attachment Bolt Stresses

The bolts on the lower impact limiter are only used for lifting when the lower impact limiter is detached from the cask body, and are rendered inoperable by securing them to the cask body as part of the assembled cask. The bolts are therefore not considered to be a structural part of the package with respect to lifting and do not need to be designed for the factor of safety against yielding. Since the arrangement of the cables or straps used to lift the lower impact limiter may vary, the total lifting load is conservatively considered simultaneously in the vertical and horizontal directions.

Bolt Tension	$T = \frac{W_{LL} \times DLF \times g}{n_b} = \frac{2600 \times 1.35 \times 9.81}{3} = 11477.7 \text{ N}$
Bolt Shear	$V = \frac{W_{LL} \times DLF \times g}{n_b} = \frac{2600 \times 1.35 \times 9.81}{3} = 11477.7 \text{ N}$
Bolt Stress Area	$A_b = 0.000817 \text{ m}^2$
Bolt Tensile Stress	$\sigma_t = \frac{T}{A_b} = \frac{11477.7}{0.000817 \times 1000} = 14048.6 \frac{\text{kN}}{\text{m}^2} = 14.0 \text{ MPa}$

Bolt Shear Stress $\tau = \frac{V}{A_b} = \frac{11477.7}{0.000817 \times 1000} = 14048.6 \frac{\text{kN}}{\text{m}^2} = 14.0 \text{ MPa}$

Maximum Principal Stress $\sigma_{p1} = \frac{1}{2} \times \left[\sigma_1 + \sqrt{\sigma_1^2 + 4 \times \tau^2} \right]$
 $= \frac{1}{2} \times \left[14.0 + \sqrt{14.0^2 + 4 \times 14.0^2} \right] = 22.7 \text{ MPa}$

Minimum Principal Stress $\sigma_{p2} = \frac{1}{2} \times \left[\sigma_1 - \sqrt{\sigma_1^2 + 4 \times \tau^2} \right]$
 $= \frac{1}{2} \times \left[14.0 - \sqrt{14.0^2 + 4 \times 14.0^2} \right] = -8.7 \text{ MPa}$

Maximum Shear Stress $\tau_{\text{max}} = \frac{\sigma_{p1} - \sigma_{p2}}{2} = \frac{22.7 - (-8.7)}{2} = 15.7 \text{ MPa}$

Bolt Yield Stress $S_y = 896.3 \text{ MPa}$

Allowable Shear Stress $S_a = 0.6 \times S_y = 537.6 \text{ MPa}$

Factor of Safety $FS = \frac{S_a}{\tau_{\text{max}}} = \frac{537.6}{15.7} = 34.2 > 3.0$

2.5.1.3.5.2 Lower Impact Limiter Thread Engagement

The minimum required thread engagement length to prevent impact limiter material failure is determined in accordance with “Machinery’s Handbook”, 26th Edition [Ref. 27]. Since the constants in the equation assume U.S. customary units, the metric units used in this calculation are converted for determination of the required engagement length. The minimum required thread engagement length that prevents upper impact limiter material failure is:

$$\text{Minimum Engagement Length } L_e = \frac{S_m \times 2 \times A_b}{S_{ct} \times \pi \times n \times D_{s,\text{min}} \times \left[\frac{1}{2 \times n} + 0.57735 \times (D_{s,\text{min}} - E_{n,\text{max}}) \right]}$$

- S_{bt} = Bolt External Thread Tensile Strength, MPa
- A_b = Stress Area of Bolt External Threads, mm²
- S_{ct} = Cask Internal Thread Tensile Strength, MPa n = Number of threads per millimeter
- $D_{s,\text{min}}$ = Minimum Major Bolt Diameter, mm
- $E_{n,\text{max}}$ = Maximum Pitch Diameter of Internal Thread, mm

Solving the equation for Minimum Engagement Length, L_e :

Minimum Engagement Length

$$L_e = \frac{150,000 \times 2 \times 1.27}{69,000 \times \pi \times 6.35 \times 1.396 \left[\frac{1}{2 \times 6.35} + 0.57735 \times (1.396 - 1.313) \right]}$$

$$= 1.56 \text{ in} = 39.5 \text{ mm}$$

Where

$$\begin{aligned} S_{bt} &= 1030 \text{ MPa} = 150,000 \text{ psi} \\ A_b &= 817.0 \text{ mm}^2 = 1.27 \text{ in}^2 \\ S_{Lt} &= 470 \text{ MPa} = 69,000 \text{ psi} \\ p &= \text{Thread Pitch} = 4.0 \text{ mm} = 0.157 \text{ in} \\ n &= \frac{1}{p} = \frac{1}{0.157} = 6.35 \text{ Threads/inch} \\ D_{s,\min} &= 35.465 \text{ mm} = 1.396 \text{ in} \\ E_{n,\max} &= 33.342 \text{ mm} = 1.313 \text{ in} \end{aligned}$$

The available thread engagement, L_{ep} , is 75 mm. Therefore, the factor of safety is

$$FS = \frac{L_{ep}}{L_e} = \frac{75.0}{39.5} = 1.90 > 1.0$$

Therefore, the lower impact limiter lifting ring configuration is acceptable for the required loads.

2.5.2 Tie-down Devices

The RT-100 cask utilizes two sets of tie down arms, as shown in Chapter 7, Figure 7.4.4-1. These tie-down arms are welded to two different tie-down plates that in turn are welded to the outer shell of the cask body. Each set of arms on opposite sides of the cask are designed to cross over and securely position the cask, and to absorb the latitudinal, longitudinal and vertical forces required by 10 CFR 71.45 [Ref. 2]. The tie-down arms and plates are a structural part of the package, and must withstand the following loads without impairing the safety of the cask:

- Two (2) times the loaded weight of the cask in the vertical direction
- Ten (10) times the loaded weight of the cask in the direction of travel
- Five (5) times the loaded weight of the cask transverse to the direction of travel

These loads are considered to act simultaneously on the cask and the tie-down arms.

The lifting pockets on the cask body are the only other parts of the cask that could possibly be used to tie down the cask. As such, these pockets are rendered inoperable for tie-down during transport by ensuring that the lift yoke retaining pins are installed in place prior to transport.

2.5.2.1 Tie-down Load Calculation

The maximum forces applicable in each of the three loading directions are calculated in this section. This calculation is accomplished by using the mass of the fully loaded cask along with the gravitational acceleration and the vertical, longitudinal and lateral factors specified in 10 CFR 71.45 [Ref. 2]. The loaded weight of the cask is specified in Chapter 1, Section 1.2.1.2.

Gravitational Acceleration:	$g = 9.81 \text{ m/s}^2$
Cask Mass:	$M_c = 34696 \text{ kg}$
Payload Mass:	$M_p = 7060 \text{ kg}$
Total Mass:	$M = M_c + M_p = 34696 \text{ kg, assume } 42000 \text{ kg}$

Total Weight:	$W = M_g = 412.02 \text{ kN}$
Vertical Acceleration	$d_v = 2$
Axial Acceleration	$d_a = 10$
Transverse Acceleration	$d_L = 5$
Vertical Load	$P_y = M \times g \times d_y = 824 \text{ kN}$
Axial Load	$P_a = M \times g \times d_a = 4120.2 \text{ kN}$
Transverse Load	$P_L = M \times g \times d_L = 2060.1 \text{ kN}$

2.5.2.2 Tie-down Force Calculation

The geometric configuration of the tie-down system is designed so that the resultant tie-down arm tensile loads are tangent to the cask surface in order to minimize the effects of out-of-plane stresses in the cask shell. Figure 2.5.2-1 and Figure 2.5.2-2 illustrate the details of the tie-down system geometry. Shear stops are utilized to convert some of the cask loads into turning moments that are restricted by the tie-down arms. As shown on drawing RT PE 1001-1Rev. F – Robatel Transport Package RT-100 General Assembly Sheet 1/2 (Chapter 1, Appendix 1.4, Attachment 1.4-2), the tie-down arms have slightly different angles in the front and rear of the casks. These differences are summarized in Table 2.5.2-1. The horizontal angles from the cask body to each arm varies from 40° and 44° on one end of the cask and 37° and 41° on the other.

Table 2.5.2-1 Tie-down Arms Horizontal Angles

Load	Arms in Tension	Angles	Average Angle
Longitudinal	L & M (Rear)	44 and 40	42
	Q & R (Front)	37 and 41	39
Lateral	M & R	40 and 41	40.5
	L & Q	44 and 37	40.5
Vertical	L, M, Q, R	44, 40, 37, 41	40.5

The analytical model for determining the reaction loads required to prevent rotation and translation of the package due to the 10 CFR 71.45 [Ref. 2] applied loads is shown in Figure 2.5.2-1 and Figure 2.5.2-2. The evaluation is bounded by analyzing the high average angle (42°) caused by longitudinal forces on the tie-down arms on the rear of the cask, and the low average angle (32°) caused by longitudinal forces on the tie-down arms on the front of the cask. The shear stop forces at the bottom of the package are represented by the orthogonal components of a single force vector, S , making an angle of γ with the global y -axis. The stresses in the members are determined by considering the component loads ($10W$, $5W$, and $2W$) individually and superimposing the results. The geometry of the arms has a slight asymmetry so that the tie downs can cross one another; this slight asymmetry is ignored and average dimensions are used for calculation purposes. A detailed force analysis is conducted using the dimensions and notations shown in the figures; other terms are defined below:

W : weight of cask, kN

T_x : tensile force in member 2 and 3 resulting from $5W$ load, kN

T_y : tensile force in member 1 and 2 resulting from $10W$ load, kN

- T_z : tensile force in each member resulting from 2W load, kN
- $T_{1,2,3,4}$: total tensile force in subscripted member, kN
- F_x : total force in the x direction resulting from 5W load, kN
- F_y : total force in the y direction resulting from 10W load, kN
- L: Effective length of tie-down arm, i.e. distance between tie-down tangent point and center of tie-down attachment eye, mm

The forces are derived in detail in Calculation Package RTL-001-CALC-ST-0202, Rev. 4 [Ref. 34] and are developed via summing the moments about the center of gravity. A summary of the values calculated using Figure 2.5.2-1 and Figure 2.5.2-2 are provided in Table 2.5.2-2. The maximum calculated forces using these values is provided in Table 2.5.2-3. The results show that the front arms with the lower horizontal angle are subjected to the greater forces. The evaluation of the longitudinal loads on the two front tie-down arms bounds the evaluation of all other load conditions on the cask. The tension calculations and safety margin evaluations contained in the following sections focuses on the front tie-down arms.

Unit: mm

R = impact limiter radius = 2587/2

r = cask radius = (2040+60)/2

d = cask C.G. elev. = 1648

t = avg. tie-down eye elev. = 1429

L = total length from the tangent point
 of the tie-down arm (to the cask body)
 to the tie-down eye

x' = avg. tie-down eye X axis offset

y' = avg. tie-down eye Y axis offset

z' = cask tangent elev.

a = L cosθ sinφ

b = L cosθ cosφ

c = L sinθ

weight	412.02	KN
R	1293.5	mm
r	1050	mm
d	1648	mm
t	1429	mm
L	605	mm
θ	0.514872	rad
φ	0.733038	rad
a	352.3409	mm
b	391.3142	mm
c	297.9163	mm
x'	427.9612	mm
y'	1093.901	mm
z'	1726.916	mm

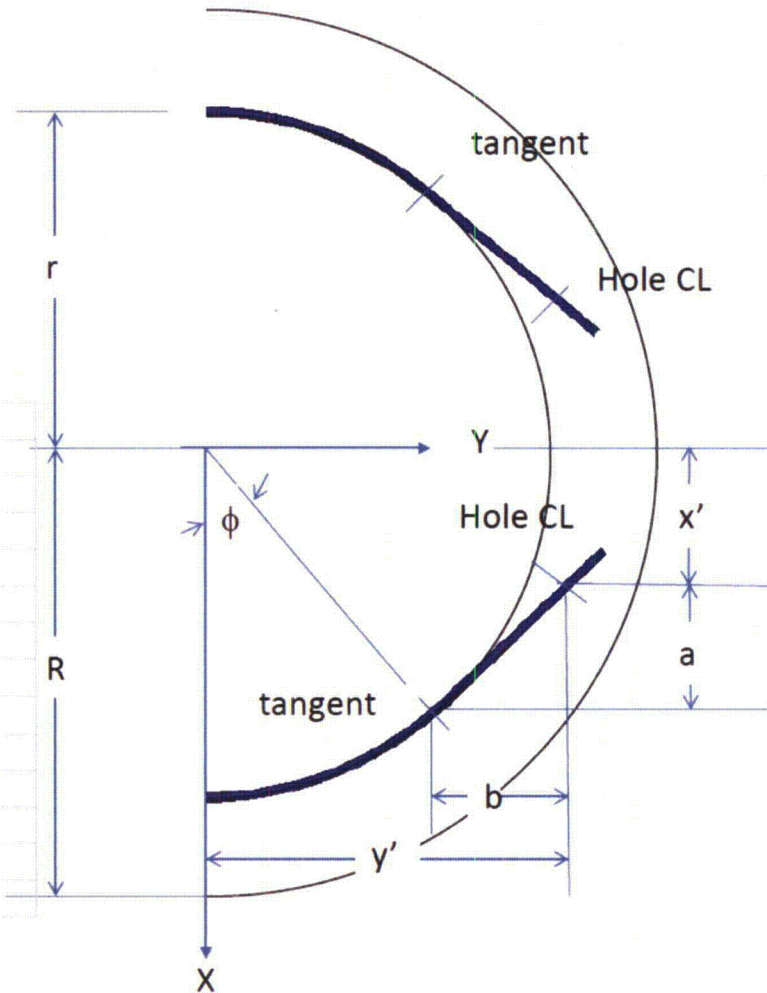


Figure 2.5.2-1 RT-100 Tie-Down Arm Geometry

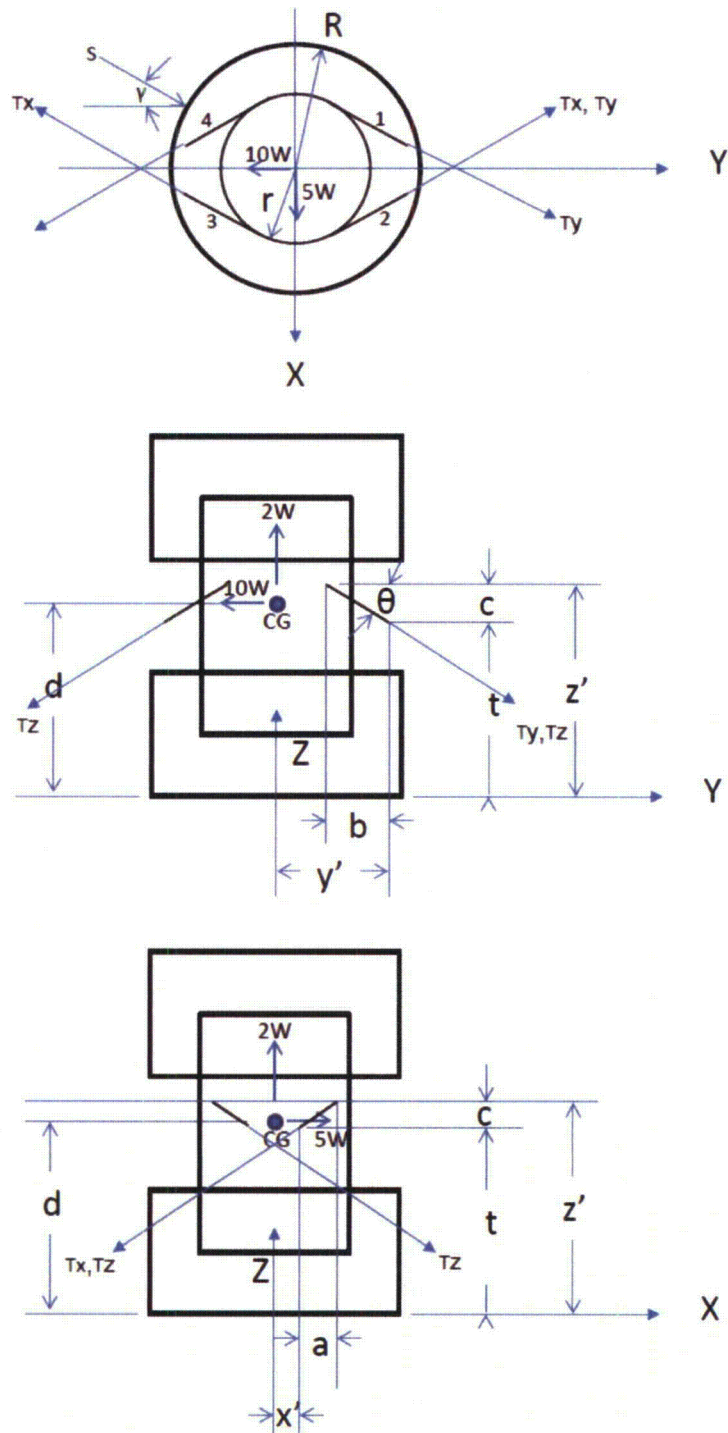


Figure 2.5.2-2 RT-100 Tie-Down Free Body Diagrams

Table 2.5.2-2 Calculated Values for Tie-Down Arms

	Rear Arms		Front Arms	
Φ	$(44^\circ \text{ \& } 40^\circ) = > 0.733038$	rad	$(41^\circ \text{ \& } 37^\circ) = > 0.680678$	rad
a	351.47	mm	365.61	mm
b	390.34	mm	451.49	mm
c	297.18	mm	328.69	mm
L	$(616 + 591)/2 = 603.5$	mm	$(682 + 653)/2 = 667.5$	mm
x'	451.13	mm	473.71	mm
y'	1113.01	mm	1131.16	mm
z'	1726.18	mm	1757.59	mm

(Note: these values calculated using parameters as defined in Figure 2.5.2-1 and Figure 2.5.2-2)

Table 2.5.2-3 Calculated Forces for Tie-Down Arms

	Rear Arms		Front Arms	
T _x	1361.26	kN	1430.82	kN
T _y	1609.56	kN	1571.40	kN
T _z	418.36	kN	418.36	kN
T _{max}	3389.18	kN	3420.58	kN
F _{xx}	474.56	kN	492.68	kN
F _{yy}	2038.07	kN	1994.43	kN
F _n	2925.80	kN	2956.73	kN
F _f	146.29	kN	147.84	kN
S _x	204.57	kN	213.28	kN
S _y	953.61	kN	931.10	kN

2.5.2.3 Tie-Down Arm Evaluation

The maximum tie-down arm load of 3420.58 kN is determined as described in Section 2.5.2.2 above. This load is applied to the tie-down arm design to ensure that stresses are within allowable limits. As show in the drawings presented in (Chapter 1, Appendix 1.4, Attachments 1.4-2 through 1.4-8) the tie-down arm is reinforced in the portion containing the attachment hole. This reinforcement ensures that the loads in this area of reduced cross-section can be transmitted safely into the rest of the tie-down arm. Stresses for the tie-down arm and its connection to the exterior cask shell are calculated as follows:

Arm Tension Stress at Hole

Arm Cross-Sectional Area at Hole, $A_{net} = 11,450 \text{ mm}^2$

Arm Tension Stress, $\sigma_{net} = T_{max} / A_{net} = 298.74 \text{ MPa}$

Stress Allowable, $\sigma_{allow} = 437.2 \text{ MPa}$ (@50°C per Table 2.2.1-1)

Factor of Safety, $FS = \sigma_{allow} / \sigma_{net} = 437.2 / 298.74 = 1.46 > 1.0$

Arm Bearing Stress at Hole

Arm Bearing Area at Hole, $A_{bear} = 7,650 \text{ mm}^2$

Arm Tension Stress, $\sigma_{net} = T_{max} / A_{bear} = 447.13 \text{ MPa}$

Stress Allowable, $\sigma_{\text{allow}} = 1.35 \times 437.2 \text{ MPa} = 590.2 \text{ MPa}$ (@50°C per Table 2.2.1-1)
Factor of Safety, $FS = \sigma_{\text{allow}} / \sigma_{\text{net}} = 590.2 / 447.13 = \underline{1.32} > 1.0$

Arm Tear-Out Stress at Hole

Arm Tear-out Area, $A_{\text{tear}} = 18,700 \text{ mm}^2$

Arm Tear-out Stress, $\tau_{\text{tear}} = T_{\text{max}} / A_{\text{tear}} = 182.92 \text{ MPa}$

Tear-out Stress Allowable, $\tau_{\text{allow}} = 0.6 \times 437.2 = 262.3 \text{ MPa}$

Factor of Safety, $FS = \tau_{\text{allow}} / \tau_{\text{tear}} = 262.3 / 182.92 = \underline{1.43} > 1.0$

Arm Tension Stress at Main Cross Section

Arm Area, $A_{\text{arm}} = 9,100 \text{ mm}^2$

Arm Tear-out Stress, $\sigma_{\text{arm}} = T_{\text{max}} / A_{\text{arm}} = 375.89 \text{ MPa}$

Tear-out Stress Allowable, $\sigma_{\text{allow}} = 437.2 \text{ MPa}$

Factor of Safety, $FS = \sigma_{\text{allow}} / \sigma_{\text{arm}} = 437.2 / 375.89 = \underline{1.16} > 1.0$

As shown in the summary above, the stresses in the limiting tie-down arm are below the yield stress allowables.

2.5.2.4 Tie-down Arm & Plate Weld Evaluation

The stresses in the welds attaching the tie-down arms to the tie-down plates and the plates to the cask body are found by applying the loads from the attachment arms to the weld around the perimeter of the plates. The maximum load on the tie-down arm welds are the sum of the loads in two connecting arms. Thus, from inspection of Figure 2.5.2-2, the maximum tie-down arm load is calculated as follows:

Tie-down Arm Weld Force, $F_{\text{total}} = 2T_x + T_y + 2T_z = 5269.76 \text{ kN}$

Weld axial load $F_x = F_{\text{total}} \times (b / L) = 3564.43 \text{ kN}$

Weld vertical load $F_y = F_{\text{total}} \times (c / L) = 2594.96 \text{ kN}$

Weld transverse load $F_z = F_{\text{total}} \times (a / L) = 2886.42 \text{ kN}$

Arm tensile strength: 437.2 MPa

Cask tensile strength: 199.3 MPa

Weld tensile strength: 450 MPa, weld between tie-down arm and plate [Ref. 34]
420 MPa, weld between tie-down plate and cask [Ref. 34]

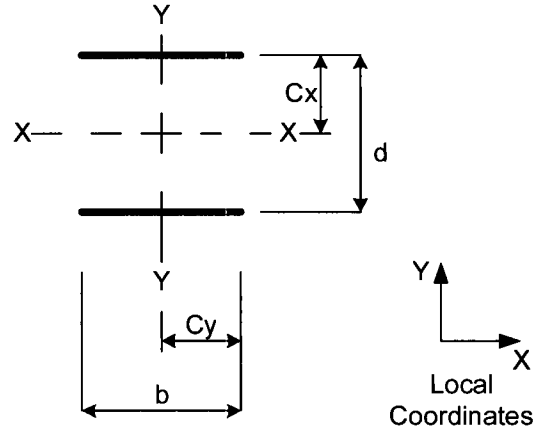
The weld length, b , is 1583.36 mm, the weld height “ d ” for the tie-down arm plate is the 260 mm height of the arm, and weld height “ d ” for the weld between tie-down plate and cask body is 388.03 mm (Calculation Package RTL-001-CALC-ST-0202 Rev. 4 [Ref. 34]). These dimensions and loads are used in the following weld stress calculations.

2.5.2.4.1 Tie Down Arm-to-Plate Weld Stress

The stresses in the welds attaching the tie-down arm to the tie-down plate are found by applying the weld loads as specified in Section 2.5.2.4. The stresses and allowables are determined as described in “Design of Welded Structures” [Ref. 25] and Calculation Package RTL-001-CALC-ST-0202, Rev. 4 [Ref. 34].

Weld properties are as follows:

$$\begin{aligned}
 b &= 1.583 \text{ m} \\
 d &= 0.260 \text{ m} \\
 C_y &= b/2 = 0.79 \text{ m} \\
 C_x &= d/2 = 0.13 \text{ m} \\
 A_w &= 2 \times b = 3.172 \text{ m}^3/\text{m} \\
 S_x &= b \times d = 0.41 \text{ m}^3/\text{m} \\
 S_y &= b^2/3 = 0.84 \text{ m}^3/\text{m} \\
 J_w &= b(3d^2 + b^2) / 6 = 0.71 \text{ m}^4/\text{m}
 \end{aligned}$$



Weld Throat Size = 0.022 m

Weld stress is calculated as follows:

$$\begin{aligned}
 f_t &= (F_z / A_w) + (M_x / S_x) + (M_y / S_y) = 911.69 \text{ kN/m} \\
 f_{vy} &= (F_y / A_w) + ((M_z \times C_y) / J_w) = 819.63 \text{ kN/m} \\
 f_{vx} &= (F_x / A_w) + ((M_z \times C_x) / J_w) = 1125.85 \text{ kN/m} \\
 f_w &= (f_t^2 + f_{vy}^2 + f_{vx}^2)^{1/2} = 1664.49 \text{ kN/m}
 \end{aligned}$$

Weld Allowable Stress = 0.6 x F_w x Weld Size x 1000 = 5940 kN/m

Weld Metal Factor of Safety, FS = 5940 / 1664.49 = 3.56 > 1.0

Tie-Down Arm Shear Allowable = 0.6 x F_w x Weld Size / 0.7071 x 1000 = 8158 kN/m

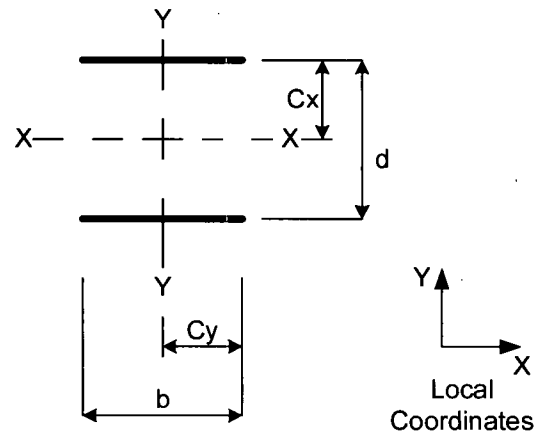
Tie-Down Arm Factor of Safety, FS = 8158 / 1664.49 = 4.90 > 1.0

2.5.2.4.2 Tie Down Plate-to-Outer Shell Weld Stress

The stresses in the welds attaching the tie-down plate to the cask outer shell are found by applying the weld loads as specified in Section 2.5.2.4. The stresses and allowables are determined as described in “Design of Welded Structures” [Ref. 25] and Calculation Package RTL-001-CALC-ST-0202, Rev. 4 [Ref. 34].

Weld properties are as follows:

$$\begin{aligned}
 b &= 1.583 \text{ m} \\
 d &= 0.388 \text{ m} \\
 C_y &= b/2 = 0.79 \text{ m} \\
 C_x &= d/2 = 0.19 \text{ m} \\
 A_w &= 2 \times b = 3.172 \text{ m}^3/\text{m} \\
 S_x &= b \times d = 0.615 \text{ m}^3/\text{m} \\
 S_y &= b^2/3 = 0.84 \text{ m}^3/\text{m} \\
 J_w &= b (3d^2 + b^2) / 6 = 0.78 \text{ m}^4/\text{m}
 \end{aligned}$$



Weld Throat Size = 0.017 m

Weld stress is calculated as follows:

$$\begin{aligned}
 f_t &= (F_z / A_w) + (M_x / S_x) + (M_y / S_y) = 911.69 \text{ kN/m} \\
 f_{vy} &= (F_y / A_w) + ((M_z \times C_y) / J_w) = 819.63 \text{ kN/m} \\
 f_{vx} &= (F_x / A_w) + ((M_z \times C_x) / J_w) = 1125.85 \text{ kN/m} \\
 f_w &= (f_t^2 + f_{vy}^2 + f_{vx}^2)^{1/2} = 1664.49 \text{ kN/m}
 \end{aligned}$$

Weld Allowable Stress = $0.6 \times F_w \times \text{Weld Size} \times 1000 = 4284 \text{ kN/m}$

Weld Metal Factor of Safety, FS = $4284 / 1664.49 = 2.57 > 1.0$

Outer Shell Shear Allowable = $0.6 \times F_w \times \text{Weld Size} / 0.7071 \times 1000 = 2.875 \text{ kN/m}$

Outer Shell Factor of Safety, FS = $2875 / 1664.49 = 1.73 > 1.0$

2.5.2.5 Tie-Down Evaluation Summary

As shown in the previous sections, all components of the tie-down components that are a structural part of the cask maintain positive safety margins when subjected to the simultaneous loadings specified in 10 CFR 71.45 [Ref. 2]. The smallest factor of safety is 1.16 against tie-down arm tension. Under excessive loading, the failure of the tie-down system occurs by yielding in the tie-down arm. This failure does not impair the package's ability to meet other regulatory requirements since the tie-down arms are welded to a plate that is in-turn welded to the cask body. Damage to the tie-down arm does not damage any component integral to the cask body and therefore, does not compromise the cask body shell.

2.6 Normal Conditions of Transport

This Section describes the RT-100 evaluation for the normal conditions of transport specified in 10 CFR 71.71 [Ref. 2]. The requirements of 10 CFR 71.71 state that the RT-100 shall be structurally adequate for the following normal conditions of transport:

- Heat
- Cold
- Reduced external pressure

- Increased external pressure
- Vibration
- Water spray, free drop
- Corner drop
- Compression, and
- Penetration.

During the free drop analyses, the cask impact orientation evaluated is the orientation that inflicts the maximum damage to the cask. Also, the requirements of 10 CFR 71.71 [Ref. 2] specify that the evaluation of the RT-100 for the normal conditions of transport be evaluated at the most unfavorable ambient temperature in the range from -29°C to +100°C. The normal conditions of transport evaluations presented in this section show that the package satisfies the applicable performance requirements specified in the 10 CFR 71.71 [Ref. 2]. The scale drop testing and analytical analyses demonstrate that there is no decrease in the RT-100 Cask Package effectiveness as follows:

- No loss or dispersal of contents
- No structural changes reducing the effectiveness of components required for shielding, for heat transfer, or for maintaining subcriticality or containment
- No changes to the package affecting its ability to withstand HAC.

The normal conditions evaluations described in the following sections are performed in accordance with the design criteria and load combinations as identified in Section 2.1.2. Each of the following subsections addresses each normal conditions requirement.

2.6.1 Heat

The RT-100 cask body and closure lids are analyzed for structural adequacy in accordance with the thermal evaluation of the RT-100 for the temperatures specified in 10 CFR 71.71(c)(1) [Ref. 2] is presented in Chapter 3. The thermal evaluation demonstrates that the cask component temperatures are maintained within their safe operating ranges for all normal conditions of transport. The following subsections discuss the structural evaluation of the RT-100 using the appropriate component temperatures as determined in Chapter 3.

2.6.1.1 Summary of Pressures and Temperatures

The pressures and temperatures occurring in the RT-100 as a result of the 10 CFR 71 [Ref. 2] normal conditions of transport thermal conditions are an important consideration for the structural evaluations presented in this chapter. The internal pressure induces stresses on the containment system; the temperatures affect the selection of temperature-dependent material properties as well as, the internal pressures that occur as a result of the ambient temperatures and solar insolation specified in 10 CFR 71.71 [Ref.2]. The material properties utilized are based on the maximum calculate temperatures of each component or higher temperatures which are conservative.

The maximum normal operating pressure evaluation for the RT-100 is presented in Chapter, 3 Section 3.3.2. As described in this section, the calculated maximum pressure for normal

conditions is 182.71 kPa (26.5 psia). For conservatism, the structural evaluations involving internal pressure use a maximum normal operating condition pressure of 342.7 kPa (49.7 psia or 35 psig).

The maximum component temperatures in the RT-100 for normal conditions are presented in Chapter 3, Table 3.1.3-1 “RT-100 Maximum Normal Condition Temperature Summary” (Found in Chapter 3). The temperatures are utilized to determine the stress allowables used in the structural evaluation for the normal conditions of transport.

2.6.1.2 Differential Thermal Expansion

As shown in Chapter 3, Table 3.1.3-1, the temperatures of the components of the cask differ by only a few degrees under normal conditions of transport thermal ambient conditions. This difference is due in part to the relatively low decay heat of the contents. The RT-100 is evaluated for differential thermal expansion as described in Section 2.6.7 in combination with normal pressure and inertial loads under the following conditions:

- Ambient temperature, 38°C
- Initial temperature, 38°C
- Heat transfer to ambient by natural convection, still air
- Heat transfer to ambient by radiation
- Steady-state solar insolation
- Internal heat load as a uniform heat flux, 13.04 W/m²

2.6.1.3 Stress Calculations

Regulatory Guide 7.6 [Ref. 4] requires that the range of primary plus secondary stress intensities during normal conditions of transport be less than 3.0 S_m. To evaluate this condition, the range of primary plus secondary stresses for the combined normal events (including heat, cold, normal operating pressure, 0.3-m end drop, and 0.3-m side drop conditions) are analyzed using the finite element model presented in 2.6.7.2.

2.6.1.4 Comparison with Allowable Stresses

The combined stress results are presented in Tables 2.6.7-1 and 2.6.7-2. Since the margins of safety are all positive, the RT-100, therefore, satisfies the requirements of 10 CFR 71.71(c)(1) [Ref. 2] for the heat (normal transport) condition.

2.6.2 Cold

The RT-100 cask body and closure lids are analyzed for structural adequacy in accordance with the thermal evaluation of the RT-100 for the temperatures specified in 10 CFR 71.71(c)(2) [Ref. 2] is presented in Chapter 3. The thermal evaluation demonstrates that the RT-100 component temperatures are maintained within their safe operating ranges for all normal conditions of transport. Using the same methodology presented in Section 2.6.1, the RT-100 is evaluated for cold conditions. The following thermal case is used to calculate the thermal stress under cold conditions:

- Ambient temperature, -40°C
- Initial temperature, -40°C

- Heat transfer to ambient by natural convection, still air
- Heat transfer to ambient by radiation
- No solar insolation, in shade
- Internal heat load as a uniform heat flux, 13.04 W/m²

The combined stress results are presented in Tables 2.6.7-1 and 2.6.7-2. Since the margins of safety are all positive, the RT-100, therefore, satisfies the requirements of 10 CFR 71.71(c)(2) [Ref. 2] for the cold (normal transport) condition.

2.6.3 Reduced External Pressure

The drop in atmospheric pressure to 24 kPa (3.5 psia), as specified in 10 CFR 71.71(c)(3) [Ref. 2], effectively results in an additional internal pressure in the cask of 77 kPa (11.2 psig). This additional pressure has a negligible effect on the RT-100 because, in Section 2.6.1.1, the cask is analyzed for a normal transport conditions internal pressure of 241 kPa (35 psig). Maximum internal pressure is included in combination with internal loads (see Tables 2.6.7-1 and 2.6.7-2). Since the margins of safety are all positive, the RT-100 satisfies the requirements of 10 CFR 71.71(c)(3) for reduced external pressure.

2.6.4 Increased External Pressure

An increased external pressure of 20 psia (5.3 psig external pressure), as specified in 10 CFR 71.71(c)(4) [Ref. 2], has a negligible effect on the RT-100 because of the thick outer shell and end closures of the cask. Section 2.6.7 addresses many different loading cases which exceed these prescribed external pressure requirements. Therefore, the requirements of 10 CFR 71.71(c)(4) [Ref. 4] are satisfied.

2.6.5 Vibration

10 CFR 71.71 (c)(5) [Ref.4] requires that “vibration normally incident to transport” be evaluated. The RT-100 package consists of thick section materials that are unaffected by vibration normally incident to transport, such as over the road vibrations.

2.6.5.1 Vibration Evaluation of the RT-100 Cask Primary Lid Bolts

The RT-100 may be subjected to a cycle range typically associated with high-cycle fatigue (> 10⁸ cycles). Therefore, the endurance limit of the material for the high cycle fatigue can be approximated by using a 60% reduction, r_h , of the ultimate tensile strength (AISC [Ref. 26]) with an additional 10% reduction r_g , for the connection surface (Machinery’s Handbook [Ref. 27]). Thus the endurance limit for the material is:

$$S_a = (1 - r_h) \times (1 - r_g) \times S_{ub}$$

where:

$$\begin{aligned} S_{ub} &= \text{Bolt Ultimate Stress} \\ &= 1030 \text{ MPa} \quad (\text{ASTM A354 Grade B, Table 2.2.1-3}) \end{aligned}$$

$$S_a = (1 - 0.60) \times (1 - 0.10) \times 1030$$

$$= 370.8 \text{ MPa}$$

NUREG-0128 [Ref. 30] gives the following RMS vibration load factors for the road travel:

$$f_v = \text{Vertical Vibration Load Factor}$$

$$= 0.52$$

$$f_L = \text{Longitudinal Vibration Load Factor}$$

$$= 0.27$$

$$f_t = \text{Transverse Vibration Load Factor}$$

$$= 0.19$$

The RT-100 is transported in the vertical orientation. The cask lid is subjected to vibration in the vertical direction. A notch factor, f_N , of 3.0 is used and is conservative (AISC [Ref. 26]). The vibration stress in the bolts is:

$$s_v = \frac{F_b \times f_N}{A_b}$$

where:

$$F_b = \text{Bolt Force due to Vibration}$$

$$= \frac{f_v \times W_{Lp} \times g}{N_b}$$

$$A_b = \text{Bolt Stress Area}$$

$$= 1470 \text{ mm}^2 \quad [\text{Ref. 27}]$$

$$W_{Lp} = \text{Cask Lid Weight}$$

$$= 3648 \text{ kg, use } 3650 \text{ kg}$$

$$N_b = \text{Number of Bolts}$$

$$= 32$$

$$F_b = \frac{0.52 \times 3650 \times 9.81}{32} \times \frac{1 \text{ kN}}{1000 \text{ N}}$$

$$= 0.58 \text{ kN}$$

$$s_v = \frac{0.58 \times 3.0}{0.001470} \times \frac{1 \text{ MPa}}{1000 \frac{\text{kN}}{\text{m}^2}}$$

$$= 1.19 \text{ MPa} \ll S_a = 370.8 \text{ MPa}$$

Since the stress in the bolts is well below the endurance limit of the material, the primary lid bolts are not subjected to transportation-related fatigue damage during their service life.

The maximum shock loading coefficient for the three orthogonal directions is specified as 2.9 (NUREG-0128 [Ref. 30]). The RT-100 primary lid is subjected to shock loading during transport. The primary lid closure bolts are shown to withstand a 125g impact load (Section 2.13.3.3), which is much larger than the 2.9W shock loading during transport. Therefore, the primary lid closure bolts are acceptable for shock loading by comparison.

2.6.5.2 Vibration Evaluation of the RT-100 Cask Secondary Lid Bolts

Per Section 2.6.5.1, the components of the package are in the high-cycle fatigue range ($> 10^8$ cycles). The endurance limit of the material for the high cycle fatigue for the secondary lid bolts is the same as for the primary lid bolts. The RT-100 lid is subjected to vibration in the vertical direction. A notch factor, f_N , of 3.0 is used and is conservative (AISC [Ref. 26]). The vibration stress in the bolts is:

$$s_v = \frac{F_b \times f_N}{A_b}$$

where:

$$F_b = \text{Bolt Force due to Vibration}$$

$$= \frac{f_v \times W_{Lp} \times g}{N_b}$$

$$A_b = \text{Bolt Stress Area}$$

$$= 817 \text{ mm}^2 \quad [\text{Ref. 27}]$$

$$W_{Ls} = \text{Cask Lid Weight}$$

$$= 857 \text{ kg}$$

$$N_b = \text{Number of Bolts}$$

$$= 18$$

All other quantities are defined in Section 2.6.5.1

$$F_b = \frac{0.52 \times 857 \times 9.81}{18} \times \frac{1 \text{ kN}}{1000 \text{ N}}$$

$$= 0.24 \text{ kN}$$

$$s_v = \frac{0.24 \times 3.0}{0.000817} \times \frac{1 \text{ MPa}}{1000 \frac{\text{kN}}{\text{m}^2}}$$

$$= 0.89 \text{ MPa} \ll S_a = 370.8 \text{ MPa}$$

Since the stress in the bolts is well below the endurance limit of the material, the secondary lid bolts are not subjected to transportation-related fatigue damage during their service life.

The maximum shock loading coefficient for the three orthogonal directions is specified as 2.9 (NUREG-0128 [Ref. 30]). The cask primary lid is subjected to shock loading during transport. The secondary lid closure bolts have been shown to withstand a 125g impact load (Section 2.12.4.1), which is much larger than the 2.9W shock loading during transport. Therefore, the secondary lid closure bolts are acceptable for shock loading by comparison.

The RT-100 satisfies the requirements for normal vibration incident to transport as required by 10 CFR 71.71(c)(5) [Ref. 2].

2.6.6 Water Spray

Water causes negligible corrosion of the stainless shell of the RT-100. The cask contents are protected in the sealed cavity. A water spray as specified in 10 CFR 71.71(c)(6) [Ref. 2] has no adverse impact on the package. The cask surface temperature specified during the water spray is between 38°C and -29°C. Consequently, the induced thermal stress in the cask components is less than the thermal stresses that occur during the extreme temperature conditions for normal transport. Therefore, the requirements of 10 CFR 71.71(c)(6) [Ref. 2] are satisfied.

2.6.7 Free Drop

The RT-100 is shown to meet the free drop requirements of 10 CFR 71.71 [Ref. 2] through a combination of classic calculations, finite element analyses and scale model drop testing (RTL-001-CALC-ST-0402, Rev. 4 [Ref. 35]). The evaluations include the qualification of the RT-100 cover bolt design for the combined effects of free drop impact force, internal pressures, thermal stress, O-ring compression force, and bolt preload following the methodology of NUREG/CR-6007 [Ref. 10] (Appendix 2.13). The combined effects of inertial loads, internal pressures, and thermal stress are considered for packaging components.

2.6.7.1 Methodology

The RT-100 is designed in accordance with Regulatory Guide 7.6 [Ref. 4]. The design criteria for NCT and HAC are presented in Table 2.1.2-2. Load combinations for the structural analysis of shipping casks for radioactive materials are defined by Regulatory Guide 7.8 [Ref. 3]. The load combinations for all normal and accident conditions and corresponding ASME service levels are shown in Table 2.1.2-1. Material properties used in this evaluation are presented in Section 2.2.1. Stress intensities caused by pressure, thermal expansion, and mechanical loads are combined before comparing to ASME, Section III, Subsection ND [Ref. 7] stress allowables, which are listed in Table 2.2.1-3.

2.6.7.2 Finite Element Analysis

The finite element code ANSYS [Ref. 28] is used to generate a three-dimensional model of the RT-100 and to determine its response to normal conditions of transport (NCT) and hypothetical accident conditions (HAC) (Section 2.7.1). Specifically, a one-half (180°) 3D model of the RT-100 inner and outer shells, outer and inner lids, bottom plate and lead shields is constructed using ANSYS [Ref. 28] solid elements. The interaction between components is modeled using gap elements. Stability of the model is assured by using weak springs. Boundary conditions are

applied to the model simulating the loading conditions the cask will experience during normal and accident transport conditions. Pressure loads are applied to the cask inner shell to simulate bounding contents loads and internal pressurization. Thermal stresses are calculated using input temperatures from the NCT thermal analyses. Bolt preloads are applied to represent the bolt torque at the time the cask is readied for shipment. Post-processing is accomplished by linearizing the stress across locations where maximum stresses are calculated. The analyses assume linear elastic behavior of the cask. Therefore, calculated stress intensities are compared to appropriate allowables (Table 2.2.1-1) and the margin of safety is calculated.

2.6.7.2.1 Model Description

Finite element analysis methods are used to perform the stress evaluation of the RT-100 for normal and accident free drop conditions. Each drop condition is analyzed using a three-dimensional finite element model using the computational modeling software ANSYS [Ref. 28]. Figure 2.6.7-1 shows the major components of the RT-100 represented in the model including the inner and outer shells, flange, bottom plate, primary and secondary lids, and closure bolts.

As shown in Figure 2.6.7-1, the model (which corresponds to half (180°) of the cask body) is generated by de-featuring the SolidWorks® solid model used to develop the manufacturing drawings and exporting the model to a .STEP file format. The .STEP file is imported directly into ANSYS [Ref.28] where the finite element model is developed following the guidance presented in ISG-21 [Ref. 53]. The resulting finite element model of the cask body is represented using solid elements, contact elements, mass elements and spring/damper elements (Figure 2.6.7-2).

The solid portion of the model is constructed using ANSYS solid (SOLID185) elements. Surface-to-surface contact elements are used to simulate the interaction between adjacent components. Specifically, contact between the cask shells and lead shielding are modeled using CONTAC174/TARGE170 surface-to-surface contact elements with zero friction, which allows the lead to float between the inner and outer shells. Contact elements are also used to bond dissimilarly meshed components. To simulate the impact limiters, the interaction between the cask body and impact limiters is modeled using CONTAC52 gap elements (Figure 2.6.7-3), which acts as a compression only element. The size of the CONTAC52 gaps is determined from nominal dimensions between the impact limiter and cask body. Spring elements (COMBIN14) are inserted automatically during the solution to help stabilize the model. ANSYS [Ref. 28] assigns low spring stiffness so their presence does not adversely affect the accuracy of the solution.

Finite element model verification and mesh density study are presented in Appendix A.4 of Calculation Package RTL-001-CALC-ST-0402, Rev. 4 [Ref. 35]. During the development of the finite element model each part and interface was considered on an individual basis. The RT-100 outer shell was meshed using the sweep method and the element size was varied until there was a sufficient number of elements across the shell thickness. The element ratio was reviewed to ensure adequate results. To test a component, in this case the outer shell, the ends were fixed and a pressure load was applied to the inner surface and a solution was obtained. If a singularity or discontinuity was noted, the mesh was refined until uniform results were obtained. As a second check, a hand calculation was performed on to ensure that the stress calculated by ANSYS

[Ref. 28] is giving expected results. Hoop stresses were also calculated and compared to the results. As the model was developed the same philosophy was applied to the intersection of the shell and bottom plate. Using Roark's equations ("Roark's Formulas for Stress and Strain" [Ref. 29]), the interface stress was checked to ensure the bending stress was in the expected range.

The choice of element type was evaluated by running a series of sensitivity studies. For this case, a high order 8-node brick element was chosen over brick element with mid-side nodes. This choice was made because of the relatively thin section of the RT-100 shell versus the length, which made it possible to increase the total number of elements without compromising the run time performance. Several cases were run to vary the total mesh density to see how the stress results varied versus performance of the model. In the extreme case, an overly dense mesh produced excessively long run times and un-converged solutions. Models with low mesh densities that were too low resulted in unrealistic stress results. After numerous runs a balance was found between consistent results and model performance with variations in stress results of less than 1% when comparing high mesh densities to adequate mesh densities. Therefore, it was concluded that the cask model was a quality model and met the intent of ISG-21 [Ref. 53].

At the time the analyses were performed, analyses were generally compared to models previously generated for other 10 CFR 71 [Ref. 2] cask designs. The results of the RT-100 cask analysis are consistent with these previous designs and where peak stress are expected. Additionally, confirmatory scale model testing of the RT-100 demonstrated that the methods used to calculate the cask accelerations and impact limiter deformation are consistent with the drop test results. Therefore, the inertial loads applied to the cask body are conservative.

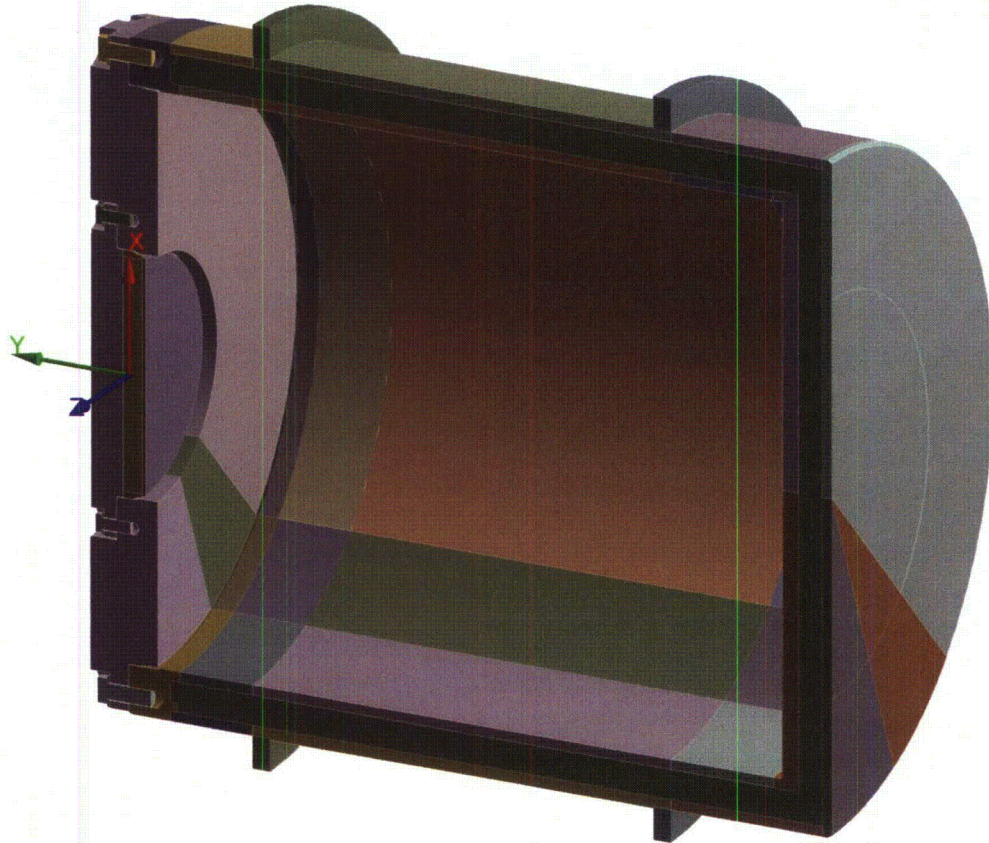


Figure 2.6.7-1 RT-100 Solid Model

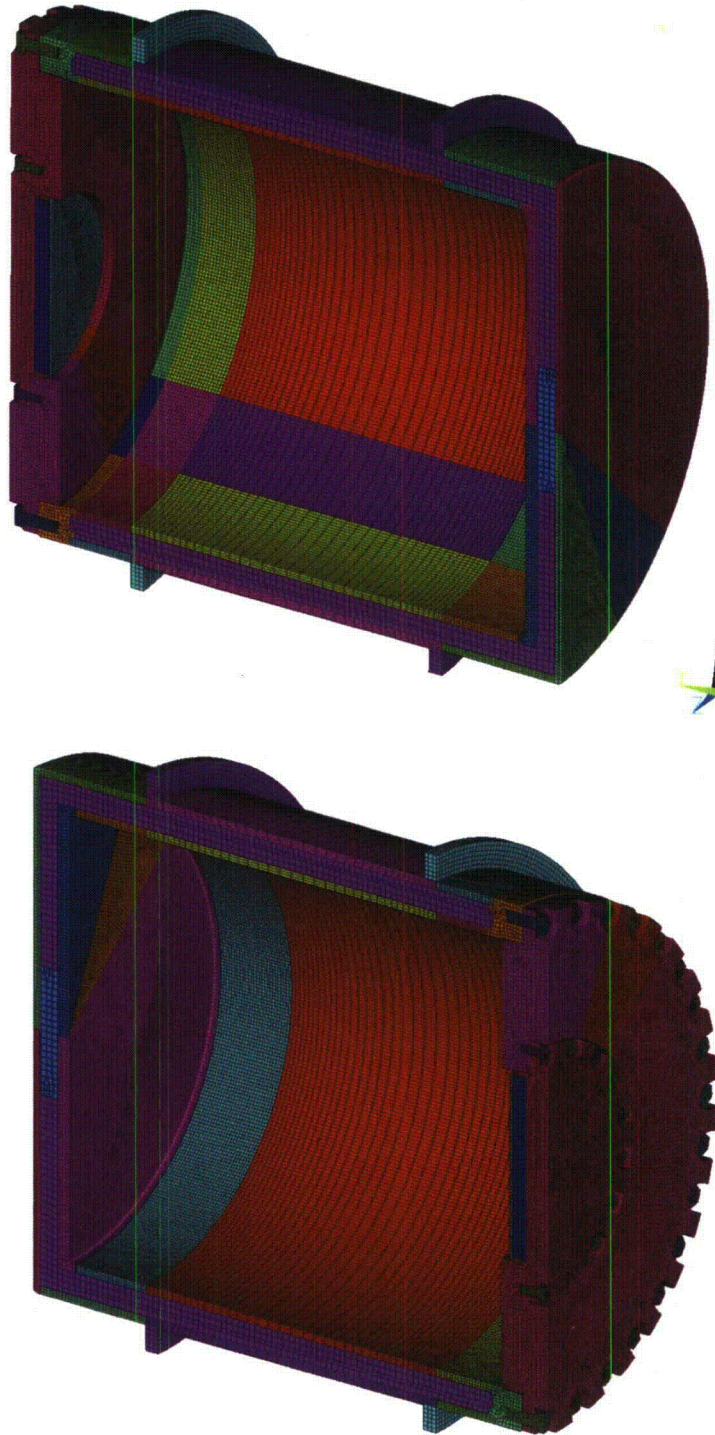


Figure 2.6.7-2 RT-100 Finite Element Model



Figure 2.6.7-3 Gap Elements Used to Represent the Impact Limiters for Side and End Drop Configurations

2.6.7.2.2 Boundary Conditions

Boundary conditions are applied to the model to simulate the loading conditions the RT-100 experiences during NCT and HAC. The five categories of cask loading considered in the free drop event are closure lid bolt preload, internal pressure load, thermal load, inertial body load and displacement.

- Closure Lid Bolt Preload: The required total bolt preloads on the cask outer and inner lid bolts are 130.6 kN and 72.2 kN, respectively (10). To apply the bolt preload ANSYS [Ref. 28] pre-tension elements (PRETS179) are used to define the 3-D pre-tension section within the meshed bolt. The PRETS179 element uses a single translation degree of freedom to define pretension direction (Figure 2.6.7-4). The pretension Section is modeled by a set of pretension elements defined by the bolt shaft.
- Pressure Loading: A pressure of 241 kPa (35 psig) is used to envelope the maximum normal operating pressure for all impact loadings considered (Calculation Package RTL-001-CALC-TH-0102, Rev. 6 [Ref. 42]). For accident conditions, a pressure value of 588 kPa (85.3 psig) is used to represent the pressure experienced during fire conditions (Calculation Package RTL-001-CALC-TH-0202, Rev. 6 [Ref. 43]). The internal pressure load is applied as an equivalent static pressure load uniformly applied on the interior surface of the cask.
- Pressure loading contents—cask end drop: For the end drop analyses, the content weight is assumed to be uniformly distributed on the cask end and over an area determined by the inside diameter of the RT-100. Therefore, one-half the contents weight of 6,804 kg (15,000 lb) is applied to the cask inner shell bottom plate. The contents pressure load is multiplied by the appropriate g-load to accurately represent the 304.8 mm (1-foot) and 9144 mm (30-foot) end drop. The pressure value is conservatively multiplied by 1.05 to account for the difference between the solid model surface and the tessellated area of the element mesh.
- Pressure loading contents—side drop: For the side drop condition, the contact area between the contents and the cask cavity is approximately 180° (90° on each side of the drop centerline). The inertial load produced by the 6,804 kg (15,000 lb) contents weight is represented as an equivalent static pressure applied on the interior surface of the RT-100. The pressure is uniformly distributed along the cavity length and is varied in the circumferential direction as a cosine distribution. The pressure value is conservatively multiplied by 1.05 to account for the difference between the solid model surface and the tessellated area of the element mesh. The maximum pressure occurs at the impact centerline; the pressure decreases to zero at locations that are 90° either side of the impact centerline, as illustrated in Figure 2.6.7-5. The following formula is used to determine the contents pressures for the side drop analyses, which

vary around the circumference.

This method uses a summation scheme to approximate the integration of the cosine-shaped pressure distribution:

$$F_{\text{total}} = \sum_{i=1}^{18} P_{\text{max}} A_i \cos(\theta_i) \cos(\theta'_i)$$
$$F_{\text{total}} = 6,804/2 \text{ kg}$$

Where

- P_{max} = maximum pressure (at impact centerline)
- θ_i = average angle of subtended arc of i^{th} element measured from centerline at point of impact to obtain vertical component of pressure
- i = i^{th} circumferential sector
- θ'_i = normalized angle to peak at 0° and to be zero at 90°
- A_i = i^{th} circumferential area over which the pressure is applied

Gap elements are defined at both ends of the cask to simulate the pressure applied by the impact limiters during side drop conditions. This is accomplished by defining the gap stiffness as a cosine function from a maximum value $175 \times 10^6 \text{ N/m}$ ($1 \times 10^6 \text{ lb/in}$) at the center line to $15.3 \times 10^6 \text{ N/m}$ ($87,156 \text{ lb/in}$) at 85° from the center line of impact, and a minimal value $175 \times 10^3 \text{ N/m}$ (100 lb/in) from 90° to 180° . The load distribution that results from the crushing of the impact limiter is shown in Figure 2.6.7-3.

- o Thermal: According to Regulatory Guide 7.8 [Ref. 3], four credible thermal conditions must be considered

Condition 1 – Hot Case 1:

- a. Ambient temperature, 38°C
- b. Initial temperature, 38°C
- c. Heat transfer to ambient by natural convection, still air
- d. Heat transfer to ambient by radiation
- e. Steady-state Solar insolation
- f. Internal heat load as a uniform heat flux, 13.04 W/m^2

Condition 2 – Hot Case 2:

- a. Ambient temperature, 38°C
- b. Initial temperature, 38°C
- c. Heat transfer to ambient by natural convection, still air
- d. Heat transfer to ambient by radiation
- e. No solar insolation, in shade
- f. Internal heat load as uniform heat flux, 13.04 W/m^2

Condition 3 – Cold Case 1:

- a. Ambient temperature, -40°C
- b. Initial temperature, -40°C
- c. Heat transfer to ambient by natural convection, still air
- d. Heat transfer to ambient by radiation
- e. No solar insolation, in shade
- f. Internal heat load as a uniform heat flux, 13.04 W/m²

Condition 4 – Cold Case 2:

- a. Ambient temperature, -29°C
- b. Initial temperature, -29°C
- c. Heat transfer to ambient by natural convection, still air
- d. Heat transfer to ambient by radiation
- e. No solar insolation
- f. Internal heat load as a uniform heat flux, 13.04 W/m²

Heat Conditions 1 and 3 bound the differential the worst case thermal expansion between dissimilar materials. Therefore, Heat Conditions 2 and 4 are not considered.

The cask temperature distributions calculated for Conditions 1 and 3 are used as inputs to the ANSYS [Ref. 28] analyses. The ANSYS analyses determine the stresses arising from the thermal expansion of the cask from its initial 21°C condition, including the effects of the differential thermal growth within the components; these effects are a result of the temperature difference across the cask walls. The cask temperature distributions are also used to determine the values of the temperature-dependent material properties.

The temperatures for the structural analysis are obtained from the results file and database file of the thermal analysis by writing the results to an ASCII file using the ANSYS BFINT command. Nodes for the structural model are transferred to the same coordinate system as used by the thermal run and the thermal results are interpolated for each thermal condition.

- Inertial body load: The inertial effects, which occur during impact, are represented by equivalent static forces, in accordance with the D'Alembert's principle. The inertial body load includes the weight of the empty cask and the weight of the cavity contents. Accelerations are calculated in Appendix 2.13. An acceleration of 44g and 52g are applied to the model to simulate end drop and side drop conditions, respectively. The inertial load is applied to the cask body using the ANSYS ACEL command equivalent to the normal and accident conditions accelerations corresponding to the 0.3 meter and 9 meter drop cases. Since the lead shield is attached to the steel shells with frictionless contact elements, the lead represents the largest physical load applied to the cask structure.

- Displacement boundary conditions: Displacement boundary conditions are applied to enforce symmetry at the cut boundary of the 3D model. All nodes on the symmetry plane are fixed in the UZ direction. The overall model is stabilized by the gap elements (CONTAC52) that represent the impact limiter, which are connected to the cask body with the outer nodes or “ground” nodes representing the impact limiter fixed.

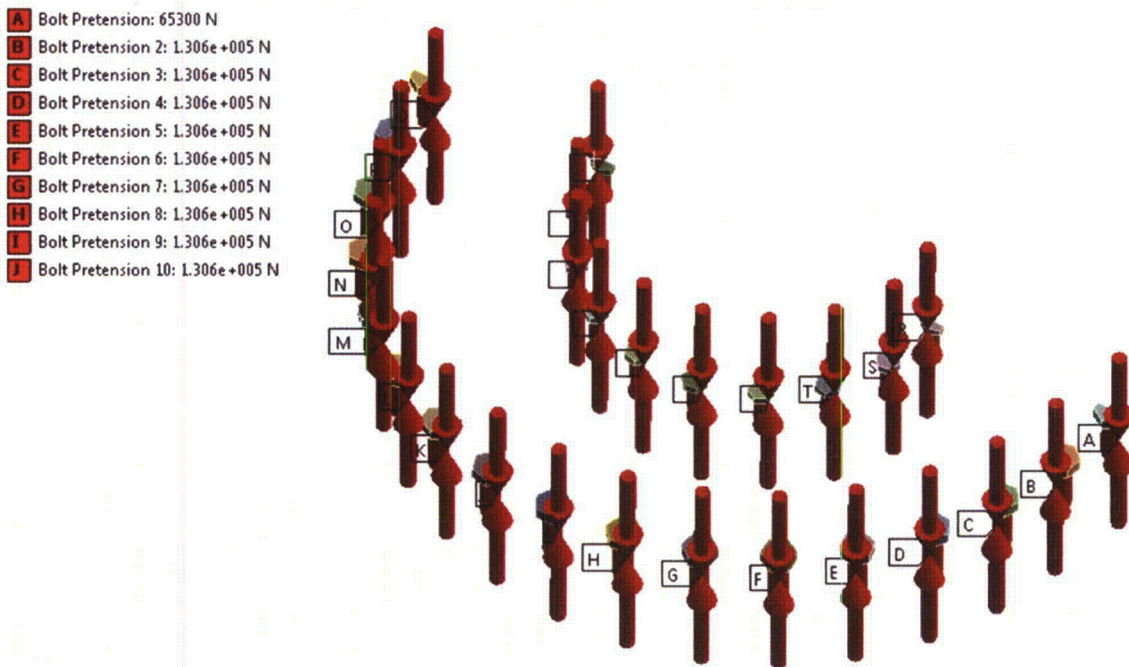


Figure 2.6.7-4 Bolt Pre-load Using ANSYS Pre-Tension Elements (PRETS179)

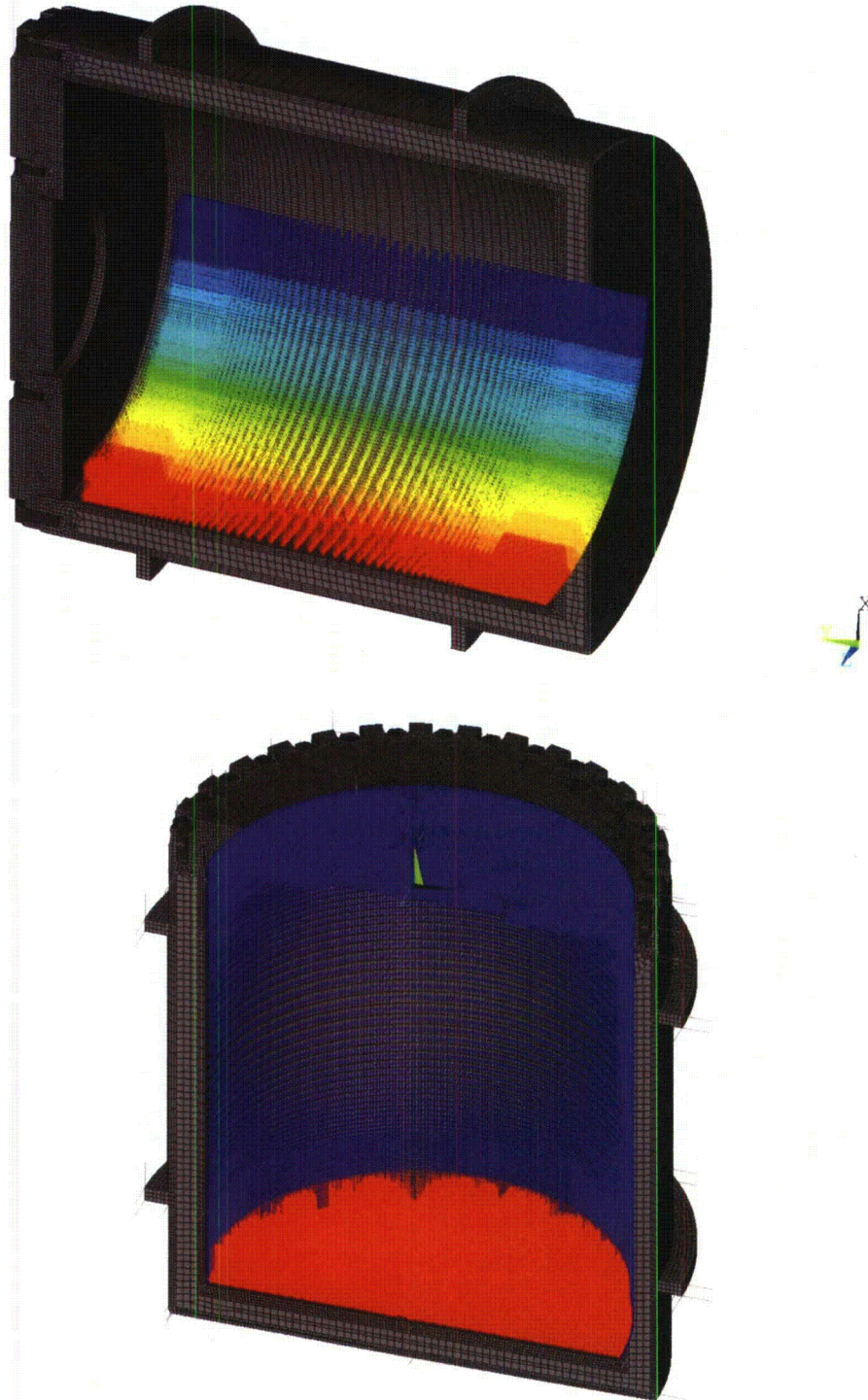


Figure 2.6.7-5 Pressure Distribution Used to Simulate the Contents

2.6.7.3 Side Drop

In accordance with the requirements of 10 CFR 71.71 [Ref. 2], the RT-100 is structurally evaluated for the normal condition of transport 0.3 meter side-drop. During the 0.3 meter side-drop event, the cask (equipped with an impact limiter over each end) falls a distance of 0.3 meter onto a flat, unyielding, horizontal surface. The cask strikes the surface in a horizontal position, thereby resulting in a side impact of the cask. The types of loading involved in a side-drop event are lid closure bolt preload, internal pressure load, thermal load, and inertial body load.

Stress results for the 0.3 meter side drop combined loading conditions discussed previously are documented in Table 2.6.7-1. The table documents the primary membrane (P_m), primary membrane plus primary bending (P_m+P_b), primary membrane plus primary bending plus secondary peak stress (P_m+P_b+Q) in accordance with the criteria presented in Regulatory Guide 7.6 [Ref. 4].

As shown in Table 2.6.7-1, the margins of safety are positive when compared to the stress intensity for each category. The most critically stressed component in the system is the inner lid. The minimum margin of safety is found to be +0.8 for primary membrane plus bending stress intensity. The locations of the critical sections correspond to the maximum stress location shown in Figures 2.6.7.3-1 through 2.6.7.3-11. The minimum margin of safety for primary plus secondary stress intensity is +1.5.

Table 2.6.7-1 NCT Side Drop Stress Summary

Component and Stress State	Stress Location	ANSYS Results (MPa)				RG 7.6 Allowable Stress	Margin of Safety (1)	
		S1	S2	S3	SINT			
INNER SHELL	P_m	5.0	-3.8	-31.6	36.6	138	2.8	
	$P_m + P_b$	Inside	5.3	-3.8	-31.4	36.7	207	4.6
		Center	5.0	-3.8	-31.6	36.6	207	4.7
		Outside	4.7	-3.8	-31.8	36.5	207	4.7
	Hot $P_m + P_b + Q$	Inside	5.3	-3.8	-31.4	36.7	414	10.3
		Center	5.0	-3.8	-31.6	36.6	414	10.3
		Outside	4.7	-3.8	-31.8	36.5	414	10.3
	Cold $P_m + P_b + Q$	Inside	5.3	-3.8	-31.4	36.7	414	10.3
		Center	5.0	-3.8	-31.6	36.6	414	10.3
		Outside	4.7	-3.8	-31.8	36.5	414	10.3
	OUTER SHELL	P_m	4.3	-3.8	-32.3	36.6	138	2.8
		$P_m + P_b$	Inside	4.4	-3.8	-32.2	36.5	207
Center			4.3	-3.8	-32.3	36.6	207	4.7
Outside			4.2	-3.9	-32.5	36.7	207	4.6
Hot $P_m + P_b + Q$		Inside	4.4	-3.8	-32.2	36.5	414	10.3
		Center	4.3	-3.8	-32.3	36.6	414	10.3
		Outside	4.2	-3.9	-32.5	36.7	414	10.3
Cold $P_m + P_b + Q$		Inside	4.4	-3.8	-32.2	36.5	414	10.3
		Center	4.3	-3.8	-32.3	36.6	414	10.3
		Outside	4.2	-3.9	-32.5	36.7	414	10.3
FLANGE		P_m	4.1	-3.9	-32.9	37.0	138	2.7
		$P_m + P_b$	Inside	4.1	-3.9	-32.7	36.8	207
	Center		4.1	-3.9	-32.9	37.0	207	4.6
	Outside		4.1	-4.0	-33.0	37.1	207	4.6
	Hot $P_m + P_b + Q$	Inside	4.1	-3.9	-32.7	36.8	414	10.2
		Center	4.1	-3.9	-32.9	37.0	414	10.2
		Outside	4.1	-4.0	-33.0	37.1	414	10.2
	Cold $P_m + P_b + Q$	Inside	4.1	-3.9	-32.7	36.8	414	10.2
		Center	4.1	-3.9	-32.9	37.0	414	10.2
		Outside	4.1	-4.0	-33.0	37.1	414	10.2
	OUTER LID	P_m	18.4	-0.3	-18.4	36.8	138	2.7
		$P_m + P_b$	Inside	51.6	9.5	7.4	44.3	207
Center			18.4	-0.3	-18.4	36.8	207	4.6
Outside			-8.9	-12.7	-47.7	38.8	207	4.3
Hot $P_m + P_b + Q$		Inside	62.8	-15.8	-41.9	104.7	414	3.0
		Center	11.4	-12.5	-39.4	50.8	414	7.1
		Outside	12.9	-2.4	-41.7	54.5	414	6.6
Cold $P_m + P_b + Q$		Inside	116.0	61.8	27.6	88.4	414	3.7
		Center	30.1	5.4	-17.7	47.8	414	7.7
		Outside	-4.4	-13.7	-55.0	50.7	414	7.2
INNER LID		P_m	-1.5	-2.6	-56.9	55.4	138	1.5
		$P_m + P_b$	Inside	-4.2	-19.9	-121.3	117.1	207
	Center		-1.5	-2.6	-56.9	55.4	207	2.7
	Outside		15.9	7.2	0.3	15.7	207	12.2
	Hot $P_m + P_b + Q$	Inside	2.4	-31.7	-161.7	164.1	414	1.5
		Center	15.2	2.8	-58.4	73.6	414	4.6
		Outside	13.5	-5.2	-23.7	37.2	414	10.1
	Cold $P_m + P_b + Q$	Inside	-8.8	-28.7	-148.7	140.0	414	2.0
		Center	4.1	-0.2	-58.8	62.9	414	5.6
		Outside	19.5	4.7	-6.9	26.4	414	14.7

Note: (1) The margin of safety is the ratio of Allowable Stress and the Stress Intensity (SINT) minus 1.

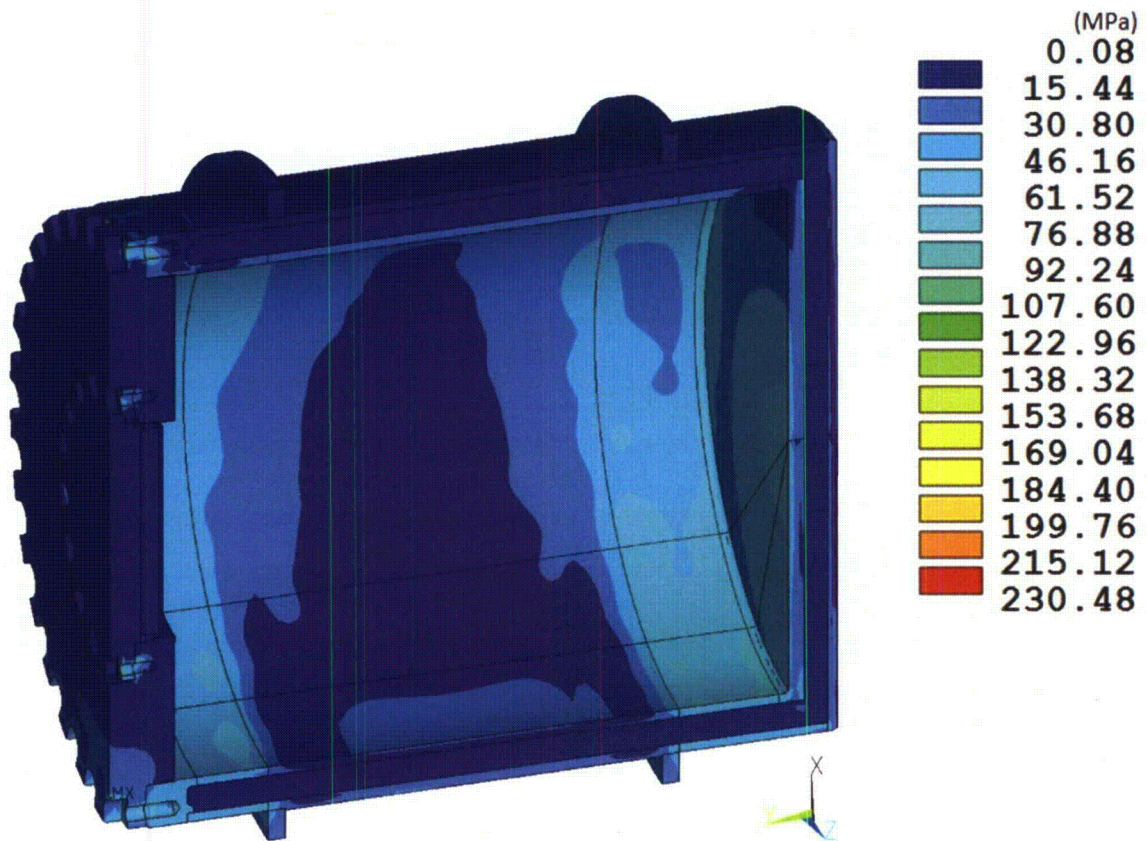


Figure 2.6.7-6 RT-100 NCT Side Drop Stress Intensity Results

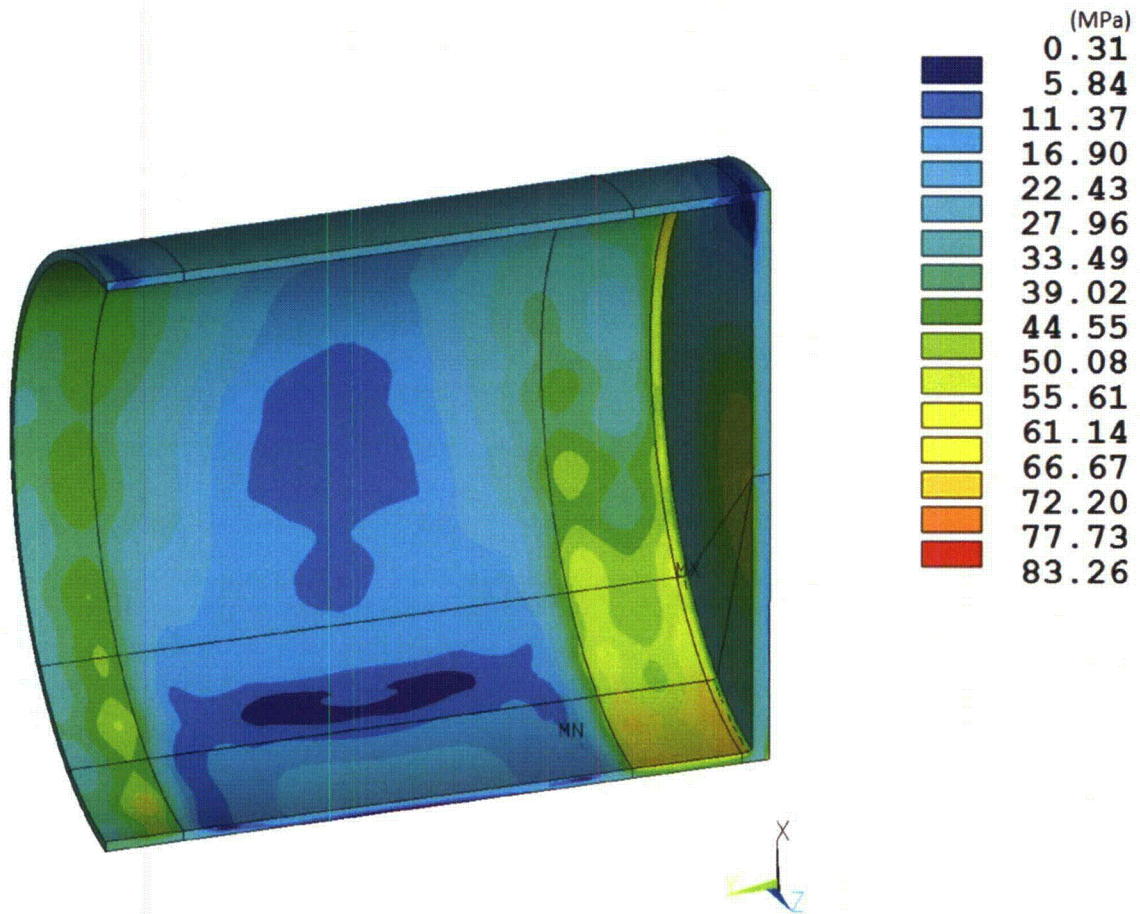


Figure 2.6.7-7 RT-100 Inner Shell NCT Side Drop Stress Intensity Results

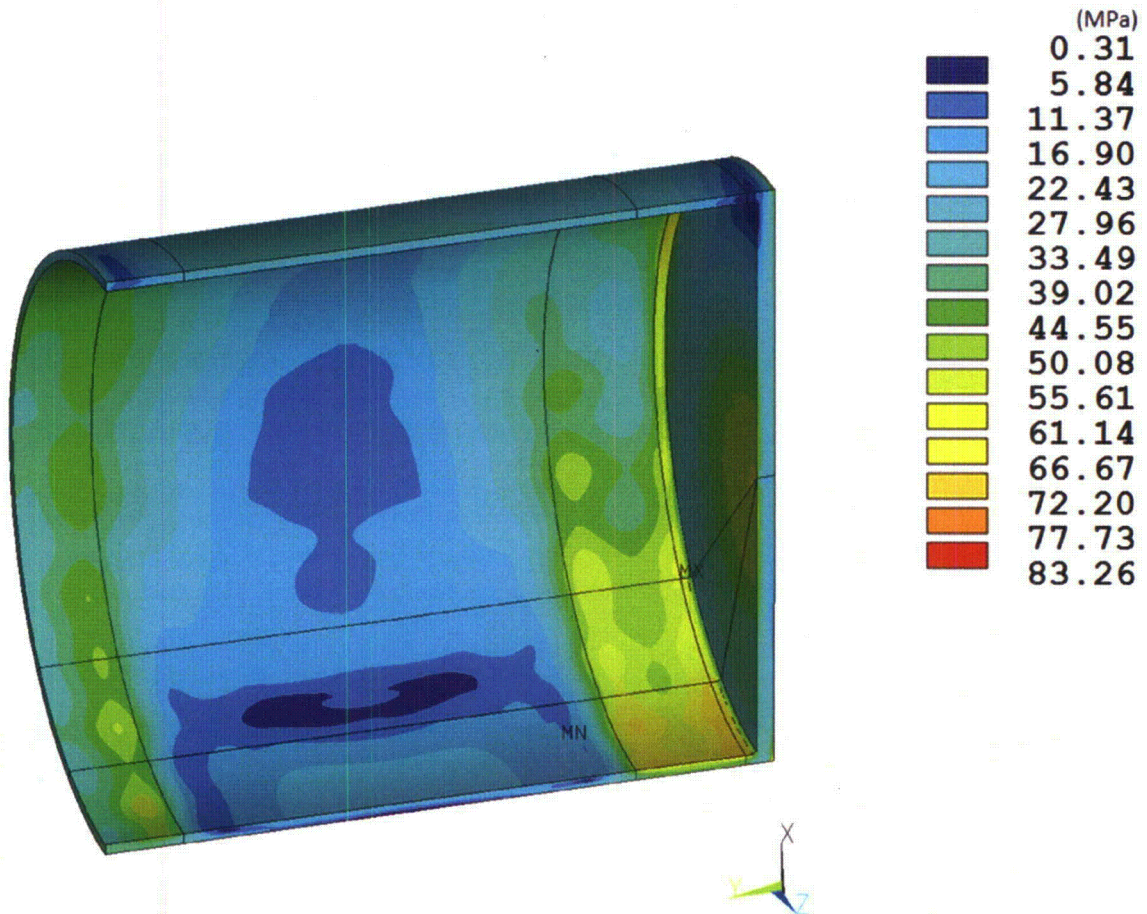


Figure 2.6.7-8 RT-100 Outer Shell NCT Side Drop Stress Intensity Results

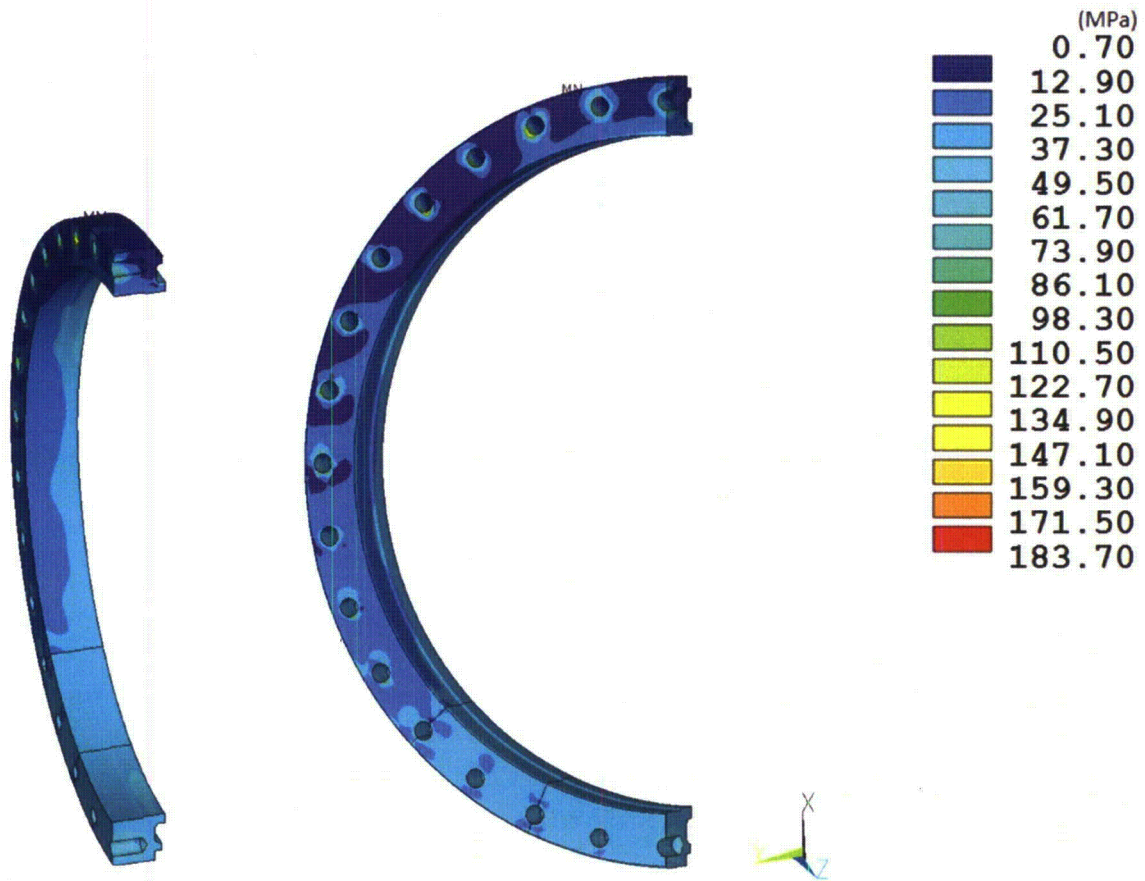


Figure 2.6.7-9 RT-100 Flange NCT Side Drop Stress Intensity Results

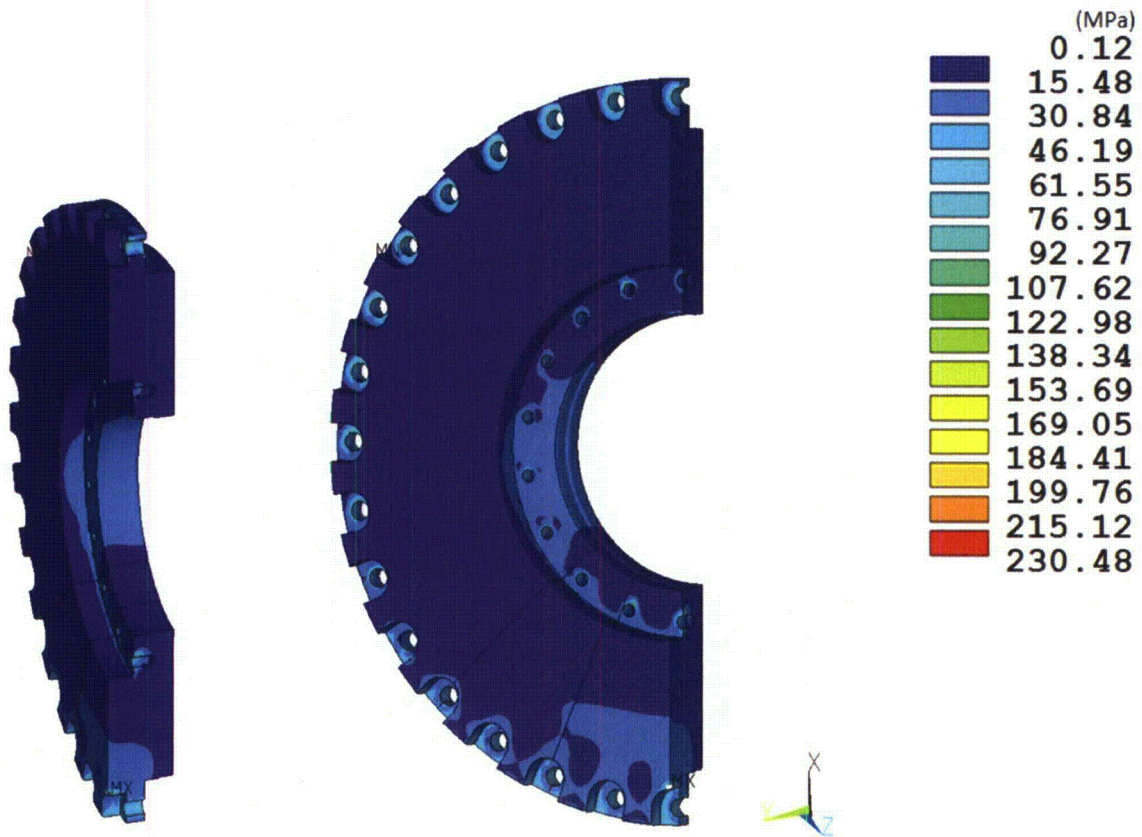


Figure 2.6.7-10 RT-100 Outer Lid NCT Side Drop Stress Intensity Results

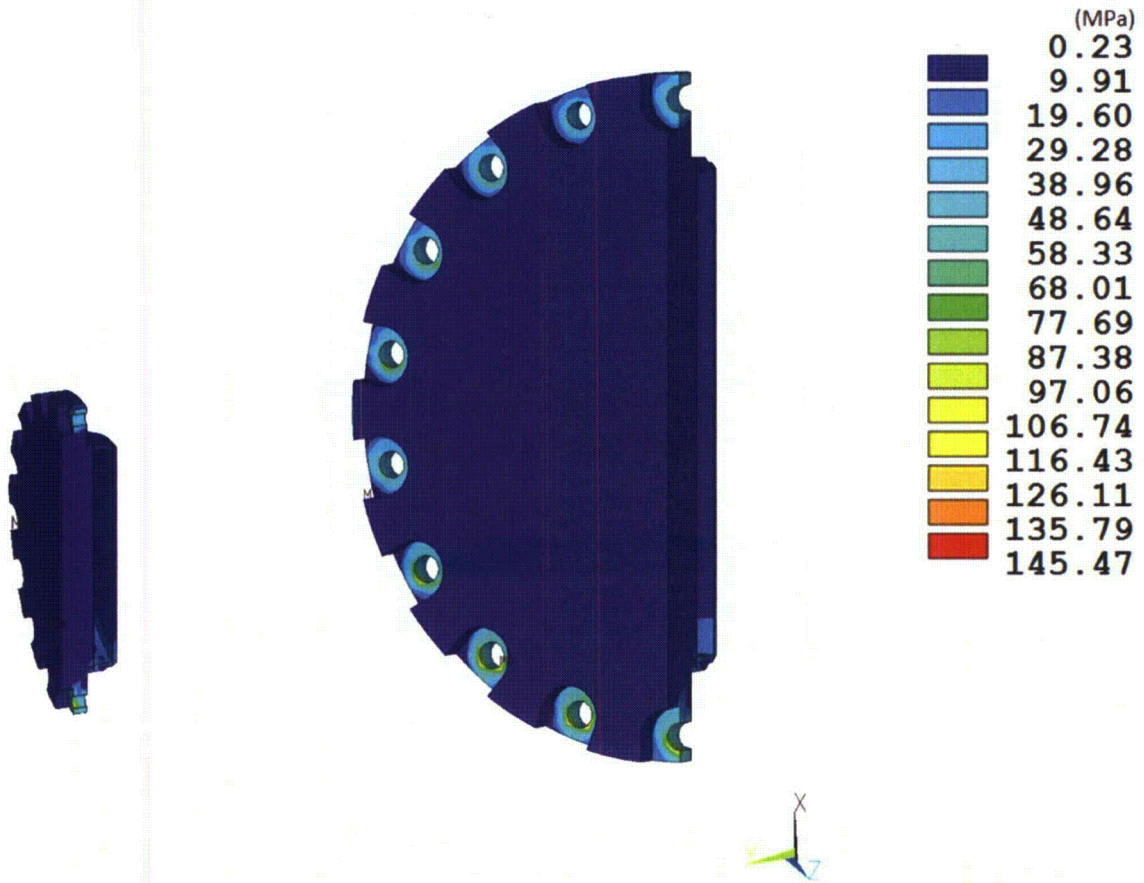


Figure 2.6.7-11 RT-100 Inner Lid NCT Side Drop Stress Intensity Results

2.6.7.4 End Drop

In accordance with the requirements of 10 CFR 71.71 [Ref. 2], the Universal Transport Cask is structurally evaluated for the normal condition of transport 0.3 m end-drop. In this event, the cask (equipped with an impact limiter over each end) falls a distance of 0.3 m onto a flat, unyielding, horizontal surface. The cask strikes the surface in a vertical position; consequently, an end impact on the bottom end or top end of the cask occurs.

As discussed previously, stress results for the 1-ft top and bottom-end drop combined loading conditions are documented in Table 2.6.7-2. The table documents the primary membrane (P_m), primary membrane plus primary bending (P_m+P_b), primary membrane plus primary bending plus secondary peak stress (P_m+P_b+Q) in accordance with the criteria presented in Regulatory Guide 7.6 [Ref. 4].

As shown in the Table 2.6.7-2, the margins of safety for the primary stress intensity category are positive for all of the 0.3 m top-end drop conditions. The most critically stressed component in the system is the cask flange region due to the bending of the flange due to the inertial load imposed by the cask lids. The minimum margin of safety is found to be +2.4 for primary membrane plus bending stress intensity. The locations of the critical sections correspond to the maximum stress location shown in Figure 2.6.7-12 through Figure 2.6.7-17. The minimum margin of safety for primary plus secondary stress intensity is +0.2.

Table 2.6.7-2 NCT End Drop Stress Summary

	Component and Stress State	Stress Location	ANSYS Results (MPa)				RG 7.6 Allowable Stress	Margin of Safety (1)	
			S1	S2	S3	SINT			
INNER SHELL	P _m		2.7	1.2	-7.8	10.5	138	12.1	
	P _m + P _b	Inside	2.7	2.0	-12.2	14.9	207	12.9	
		Center	2.7	1.2	-7.8	10.5	207	18.7	
		Outside	2.9	0.2	-3.6	6.6	207	30.5	
	Hot P _m + P _b + Q	Inside	2.7	2.0	-12.2	14.9	414	26.8	
		Center	2.7	1.2	-7.8	10.5	414	38.3	
		Outside	2.9	0.2	-3.6	6.6	414	61.9	
	Cold P _m + P _b + Q	Inside	2.7	2.0	-12.2	14.9	414	26.8	
		Center	2.7	1.2	-7.8	10.5	414	38.3	
		Outside	2.9	0.2	-3.6	6.6	414	61.9	
	OUTER SHELL	P _m		6.5	-0.9	-3.4	9.9	138	12.9
		P _m + P _b	Inside	7.5	1.0	-2.7	10.2	207	19.3
Center			6.5	-0.9	-3.4	9.9	207	19.9	
Outside			6.9	0.7	-9.0	15.9	207	12.0	
Hot P _m + P _b + Q		Inside	113.3	39.9	-63.2	176.5	414	1.3	
		Center	22.5	-10.9	-16.7	39.2	414	9.5	
		Outside	25.4	0.5	-33.5	58.9	414	6.0	
Cold P _m + P _b + Q		Inside	10.7	0.5	-4.5	15.3	414	26.1	
		Center	18.7	5.7	-4.7	23.5	414	16.6	
		Outside	10.4	2.4	-9.5	19.9	414	19.8	
FLANGE		P _m		5.9	1.5	-12.3	18.1	138	6.6
		P _m + P _b	Inside	0.1	-3.3	-19.5	19.6	207	9.5
	Center		5.9	1.5	-12.3	18.1	207	10.4	
	Outside		20.1	6.3	-13.6	33.7	207	5.1	
	Hot P _m + P _b + Q	Inside	48.0	24.1	-219.4	267.4	414	0.5	
		Center	12.9	-5.7	-23.8	36.6	414	10.3	
		Outside	74.0	34.2	-53.9	127.9	414	2.2	
	Cold P _m + P _b + Q	Inside	32.8	-42.6	-105.1	137.9	414	2.0	
		Center	14.2	2.1	-24.1	38.3	414	9.8	
		Outside	92.7	71.4	-36.7	129.4	414	2.2	
	OUTER LID	P _m		-0.9	-4.0	-14.6	13.7	138	9.1
		P _m + P _b	Inside	-7.7	-17.0	-52.6	45.0	207	3.6
Center			-0.9	-4.0	-14.6	13.7	207	14.1	
Outside			24.2	9.0	5.1	19.0	207	9.9	
Hot P _m + P _b + Q		Inside	280.5	36.7	-55.4	336.0	414	0.2	
		Center	35.3	20.9	-4.7	40.0	414	9.3	
		Outside	41.6	16.7	-56.7	98.3	414	3.2	
Cold P _m + P _b + Q		Inside	-35.0	-71.0	-163.6	128.5	414	2.2	
		Center	14.0	4.5	-14.8	28.8	414	13.4	
		Outside	21.6	-0.3	-22.2	43.8	414	8.4	

Table 2.6.7-2 (Continued)

Component and Stress State	Stress Location	ANSYS Results (MPa)				RG 7.6 Allowable Stress	Margin of Safety (1)
		S1	S2	S3	SINT		
P _m		5.7	-2.3	-35.4	41.1	138	2.4
P _m + P _b	Inside	-6.5	-10.3	-67.7	61.3	207	2.4
	Center	5.7	-2.3	-35.4	41.1	207	4.0
	Outside	20.8	6.0	-6.5	27.3	207	6.6
Hot P _m + P _b + Q	Inside	-14.6	-27.5	-112.1	97.5	414	3.2
	Center	28.9	11.0	-26.3	55.2	414	6.5
	Outside	18.9	-8.7	-36.5	55.3	414	6.5
Cold P _m + P _b + Q	Inside	-18.9	-23.7	-93.0	74.1	414	4.6
	Center	9.7	-1.3	-39.2	49.0	414	7.4
	Outside	23.4	3.1	-13.5	36.8	414	10.2

Note: The margin of safety is the ratio of the Allowable Stress and the Stress Intensity (SINT) minus 1.

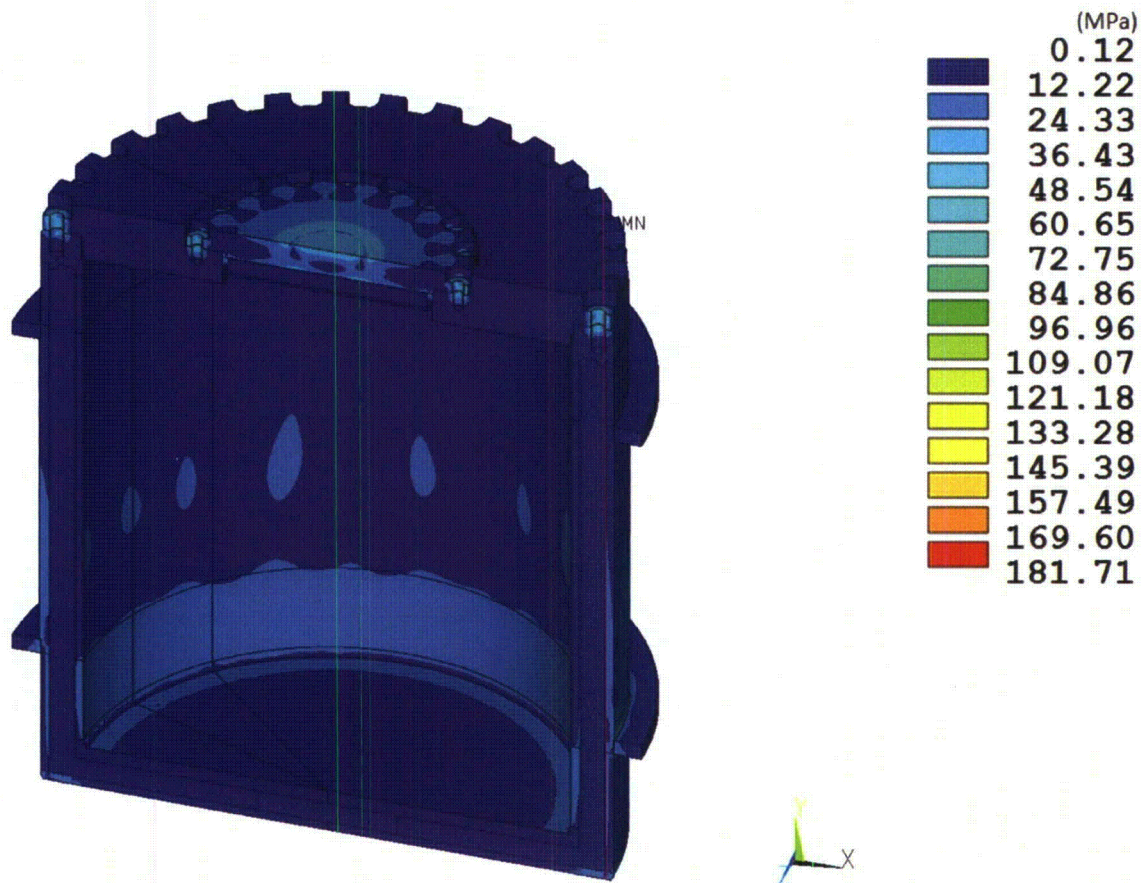


Figure 2.6.7-12 RT-100 NCT Bottom Drop Stress Intensity Results

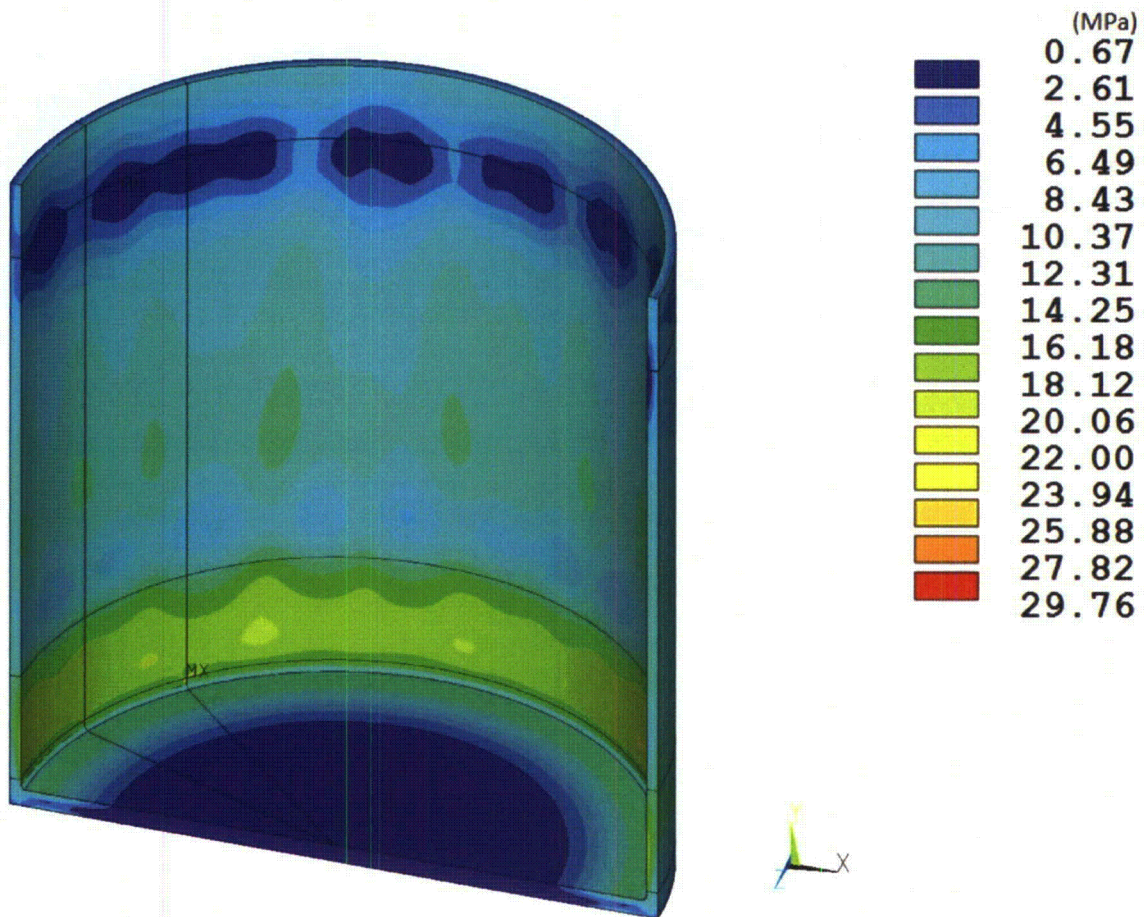


Figure 2.6.7-13 RT-100 Inner Shell NCT End Drop Stress Intensity Results

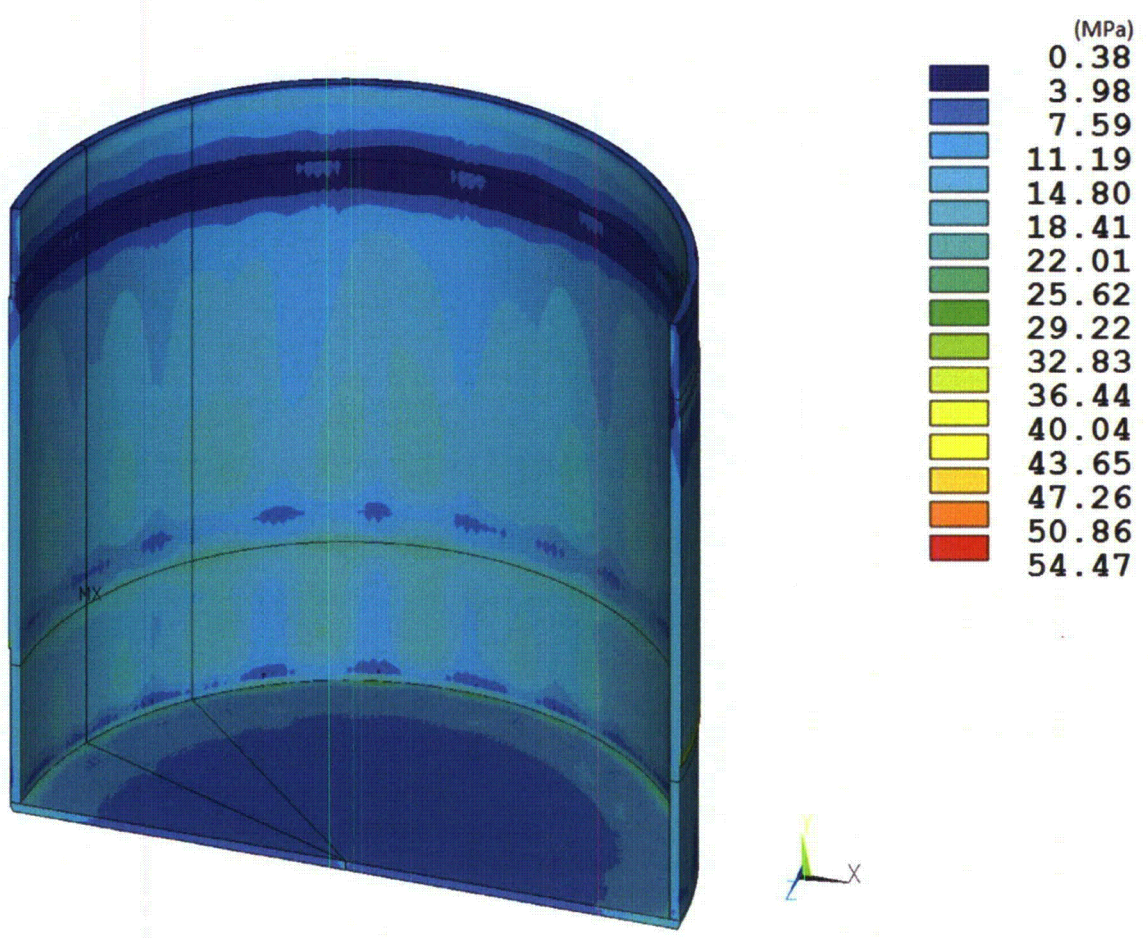


Figure 2.6.7-14 RT-100 Outer Shell NCT End Drop Stress Intensity Results



Figure 2.6.7-15 RT-100 Flange NCT End Drop Stress Intensity Results

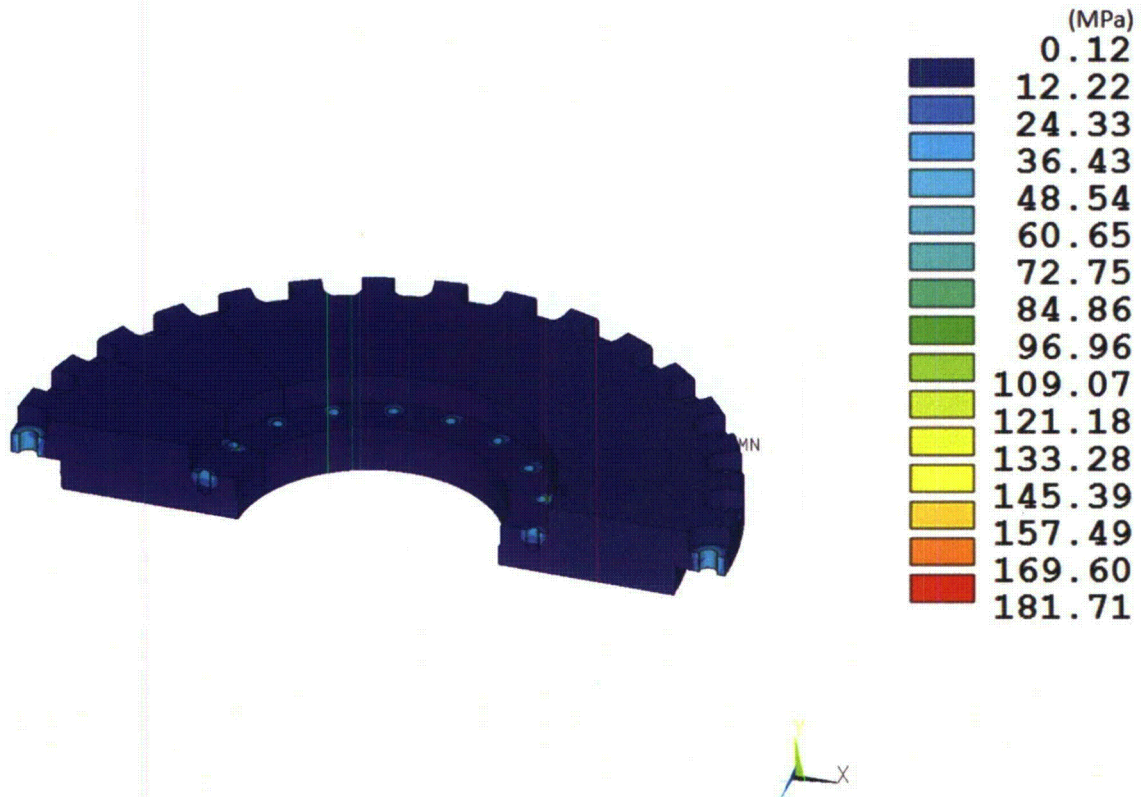


Figure 2.6.7-16 RT-100 Outer Lid NCT End Drop Stress Intensity Results

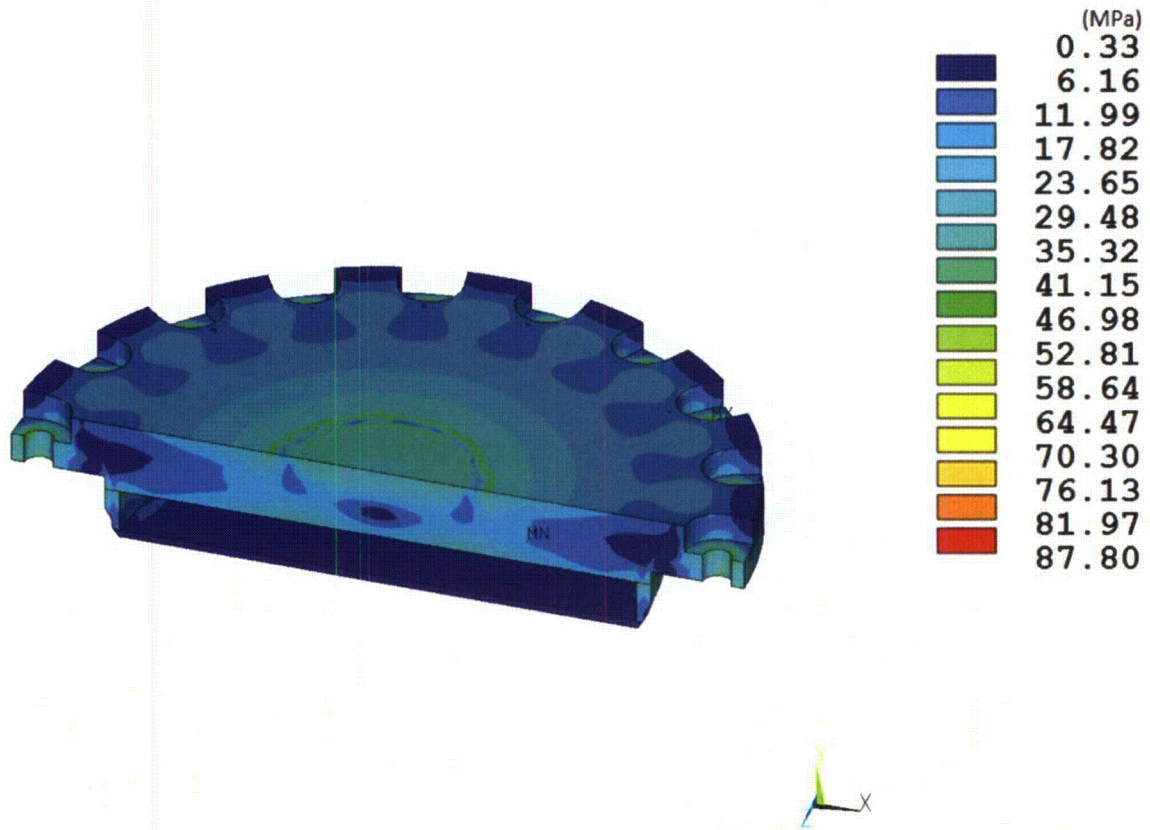


Figure 2.6.7-17 RT-100 Inner Lid NCT End Drop Stress Intensity Results

2.6.8 Corner Drop

The RT-100 is composed of materials other than fiberboard or wood. Also, the weight of the RT-100 exceeds 100 kg. According to 10 CFR 71.71(c)(8) [Ref. 2], the corner drop test is not applicable to the RT-100.

2.6.9 Compression

According to 10 CFR 71.71(c)(9) [Ref. 2], the compression test is not applicable to the RT-100 because the package weight is greater than 5,000 kg.

2.6.10 Penetration

According to 10 CFR 71.71(c)(10) [Ref. 2], a penetration test involving a 13-lb (6-kg) penetration cylinder dropped from a height of 1 m is required for evaluation of packages during normal conditions of transport. However, Regulatory Guide 7.8 [Ref. 3] states that “the penetration test of 10 CFR 71.71 [Ref. 2] is not considered by the NRC staff to have structural significance for large shipping casks (except for unprotected valves and rupture disks) and is not considered as a general requirement.” A penetration test is not performed since the RT-100 has no unprotected valves or rupture disks that could be affected by normal conditions of transport.

2.7 Hypothetical Accident Conditions

The RT-100 Cask meets the standards specified in 10 CFR 71.51 [Ref. 2] when subjected to the conditions and tests specified in 10 CFR 71.73 [Ref. 2] for hypothetical accidents. In accordance with 10 CFR 71.73 [Ref. 2], the RT-100 is structurally evaluated for hypothetical accident scenarios of free drop, puncture, fire, crush, and water immersion. In the free-drop and puncture analyses, the cask impact orientation evaluated is the one that inflicts the maximum damage to the cask. The most unfavorable ambient temperature condition during operation in the range from -40°C to 38°C is assumed. The following sections contain the evaluation of the cask for structural integrity under the hypothetical accident conditions.

2.7.1 Free Drop

The RT-100 Cask is required by 10 CFR 71.73(c)(1) [Ref. 2] to demonstrate structural adequacy for a free drop through a distance of 9 meters onto a flat, unyielding, horizontal surface. The cask payload is oriented to strike the surface to inflict the maximum damage. In determining the orientation that produces the maximum damage, the cask is evaluated for impact orientations in which the cask strikes the impact surface on its bottom end and side. Evaluation of each drop orientation is performed by using finite element analysis techniques. A complete description of the 3-D model used to analyze the cask body is presented in Section 2.6.7.2. The results of each drop orientation listed above are presented in this section. The impact limiters are evaluated in Appendix 2.12 for all loading conditions and orientations. These analyses provide the inertial loads (maximum “g-loads”) imparted to the cask for each drop orientation (Table 2.12.6-1). Cask body decelerations used in NCT and HAC finite element analyses are shown in Table 2.7.1-1.

Table 2.7.1-1 Deceleration Loadings in RT-100 Cask Body Finite Element Analyses

Case	End Drop (g)	Side Drop (g)
HAC (Drop Height = 9.0 m)	123	226
NCT (Drop Height = 0.3 m)	44	52

The mass of the contents is considered when evaluating impact and environmental temperature for the drop is between -40°C and 38°C. For the accident condition, stresses arising from thermal expansion are not considered. However, for determination of properties, the temperatures are considered. The mean normal operating pressure of 241 (kPa) 35 psig is applied in the finite element models to produce the bounding critical stress condition in conjunction with the other loads previously discussed. A separate analysis evaluates the stresses associated with the accident pressure of 588 kPa (85.3 psig) that results from the regulatory fire event. Closure lid bolt preload is considered (Appendix 2.13 and Section 2.6.7.2.2) and fabrication stresses are discussed (Appendix 2.14). The following method and assumptions are adopted in all the hypothetical accident drop analyses:

The following sections contain the evaluation of the RT-100 for impact orientations in which the cask strikes the impact surface on its bottom end and side. The impact conditions (in accordance with Regulatory Guide 7.8 [Ref. 3] and the categories of load to be considered for the hypothetical accident conditions) are similar to those for the 0.3 meter free drops under normal conditions of transport as discussed in Section 2.6.7. Therefore, the discussions in the following sections refer to Section 2.6.7 wherever applicable.

Three categories of load—closure lid bolt preload, internal pressure, and inertial body loads—are considered on the cask. The inertia loads imposed upon the cask by the impact limiter result from the mass of the entire assembly being acted upon by a design deceleration value of 123 g for the 30-ft end-drop case. The closure lid bolt preload, internal pressure load, and contents loads considered for the 30-ft end-drop condition are similar to those considered for 1-ft end-drop condition in Section 2.6.7.2, with the exception that thermal stresses are not considered for accident conditions. The material properties of the components are considered to be temperature dependent.

The allowable stress limits criteria are discussed in Section 2.6.7.1. These criteria are used to determine the allowable stresses for each cask component, conservatively using the maximum operating temperature within a given component to determine the allowable stress throughout that component. For cask body analyses presented in this section, the maximum heat conditions (thermal condition 1) are 38°C ambient temperature, maximum decay heat load, and maximum solar insolation.

During fabrication of the RT-100, thermal stresses can be introduced in the inner and outer shells as a result of pouring molten lead between them. Residual stresses may be induced in the inner shell (containment boundary) and the outer shell due to shrinkage of the lead shielding subsequent to lead pouring operations; however, these stresses are relieved early in the life of the cask because of the low creep strength of lead. Therefore, the effects of stresses resulting from the cask fabrication processes are considered negligible. Further discussion of fabrication stresses is

provided in Appendix 2.14.

2.7.1.1 End Drop

In accordance with the requirements of 10 CFR 71.73(c)(1) [Ref. 2], the RT-100 is structurally evaluated for the 30-foot end-drop condition. In this hypothetical accident, the cask including the payload, spacer (if appropriate), and the impact limiters falls 30 feet onto a flat, unyielding, horizontal surface. The cask strikes the surface in a vertical position and results in an end impact on the bottom of the cask. The types of loading involved in an end-drop accident are closure lid bolt preload, internal pressure, and inertial body load. Section 2.6.7.2 describes the application of each loading condition.

2.7.1.1.1 End Drop Evaluation

In accordance with the requirements of 10 CFR 71.73(c)(1) [Ref. 2], the RT-100 is structurally evaluated for the 30-foot end-drop condition. In this hypothetical accident, the cask including the payload and the impact limiters falls 30 feet onto a flat, unyielding, horizontal surface. The cask strikes the surface in a vertical upright position. For the RT-100 cask, the bottom end drop is bounding. In the bottom down position, the prying load on the closure bolts is maximized.

Stress results for the 9-meter bottom end drop combined are documented in Table 2.7.1-2. The table documents the primary membrane (P_m), primary membrane plus primary bending (P_m+P_b) stresses in accordance with the criteria presented in Regulatory Guide 7.6 [Ref. 4].

As shown in Table 2.7.1-2, the margins of safety when compared to the stress intensity for each category are positive. The most critically stressed component in the system is the flange; this result is due to bending as a result of the inertial loads on the cask lids. The minimum margin of safety is found to be +1.5 for primary membrane plus bending stress intensity. The locations of the critical sections correspond to the maximum stress location shown in Figure 2.7.1-1 through Figure 2.7.1-6.

2.7.1.1.2 Lead Slump Evaluation

The following sections provide the lead slump evaluation of the RT-100. During an end drop accident, the shielding capability of the RT-100 cask may be reduced as a result of lead slump.

2.7.1.1.2.1 Elastic Deformation

The maximum lead slump occurs during the previously analyzed bottom end drop in Section 2.7.1.1.1. The relative displacement is obtained from the finite element analysis. Figure 2.7.1-7 shows the exaggerated displacement plot under this drop orientation. The total elastic displacement of the lead column is 1.62 mm.

2.7.1.1.2.2 Plastic Deformation with Maximum Gap

Maximum plastic deformation of the lead shield occurs when the package experiences extreme cold conditions prior to the end drop. During extreme cold conditions, the contraction of the lead shield forms a small gap at the top of the lead column. The reduced height of the lead shield due to contraction is:

$$h_{\text{lead}} = h_{\text{lead}} (1 + \alpha\Delta T) = 2037.4 \text{ mm}$$

Where,

$h_{\text{lead}} = 2040.9 \text{ mm}$	Initial height of lead shield at 21.1°C
$\alpha = 2.78 \times 10^{-5} \text{ mm/mm/}^\circ\text{C}$	Coefficient of thermal expansion for lead at -40°C
$\Delta T = -40^\circ\text{C} - 21.1^\circ\text{C} = -61.1^\circ\text{C}$	Temperature difference

The reduced height of the annular column formed by the steel shells due to contraction is:

$$h_{\text{steel}} = h_{\text{steel}} (1 + \alpha\Delta T) = 2039.0 \text{ mm}$$

Where,

$h_{\text{steel}} = 2040.9 \text{ mm}$	Initial height of annular column at 21.1°C
$\alpha = 1.48 \times 10^{-5} \text{ mm/mm/}^\circ\text{C}$	Coefficient of thermal expansion for steel at -40°C
$\Delta T = -40^\circ\text{C} - 21.1^\circ\text{C} = -61.1^\circ\text{C}$	Temperature difference

Radial Thermal Expansion

In addition to the gap formed in the axial direction, radial gaps also form during extreme cold conditions. For this evaluation, the interference fit between the cask inner shell and lead shield is ignored because during thermal contraction, the lead applies pressure to the steel inner shell. Since the yield strength of lead is low compared to the steel shell, the lead will conform to the shape of the inner shell. Therefore, the lead volume is not lost during the contraction process and the physical gap between lead and outer shell if any will be significantly less than the values predicted in this calculation. The reduced outside radius of the lead shield at -40°C is:

$$r_o = r_{\text{outer}} (1 + \alpha\Delta T) = 983.3 \text{ mm}$$

Where,

$r_{\text{outer}} = 985.0 \text{ mm}$	Initial outside radius of lead shield = inner radius of steel outer shell at 21.1°C
$\alpha = 2.78 \times 10^{-5} \text{ mm/mm/}^\circ\text{C}$	Coefficient of thermal expansion for lead at -40°C
$\Delta T = -40^\circ\text{C} - 21.1^\circ\text{C} = -61.1^\circ\text{C}$	Temperature difference

The change in inside radius of lead shield at -40°C:

$$r_i = r_{\text{inner}} (1 + \alpha\Delta T) = 893.6 \text{ mm}$$

Where,

$r_{\text{inner}} = 895.1 \text{ mm}$	Inner radius of lead shield at 21.1°C
$\alpha = 2.78 \times 10^{-5} \text{ mm/mm/}^\circ\text{C}$	Coefficient of thermal expansion for lead at -40°C
$\Delta T = -40^\circ\text{C} - 21.1^\circ\text{C} = -61.1^\circ\text{C}$	Temperature difference

The reduced inside radius of the outer steel shell at -40°C:

$$r_o = r_{\text{int}} (1 + \alpha\Delta T) = 984.1 \text{ mm}$$

Where,

$r_{\text{int}} = 985.0 \text{ mm}$	Inner radius of steel outer shell at 21.1°C
-------------------------------------	---

$$\begin{aligned}\alpha &= 1.48 \times 10^{-5} \text{ mm/mm/}^\circ\text{C} && \text{Coefficient of thermal expansion for steel at } -40^\circ\text{C} \\ \Delta T &= -40^\circ\text{C} - 21.1^\circ\text{C} = -61.1^\circ\text{C} && \text{Temperature difference}\end{aligned}$$

The change in outside radius of inner steel shell is at -40°C :

$$r_i = r_{\text{inner}} (1 + \alpha \Delta T) = 894.3 \text{ mm}$$

Where,

$$\begin{aligned}r_{\text{inner}} &= 895.1 \text{ mm} && \text{Inner radius of lead shield at } 21.1^\circ\text{C} \\ \alpha &= 1.48 \times 10^{-5} \text{ mm/mm/}^\circ\text{C} && \text{Coefficient of thermal expansion for steel at } -40^\circ\text{C} \\ \Delta T &= -40^\circ\text{C} - 21.1^\circ\text{C} = -61.1^\circ\text{C} && \text{Temperature difference}\end{aligned}$$

Lead Shield Volume

The previous section shows that the relative contraction of materials during extreme cold conditions results in a small gap between the lead shield and outer steel shell. The small gap formed in the radial directions is sufficient to allow the lead shield to slump during an HAC bottom impact. Following exposure to extreme cold conditions (-40°C), the available volume of the lead column is:

$$V_f = A_f \times h_c = 1.0784 \times 10^9 \text{ mm}^3$$

Where,

$$\begin{aligned}A_f &= \pi (r_o^2 - r_i^2) = 5.293 \times 10^5 \text{ mm}^2 && \text{Cross-sectional area of lead shield} \\ r_o &= 983.3 \text{ mm} && \text{Outside radius of lead shield at } -40^\circ\text{C} \\ r_i &= 893.6 \text{ mm} && \text{Inner radius of lead shield at } -40^\circ\text{C} \\ h_c &= 2037.4 \text{ mm} && \text{Height of lead column at } -40^\circ\text{C}\end{aligned}$$

The cross sectional area of the annulus between the inner and outer shells following exposure to extreme cold conditions (-40°C) is:

$$A_i = \pi (r_o^2 - r_i^2) = 5.3013 \times 10^5 \text{ mm}^2$$

Where,

$$\begin{aligned}r_o &= 984.1 \text{ mm} && \text{Inside radius of steel outer shell at } -40^\circ\text{C} \\ r_i &= 894.3 \text{ mm} && \text{Outside radius of steel inner shell } -40^\circ\text{C}\end{aligned}$$

Lead Slump

Accounting for the contraction of the steel shells and lead shield the reduced height of the lead column based on the net gap is:

$$h_{\text{final}} = V_f / A_i = 2034.2 \text{ mm}$$

Subtracting the reduced height of the lead column from the height of the annular region and ignoring the elastic deformation, the lead slump is:

$$h_{\text{slump}} = h_{\text{steel}} - h_{\text{final}} = 2039.0 - 2034.2 = 4.8 \text{ mm}$$

Table 2.7.1-2 HAC End Drop Stress Summary

Component and Stress State	Stress Location	ANSYS Results				RG 7.6 Allowable Stress	Margin of Safety (1)
		S1	S2	S3	SINT		
INNER SHELL		MPa	MPa	MPa	MPa	MPa	
Pm		7.5	5.7	-30.9	38.4	331	7.6
Pm + Pb	<i>Inside</i>	12.8	6.5	-51.3	64.1	496	6.7
	<i>Center</i>	7.5	5.7	-30.9	38.4	496	11.9
	<i>Outside</i>	8.2	-0.5	-11.2	19.4	496	24.6
OUTER SHELL		MPa	MPa	MPa	MPa	MPa	
Pm		10.7	0.1	-22.0	32.8	331	9.1
Pm + Pb	<i>Inside</i>	7.2	-0.2	-26.3	33.5	496	13.8
	<i>Center</i>	10.7	0.1	-22.0	32.8	496	14.2
	<i>Outside</i>	14.2	0.5	-17.8	32.0	496	14.5
FLANGE		MPa	MPa	MPa	MPa	MPa	
Pm		-5.2	-11.9	-19.5	14.3	331	22.2
Pm + Pb	<i>Inside</i>	-5.9	-13.2	-20.2	14.2	496	33.8
	<i>Center</i>	-5.2	-11.9	-19.5	14.3	496	33.8
	<i>Outside</i>	4.7	-14.9	-23.9	28.6	496	16.3
OUTER LID		MPa	MPa	MPa	MPa	MPa	
Pm		10.1	-2.3	-30.1	40.3	331	7.2
Pm + Pb	<i>Inside</i>	-29.7	-48.1	-104.5	74.8	496	5.6
	<i>Center</i>	10.1	-2.3	-30.1	40.3	496	11.3
	<i>Outside</i>	68.5	45.1	24.1	44.4	496	10.2
INNER LID		MPa	MPa	MPa	MPa	MPa	
Pm		45.2	31.4	9.3	35.9	331	8.2
Pm + Pb	<i>Inside</i>	47.0	-14.6	-143.5	190.4	496	1.6
	<i>Center</i>	45.2	31.4	9.3	35.9	496	12.8
	<i>Outside</i>	172.0	77.5	33.6	138.4	496	2.6

Note: (1) The margin of safety is the ratio of the Allowable Stress and the Stress Intensity (SINT) minus 1.

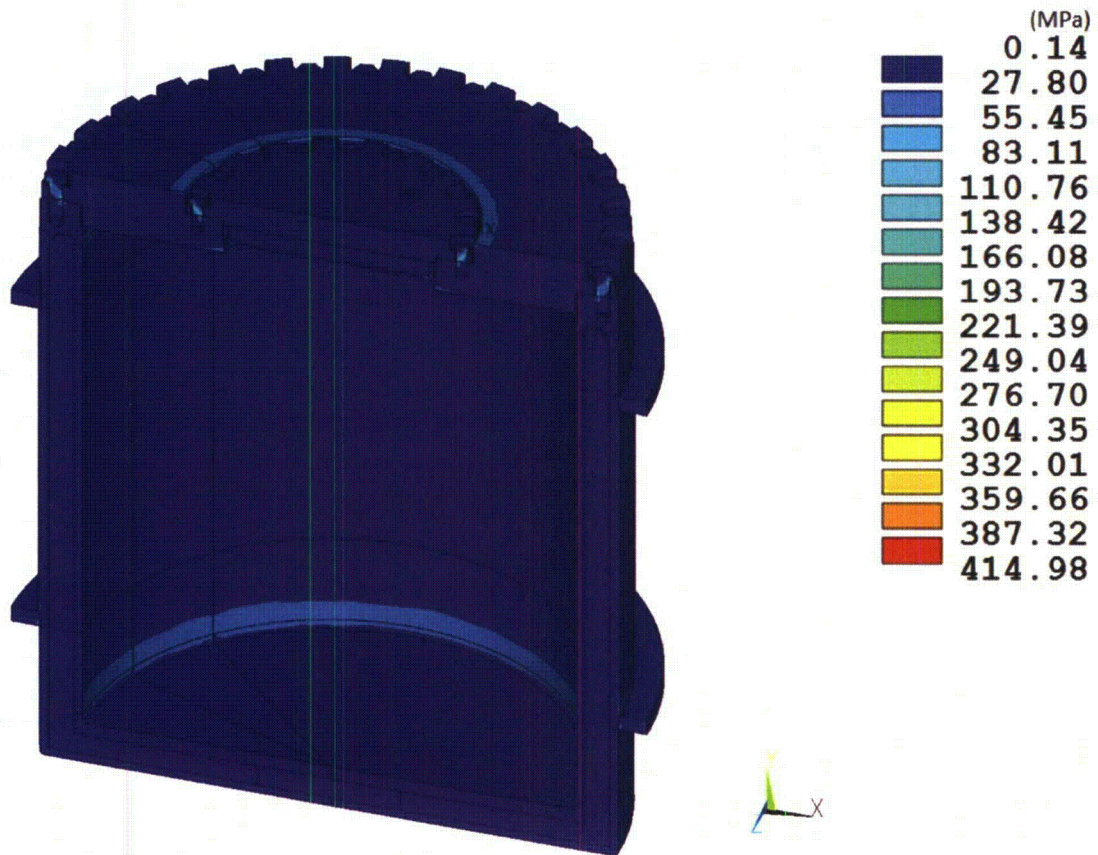


Figure 2.7.1-1 RT-100 HAC End Drop Stress Intensity Results

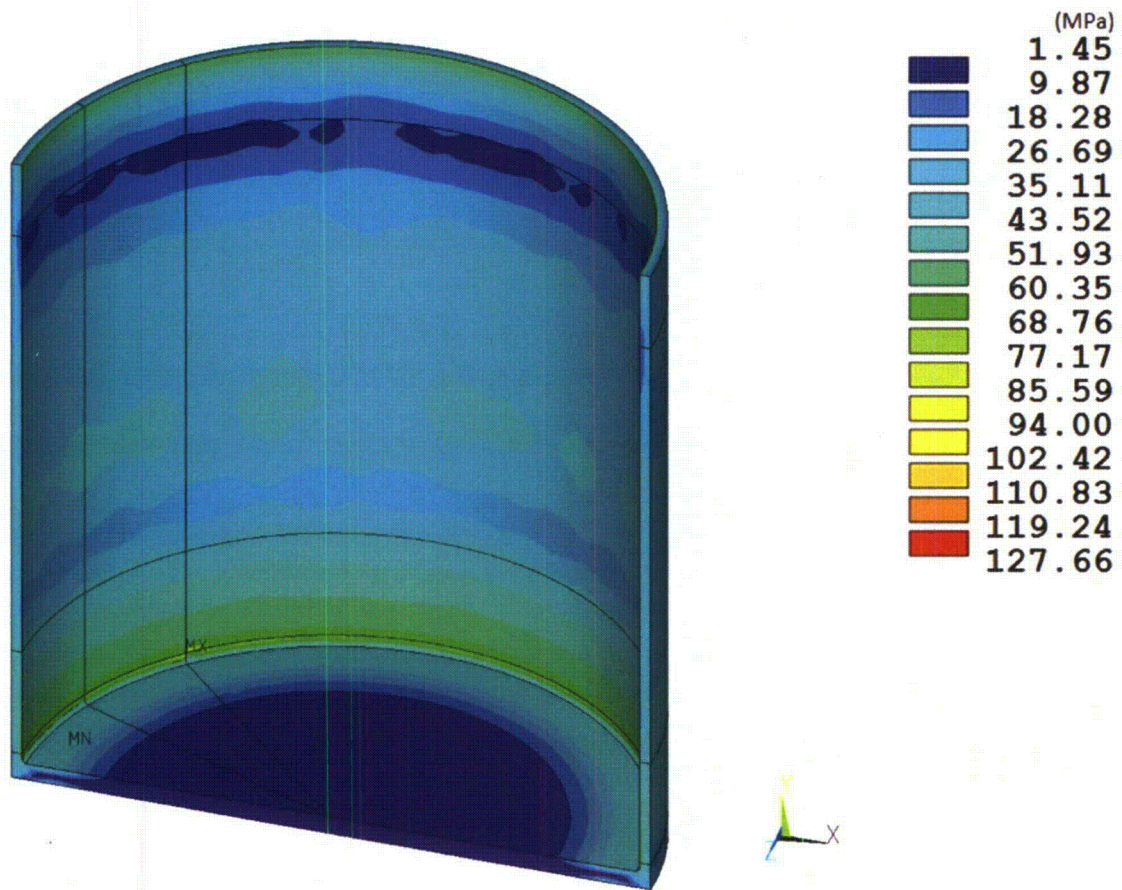


Figure 2.7.1-2 RT-100 Inner Shell HAC End Drop Stress Intensity Results

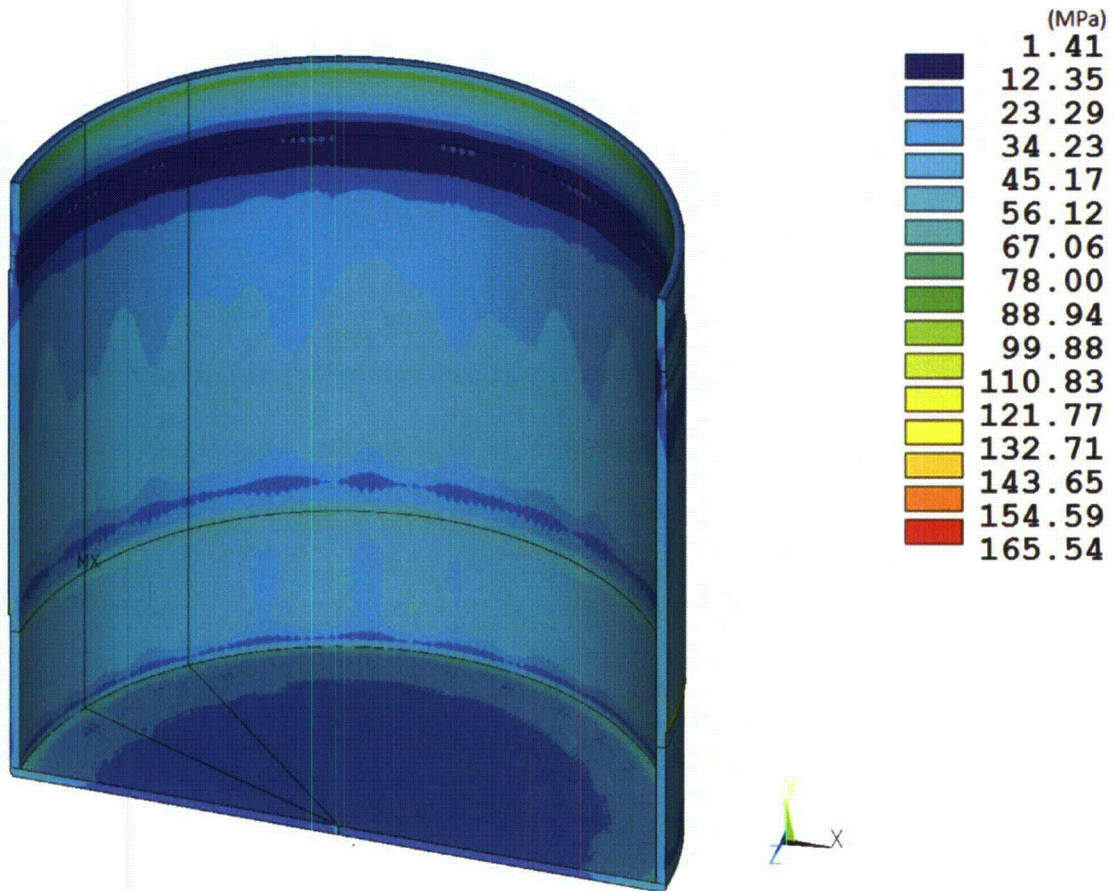


Figure 2.7.1-3 RT-100 Outer Shell HAC End Drop Stress Intensity Results



Figure 2.7.1-4 RT-100 Flange HAC End Drop Stress Intensity Results

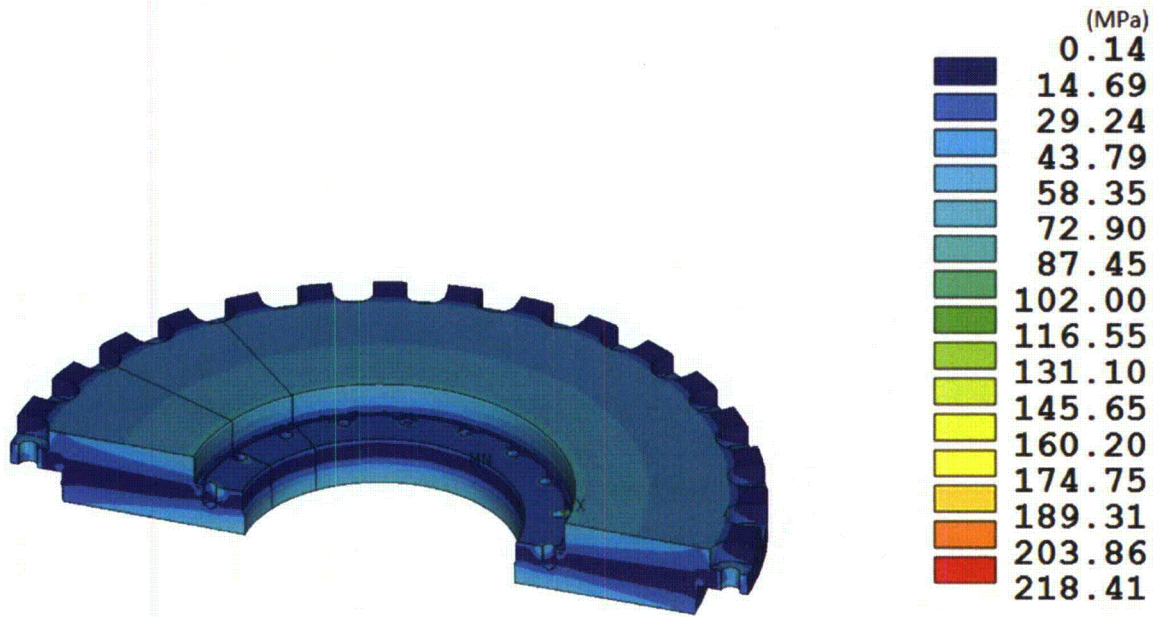


Figure 2.7.1-5 RT-100 Outer Lid HAC End Drop Stress Intensity Results

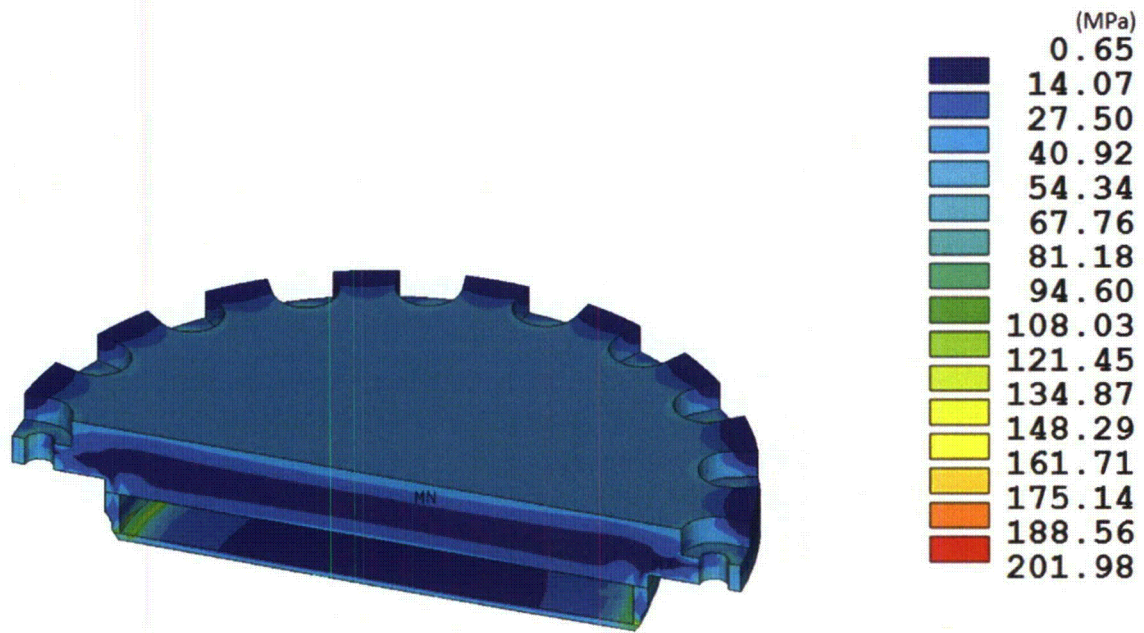


Figure 2.7.1-6 RT-100 Inner Lid HAC End Drop Stress Intensity Results

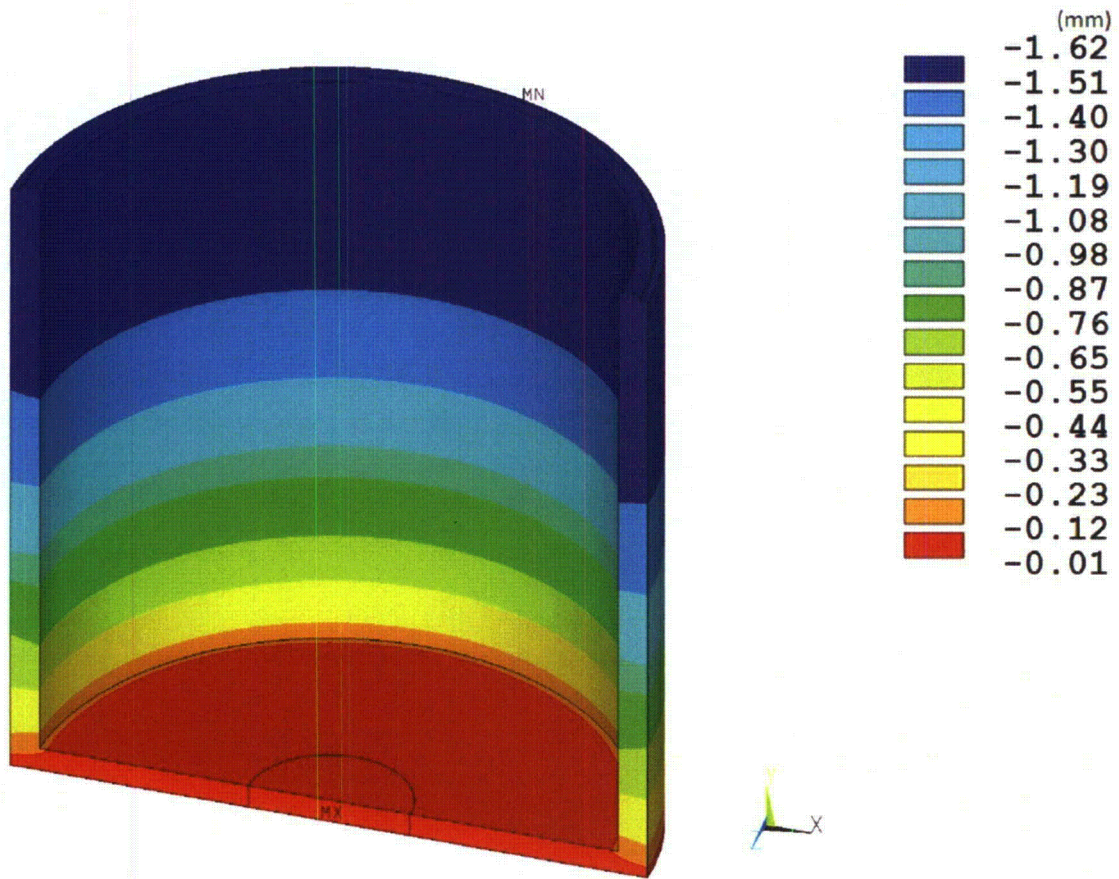


Figure 2.7.1-7 RT-100 Lead Slump

2.7.1.2 Side Drop

In accordance with the requirements of 10 CFR 71.73(c)(1) [Ref. 2], the RT-100 is structurally evaluated for the hypothetical accident 30-foot side drop condition. In this event, the cask including the payload and impact limiters falls 30 feet onto a flat, unyielding, horizontal surface. The package strikes the surface in a horizontal position resulting in a side impact. The types of loading involved in a side drop accident are closure lid bolt preload, internal pressure, and inertial body load.

As previously discussed, stress results for the 9-meter side drop combined loading conditions are documented in Table 2.7.1-3. The table documents the primary membrane (P_m), primary membrane plus primary bending (P_m+P_b), stresses in accordance with the criteria presented in Regulatory Guide 7.6 [Ref. 4].

As shown in Table 2.7.1-3, the margins of safety are positive when compared to the stress intensity for each category. The most critically stressed component in the system is the cask outer shell; this condition is due to ovalization of the cask body and the inertial load of the lead shield. The minimum margin of safety is found to be +0.2 for primary membrane plus bending stress intensity. The locations of the critical sections correspond to the maximum stress location shown in Figure 2.7.1-8 through Figure 2.7.1-13.

Table 2.7.1-3 HAC Side Drop Stress Summary

Component and Stress State	Stress Location	ANSYS Results				RG 7.6 Allowable Stress	Margin of Safety (1)
		S1	S2	S3	SINT		
INNER SHELL		MPa	MPa	MPa	MPa	MPa	
	Pm	19.1	-13.7	-140.4	159.6	331	1.1
Pm + Pb	<i>Inside</i>	20.0	-13.9	-139.7	159.7	496	2.1
	<i>Center</i>	19.1	-13.7	-140.4	159.6	496	2.1
	<i>Outside</i>	18.3	-13.5	-141.3	159.6	496	2.1
OUTER SHELL		MPa	MPa	MPa	MPa	MPa	
	Pm	-14.2	-129.8	-201.4	187.1	331	0.8
Pm + Pb	<i>Inside</i>	-66.9	-166.2	-472.2	405.3	496	0.2
	<i>Center</i>	-14.2	-129.8	-201.4	187.1	496	1.7
	<i>Outside</i>	73.5	36.5	-95.5	169.0	496	1.9
FLANGE		MPa	MPa	MPa	MPa	MPa	
	Pm	17.1	-12.5	-145.1	162.2	331	1.0
Pm + Pb	<i>Inside</i>	16.9	-12.6	-144.6	161.5	496	2.1
	<i>Center</i>	17.1	-12.5	-145.1	162.2	496	2.1
	<i>Outside</i>	17.3	-12.4	-145.5	162.8	496	2.0
OUTER LID		MPa	MPa	MPa	MPa	MPa	
	Pm	95.6	0.3	-104.9	200.5	331	0.7
Pm + Pb	<i>Inside</i>	289.3	35.4	-7.0	296.3	496	0.7
	<i>Center</i>	95.6	0.3	-104.9	200.5	496	1.5
	<i>Outside</i>	-34.4	-94.7	-206.7	172.3	496	1.9
INNER LID		MPa	MPa	MPa	MPa	MPa	
	Pm	-4.3	-14.3	-164.4	160.1	331	1.1
Pm + Pb	<i>Inside</i>	-20.9	-70.1	-371.6	350.6	496	0.4
	<i>Center</i>	-4.3	-14.3	-164.4	160.1	496	2.1
	<i>Outside</i>	64.8	33.1	-1.4	66.3	496	6.5

Note: (1) The margin of safety is the ratio of the Allowable Stress and the Stress Intensity (SINT) minus 1.

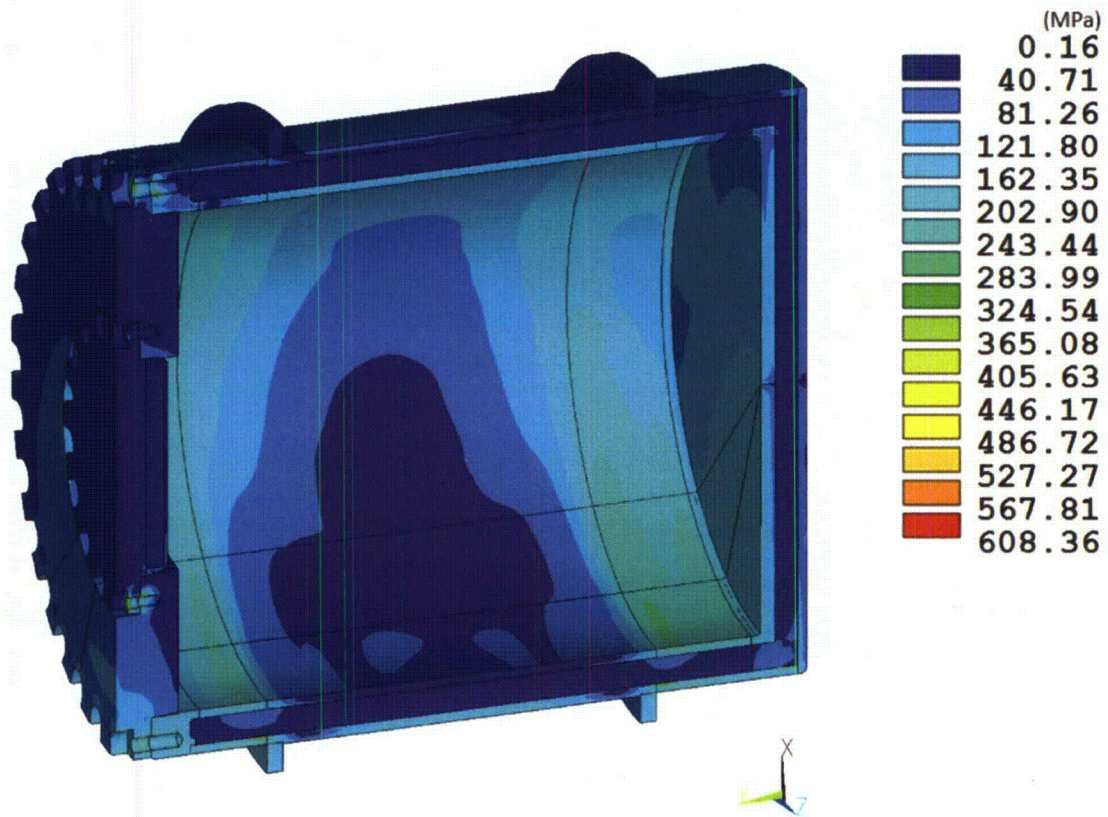


Figure 2.7.1-8 RT-100 HAC Side Drop Stress Intensity Results

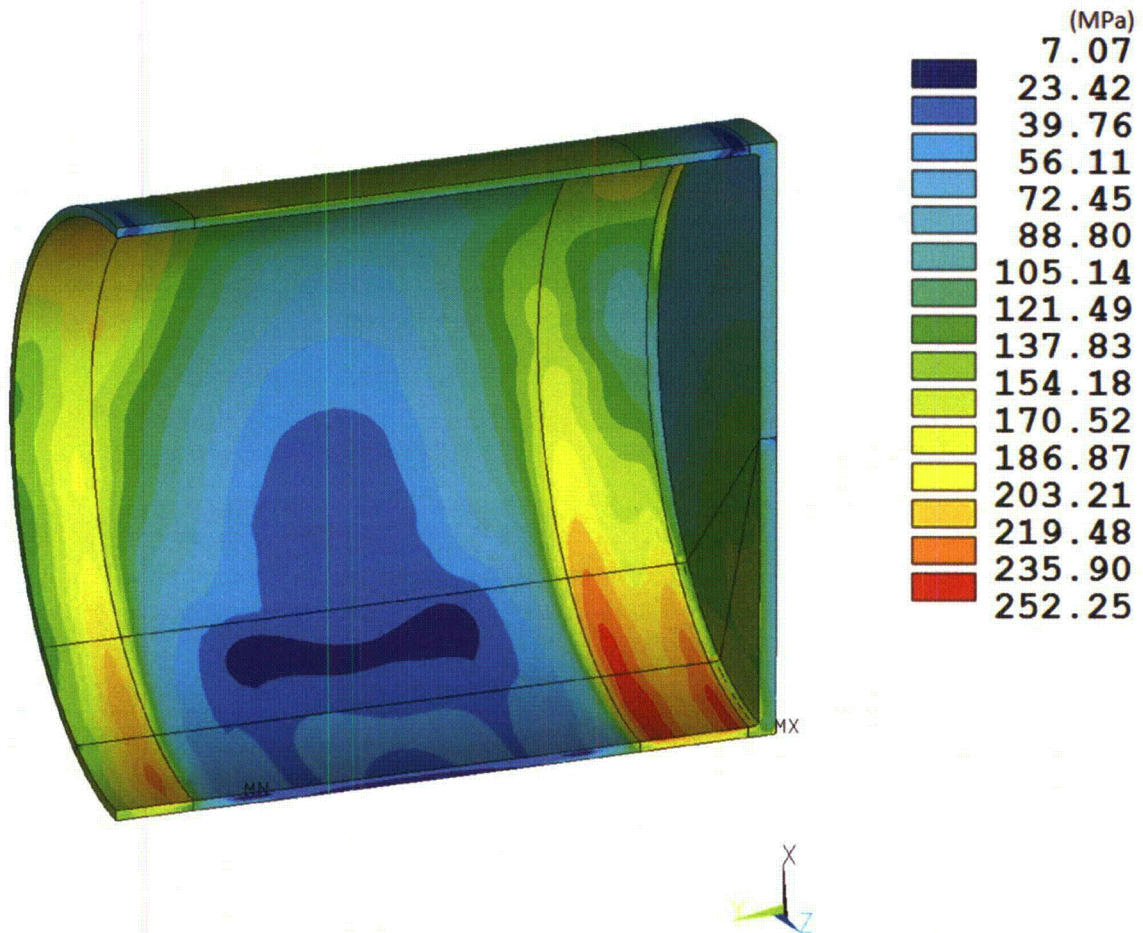


Figure 2.7.1-9 RT-100 Inner Shell HAC Side Drop Stress Intensity Results

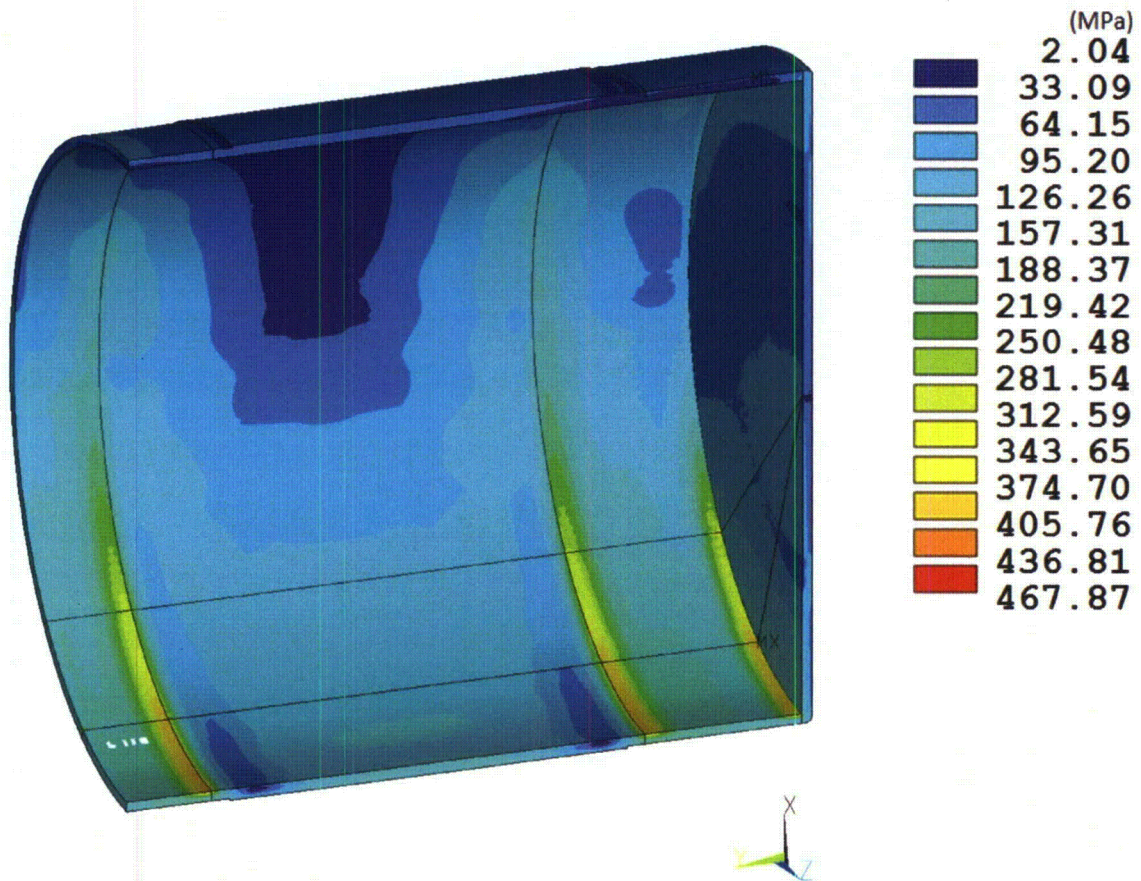


Figure 2.7.1-10 RT-100 Outer Shell HAC Side Drop Stress Intensity Results

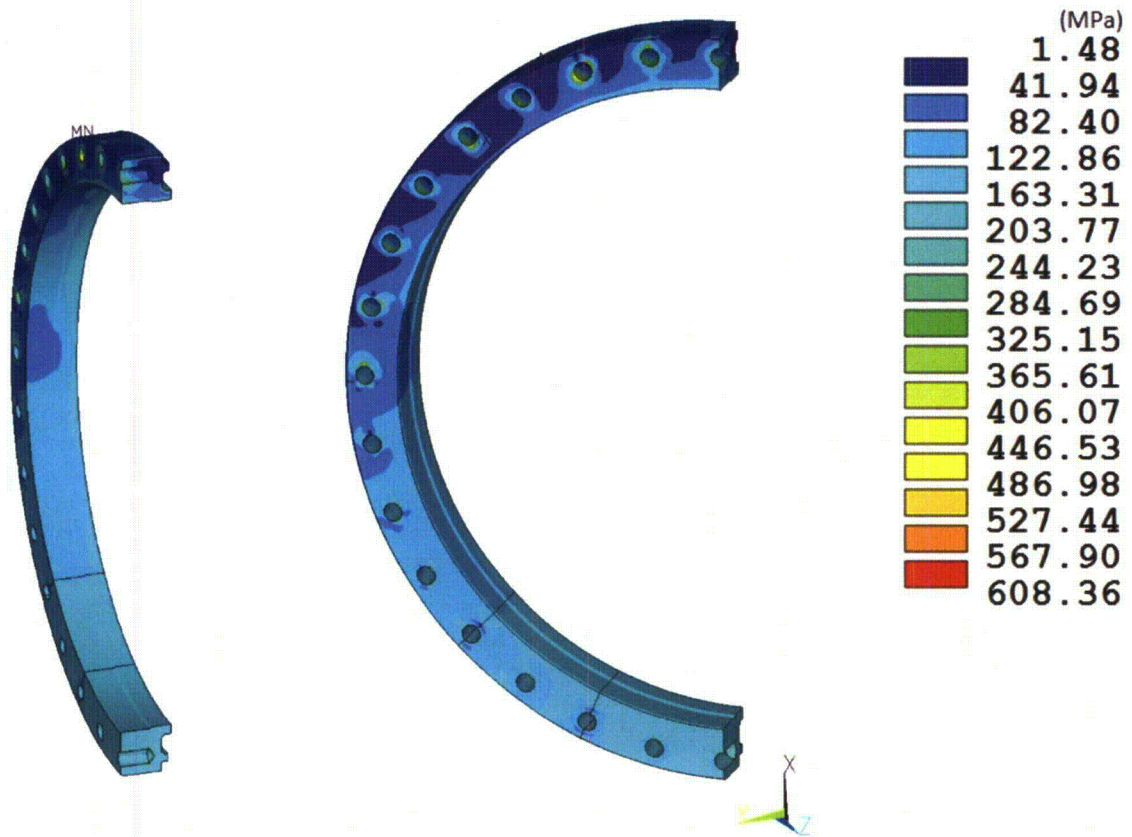


Figure 2.7.1-11 RT-100 Flange HAC Side Drop Stress Intensity Results

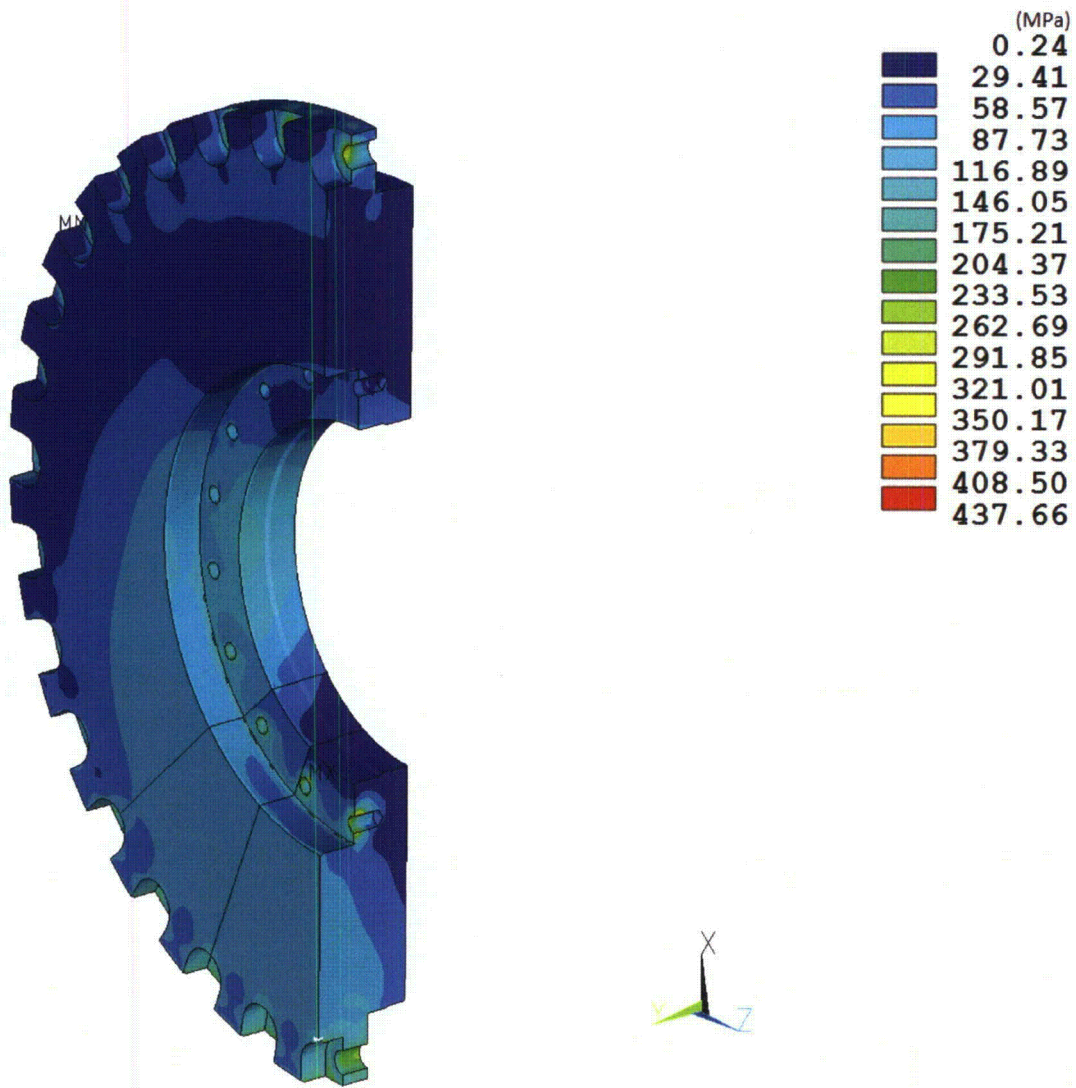


Figure 2.7.1-12 RT-100 Outer Lid HAC Side Drop Stress Intensity Results

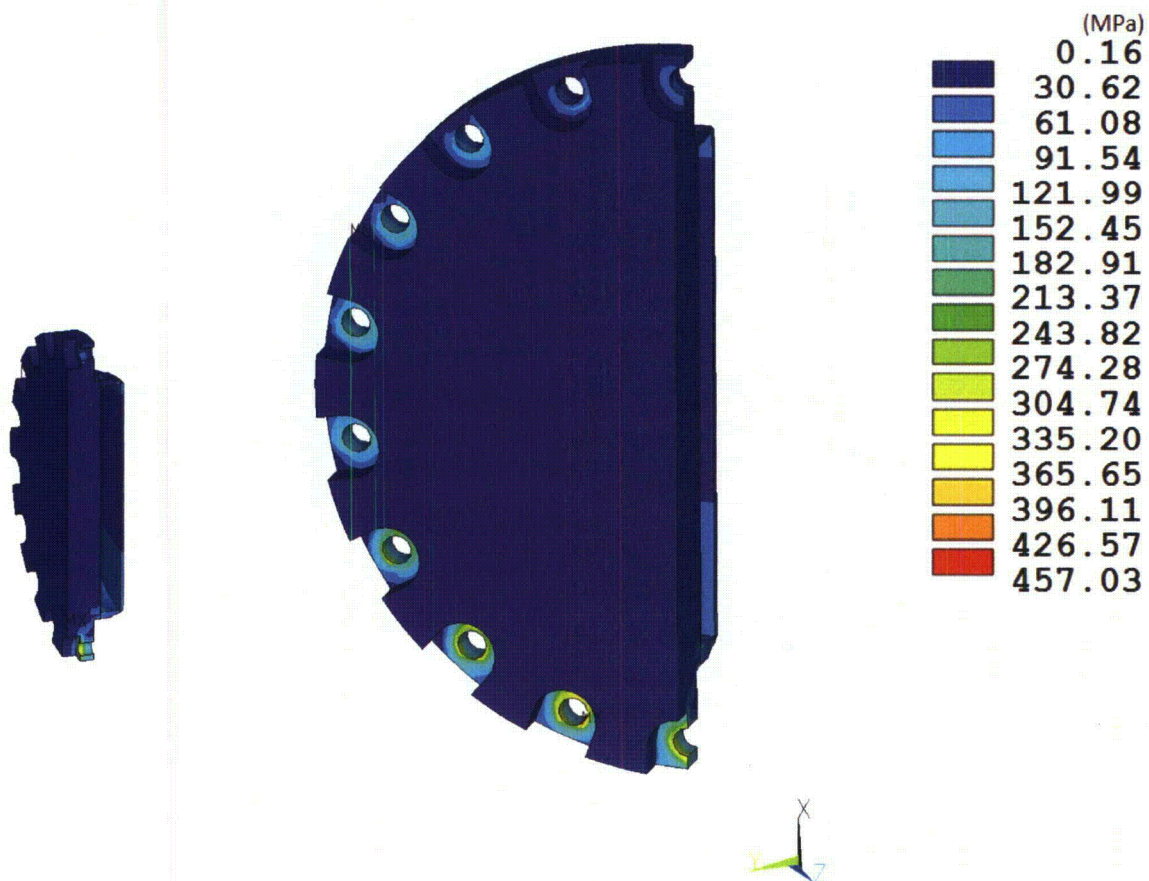


Figure 2.7.1-13 RT-100 Inner Lid HAC Side Drop Stress Intensity Results

2.7.1.3 Corner Drop

In accordance with the requirements of 10 CFR 71.73(c)(1) [Ref. 2], the RT-100 is structurally evaluated for the hypothetical accident 30-foot corner drop condition. Based on the impact limiter analysis provided in Appendix 2.12, Table 2.7.1-4 demonstrates that the end and side drop accelerations bound the CG over corner drop acceleration.

Table 2.7.1-4 Corner Drop Component Accelerations

Side Drop Acceleration (g)	End Drop Acceleration (g)	Corner Drop Acceleration (g)	Corner Drop Axial Component (g)	Corner Drop Lateral Component (g)
226	123	116	91.4	71.4

To evaluate the stresses generated in the RT-100 during the corner drop (38° from vertical), the ANSYS [Ref. 28] stress results for the side and end drop evaluations are scaled by the ratio of the end and side drop accelerations and the corner drop axial and lateral component accelerations. Once scaled, the resulting axial and lateral component stresses are summed and compared to the allowable stress intensity.

Stress results for the 9-meter corner drop combined loading conditions are documented in Table 2.7.1-5. The table documents the primary membrane (P_m), primary membrane plus primary bending (P_m+P_b) stresses in accordance with the criteria presented in Regulatory Guide 7.6 [Ref. 4].

As shown in Table 2.7.1-5, the margins of safety when compared to the stress intensity for each category are positive. The most critically stressed component in the system is the inner lid. The minimum margin of safety is found to be +1.0 for primary membrane plus bending stress intensity.

Table 2.7.1-5 HAC Corner Drop Stress Summary

Stress State	End Drop SINT	Side Drop SINT	Corner SINT	RG 7.6 Allowable Stress	Margin of Safety(1)
INNER SHELL	MPa	MPa	MPa	MPa	
Pm	38.4	159.6	79.0	331	3.2
Pm + Pb	64.1	159.7	98.1	496	4.1
	38.4	159.6	79.0	496	5.3
	19.4	159.6	64.9	496	6.7
OUTER SHELL	MPa	MPa	MPa	MPa	
Pm	32.8	187.1	83.5	331	3.0
Pm + Pb	33.5	405.3	153.0	496	2.2
	32.8	187.1	83.5	496	4.9
	32.0	169.0	77.2	496	5.4
FLANGE	MPa	MPa	MPa	MPa	
Pm	14.3	162.2	61.9	331	4.4
Pm + Pb	14.2	161.5	61.6	496	7.1
	14.3	162.2	61.9	496	7.0
	28.6	162.8	72.7	496	5.8
OUTER LID	MPa	MPa	MPa	MPa	
Pm	40.3	200.5	93.3	331	2.5
Pm + Pb	74.8	296.3	149.2	496	2.3
	40.3	200.5	93.3	496	4.3
	44.4	172.3	87.4	496	4.7
INNER LID	MPa	MPa	MPa	MPa	
Pm	35.9	160.1	77.3	331	3.3
Pm + Pb	190.4	350.6	252.3	496	1.0
	35.9	160.1	77.3	496	5.4
	138.4	66.3	123.8	496	3.0

Note: (1) The margin of safety is the ratio of the Allowable Stress and the Stress Intensity (SINT) minus 1.

2.7.1.4 Oblique Drops

In accordance with the requirements of 10 CFR 71.73(c)(1) [Ref. 2], the RT-100 is structurally evaluated for the hypothetical accident 30-foot oblique drop condition. Based on the following analysis, the cask velocities and stresses generated by an oblique-angle drop are bounded by those produced by the side drop. For a shallow angle drop, it is assumed that no energy is absorbed by the first impact limiter that contacts the impact surface, which causes all of the rotational inertia generated by the cask into the second impact limiter. The analysis is performed according to the following basic inertial equations in “Standard Handbook for Mechanical Engineers, 7th Edition” [Ref. 51]

Assumptions:

- The rotational inertia of the cask is approximated by a solid cylinder
- The cask does not slide along the impact surface
- No gravitational acceleration is assumed to occur after initial contact of the cask with the impact surface

The equation for the rotational inertia of a cylinder is:

$$I_{cyl} = I_{cyl} = \frac{1}{4} \times M \times \left(r^2 + \frac{l^2}{3} \right)$$

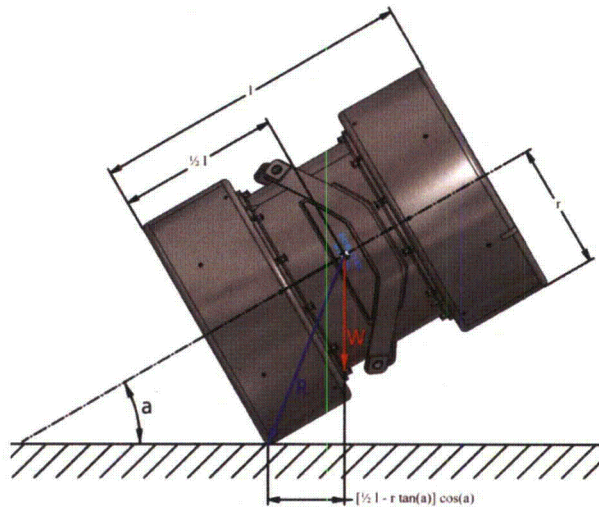
Where M = mass of cask

r = radius of cask

l = length of cask

R = distance from CG to corner of impact limiter

a = angle of the cask at impact



For this configuration, the angular momentum of the cask before impact, L_1 , is represented by:

$$L_1 = M \times v_1 \times \left(\frac{l}{2} - \tan(a) \right) \times \cos(a)$$

Where v_1 = impact velocity

After impact the angular momentum, L_2 , of the cask is:

$$L_2 = I_{imp} \times \omega_2$$

Where $I_{imp} = I_{cyl} + M \times R^2$

ω_2 = angular velocity of cask following impact

Substituting the rotational inertia for a cylinder, I_{cyl} :

$$I_{imp} = M \times \left(\frac{r^2}{4} + \frac{l^2}{12} + R^2 \right)$$

Because no external moments are applied to the cask, angular momentum is conserved.

Therefore:

$$L_1 = L_2$$

Substituting:

$$M \times v_1 \times \left(\frac{1}{2} - r \times \tan(a) \right) \times \cos(a) = M \times \left(\frac{r^2}{4} + \frac{l^2}{12} + R^2 \right) \times \omega_2$$

Solving for the angular velocity, ω_2 , gives:

$$\omega_2 = v_1 \times \frac{\left(\frac{1}{2} - r \times \tan(a) \right) \times \cos(a)}{\frac{r^2}{4} + \frac{l^2}{12} + R^2}$$

The maximum angular velocity occurs when the impact angle equals zero. Therefore, the velocity of the secondary impact is:

$$v_s = l \times \omega_2$$

Substituting the angular velocity:

$$v_s = l \times v_1 \times \frac{\left(\frac{1}{2} - r \times \tan(a) \right) \times \cos(a)}{\frac{r^2}{4} + \frac{l^2}{12} + R^2}$$

The limiting case occurs when the secondary impact velocity equals the initial impact velocity.

Therefore:

$$v_s = v_1 \text{ when the angle } a = 0$$

Solving:

$$1 = \frac{\frac{l^2}{2}}{\frac{r^2}{4} + \frac{l^2}{12} + R^2}$$

From the figure above:

$$R^2 = \frac{l^2}{4} + r^2$$

Substituting and solving:

$$\frac{l^2}{2} = r^2 + \frac{l^2}{12} + \frac{l^2}{4} + r^2 \Rightarrow \frac{4}{12} l^2 = \frac{5}{4} r^2 \Rightarrow \frac{l^2}{r^2} = 7.5 \Rightarrow \frac{l}{r} = 2.74$$

Therefore:

$$\frac{l}{D} = 1.37$$

Where D = diameter of cask

This evaluation shows that cask designs with a length-to-diameter ratio greater than 1.37 may result in oblique impact velocities greater than the side drop. However, the length of the

RT-100 is 3316 mm and the diameter is 2587 mm for a length-to-diameter ratio of 1.28. Therefore, impact velocities and resulting stresses in the RT-100 during the oblique drop event are less than those experienced during the side drop.

2.7.1.5 Summary of Results

Structural analyses are performed for the RT-100 for hypothetical accident conditions free drop conditions. To evaluate the RT-100, 3D ANSYS [Ref. 28] is used to analyze the governing drop cases. All structural members have a positive margin of safety under worst case loading conditions. It is concluded that the RT-100 is structurally adequate for the HAC free drop conditions. Therefore, the requirements of 10 CFR 71.73(c)(1) [Ref. 2] have been satisfied.

2.7.2 Crush

In accordance with the requirements of 10 CFR 71.73(c)(2) [Ref. 2], the RT-100 is to be subjected to a dynamic crush test by evaluating the package on essentially unyielding horizontal surface so as to suffer maximum damage by the drop of a 500-kg mass from 9 m onto the package. The mass must consist of a solid mild steel plate 1 m × 1 m and must fall in a horizontal attitude. The crush test is required only when the specimen has a mass not greater than 500 kg, and overall density not greater than 1000 kg/m³ based on external dimension. The crush condition is not applicable since the RT-100 weighs more than 500 kg and overall density is greater than 1000 kg/m³.

2.7.3 Puncture

In accordance with the requirements of 10 CFR 71.73(c)(3) [Ref. 2] related to puncture (hypothetical accident condition), the RT-100 Cask is analyzed for structural adequacy (Calculation Package RTL-001-CALC-ST-0403 Rev. 4 [Ref. 36]). The cask is assumed to be in a horizontal position and dropped 1 m onto a 15 cm diameter, mild steel bar, oriented vertically on an unyielding surface. The structural evaluation of the RT-100 is performed by classical elastic analysis and finite element analysis methods.

2.7.3.1 Lid Puncture

Finite element analysis methods are used to perform the stress evaluation of the RT-100 for the end puncture conditions. The end puncture is analyzed using a three-dimensional finite element model using the computational modeling software ANSYS [Ref. 28]. To simplify the pin puncture analysis, only the upper end of the cask is considered for this evaluation. Figure 2.7.3-1 shows the pin puncture model.

2.7.3.1.1 Lid Puncture Boundary Conditions

The puncture load is applied to a 152 mm (6 in) diameter region which corresponds to a 152 mm diameter pin. The load is simulated with an evenly distributed pressure load equal to the dynamic flow stress of the pin; the dynamic flow stress is taken to be 324 MPa (47,000 psi). As discussed in the cask body analysis, the preload torque is included as an initial condition. In addition, the maximum normal operating pressure of 241 KPa (35 psig) is applied to the interior surface of the RT-100.

2.7.3.1.2 Lid Puncture Results

Stress results for the 1-meter pin puncture combined loading conditions are documented in Table 2.7.3-1. The table documents the primary membrane (Pm), primary membrane plus primary bending (P_m+P_b) stresses in accordance with the criteria presented in Regulatory Guide 7.6 [Ref. 4]. Stresses are linearized across critical sections to determine the membrane and bending stresses and subsequently, are compared with allowable stress intensities.

As shown in Table 2.7.3-1, the margins of safety are positive when compared to the stress intensity for each category. The most critically stressed component in the system is the flange; this condition is due to bending as a result of the pin puncture probe striking the center of the lid. The minimum margin of safety is found to be +0.2 for primary membrane plus bending stress intensity. The locations of critical section correspond to the maximum stress location are shown in Figure 2.7.3-2.

Table 2.7.3-1 HAC Pin Puncture Stress Summary

Stress State	Location	S1	S2	S3	SINT	RG 7.6 Allowable Stress	Margin of Safety
<i>INNER LID</i>		MPa	MPa	MPa	MPa	MPa	
Pm		-108.6	-109.8	-191.5	82.9	331	3.0
Pm + Pb	<i>Inside</i>	383.4	382.9	-37.7	421.1	485	0.2
	<i>Center</i>	-108.6	-109.8	-191.5	82.9	485	4.9
	<i>Outside</i>	-342.9	-602.3	-603.3	260.4	485	0.9

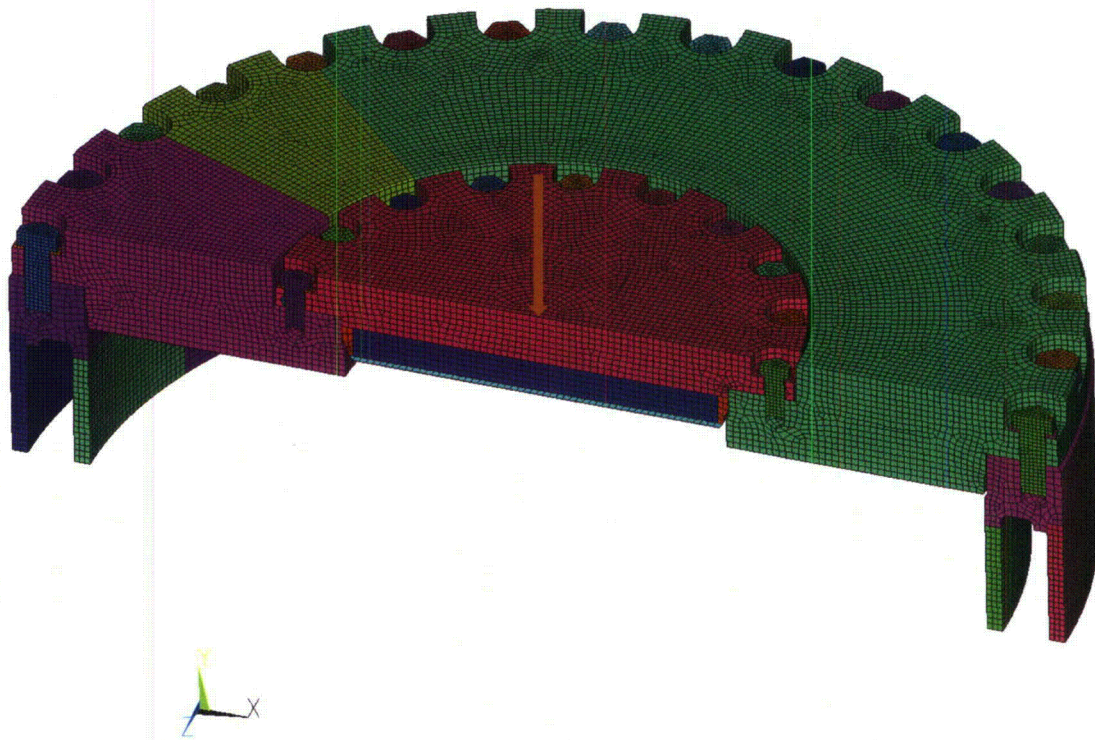


Figure 2.7.3-1 RT-100 ANSYS Puncture Model

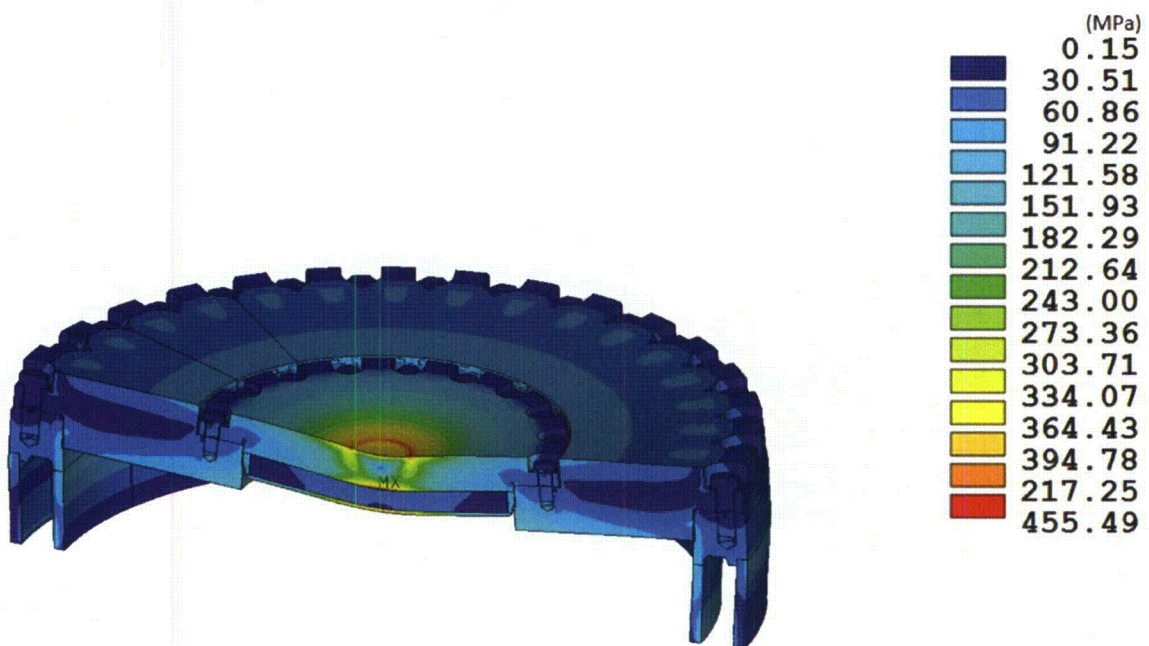


Figure 2.7.3-2 RT-100 Pin Puncture Stress Intensity Results

2.7.3.2 Cask Side Puncture

The following sections describe the cask side puncture analysis.

2.7.3.2.1 Cask Side Puncture Minimum Wall Thickness

A series of pin puncture tests (performed at Oak Ridge National Laboratory) are used to develop an empirical equation to determine the stress in the outer wall of a multi-wall cask as a function of the mass of the cask and the thickness of the cask outer wall material. This equation (Nelm's equation [Ref. 59]) applies to steel-lead-steel cask wall construction and is used to demonstrate pin puncture adequacy for casks with stainless steel walls; this equation has been the basis for the puncture analysis of several previously licensed casks. Solving Nelm's equation [Ref.59] for the RT-100 outer shell:

$$t = \left(\frac{W}{S}\right)^{0.71} = 1.16 \text{ in (29mm)} < 35 \text{ mm}$$

where,

$$W = 92,594 \text{ lb (42,000 kg), maximum gross weight of the package}$$

$$S = 75,000 \text{ psi (517.1 MPa), ultimate tensile strength of the outer shell}$$

Nelm's equation [Ref. 59] shows that the cask outer shell is sufficient to resist puncture.

2.7.3.2.2 Cask Sidewall Bending Stresses

When the cask sidewall impacts the puncture pin, the bending force is:

$$\sigma_b = \frac{M \times c}{I} = 15.3 \text{ MPa}$$

Conservatively assuming the compressive and tensile stresses occur at the same location, the stress intensity is doubled to 30.6 MPa. Therefore, the factor of safety is:

$$FS = \frac{517.1}{30.6} = 15.7 > 1$$

where,

$$M = \frac{F_i \times m}{4} = 1589.2 \text{ kN-m, moment due to impact force}$$

$$m = \frac{L}{2} = 1.16 \text{ m, moment arm resulting from impact}$$

$$L = h_{\text{tot}} - h_U - h_L = 2.32 \text{ m, sidewall length}$$

$$h_{\text{tot}} = 3312.8 \text{ mm, cask total height}$$

$$h_U = 498 \text{ mm, upper impact limiter height}$$

$$h_L = 494 \text{ mm, lower impact limiter height}$$

$$F_i = K_s \times A_i = 5478.2 \text{ kN, impact force}$$

$$K_s = 324 \text{ MPa, dynamic flow stress for mild steel (3)}$$

$$A_i = \frac{\pi}{4} \times d_p^2 = 0.0177 \text{ m}^2, \text{ puncture probe area}$$

$$d_p = 0.15 \text{ m, puncture probe diameter}$$

Therefore, the RT-100 sidewall successfully resists the regulatory puncture drop.

2.7.3.3 Lead Deformation during Side Puncture

Following the postulated side puncture of The RT-100, the cask may experience localized deformation in the outer shell. Behind this localized deformation a slight flattening may occur, and results in shielding loss. To quantify this loss, the local stiffness of the cask wall is determined to calculate the energy absorbed by the package. To calculate the total deformation of the lead shield, it is conservatively assumed that the available potential energy of the 1 meter puncture drop is converted to strain energy.

The maximum deformation occurs during postulated puncture event when the cask strikes the puncture probe approximately mid-span on the cask outer shell. Figure 2.7.3-3 shows the side puncture details. For the purposes of this evaluation, the cask is considered a closed cylinder subjected to a concentrated load at the mid-span. The deformation is obtained from Table 31, Case 9 of "Roark's Formulas for Stress and Strain, 6th Edition" [Ref. 29]. The deflection of the outer shell due to the applied load is:

$$y = \frac{P}{Et} \left[0.48 \times \left(\frac{L}{R} \right)^{0.5} \times \left(\frac{R}{t} \right)^{1.22} \right]$$

where:

L = length of the cylinder

R = mean radius of the shell

P = applied load

E = Young's modulus

Solving for the stiffness

$$k = \frac{P}{y} = \frac{Et}{\left[0.48 \times \left(\frac{L}{R} \right)^{0.5} \times \left(\frac{R}{t} \right)^{1.22} \right]}$$

The RT-100 is considered a composite cylinder comprised of an outer shell, lead shield, and inner shell. The resulting stiffness of each component is shown below.

2.7.3.3.1 Outer Shell Stiffness

$$k_1 = \frac{1.989 \times 10^{10} \times 3.505 \times 10^{-2}}{\left[0.48 \times \left(\frac{1.946}{1.003} \right)^{0.5} \times \left(\frac{1.003}{3.505 \times 10^{-2}} \right)^{1.22} \right]} = 1.743 \times 10^7 \text{ N/m}$$

where:

L = 1.946 m

R = 1.003 m

$$\begin{aligned}t &= 3.505 \times 10^{-2} \text{ m} \\P &= 6.972 \times 10^8 \text{ N} \\E &= 1.989 \times 10^{10} \text{ Pa}\end{aligned}$$

2.7.3.3.2 Lead Stiffness

$$k_2 = \frac{1.602 \times 10^9 \times 8.992 \times 10^{-2}}{\left[0.48 \times \left(\frac{1.946}{9.401 \times 10^{-1}} \right)^{0.5} \times \left(\frac{9.401 \times 10^{-1}}{8.992 \times 10^{-2}} \right)^{1.22} \right]} = 1.191 \times 10^7 \text{ N/m}$$

where:

$$\begin{aligned}L &= 1.946 \text{ m} \\R &= 9.401 \times 10^{-1} \text{ m} \\t &= 8.992 \times 10^{-2} \text{ m} \\P &= 1.441 \times 10^8 \text{ N} \\E &= 1.602 \times 10^9 \text{ Pa}\end{aligned}$$

2.7.3.3.3 Inner Shell Stiffness

$$k_3 = \frac{1.989 \times 10^{10} \times 1.905 \times 10^{-2}}{\left[0.48 \times \left(\frac{1.946}{8.801 \times 10^{-1}} \right)^{0.5} \times \left(\frac{8.801 \times 10^{-1}}{1.905 \times 10^{-2}} \right)^{1.22} \right]} = 4.945 \times 10^6 \text{ N/m}$$

where:

$$\begin{aligned}L &= 1.946 \text{ m} \\R &= 8.801 \times 10^{-1} \text{ m} \\t &= 1.905 \times 10^{-2} \text{ m} \\P &= 3.789 \times 10^8 \text{ N} \\E &= 1.989 \times 10^{10} \text{ Pa}\end{aligned}$$

2.7.3.3.4 Lead Deformation due to Puncture Load

The effective stiffness of the composite section of the cask is:

$$k_{\text{eff}} = k_1 + k_2 + k_3 = 3.428 \times 10^7 \text{ N/m}$$

The energy absorbed during impact is:

$$U = \frac{1}{2} k_{\text{eff}} \times \delta^2$$

Assuming the energy absorbed is equal to the total potential energy, the potential energy is calculated as:

$$\text{P.E.} = W \times h$$

Setting the energy absorbed during impact equal to the total potential energy the outer shell deformation is:

$$\frac{1}{2} k_{\text{eff}} \times \delta^2 = W \times h \Rightarrow \delta = \sqrt{\frac{2(W \times h)}{k_{\text{eff}}}} = 0.050 \text{ m}$$

where:

$$W = 42,000 \text{ kg}$$

$$H = 1.016 \text{ m}$$

The deformation of the lead is calculated from the ratio of the effective stiffness and lead stiffness:

$$\delta_{\text{lead}} = \delta \times \frac{k_2}{k_{\text{eff}}} = 0.017 \text{ m}$$

Although the deformation is comprised of an elastic and inelastic component, the entire deformation is conservatively assumed to be permanent.

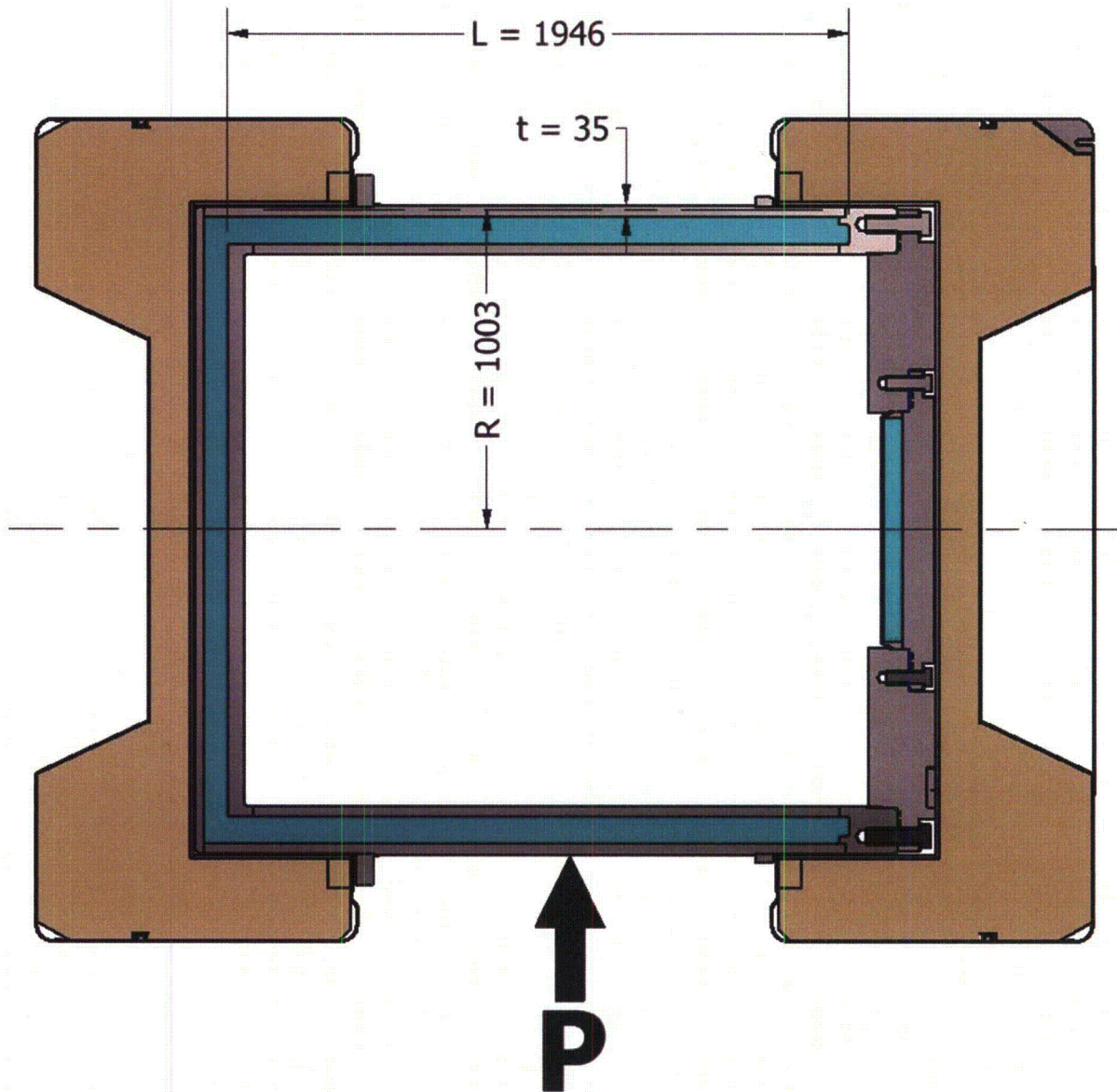


Figure 2.7.3-3 RT-100 Side Puncture Details

2.7.4 Thermal

For hypothetical accident conditions, the RT-100 cask body provides protection and containment of the contents. Thermal expansion of the bolts is evaluated to ensure the containment boundary is maintained. Similarly, the cask body is evaluated for pressures associated with the fire accident; during the accident, the cask is assumed to be subjected to a fire that produces a surrounding environment of 800°C for a period of 30 minutes. The thermal evaluation of the hypothetical fire transient is presented Section in 3.4.

2.7.4.1 Summary of Pressures and Temperatures

Cask components temperatures under varying conditions are evaluated using the ANSYS finite element computer code [Ref. 28]. The cask cavity pressure is estimated based on the surface averaged temperature of the inner shell at the cavity side. The detail of the thermal analyses is documented in Chapter 3, Section 3.1. Table 3.1.3-1 presents the normal condition maximum temperature along with the maximum surface averaged temperature of inner shell surface at the cavity side. Chapter 3, Table 3.1.3-2 presents the maximum temperatures under hypothetical accident conditions along with the maximum surface averaged temperature of inner shell surface at the cavity side. The surface averaged temperature of the inner shell at the cavity side is used to predict the gas pressure inside the cask; Chapter 3, Table 3.1.4-1 summarizes the maximum NCT and HAC pressures.

2.7.4.2 Differential Thermal Expansion

For the RT-100 Cask, the closure bolts are the only components of concern during the fire accident that may experience thermal expansion. The bolting evaluation in Appendix 2.13 evaluates the effects of thermal expansion on the closure bolts.

2.7.4.3 Stress Calculations

The following Section evaluates the stresses in the bolts and cask body during hypothetical accident conditions.

2.7.4.3.1 Bolt stresses during fire accident

The bolt stress evaluation is presented in Appendix 2.13. The evaluation shows that the bolt stresses are less than the allowables. Therefore, the bolts continue to provide a tight seal and containment is maintained.

2.7.4.3.2 Pressure stress during fire accident

In accordance with the requirements of 10 CFR 71.73(c)(4), the RT-100 Cask is structurally evaluated when subjected to an accident internal pressure of 689.4 kPa (100 psia). The pressure is based upon an average cask temperature of 73.1°C. For conservatism, the stress intensity values are compared to allowable stress values at 150°C. To obtain pressure stress results, a uniform internal pressure is applied to the ANSYS finite element model.

2.7.4.4 Comparison with Allowable Stresses

The accident pressure stresses are presented in Table 2.7.4-1. The table documents the primary membrane (P_m), primary membrane and plus primary bending (P_m+P_b) stresses in accordance with the criteria presented in Regulatory Guide 7.6. As Table 2.7.4-1 shows, the margins of

safety are positive when compared to the stress intensity for each category. The most critically stressed component in the system is the inner lid; this condition is due to prying load at the interface of the closure bolt and lid. The minimum margin of safety is found to be +6.4 for primary membrane plus bending stress intensity. The margins of safety are all positive and thus, the RT-100 satisfies the requirements of 10CFR71.73(c)(4) for thermal HAC.

Table 2.7.4-1 HAC Pressure Stress Summary

Component and Stress State	Stress Location	ANSYS Results				RG 7.6 Allowable Stress	Margin of Safety (1)
		S1	S2	S3	SINT		
INNER SHELL		MPa	MPa	MPa	MPa	MPa	
Pm		1.2	0.0	-1.0	2.2	331	Large
Pm + Pb	<i>Inside</i>	1.2	0.0	-1.1	2.3	496	Large
	<i>Center</i>	1.2	0.0	-1.0	2.2	496	Large
	<i>Outside</i>	1.2	0.0	-0.9	2.1	496	Large
OUTER SHELL		MPa	MPa	MPa	MPa	MPa	
Pm		1.2	0.0	-0.7	1.9	331	Large
Pm + Pb	<i>Inside</i>	1.2	0.0	-0.7	2.0	496	Large
	<i>Center</i>	1.2	0.0	-0.7	1.9	496	Large
	<i>Outside</i>	1.2	0.0	-0.6	1.8	496	Large
FLANGE		MPa	MPa	MPa	MPa	MPa	
Pm		1.2	0.0	-0.4	1.6	331	Large
Pm + Pb	<i>Inside</i>	1.2	0.0	-0.5	1.7	496	Large
	<i>Center</i>	1.2	0.0	-0.4	1.6	496	Large
	<i>Outside</i>	1.2	0.0	-0.4	1.5	496	Large
OUTER LID		MPa	MPa	MPa	MPa	MPa	
Pm		1.1	0.1	-0.2	1.3	331	Large
Pm + Pb	<i>Inside</i>	1.1	0.1	-0.3	1.4	496	Large
	<i>Center</i>	1.1	0.1	-0.2	1.3	496	Large
	<i>Outside</i>	1.0	0.1	-0.2	1.2	496	Large
INNER LID		MPa	MPa	MPa	MPa	MPa	
Pm		0.2	-2.1	-36.5	36.7	331	Large
Pm + Pb	<i>Inside</i>	-2.1	-6.2	-64.0	61.9	496	Large
	<i>Center</i>	0.2	-2.1	-36.5	36.7	496	Large
	<i>Outside</i>	4.1	2.0	-10.6	14.7	496	Large

2.7.5 Immersion – Fissile Material

This Section is not applicable. The RT-100 does not have any fissile material subject to the requirements of 10 CFR 71.55 [Ref. 2].

2.7.6 Immersion – All Package

According to the requirements of 10 CFR 71.73(c)(6) [Ref.2], a package must be subjected to water pressure that is equivalent to: immersion under a head of water of at least 15 meters for a period of 8 hours. Also, 10 CFR 71.61 [Ref. 2] requires that a package's undamaged containment system be able to withstand an external water pressure of 2000 kPa for a period of not less than one hour without collapse, buckling or in-leakage of water. The outer lid is shown to be structurally adequate for a maximum external dynamic crush pressure of the top impact limiter. Therefore, the RT-100 satisfies all of the immersion requirements for a package that is used for the international shipment of radioactive materials.

2.7.7 Deep Water Immersion Test (for Type B Packages Containing More than 10^5 A₂)

This Section is not applicable. The RT-100 is limited to a maximum of 3000 A₂.

2.7.8 Summary of Damage

The analytical results reported in Section 2.7.1 through 2.7.7 indicate that the damage incurred by the RT-100 during the hypothetical accident is minimal, and such damage does not diminish the cask ability to maintain the containment boundary. A 9-meter drop or a 1-meter pin puncture accident may damage the outer shell and result in a localized reduction in shielding ability. However, the shielding remains intact to satisfy the accident shielding criteria. Based on the analyses of Section 2.7 through 2.7.7, the RT-100 fulfills the structural and shielding requirements of 10 CFR 71 [Ref. 2] for all of the hypothetical accident conditions.

2.8 Accident Conditions for Air Transport of Plutonium

This Section is not applicable. The RT-100 cask is not to be used to transport Plutonium by air transport.

2.9 Accident Conditions for Fissile Material Packages for Air Transport

This Section is not applicable. The RT-100 is limited by 10 CFR 71 [Ref. 2] for quantities of fissile material. However, the RT-100 is not used to transport any fissile material by air transport.

2.10 Special Form

This Section is not applicable. The RT-100 is not to be used to transport special form materials as specified in 10 CFR 71.75 [Ref. 2].

2.11 Fuel Rods

This Section is not applicable. The RT-100 is not to be used to transport fuel rods.

**WITHHELD PER
10 CFR 2.390**

2.13 Appendix – Closure Bolt Evaluation

The RT-100 package is designed with two sets of closure bolts: 18 M36 hex head bolts at the secondary lid and 32 M48 hex head bolts at the primary lid. These two sets of bolts are credited with maintaining positive closure of the package under all accident conditions. The purpose of this evaluation is to structurally qualify these bolts for the loadings associated with the normal conditions of transport and the hypothetical accident conditions.

2.13.1 Methodology

Bolt loadings under the various normal and accident conditions are determined in accordance with the recommendations of NUREG/CR-6007 [Ref.10]. Stresses resulting from these loads are compared with the design criteria in Section 2.1.2.2. Note that in many cases, calculations are made using exact values, not the rounded numbers shown in intermediate steps. In certain situations, the numbers displayed may not be capable of providing the exact final solution. Using the exact numbers, however, provides the most accurate solution possible. Calculation Package RTL-001-CALC-ST-0203, Rev. 6 [Ref. 60] provides additional information.

2.13.2 Loads

The following loads are evaluated in this section:

- Internal pressure loads
- Temperature loads
- Bolt preload
- Impact loads
- Puncture loads
- External pressure loads
- Gasket seating load

These loads are combined per NUREG/CR-6007 [Ref. 10] in Section 2.13.3.

2.13.2.1 Internal Pressure Loads

Per Table 4.3 of NUREG/CR-6007 [Ref. 10], the forces and moments generated under the internal pressure load are a tensile load F_{ap} , a shear load F_{sp} , a fixed edge closure force F_{fp} , and a fixed edge closure moment M_{fp} . These factors are evaluated for the primary and secondary lid bolts.

2.13.2.1.1 Internal Pressure Loads for Primary Lid Closure Bolts

The tensile force per bolt due to internal pressure, F_{ap} , is:

$$F_{ap} = \frac{\pi x D_{lg}^2 x (P_{li} - P_{lo})}{4x N_b}$$

where,

$$\begin{aligned} D_{lg} &= \text{Outer Seal Diameter} \\ &= 1835 \text{ mm} \\ N_b &= \text{Number of Bolts} \\ &= 32 \\ P_{li} &= \text{Internal Pressure} \\ &= 35 \text{ psi} = 241.3 \text{ kN/m}^2 \text{ use } 250 \text{ kN/m}^2 \text{ (Calc TH-102)} \\ P_{lo} &= \text{External Pressure} \\ &= 0 \text{ kN/m}^2 \text{ (conservative)} \end{aligned}$$

Thus,

$$F_{ap} = \frac{(1.835)^2 \times (250 - 0)}{4 \times 32} = 20.7 \text{ kN/bolt}$$

The shear force per bolt due to internal pressure F_{sp} is:

$$F_{sp} = \frac{\pi \times E_t \times t_t \times (P_{li} - P_{lo}) \times D_{lb}^2}{2 \times N_b \times E_c \times t_c \times (1 - N_{ul})}$$

where,

$$\begin{aligned} E_l &= \text{Primary Lid Material Elastic Modulus, it means the} \\ &\quad \text{(SA 240 TYP304/304L)} \\ &= 195 \text{ GPa at } 20^\circ \text{ C} \quad \text{(Table 2.2.1-1)} \\ D_{lb} &= \text{Primary Lid Bolt Circle Diameter} \\ &= 1920 \text{ mm} \\ N_{ul} &= \text{Primary Lid Material Poisson's} \\ &\quad \text{Ratio, (SA 240 TYPE 304/304L)} \\ &= 0.31 \quad \text{(Table 2.2.1-2)} \\ E_c &= \text{Cask Material Elastic Modulus,} \\ &\quad \text{(SA 240 TYPE 304/304L)} \\ &= 195 \text{ GPa at } 20^\circ \text{ C} \quad \text{(Table 2.2.1-1)} \\ t_l &= \text{Primary Lid Thickness} \\ &= 210 \text{ mm} \\ t_c &= \text{Cask Wall Thickness} \\ &= 65 \text{ mm (neglecting lead)} \end{aligned}$$

The remaining terms are as previously defined. However, this expression for shear force does not apply to the RT-100 cask design because the *maximum* gap between the lid and cask body (4 mm = 1741 – 1737) per RT100 PE 1001-1 Rev. H, Detail 1, Chapter 1, Appendix 1.4, Attachment 1.4-2) is less than the *minimum* gap between the bolt clearance holes and bolt shank (5.5 mm = 52.5- 47) per RT100 PE 1001-1 Rev. H (Chapter1, Appendix 1.4, Attachment 1.4-2) and Machinery's Handbook [Ref. 27]). Thus, the RT-100 primary lid bolts are not subjected to any shear loads. Therefore,

$$F_{sp} = 0.0 \text{ kN/bolt.}$$

The fixed edge closure force F_{fp} and moment M_{fp} are:

$$F_{fp} = \frac{D_{lb} \times (P_{li} - P_{lo})}{4} = \frac{1.920 \times (250 - 0)}{4} = 120.0 \text{ kN/m}$$

and,

$$M_{fp} = \frac{(P_{li} - P_{lo}) \times D_{lb}^2}{32} = \frac{(250 - 0) \times 1.920^2}{32} = 28.8 \text{ kN-m/m}$$

2.13.2.1.2 Internal Pressure Load for Secondary Lid Closure Bolts

The secondary lid closure bolt forces and moments are determined using the same methodology as shown for the primary lid bolts (Section 2.13.2.1.1), except that the secondary lid features are incorporated.

The tensile force per bolt due to internal pressure F_{as} is:

$$F_{as} = \frac{\pi \times D_{lg}^2 \times (P_{li} - P_{lo})}{4 \times N_b}$$

where,

$$\begin{aligned} D_{lg} &= \text{Outer Seal Diameter} \\ &= 850 \text{ mm} \\ N_b &= \text{Number of Bolts} \\ &= 18 \\ P_{li} &= \text{Internal Pressure} \\ &= 35 \text{ psi} = 241.3 \text{ kN/m}^2 \text{ use } 250 \text{ kN/m}^2 \text{ [Ref. 38]} \\ P_{lo} &= \text{External Pressure} \\ &= 0 \text{ kN/m}^2 \text{ (conservative)} \end{aligned}$$

Thus,

$$\begin{aligned} F_{as} &= \frac{\pi \times (0.850)^2 \times (250 - 0)}{4 \times 18} \\ &= 7.9 \text{ kN/bolt} \end{aligned}$$

The *maximum* gap between the lid and cask body (just 4 mm = 748 – 744) is less than the *minimum* gap between the bolt clearance holes and bolt shank (5.5 mm = 40.5- 35). As with the primary lid (Section 2.13.2.1.1), the shear force per bolt due to internal pressure F_{ss} is:

$$F_{ss} = 0.0 \text{ kN/bolt.}$$

The fixed edge closure force F_{fs} and moment M_{fs} are:

$$F_{fs} = \frac{D_{lb} \times (P_{li} - P_{lo})}{4}$$

and,

$$M_{fs} = \frac{(P_{li} - P_{lo}) \times D_{lb}^2}{32}$$

where, D_{lb} = Secondary Lid Bolt Diameter
= 926 mm

All other terms are previously defined. Thus,

$$F_{fs} = \frac{D_{lb} \times (P_{li} - P_{lo})}{4} = \frac{0.926 \times (250 - 0)}{4} = 57.9 \text{ kN/m}$$

and,

$$M_{fs} = \frac{(P_{li} - P_{lo}) \times D_{lb}^2}{32} = \frac{(250 - 0) \times 0.926^2}{32} = 6.7 \text{ kN-m/m}$$

2.13.2.2 Temperature Loads

Temperature differentials and/or differences in the thermal-expansion coefficients of the joint components induce bolt loads. These forces are evaluated Per Table 4.4 of NUREG/CR-6007, [Ref. 10].

2.13.2.2.1 Temperature Loads for Primary Lid Closure Bolts

The tensile force per bolt due to temperature F_{atp} is:

$$F_{atp} = 0.25 \times \pi \times D_b \times E_b \times (\alpha_l \times T_l - \alpha_b \times T_b)$$

where,

D_b = Nominal Bolt diameter
= 48 mm
 E_b = Bolt Material Elastic Modulus,
(SA 354 Grade BD)
= 202 GPa at 20° C (Table 2.2.1-1)

α_l	=	Primary Lid Material Coefficient of Thermal Expansion
	=	16.6×10^{-6} m/m/°C (Table 2.2.1-1)
α_b	=	Bolt Material Coefficient of Thermal Expansion
	=	11.5×10^{-6} m/m/°C (Table 2.2.1-1)
T_l	=	Maximum Primary Lid Temperature under NCT conditions
	=	71°C (conservatively use 100 °C) (Table 3.1.3-1)
T_b	=	Minimum Bolt Temperature under NCT conditions
	=	-20 °C (10 CFR 71.71 [Ref. 2])

Thus,

$$F_{atp} = 0.25 \times \pi \times 0.048^2 \times 202 \times 10^6 \times (16.6 \times 10^{-6} \times 100 - 11.5 \times 10^{-6} \times -20) \\ = 690.9 \text{ kN/bolt}$$

Shear force per bolt due to temperature F_{stp} is considered zero because the clamped components (primary lid and cask forged ring) have essentially the same temperature.

2.13.2.2.2 Temperature Loads for Secondary Lid Closure Bolts

The secondary lid closure bolt forces are determined using the same methodology as shown for the primary lid bolts (Section 2.13.2.2.1) and incorporating the secondary lid geometry, material properties and temperatures. Only the bolt diameter in the previous equation must be changed since the primary and secondary lids are constructed of the same materials and experience essentially the same temperature. The secondary bolt diameter is 36 mm. Thus, the tensile force per unit bolt due to temperature F_{stl} is:

$$F_{atl} = 0.25 \times \pi \times 0.036^2 \times 202 \times 10^6 \times (16.6 \times 10^{-6} \times 100 - 11.5 \times 10^{-6} \times -20) \\ = 388.6 \text{ kN/bolt}$$

As with the primary lid, the shear force per bolt due to temperature F_{sts} is considered zero since the clamped components (primary and secondary lids) have essentially the same temperature.

2.13.2.3 Bolt Preloads

Tightening torques for the primary and secondary lid bolts are respectively, 850 N-m +/-10 % and 350 +/-10 % per Chapter 7, Table 7.4.5-1. The method of analysis is described in Table 4.1 of NUREG/CR-6007 [Ref.10].

2.13.2.3.1 Bolt Preload for Primary Lid Closure Bolts

The primary lid bolt preload F_{pl} is determined as follows (Table 4.1 of NUREG/CR-6007 [Ref. 10]):

$$F_{pl} = \frac{T}{K_L \times D_b}$$

D_b	=	Nominal Bolt diameter
	=	48 mm
K	=	Nut Factor for empirical relation between applied torque and the achieved preload
	=	0.15 (lubricated) minimum (EPRI Good Bolting Practices)
	=	0.30 (dry) maximum
T	=	Applied Torque
	=	850 N-m +/-10%

To determine maximum preload F_{plmax} for the primary lid bolts, minimum nut factor, K , of 0.15 (lubricated) and maximum tightening torque of 940 N-m (conservatively bounds the 850 N-m +10% maximum):

$$F_{pl} = \frac{T}{K_L \times D_b} = \frac{940}{0.15 \times 0.048} \times \frac{1 \text{ kN}}{1000 \text{ N}}$$
$$= 130.6 \text{ kN}$$

The residual torsion moment M_{rl} is:

$$M_{rl} = 0.5 \times T_{max} = 0.5 \times 940$$
$$= 470 \text{ N-m}$$

The residual tensile bolt force F_{arl} is

$$F_{arl} = F_{plmax} = 130.6 \text{ kN}$$

2.13.2.3.2 Bolt Preload for Secondary Lid Closure Bolts

The maximum secondary lid bolt preload F_{psmax} is determined in a manner similar to the primary bolt lids (Section 2.13.2.3.1). Thus,

$$F_{pl} = \frac{T}{K_L \times D_b}$$

where,

D_b	=	Nominal Bolt diameter
	=	36 mm
T	=	Applied Torque
	=	350 N-m +/-10%

Other terms are as previously defined. The maximum preload F_{psmax} for the secondary lid bolts is

obtained by using a nut factor K of 0.15 (lubricated) and a tightening torque of 390 N-m (conservatively bounding the 350 N-m+10% maximum).

$$F_{psmax} = \frac{T_{max}}{K_L \times D_b} = \frac{390}{0.15 \times 36} \\ = 72.2 \text{ kN}$$

The residual tensile bolt force M_{rs} is:

$$M_{rs} = 0.5 \times T_{max} = 0.5 \times 390 \\ = 195.0 \text{ N-m}$$

The residual tensile bolt force F_{ars} is

$$F_{ars} = F_{psmax} = 72.2 \text{ kN}$$

2.13.2.4 Impact Loads

Maximum tension and shear loads in the closure bolts due to the regulatory impact drops are evaluated in accordance with NUREG/CR-6007 [Ref. 10]. Using the NUREG terminology, the primary lid bolts are evaluated as closure bolts for an *unprotected* lid, and the secondary bolts are evaluated as components of a *protected* lid. This approach means the primary bolt evaluation includes the impact or inertial forces of the entire cask; the secondary lid bolts are evaluated only for the forces due to the inertia of the secondary lid.

2.13.2.4.1 Dynamic Load Factors

Drop impact loadings are generally considered triangular or half-sine loadings; NUREG/CR-3966 [Ref. 17] presents dynamic load factor (DLF) charts for either pulse shape. For this analysis, results are compared and loading with the higher DLF is utilized.

Dynamic load factors for triangular and half sine loadings are shown in Figures 2.3 and Figure 2.15 of NUREG/CR-3966 [Ref. 17]. This information is presented as graphs where the DLF is the ordinate and t_d/T is the abscissa. The latter quantity t_d/T is the ratio of the impact duration t_d and the natural period of the impacting object T.

The period of the lids T is considered for bolt closure analyses. T is determined by the lid's lowest mode frequency.

Dynamic Load Factors for Primary Lid Closure Bolts

To determine the primary lid frequency, the primary lid and secondary lid are considered a single simply-supported flat circular plate. Thus, (Table 36, Case 11a of "Roark's Formulas for Stress and Strain" [Ref. 29]):

Resonant Frequency of Primary Lid (with secondary lid attached):

$$f_i = \frac{4.99}{2\pi} \sqrt{\frac{Dg_c}{wr^4}}$$

where,

$$\begin{aligned} D &= \text{Lid Flexural Rigidity} \\ &= \frac{E_1 t_1^3}{12(1-\nu_1^2)} \\ g_c &= \text{conversion factor} \\ &= 1000 \text{ kg-mm/s}^2\text{-N} \\ w &= \text{weight per unit area} \\ r &= \text{lid bolt radius} \\ &= D_{lb}/2 \\ &= 960 \text{ mm} \end{aligned}$$

RT100 PE 1001-1, Rev. H Appendix 1.4, the primary lid weighs 3648 kg and the secondary lid weighs 857 kg. Thus,

$$\begin{aligned} W &= \frac{(3648+857)}{\pi \cdot 960^2} \\ &= 0.001556 \text{ kg/mm}^2 \end{aligned}$$

D may be determined from previously defined values:

$$\begin{aligned} D &= \frac{195 \times 10^3 \times 210^3}{12 \times (1 - 0.31^2)} \\ &= 1.665 \times 10^{11} \text{ N-mm} \end{aligned}$$

The frequency of the primary lid (with attached secondary lid) is:

$$\begin{aligned} f_i &= 0.7942 \times \sqrt{\frac{1.665 \times 10^{11} \times 1000}{0.001556 \times 960^4}} \\ &= 282 \text{ Hz} \end{aligned}$$

The period of the primary lid is equal to $1/f_i$, or $T = 1/282 = 0.00354$ s. Impact durations for the NCT and HAC impacts range from 0.012 s to 0.045 s (RTL-001-CALC-ST-0401, Rev. 6 [Ref.40]). Thus, the smallest value of the ratio t_d/T is 3.389 and the largest is 12.71. With these values, the maximum DLF is determined from Figures 2.3 and 2.15 (NUREG/CR-3966 [Ref.17]) to be less than 1.15. Thus, it is concluded that the DLF for the primary lid bolts may be conservatively bounded by a value of 1.15 for both NCT and HAC drops.

Dynamic Load Factors for Secondary Lid Closure Bolts

To determine the secondary lid frequency, the secondary lid is considered a simply-supported flat circular plate. Thus, (Table 36, Case 11a of "Roark's Formulas for Stress and Strain" [Ref. 29]):

Resonant Frequency of Secondary Lid:

$$f_l = 0.7942 \sqrt{\frac{Dg_c}{wr^4}}$$

where,

$$\begin{aligned} D &= \text{Lid Flexural Rigidity} \\ &= \frac{E_1 t_1^3}{12(1-\nu_{ul}^2)} \\ g_c &= \text{conversion factor} \\ &= 1000 \text{ kg}\cdot\text{mm}/\text{s}^2\cdot\text{N} \\ w &= \text{weight per unit area} \\ r &= \text{lid bolt radius} \\ &= D_{lb}/2 \\ &= 463 \text{ mm} \end{aligned}$$

The secondary lid weighs 857 kg. Furthermore,

$$\begin{aligned} E_1 &= \text{Secondary Lid Material Elastic Modulus, (SA 240 TYPE 304/304L)} \\ &= 195 \text{ GPa at } 20^\circ \text{ C} \quad (\text{Table 2.2.1-1}) \\ D_{lb} &= \text{Secondary Lid Bolt Circle Diameter} \\ &= 926 \text{ mm} \\ \nu_{ul} &= \text{Secondary Lid Material Poisson's Ratio, (SA 240 TYPE 304/304L)} \\ &= 0.31 \quad (\text{Table 2.2.1-2}) \\ t_1 &= \text{Secondary Lid Thickness} \\ &= 110 \text{ mm (stainless steel only)} \end{aligned}$$

Thus,

$$\begin{aligned} w &= \frac{857}{\pi \cdot 463^2} \\ &= 0.001272 \text{ kg}/\text{mm}^2 \end{aligned}$$

D may be determined from previously defined values:

$$D = \frac{195 \times 10^3 \times 110^3}{12 \times (1 - 0.31^2)}$$

$$= 2.395 \times 10^{10} \text{ N-mm}$$

The frequency of the secondary lid is:

$$f_l = 0.7942 \times \sqrt{\frac{2.395 \times 10^{10} \times 1000}{0.001272 \times 463^4}}$$

$$= 508 \text{ Hz}$$

The period of the secondary lid is equal to $1/f_l$, or $T = 1/508 = 0.00197$ s. Impact durations for the NCT and HAC impacts range from 0.012 s to 0.045 s (RTL-001-CALC-ST-0401, Rev. 6 [Ref.40]). Thus, the value of t_d/T is 4.6 or more. With this value, the maximum DLF can be determined from Figures 2.3 and 2.15 (NUREG/CR-6007 [Ref. 10]) to be approaching unity. For consistency with the primary lid bolt analyses, the DLF for the secondary lid bolts is set conservatively to 1.15 for both NCT and HAC drops.

2.13.2.4.2 End Drop Loads

The following subsections detail calculations for the end drop load.

2.13.2.4.2.1 Primary Lid Bolts

Impact loads in the primary lid bolts due to an end drop are determined using the formulas for evaluating bolt forces/moments generated by impact load applied to an unprotected closure in Table 4.5 of NUREG/CR-6007 [Ref. 10]. An acceleration of 125 g is used in this analysis (which bounds the 123 g maximum reported in Section 2.12.4.1).

The non-prying tensile bolt force per primary lid bolt F_{tp} is:

$$F_{tp} = \frac{1.34 \times \sin(x_i) \times DLF \times a_i \times (W_L + W_c) \times g}{N_b}$$

where,

- x_i = End Drop Impact Angle
= 90°
- DLF = 1.15 (Section 2.13.2.4.1)
- a_i = Maximum Impact Acceleration
= 123 g (use 125 g) [Ref. 40]
- W_L = Closure Lid Weight
= 3648 kg (use 3650 kg)
- W_c = Cask Payload Weight
= 6804 kg (use 7000kg)
- N_b = Number of Bolts

$$= 32$$

Thus,

$$F_{tp} = \frac{1.34 \times \sin(90.0) \times 1.15 \times 125 \times (3650 + 7000) \times 9.81}{32} \times \frac{1 \text{ kN}}{1000 \text{ N}}$$

$$= 628.9 \text{ kN/bolt}$$

As discussed in Section 2.13.2.1.1, the RT-100 primary lid bolts are not subjected to any shear loads. Thus,

$$F_{sp} = 0.0 \text{ kN/bolt.}$$

The fixed edge closure lid force F_f is:

$$F_f = \frac{1.34 \times \sin(x_i) \times \text{DLF} \times a_i \times (W_L + W_c) \times g}{\pi \times D_{lb}}$$

where,

$$D_{lb} = \text{Primary Lid Bolt Diameter}$$

$$= 1920 \text{ mm}$$

The remaining terms are as previously defined. Thus,

$$F_f = \frac{1.34 \times \sin(90.0) \times 1.15 \times 125 \times (3650 + 7000) \times 9.81}{\pi \times 1.920} \times \frac{1 \text{ kN}}{1000 \text{ N}}$$

$$= 3336.4 \text{ kN/m}$$

The fixed edge closure lid moment M_f is:

$$M_f = \frac{1.34 \times \sin(x_i) \times \text{DLF} \times a_i \times (W_L + W_c) \times g}{\pi \times 8}$$

All other terms are as previously defined. Thus,

$$M_f = \frac{1.34 \times \sin(90.0) \times 1.15 \times 125 \times (3650 + 7000) \times 9.81}{\pi \times 8} \times \frac{1 \text{ kN}}{1000 \text{ N}}$$

$$= 800.7 \text{ kN-m/m}$$

The additional tensile bolt force per bolt F_{tp} caused by the prying action of the primary lid is (Table 2.1 of NUREG/CR-6007 [Ref. 10]):

$$F_{tp} = \left(\frac{\pi \times D_{lb}}{N_b} \right) \times \left[\frac{2 \times M_f}{D_{lo} - D_{lb}} - C1 \times (B - F_f) - C2 \times (B - P) \right] \div (C1 + C2)$$

where,

$$\begin{aligned}
 P &= \text{Bolt Preload per unit Length of Bolt Circle} \\
 &= F_{\text{plmax}} \times \frac{N_b}{\pi \times D_{lb}} B \\
 &= \text{Non-prying Tensile Bolt Force} \\
 &= \text{MAX}(F_f, P) \\
 C1 &= \text{Force Constant} \\
 &= 1.0 \\
 C2 &= \text{Second Force Constant} \\
 &= \left(\frac{8}{3 \times (D_{lo} - D_{lb})^2} \right) \times \left[\frac{E_l \times t_l^3}{1 - N_{ul}} + \frac{(D_{lo} - D_{li}) \times E_{lf} \times t_{lf}^3}{D_{lb}} \right] \\
 &\quad \times \left(\frac{L_b}{N_b \times D_b^2 \times E_b} \right)
 \end{aligned}$$

$$\begin{aligned}
 D_{lo} &= \text{Closure Lid Diameter at Outer Edge} \\
 &= 2016 \text{ mm}
 \end{aligned}$$

$$\begin{aligned}
 D_{li} &= \text{Closure Lid Diameter at Inner Edge} \\
 &= 1730 \text{ mm}
 \end{aligned}$$

$$\begin{aligned}
 t_{lf} &= \text{Closure Lid Flange Thickness} \\
 &= 120 \text{ mm}
 \end{aligned}$$

$$\begin{aligned}
 E_{lf} &= \text{Primary Lid Flange Material Elastic Modulus,} \\
 &\quad \text{(SA 240 TYPE 304/304L)}
 \end{aligned}$$

$$\begin{aligned}
 L_b &= \text{Bolt length between the top and bottom surfaces of the closure lid} \\
 &\quad \text{at the bolt circle} \\
 &= 67 \text{ mm}
 \end{aligned}$$

Other terms are as previously defined. Thus,

$$C2 = \left(\frac{8}{3 \times (D_{lo} - D_{lb})^2} \right) \times \left[\frac{E_l \times t_l^3}{1 - N_{ul}} + \frac{(D_{lo} - D_{li}) \times E_{lf} \times t_{lf}^3}{D_{lb}} \right] \times \left(\frac{L_b}{N_b \times D_b^2 \times E_b} \right)$$

$$\begin{aligned}
 C2 &= \left(\frac{8}{3 \times (2.016 - 1.920)^2} \right) \\
 &\quad \times \left[\frac{195 \times 10^6 \times 0.210^3}{1 - 0.31} + \frac{(2.016 - 1.730) \times 195 \times 10^6 \times 0.120^3}{1.920} \right] \\
 &\quad \times \left(\frac{0.067}{32 \times 0.048^2 \times 202 \times 10^6} \right)
 \end{aligned}$$

$$C2 = 3.47$$

$$P = \frac{130.6 \times \frac{32}{\pi \times 1.920}}{\pi \times 1.920}$$

$$= 692.9 \text{ kN/m}$$

and

$$F_{tp} = \left(\frac{\pi \times 1.920}{32} \right) \times \left[\frac{2 \times 800.7}{2.016 - 1.920} - 1 \times (3336.4 - 3336.4) - 3.47 \times (3336.4 - 692.9) \right] \frac{1}{1 + 3.47}$$

$$= 316.2 \text{ kN/bolt}$$

The total tension force F_a is

$$F_a = F_t + F_{tp}$$

$$= 628.9 + 316.2$$

$$= 945.1 \text{ kN/bolt}$$

The shear force F_s is 0.

The maximum bending moment generated by the applied loads M_{bb} is:

$$M_{bb} = \left(\frac{\pi \times D_{lb}}{N_b} \right) \times \left(\frac{Kb}{Kb + KI} \right) \times Mf$$

where,

$$Kb = \left(\frac{N_b}{L_b} \right) \times \left(\frac{E_b}{D_{lb}} \right) \times \left(\frac{D_b^4}{64} \right)$$

$$= \left(\frac{32}{0.067} \right) \times \left(\frac{202 \times 10^6}{1.920} \right) \times \left(\frac{0.048^4}{64} \right)$$

$$= 4,167 \text{ kN}$$

$$KI = \frac{E_1 \times t_1^3}{3 \times \left[(1 - N_{ul}^2) + (1 - N_{ul})^2 \times \left(\frac{D_{lb}}{D_{lo}} \right)^2 \right]} \times D_{lb}$$

$$= \frac{195 \times 10^6 \times 0.210^3}{3 \times \left[(1 - 0.31^2) + (1 - 0.31)^2 \times \left(\frac{1.920}{2.016} \right)^2 \right]} \times 1.920$$

$$= 234,719 \text{ kN}$$

Thus,

$$M_{bb} = \left(\frac{\pi \times D_{lb}}{N_b} \right) \times \left(\frac{Kb}{Kb + K1} \right) \times Mf$$

$$= \left(\frac{\pi \times 1.920}{32} \right) \times \left(\frac{4167}{4167 + 234719} \right) \times 800.7$$

$$= 2.6 \text{ kN-m}$$

2.13.2.4.2.2 Secondary Lid Bolts

Impact loads in the secondary lid bolts due to an end drop are determined similarly as for the primary lid bolts in Section 2.13.2.4.2.1.

The non-prying tensile bolt force per secondary lid bolt F_{ts} is:

$$F_{ts} = \frac{1.34 \times \sin(x_i) \times DLF \times a_i \times (W_L + W_{cs}) \times g}{N_b}$$

where,

- x_i = End Drop Impact Angle
= 90°
- DLF = 1.15 (Section 2.13.2.4.1)
- a_i = Maximum Impact Acceleration
= 123 g (use 125 g) [Ref. 40]
- W_L = Closure Lid Weight
= 857 kg (use 860 kg)
- W_{cs} = Payload Weight borne by Secondary Lid
- N_b = Number of Bolts
= 18

Since the payload weight is assumed to be evenly distributed across both the primary and secondary lids, the weight borne by the secondary lid can be obtained by multiplying the payload weight by the ratio of areas, i.e.,

$$W_{cs} = \frac{A_s}{A_p} \times W_c = \left(\frac{D_s}{D_p} \right)^2 \times W_c$$

$$= \left(\frac{0.785}{3.192} \right) \times 7000$$

$$= 1674 \text{ kg}$$

Thus,

$$F_{ts} = \frac{1.34 \times \sin(90.0) \times 1.15 \times 125 \times (860 + 1674) \times 9.81}{18} \times \frac{1 \text{ kN}}{1000 \text{ N}}$$
$$= 266.0 \text{ kN/bolt}$$

As discussed in Section 2.13.2.1.1.2, the RT-100 secondary lid bolts are not subjected to any shear loads. Thus,

$$F_s = 0.0 \text{ kN/bolt}$$

The fixed edge closure lid force F_f is:

$$F_f = \frac{1.34 \times \sin(x_i) \times DLF \times a_i \times (W_L + W_{cs}) \times g}{\pi \times D_{lb}}$$

where,

$$D_{lb} = \text{Secondary Lid Bolt Diameter}$$
$$= 926 \text{ mm}$$

The remaining terms are as previously defined. Thus,

$$F_f = \frac{1.34 \times \sin(90.0) \times 1.15 \times 125 \times (860 + 1674) \times 9.81}{\pi \times 0.926} \times \frac{1 \text{ kN}}{1000 \text{ N}}$$
$$= 1646.1 \text{ kN/m}$$

The fixed edge closure lid moment M_f is:

$$M_f = \frac{1.34 \times \sin(x_i) \times DLF \times a_i \times (W_L + W_{cs}) \times g}{\pi \times 8}$$

where all terms are as previously defined. Thus,

$$M_f = \frac{1.34 \times \sin(90.0) \times 1.15 \times 125 \times (860 + 1674) \times 9.81}{\pi \times 8} \times \frac{1 \text{ kN}}{1000 \text{ N}}$$
$$= 190.5 \text{ kN-m/m}$$

The additional tensile bolt force per bolt F_{tp} caused by the prying action of the secondary lid is (Table 2.1 of NUREG/CR-6007 [Ref. 10]):

$$F_{ip} = \left(\frac{\pi \times D_{lb}}{N_b} \right) \times \left[\frac{2 \times M_f - C1 \times (B - F_f) - C2 \times (B - P)}{D_{lo} - D_{lb}} \right] \frac{1}{C1 + C2}$$

$$= 173.5 \text{ kN/bolt}$$

where,

P = Bolt Preload per unit Length of Bolt Circle

$$= F_{plmax} \times \frac{N_b}{\pi \times D_{lb}} = 72.2 \times \frac{18}{\pi \times 0.926}$$

$$= 446.7 \text{ kN/m}$$

B = Non-prying Tensile Bolt Force

$$= \text{MAX}(F_f, P)$$

C1 = Force Constant

$$= 1.0$$

C2 = Second Force Constant

$$= \left(\frac{8}{3 \times (D_{lo} - D_{lb})^2} \right) \times \left[\frac{E_l \times t_l^3}{1 - N_{ul}} + \frac{(D_{lo} - D_{li}) \times E_{lf} \times t_{lf}^3}{D_{lb}} \right]$$

$$\times \left(\frac{L_b}{N_b \times D_b^2 \times E_b} \right)$$

$$= 1.79$$

D_{lo} = Closure Lid Diameter at Outer Edge

$$= 1000 \text{ mm}$$

D_{li} = Closure Lid Diameter at Inner Edge

$$= 745 \text{ mm}$$

t_{lf} = Closure Lid Flange Thickness

$$= 80 \text{ mm}$$

E_{lf} = Secondary Lid Flange Material Elastic Modulus,
(SA 240 TYPE 304/304L)

$$= 195 \text{ GPa at } 20^\circ\text{C} \quad (\text{Table 2.2.1-1})$$

L_b = Bolt length between the top and bottom surfaces of the
Closure lid at the bolt circle

$$= 43 \text{ mm}$$

The total tension force of F_a is:

$$\begin{aligned} F_a &= F_t + F_{tp} \\ &= 266.0 + 173.5 \\ &= 439.5 \text{ kN/bolt} \end{aligned}$$

The shear force F_s is 0.

The maximum bending moment generated by the applied loads M_{bb} is (Table 2.2 NUREG/CR-6007 [Ref. 10]):

$$\begin{aligned} M_{bb} &= \left(\frac{\pi \times D_{lb}}{N_b} \right) \times \left(\frac{Kb}{Kb + K1} \right) \times Mf \\ Kb &= \left(\frac{N_b}{L_b} \right) \times \left(\frac{E_b}{D_{lb}} \right) \times \left(\frac{D_b^4}{64} \right) \\ &= \left(\frac{18}{0.043} \right) \times \left(\frac{202 \times 10^6}{0.926} \right) \times \left(\frac{0.036^4}{64} \right) \\ &= 2,396.5 \text{ kN} \\ K1 &= \frac{E_t \times t_1^3}{3 \times \left[(1 - N_{ul}^2) + (1 - N_{ul})^2 \times \left(\frac{D_{lb}}{D_{lo}} \right)^2 \right]} \times D_{lb} \\ &= \frac{195 \times 10^6 \times 0.110^3}{3 \times \left[(1 - 0.31^2) + (1 - 0.31)^2 \times \left(\frac{0.926}{1.000} \right)^2 \right]} \times 0.926 \\ &= 71,203 \text{ kN} \end{aligned}$$

Thus,

$$\begin{aligned} M_{bb} &= \left(\frac{\pi \times D_{lb}}{N_b} \right) \times \left(\frac{Kb}{Kb + K1} \right) \times Mf \\ &= \left(\frac{\pi \times 0.926}{18} \right) \times \left(\frac{2.40}{2.40 + 71.20} \right) \times 190.5 \\ &= 1.0 \text{ kN-m} \end{aligned}$$

2.13.2.4.3 Corner Drop Evaluations

The closure bolt evaluations for the corner drop impact are conducted very similarly to the end drop analyses in Section 2.13.2.1.2. The cask body acceleration is changed and the impact angle x_i is set equal to 52.5° (corresponding to a 37.5° angle between cask axis and vertical line).

Additionally, an acceleration of 120 g is used in this analysis (which bounds the 116 g maximum reported in Section 2.12.4.1). Results are summarized in Table 2.13.2-1.

Table 2.13.2-1 Closure Bolt Loads for 9.0 m Corner-Drop

BOLT/LOCATION	Non-Prying Tensile Force, F_t (kN/bolt)	Prying Force, F_{tp} (kN/m)	Bending Moment, M_{bb} (kN-m/bolt)	Shear Force, F_s (kN/bolt)
M48x170 Bolts /Primary Lid	479.0	265.0	2.0	0.0
M36x120 Bolts /Secondary Lid	211.4	147.4	0.8	0.0

2.13.2.4.4 Side Drop Evaluations

As shown in Sections 2.13.2.1.1 and 2.13.2.1.2, the gap between the cask body and the primary and second lids is smaller than the gap between the bolts and the bolt clearance holes. Therefore, no shear load is imparted to the bolts from the cask body. Since the side impact drop primarily generates shear loads with respect to the bolts, the primary and secondary closure lid bolts do not receive any significant loading from the side impact drop and are acceptable with respect to the end and corner impact drop.

2.13.2.5 Puncture Loads

This section evaluates the results of the various puncture loads.

2.13.2.5.1 End Puncture

Puncture loads in the primary and secondary closure lid bolts due to a puncture are determined using the formulas for evaluating bolt forces/moments in Table 4.7 of NUREG/CR-6007 [Ref. 10].

2.13.2.5.1.1 Primary Lid Bolts

The non-prying tensile bolt force per primary lid bolt F_{tp} is:

$$F_{tp} = \frac{\sin(x_i) \times P_{un}}{N_b}$$

where,

- x_i = End Drop Impact Angle
= 90°
- P_{un} = MIN (P_{un1} , P_{un2})
- N_b = Number of Bolts
= 32

The term P_{un} is the maximum impact force that can be generated by puncture pin during a

normal impact. It is the smaller of:

$$P_{un1} = 0.75 \times \pi \times D_{pb}^2 \times S_{y1}$$
$$P_{un2} = 0.6 \times \pi \times D_{pb} \times t_l \times S_{ul}$$

where,

$$D_{pb} = \text{Puncture bar diameter}$$
$$= 150 \text{ mm} \quad (10 \text{ CFR } 71.73 \text{ (c)(3) [Ref. 2]})$$
$$t_l = \text{Closure Lid Thickness}$$
$$= 110 \text{ mm}$$

(the secondary lid thickness neglecting the lead)

$$S_{y1} = \text{Yield Strength of Closure Lid Material}$$

(SA 240 304L)

$$= 172 \text{ MPa at } 20^\circ\text{C} \quad (\text{Table 2.2.1-1})$$
$$S_{ul} = \text{Ultimate Strength of Closure Lid Material}$$

(SA 240 304L)

$$= 483 \text{ MPa at } 20^\circ\text{C} \quad (\text{Table 2.2.1-1})$$

thus,

$$P_{un1} = 0.75 \times \pi \times 0.150^2 \times 172000$$
$$= 9,118.5 \text{ kN}$$
$$P_{un2} = 0.6 \times \pi \times 0.150 \times 0.110 \times 483000$$
$$= 15,022 \text{ kN}$$
$$P_{un} = \text{MIN} (9118.5, 15022 \text{ kN})$$
$$= 9,118.5 \text{ kN}$$

and,

$$F_{tp} = \frac{\sin(90) \times 9118.5}{32}$$
$$= 285.0 \text{ kN/bolt.}$$

As shown in Sections 2.13.2.1.1 and 2.13.2.1.2, the design of the primary and secondary lids prevents shear loads from being applied to the bolts. Thus,

$$F_{sp} = 0$$

It is noted that the equation given for F_{sp} in NUREG/CR6007 [Ref. 10] also shows $F_{sp} = 0$.

The fixed edge closure lid force F_f is:

$$F_f = \frac{\sin(x_i) \times P_{un}}{\pi \times D_{lb}}$$

where,

$$\begin{aligned} D_{lb} &= \text{Primary Lid Bolt Circle Diameter} \\ &= 1920 \text{ mm} \end{aligned}$$

The remaining terms are as previously defined. Thus,

$$\begin{aligned} F_f &= \frac{\sin(90) \times 9118.5}{\pi \times 1.920} \\ &= 1,511.7 \text{ kN/m} \end{aligned}$$

The fixed edge closure lid moment M_f is:

$$M_f = \frac{\sin(x_i) \times P_{un}}{4 \times \pi}$$

thus,

$$\begin{aligned} M_f &= \frac{\sin(90) \times 9118.5}{4 \times \pi} \\ &= 725.6 \text{ kN-m/m} \end{aligned}$$

The additional tensile bolt force per bolt F_{tp} caused by the prying action of the primary lid is (NUREG/CR-6007 Table 2.1 [Ref. 10]):

$$\begin{aligned} F_{tp} &= \left(\frac{\pi \times D_{lb}}{N_b} \right) \times \left[\frac{2 \times M_f}{D_{io} - D_{lb}} - C1 \times (B - F_f) - C2 \times (B - P) \right] \\ &= 517.3 \text{ kN/bolt} \end{aligned}$$

where,

$$\begin{aligned} P &= \text{Bolt Preload per unit Length of Bolt Circle} \\ &= 692.9 \text{ kN/m (as shown in Section 2.13.2.4.2.1)} \\ B &= \text{Non-prying Tensile Bolt Force} \\ &= \text{MAX}(F_f, P) \\ C1 &= \text{Force Constant} \\ &= 1.0 \end{aligned}$$

$$\begin{aligned}
C2 &= \text{Second Force Constant} \\
&= \left(\frac{8}{3 \times (D_{lo} - D_{lb})^2} \right) \times \left[\frac{E_l \times t_l^3}{1 - N_{ul}} + \frac{(D_{lo} - D_{li}) \times E_{lf} \times t_{lf}^3}{D_{lb}} \right] \\
&\quad \times \left(\frac{L_b}{N_b \times D_b^2 \times E_b} \right) \\
&= 3.47 \quad (\text{as shown in Section 2.13.2.4.2.1}) \\
D_{lo} &= \text{Closure Lid Diameter at Outer Edge} \\
&= 2016 \text{ mm} \\
D_{li} &= \text{Closure Lid Diameter at Inner Edge} \\
&= 1730 \text{ mm} \\
t_{lf} &= \text{Closure Lid Flange Thickness} \\
&= 120 \text{ mm} \\
E_{lf} &= \text{Primary Lid Flange Material Elastic Modulus,} \\
&\quad ((SA 240 TYPE 304L)) \\
&= 195 \text{ GPa at } 20^\circ\text{C} \quad (\text{Table 2.2.1-1}) \\
L_b &= \text{Bolt length between the top and bottom surfaces of the} \\
&\quad \text{closure lid at the bolt circle} \\
&= 67 \text{ mm}
\end{aligned}$$

The total tension force F_a is:

$$\begin{aligned}
F_a &= F_t + F_{tp} \\
&= 285.0 + 517.3 \\
&= 802.3 \text{ kN/bolt}
\end{aligned}$$

The shear force F_s is 0.

The maximum bending moment generated by the applied loads M_{bb} is:

$$\begin{aligned}
M_{bb} &= \left(\frac{\pi \times D_{lb}}{N_b} \right) \times \left(\frac{Kb}{Kb + Kl} \right) \times Mf \\
&= 2.4 \text{ kN-m}
\end{aligned}$$

where,

$$\begin{aligned}
Kb &= \left(\frac{N_b}{L_b} \right) \times \left(\frac{E_b}{D_{lb}} \right) \times \left(\frac{D_b^4}{64} \right) \\
&= 4,167.8 \text{ kN}
\end{aligned}$$

$$\begin{aligned} K1 &= \frac{E_l \times t_l^3}{3 \times \left[(1 - N_{ul}^2) + (1 - N_{ul})^2 \times \left(\frac{D_{lb}}{D_{lo}} \right)^2 \right] \times D_{lb}} \\ &= 234,719 \text{ kN} \end{aligned}$$

2.13.2.5.1.2 Secondary Lid Bolts

The non-prying tensile bolt force per secondary lid bolt F_{ts} is:

$$F_{ts} = \frac{\sin(x_i) \times P_{un}}{N_b}$$

where,

$$\begin{aligned} x_i &= \text{End Drop Impact Angle} \\ &= 90^\circ \\ P_{un} &= \text{MIN}(P_{un1}, P_{un2}) \\ N_b &= \text{Number of Bolts} \\ &= 18 \end{aligned}$$

P_{un} was evaluated in Section 2.13.2.5.1.1:

$$P_{un} = 9,118.5 \text{ kN}$$

As shown in Figure 2.7.3-2, the primary and secondary lids act together under the pin puncture load. Therefore, the secondary lid receives only a portion of the impact load from the pin; P_{un} is reduced by the ratio of the secondary lid volume to the total lid volume.

$$\begin{aligned} V_s &= \text{Secondary Lid Volume} \\ &= \frac{\pi}{4} \times D_{lb}^2 \times t_l \\ V_t &= \text{Total Lid Volume} \\ &= \frac{\pi}{4} \times D_{lbp}^2 \times t_{la} \end{aligned}$$

where,

$$\begin{aligned} D_{lbp} &= \text{Closure Lid Bolt Diameter at Primary Lid Bolts} \\ &= 1920 \text{ mm} \\ t_{lp} &= \text{Closure Lid Thickness at Primary Lid Bolts} \\ &= 210 \text{ mm} \end{aligned}$$

$$\begin{aligned}t_{la} &= \text{Average Lid Thickness} \\ &= \frac{t_l + t_{lp}}{2}\end{aligned}$$

thus,

$$\begin{aligned}t_{la} &= \frac{110 + 210}{2} \\ &= 160 \text{ mm} \\ V_s &= \frac{\pi}{4} \times 0.926^2 \times 0.110 \\ &= 0.067 \text{ m}^3 \\ V_t &= \frac{\pi}{4} \times 1.920^2 \times 0.160 \\ &= 0.463 \text{ m}^3 \\ P_{un} &= P_{un}' \times \frac{V_s}{V_t} \\ P_{un} &= 9118.5 \times \frac{0.067}{0.463} \\ &= 1325.6 \text{ kN}\end{aligned}$$

and

$$\begin{aligned}F_{ts} &= \frac{\sin(90) \times 1325.6}{18} \\ &= 73.6 \text{ kN/bolt.}\end{aligned}$$

As shown in Sections 2.13.2.1.1 and 2.13.2.1.2, the design of the primary and secondary lids prevents shear loads being applied to the bolts. Thus,

$$F_{ss} = 0$$

It is noted that the equation given for F_{ss} in NUREG/CR6007 [Ref. 10] also shows $F_{ss} = 0$.

The fixed edge closure lid force F_f is:

$$\begin{aligned}F_f &= \frac{\sin(x_i) \times P_{un}}{\pi \times D_{lb}} \\ &= 455.7 \text{ kN/m}\end{aligned}$$

where,

$$\begin{aligned}D_{lb} &= \text{Secondary Lid Bolt Circle Diameter} \\ &= 926 \text{ mm}\end{aligned}$$

The fixed edge closure lid moment M_f is:

$$M_f = \frac{\sin(x_i) \times P_{un}}{4 \times \pi}$$

thus,

$$\begin{aligned} M_f &= \frac{\sin(90) \times 1325.6}{4 \times \pi} \\ &= 105.5 \text{ kN-m/m} \end{aligned}$$

The additional tensile bolt force per bolt F_{ts} caused by the prying action of the secondary lid is (NUREG/CR-6007 Table 2.1 [Ref. 10]):

$$\begin{aligned} F_{ts} &= \left(\frac{\pi \times D_{lb}}{N_b} \right) \times \left[\frac{2 \times M_f}{D_{to} - D_{lb}} - C1 \times (B - F_f) - C2 \times (B - P) \right] \\ &= 164 \text{ kN/bolt} \end{aligned}$$

where,

- P = Bolt Preload per unit Length of Bolt Circle
= 446.7 kN/m (as shown in Section 2.13.2.4.2.2)
- B = Non-prying Tensile Bolt Force
= MAX(F_f , P)
- C1 = Force Constant
= 1.0
- C2 = Second Force Constant
= $\left(\frac{8}{3 \times (D_{lo} - D_{lb})^2} \right) \times \left[\frac{E_l \times t_l^3}{1 - N_{ul}} + \frac{(D_{lo} - D_{li}) \times E_{lf} \times t_{lf}^3}{D_{lb}} \right]$
= $\left(\frac{L_b}{N_b \times D_b^2 \times E_b} \right)$
= 1.79 (as shown in Section 2.13.2.4.2.2)
- D_{lo} = Closure Lid Diameter at Outer Edge
= 1000 mm
- D_{li} = Closure Lid Diameter at Inner Edge
= 745 mm
- t_{lf} = Closure Lid Flange Thickness
= 80 mm
- E_{lf} = Secondary Lid Flange Material Elastic Modulus,
(SA 240 TYPE 304L)
= 195 GPa at 20°C (Table 2.2.1-1)

$$\begin{aligned} L_b &= \text{Bolt length between the top and bottom surfaces of the} \\ &\quad \text{closure lid at the bolt circle} \\ &= 43 \text{ mm} \end{aligned}$$

The total tension force F_a is:

$$\begin{aligned} F_a &= F_t + F_{ts} \\ &= 73.6 + 164 \\ &= 237.6 \text{ kN/bolt} \end{aligned}$$

The shear force F_s is 0.

The maximum bending moment generated by the applied loads M_{bb} is:

$$\begin{aligned} M_{bb} &= \left(\frac{\pi \times D_{lb}}{N_b} \right) \times \left(\frac{K_b}{K_b + K_l} \right) \times M_f \\ &= 0.6 \text{ kN/m} \end{aligned}$$

where,

$$\begin{aligned} K_b &= \left(\frac{N_b}{L_b} \right) \times \left(\frac{E_b}{D_{lb}} \right) \times \left(\frac{D_b^4}{64} \right) \\ &= 2,396.5 \text{ kN} \quad (\text{as shown in Section 2.13.2.4.2.2}) \end{aligned}$$

$$\begin{aligned} K_l &= \frac{E_l \times t_l^3}{3 \times \left[(1 - N_{ul}^2) + (1 - N_{ul})^2 \times \left(\frac{D_{lb}}{D_{lo}} \right)^2 \right]} \times D_{lb} \\ &= 71,203 \text{ kN} \quad (\text{as shown in Section 2.13.2.4.2.2}) \end{aligned}$$

2.13.2.5.2 Side Puncture

In Section 2.13.2.1.1, the gap between the cask body and the primary lid is shown to be smaller than the gap between the M48 bolts and the bolt clearance holes. Therefore, no shear load is imparted to the bolts from the cask body. Further, there are no other loads resulting from side puncture at the bolts. Thus, no significant loads are imparted to the primary and secondary closure lid bolts during a side puncture event.

2.13.2.6 External Pressure

Loads in the primary and secondary closure lid bolts due to external pressure are evaluated using the formulas for evaluating bolt forces/moments in Table 4.3 of NUREG/CR-6007 [Ref. 10].

2.13.2.6.1 Primary Lid Bolts

The pressure outside the cask P_{lo} in the case of immersion is assumed to be 350 kPa (Calculation Package RTL-001-CALC-TH-0102, Rev. 6 [Ref. 42]). The pressure inside the cask P_{li} is conservatively taken to be 0 kPa.

The axial force per bolt due to external pressure is:

$$F_a = \frac{\pi \times D_{lg}^2 \times (P_{li} - P_{lo})}{4 \times N_b} \quad (\text{Table 4.3 of NUREG/CR-6007 [Ref. 10]})$$

where,

$$\begin{aligned} D_{lg} &= \text{Outside Seal Diameter} \\ &= 1835 \text{ mm} \\ N_b &= \text{Number of Bolts} \\ &= 32 \end{aligned}$$

Since this force is negative (inward acting), the actual resulting bolt force is $F_a = 0$ since the applied load is supported by the cask wall and not by the bolts.

The fixed edge closure lid force is:

$$F_f = \frac{D_{lb} \times (P_{li} - P_{lo})}{4} \quad (\text{Table of 4.3 NUREG/CR-6007 [Ref. 10]})$$

where,

$$\begin{aligned} D_{lb} &= \text{Bolt Circle Diameter} \\ &= 1920 \text{ mm} \end{aligned}$$

thus,

$$\begin{aligned} F_f &= \frac{1.920 \times (0 - 350)}{4} \\ &= -168.0 \text{ kN/m} \end{aligned}$$

The fixed edge closure lid moment is:

$$\begin{aligned} M_f &= \frac{(P_{li} - P_{lo}) \times D_{lb}^2}{32} \quad (\text{Table of 4.3 NUREG/CR-6007 [Ref. 10]}) \\ &= \frac{(0 - 350) \times 1.920^2}{32} \\ &= -40.32 \text{ kN-m/m} \end{aligned}$$

The shear bolt force per bolt is:

$$\begin{aligned} F_s &= \frac{\pi \times E_l \times t_l \times (P_{li} - P_{lo}) \times D_{lb}^2}{2 \times N_b \times E_c \times t_c \times (1 - N_{ul})} \text{ (NUREG/CR-6007 [Ref.10])} \\ &= -296.5 \text{ kN/bolt} \end{aligned}$$

The *maximum* gap between the lid and cask body is less than the *minimum* gap between the bolt clearance holes and bolt shank (see Section 2.13.2.1.1). Thus, the RT-100 primary lid bolts are not subjected to any shear loads. Therefore,

$$F_s = 0.0 \text{ kN/bolt.}$$

2.13.2.6.2 Secondary Lid Bolts

The pressure outside the cask P_{lo} in the case of immersion is assumed to be 350 kPa (Calculation Package RTL-001-CALC-TH-0102 Rev. 6 [Ref. 42]). The pressure inside the cask P_{li} is conservatively taken to be 0 kPa.

The axial force per bolt due to external pressure is:

$$\begin{aligned} F_a &= \frac{\pi \times D_{lg}^2 \times (P_{li} - P_{lo})}{4 \times N_b} \\ &= -11.0 \text{ kN/bolt} \end{aligned}$$

Thus,

$$\begin{aligned} D_{lg} &= \text{Outside Seal Diameter} \\ &= 850 \text{ mm} \\ N_b &= \text{Number of Bolts} \\ &= 18 \end{aligned}$$

Since this force is negative (inward acting), the actual resulting bolt force is $F_a = 0$ (the load is supported by the cask wall and not by the bolts).

The fixed edge closure lid force is:

$$\begin{aligned} F_f &= \frac{D_{lb} \times (P_{li} - P_{lo})}{4} \\ &= -81.0 \text{ kN/m} \end{aligned}$$

where,

$$\begin{aligned} D_{lb} &= \text{Bolt Circle Diameter} \\ &= 926 \text{ mm} \end{aligned}$$

The fixed edge closure lid moment is:

$$\begin{aligned} M_f &= \frac{(P_{li} - P_{lo}) \times D_{lb}^2}{32} \\ &= \frac{(0 - 350) \times 0.926^2}{32} \\ &= -9.4 \text{ kN-m/m} \end{aligned}$$

The shear bolt force per bolt is:

$$\begin{aligned} F_s &= \frac{\pi \times E_l \times t_l \times (P_{li} - P_{lo}) \times D_{lb}^2}{2 \times N_b \times E_c \times t_c \times (1 - N_{ul})} \\ &= -64.2 \end{aligned}$$

The *maximum* gap between the lid and cask body is less than the *minimum* gap between the bolt clearance holes and bolt shank (see Section 2.13.2.1.2). Thus, the RT-100 secondary lid bolts are not subjected to any shear loads. Therefore,

$$F_s = 0.0 \text{ kN/bolt.}$$

2.13.2.7 Gasket Seating Load

A small closure force is required to maintain a positive seal between the cask lid and the cask body. However, this closure force is much less than the minimum preloads provided for the closure bolts at the primary and secondary lids. Therefore, the gasket seating load is negligible, and $F_s = 0$.

2.13.3 Load Combinations

The loadings in Section 2.13.2 are combined to form load cases for the closure bolt analysis per NUREG/CR-6007 [Ref. 10]. The corresponding bolt stresses are obtained and compared to the criteria defined in Section 2.1.2.2. A summary of the loads on the bolts for the primary and secondary lids under the normal conditions of transport and the hypothetical accident conditions is presented in Table 2.13.3-1 and Table 2.13.3-2, respectively.

Table 2.13.3-1 Primary Lid Bolt Load Summary

Load Case	Applied Load		Non-Prying Tensile Force F_t (kN/bolt)	Torsional Moment M_t (kN-m/bolt)	Prying Force F_r (kN/m)	Prying Moment M_r (kN-m/m)
Preload	Residual Torque	Minimum	52.8	0.2	0.0	0.0
		Maximum	130.6	0.5	0.0	0.0
Gasket	Seating Load		0.0	0.0	0.0	0.0
Internal Pressure	250 kN/m ² (35 psi) pressure		20.7	0.0	120.0	28.8
Thermal	100°C		690.9	0.0	0.0	0.0
Puncture	Drop on 15 cm diameter pin		285.0	2.4	1511.7	725.6
External Pressure	350 kPa pressure		0.0	0.0	-168.0	-40.3
Free Drop	Drop from 9 m height		628.9	2.6	3336.4	800.7

Table 2.13.3-2 Secondary Lid Bolt Load Summary

Load Case	Applied Load		Non-Prying Tensile Force F_t (kN/bolt)	Torsional Moment M_t (kN-m/bolt)	Prying Force F_r (kN/m)	Prying Moment M_r (kN-m/m)
Preload	Residual Torque	Minimum	29.6	0.1	0.0	0.0
		Maximum	72.2	0.2	0.0	0.0
Gasket	Seating Load		0.0	0.0	0.0	0.0
Internal Pressure	250 kN/m ² (35 psi) pressure		7.9	0.0	57.9	6.7
Thermal	100°C		388.6	0.0	0.0	0.0
Puncture	Drop on 15 cm diameter pin		237.7	0.6	455.7	105.5
External Pressure	350 kPa pressure		0.0	0.0	-81.0	-9.4
Free Drop	Drop from 9 m height		266.0	1.0	1646.1	190.5

2.13.3.1 Primary Lid Closure Bolt Evaluation under Normal Conditions of Transport

The maximum tension, shear and bolt bearing loads in the primary lid bolts due to the combined NCT loads are evaluated in accordance with NUREG/CR-6007 [Ref. 10], with due consideration given to the prying effects on the fixed lid. Since the prying forces act inward, normal to the cask lid, an additional prying force is generated (NUREG/C-6007 [Ref. 10]). For the NCT condition, the controlling load case is the summation of the bolt preload, the internal pressure

load and the thermal expansion load. The maximum bolt tension load F_t , shear load F_s , and torsional moment M_t for the primary lid bolts are (see Table 2.13.3-1):

$$\begin{aligned}
 F_t &= F_p + F_{ap} + F_{atp} \\
 &= 130.6 + 20.7 + 690.9 \\
 &= 842.1 \text{ kN/bolt} \\
 F_s &= F_{sp} + F_{st} \\
 &= 0.0 + 0.0 \\
 &= 0.0 \text{ kN/bolt} \\
 M_t &= M_{pt} + M_{at} + M_{st} \\
 &= 0.5 + 0.0 + 0.0 \\
 &= 0.5 \text{ kN-m/bolt}
 \end{aligned}$$

Conservatively, the fixed-edge closure lid prying is taken from the external pressure load case. This accident load case bounds all normal conditions and provides a conservative result. The additional tensile bolt force per bolt F_{tp} caused by the prying action of the primary lid is (Table 2.1 of NUREG/CR-6007 [Ref.10]):

$$\begin{aligned}
 F_{tp} &= \left(\frac{\pi \times D_{lb}}{N_b} \right) \times \left[\frac{2 \times M_f - C1 \times (B - F_f) - C2 \times (B - P)}{C1 + C2} \right] \\
 &= -18.4 \text{ kN/m-m}
 \end{aligned}$$

where,

$$\begin{aligned}
 F_f &= \text{Fixed Edge Closure Force} \\
 &= -168.0 \text{ kN/m} \quad (\text{Table 2.13.3-1}) \\
 M_f &= \text{Fixed Edge Closure Moment} \\
 &= -40.32 \text{ kN-m/m} \quad (\text{Table 2.13.3-1})
 \end{aligned}$$

Since this bolt load is less than the load generated by the minimum bolt preload (130.6 kN > -18.3 kN) the prying force generated by the external pressure is not critical with respect to bolt stress and does not result in the loss of lid seal.

The total tension force F_a is:

$$\begin{aligned}
 F_a &= F_t + F_{tp} \\
 &= 842.1 + (-18.4) \\
 &= 823.7 \text{ kN/bolt}
 \end{aligned}$$

The maximum bending moment generated by the applied loads M_{bb} is:

$$\begin{aligned} M_{bb} &= \left(\frac{\pi \times D_{lb}}{N_b} \right) \times \left(\frac{K_b}{K_b + K_1} \right) \times M_f \\ &= -0.13 \text{ kN-m} \end{aligned}$$

The average bolt stresses from the combined NCT loads are determined in accordance with Table 5.1 of NUREG/CR-6007 [Ref. 10]. The bolt stress diameter D is:

$$\begin{aligned} D &= D_b - 0.9382 \times p \\ &= 0.043 \text{ m} \end{aligned}$$

where,

$$\begin{aligned} p &= \text{Bolt Pitch} \\ &= 5.0 \text{ mm} \quad (\text{Machinery Handbook [Ref.27]}) \end{aligned}$$

The average tensile stress S_{ba} , average shear stress S_{bs} , maximum bending stress S_{bb} , and maximum torsional stress S_{bt} (Table 5.1 of NUREG/CR-6007 [Ref. 10]) are:

$$\begin{aligned} S_{ba} &= \frac{1.2732 \times F_a}{D^2} \\ &= 559.1 \text{ MPa} \\ S_{bs} &= \frac{1.2732 \times F_s}{D^2} \\ &= 0.0 \text{ MPa} \\ S_{bb} &= \frac{10.186 \times M_{bb}}{D_b^3} \\ &= -12.2 \text{ MPa} \\ S_{bt} &= \frac{5.093 \times M_t}{D_b^3} \\ &= 21.6 \text{ MPa} \end{aligned}$$

The allowable stresses for the bolts are:

$$\begin{aligned} \sigma_{ta} &= \text{Allowable Tensile Stress} \\ &= 0.7 \times S_u \\ &= 721 \text{ MPa} \\ \sigma_{sa} &= \text{Allowable Shear Stress} \\ &= 0.42 \times S_u \\ &= 432.6 \text{ MPa} \\ \sigma_{ba} &= \text{Allowable Bending Stress} \end{aligned}$$

$$\begin{aligned} &= 1.5 \times S_{mn} \\ &= 514.5 \text{ MPa} \end{aligned}$$

where,

$$\begin{aligned} S_u &= \text{Primary Bolt Ultimate Stress (SA 354 Grade BD)} \\ &= 1034.2 \text{ MPa at } 20^\circ \text{ C} \quad (\text{Table 2.2.1-1}) \\ S_{mn} &= \text{Primary Bolt Membrane Stress (SA 354 Grade BD)} \\ &= 434.4 \text{ MPa at } 20^\circ \text{ C} \quad (\text{Table 2.2.1-1}) \end{aligned}$$

Therefore, the maximum interaction ratio for the combined shear and tension loads is:

$$\begin{aligned} \text{I.R.} &= \left(\frac{S_{ba}}{\sigma_{ta}} \right)^2 + \left(\frac{S_{bs}}{\sigma_{sa}} \right)^2 \\ &= 0.601 \end{aligned}$$

The minimum factor of safety is:

$$\begin{aligned} \text{FS} &= \frac{1}{\text{I.R.}} \\ &= 1.66 > 1.0 \end{aligned}$$

thus, the maximum interaction ratio for the bending load is:

$$\begin{aligned} \text{I.R.} &= \left(\frac{S_{bb}}{\sigma_{ba}} \right)^2 \\ &= 0.00056 \end{aligned}$$

The minimum factor of safety is:

$$\begin{aligned} \text{FS} &= \frac{1}{\text{I.R.}} \\ &= 1774.7 > 1.0 \end{aligned}$$

The maximum stress intensity in the primary lid bolts under the combined loads S_{bi} is:

$$\begin{aligned} S_{bi} &= \sqrt{(S_{ba} + S_{bb})^2 + 4 \times (S_{bs} + S_{bt})^2} \\ &= 548.6 \text{ MPa} \end{aligned}$$

The primary lid closure bolts utilize a custom washer for the bolts with an outer diameter d_{ow} of 130 mm and a hole diameter d_{oh} of 52 mm. Therefore, the bearing stress under the bolt head S_{brg} is:

$$\begin{aligned} S_{brg} &= \frac{F_a}{A_{brg}} \\ &= 73.9 \text{ MPa} \end{aligned}$$

where,

$$\begin{aligned} A_{brg} &= \text{Bolt Bearing Area} \\ &= \frac{\pi}{4} \times (d_{ow}^2 - d_{oh}^2) \\ &= \frac{\pi}{4} \times (0.130^2 - 0.052^2) \\ &= 0.0111 \text{ m}^2 \end{aligned}$$

The allowable normal condition bearing stress on the lid is taken to be the yield stress of the lid material at 250 °C. The maximum interaction ratio for the bearing load is therefore:

$$\begin{aligned} \text{I.R.} &= \frac{S_{brg}}{S_{yl}} \\ &= 0.65 \end{aligned}$$

where,

$$\begin{aligned} S_{yl} &= \text{Primary Lid Material Yield Stress,} \\ &\quad (\text{SA 240 TYPE 304L}) \\ &= 114 \text{ MPa at } 250 \text{ }^\circ\text{C} \quad (\text{Table 2.2.1-1}) \end{aligned}$$

The minimum factor of safety is:

$$\begin{aligned} \text{FS} &= \frac{1}{\text{I.R.}} \\ &= 1.54 > 1.0 \end{aligned}$$

Because the cask material is weaker than the bolting material, failure occurs at the root of the cask material threads. The minimum required thread engagement length to prevent cask material failure is determined in accordance with the Machinery's Handbook [Ref. 27]. Since the constants in the equation assume customary units, the metric units used for the cask design are converted into English Units for determination of the required engagement length. Thus, the minimum engagement length L_e for the cask is:

$$\begin{aligned} L_e &= \frac{S_{ub} \times 2 \times A_b}{S_{ul} \times \pi \times n \times D_{s,min} \times \left[\frac{1}{2 \times n} + 0.57735 \times (D_{s,min} - E_{n,max}) \right]} \\ &= 43.5 \text{ mm} < L_{ep} = 72.0 \text{ mm} \end{aligned}$$

where,

$$S_{ub} = \text{Primary Bolt External Thread Tensile Strength}$$

$$\begin{aligned}
& \text{(SA 354 Grade BD)} \\
& = 149,389 \text{ psi (1,030 MPa) at } 20^\circ \text{C} \quad \text{(Table 2.2.1-1)} \\
& \approx 150,000 \text{ psi} \\
S_{ul} & = \text{Cask Internal Thread Tensile Strength} \\
& \text{(SA 240 TYPE 304L)} \\
& = 70,000 \text{ psi (482.6 MPa) at } 20^\circ \text{C} \quad \text{(Table 2.2.1-1)} \\
A_b & = \text{Stress Area of Primary Bolt External Threads} \\
& = 2.28 \text{ in}^2 \text{ (1470 mm}^2\text{) (Machinery's Handbook [Ref. 27])} \\
p & = \text{Bolt Pitch} \\
& = 0.197 \text{ in (5.0 mm) (Machinery's Handbook [Ref. 27])} \\
n & = \text{Number of Threads per Inch} \\
& = \frac{1}{p} = 5.08 \text{ threads/in} \\
D_{s,min} & = \text{Minimum Major Bolt Diameter} \\
& = 1.866 \text{ in (47.399 mm)} \quad \text{(ASME [Ref. 44])} \\
E_{n,max} & = \text{Maximum Pitch Diameter of Internal Thread} \\
& = 1.705 \text{ in (43.297 mm)} \quad \text{(ASME [Ref. 44])} \\
L_{ep} & = \text{Provided Engagement Length} \\
& = 72.0 \text{ mm}
\end{aligned}$$

Therefore, the primary closure lid bolts are acceptable for the normal conditions of transport.

2.13.3.2 Secondary Lid Closure Bolt Evaluation under Normal Conditions of Transport

The maximum tension, shear and bolt bearing loads in the secondary lid bolts due to the combined NCT loads are evaluated in accordance with NUREG/CR-6007 [Ref. 10], with due consideration given to the prying effects on the fixed lid. An additional prying force is generated (NUREG/CR-6007 [Ref. 10]) due to the prying forces acting inward and normal to the cask lid. For the NCT, the controlling load case is the summation of the bolt preload, the internal pressure load, and the thermal expansion load. The maximum bolt tension load F_t , shear load F_s , and torsional moment M_t for the primary lid bolts are (see Table 2.13.3-2):

$$\begin{aligned}
F_t & = F_p + F_{ap} + F_{atp} \\
& = 72.2 + 7.9 + 388.6 \\
& = 468.7 \text{ kN/bolt} \\
F_s & = F_{sp} + F_{st} \\
& = 0.0 + 0.0 \\
& = 0.0 \text{ kN/bolt} \\
M_t & = M_{pt} + M_{at} + M_{st} \\
& = 0.2 + 0.0 + 0.0 \\
& = 0.2 \text{ kN-m/bolt}
\end{aligned}$$

Conservatively, the fixed-edge closure lid prying is taken from the external pressure load case. This accident load case bounds all normal conditions and provides a conservative result. The additional tensile bolt force per bolt F_{tp} caused by the prying action of the secondary lid is (Table 2.1 NUREG/CR-6007 [Ref. 10]):

$$F_{tp} = \left(\frac{\pi \times D_{lb}}{N_b} \right) \times \left[\frac{2 \times M_f - C1 \times (B - F_f) - C2 \times (B - P)}{C1 + C2} \right]$$

$$= -24.5 \text{ kN-m/m}$$

where,

$$F_f = \text{Fixed Edge Closure Force}$$

$$= -81.0 \text{ kN/m} \quad (\text{Table 2.13.3-2})$$

$$M_f = \text{Fixed Edge Closure Moment}$$

$$= -9.4 \text{ kN-m/m} \quad (\text{Table 2.13.3-2})$$

Since this bolt load is less than the load generated by the minimum bolt preload ($69.5 \text{ kN} > -24.5 \text{ kN}$), the prying force generated by the external pressure is not critical with respect to bolt stress and does not result in the loss of lid closure seal.

The total tension force F_a is:

$$F_a = F_t + F_{tp}$$

$$= 468.7 + (-24.5)$$

$$= 444.1 \text{ kN/bolt}$$

The maximum bending moment generated by the applied loads M_{bb} is:

$$M_{bb} = \left(\frac{\pi \times D_{lb}}{N_b} \right) \times \left(\frac{Kb}{Kb + K1} \right) \times Mf$$

$$= -0.05 \text{ kN-m}$$

The average bolt stresses from the combined NCT loads are determined in accordance with Table 5.1 of NUREG/CR-6007 [Ref. 10]. The bolt stress diameter D is:

$$D = D_b - 0.9382 \times p$$

$$= 0.032 \text{ m}$$

where,

$$p = \text{Bolt Pitch}$$

$$= 4.0 \text{ mm} \quad [\text{Ref. 27}]$$

The average tensile stress S_{ba} , average shear stress S_{bs} , maximum bending stress S_{bb} , and

maximum torsional stress Sbt are:

$$\begin{aligned} S_{ba} &= \frac{1.2732 \times F_a}{D^2} \\ &= 543.8 \text{ MPa} \end{aligned}$$

$$\begin{aligned} S_{bs} &= \frac{1.2732 \times F_s}{D^2} \\ &= 0.0 \text{ MPa} \end{aligned}$$

$$\begin{aligned} S_{bb} &= \frac{10.186 \times M_{bb}}{D_b^3} \\ &= -10.8 \text{ MPa} \end{aligned}$$

$$\begin{aligned} S_{bt} &= \frac{5.093 \times M_t}{D_b^3} \\ &= 21.3 \text{ MPa} \end{aligned}$$

The allowable stresses for the bolts are as previously defined. The maximum interaction ratio for the combined shear and tension loads is therefore:

$$\begin{aligned} \text{I.R.} &= \left(\frac{S_{ba}}{\sigma_{ta}} \right)^2 + \left(\frac{S_{bs}}{\sigma_{sa}} \right)^2 \\ &= 0.569 \end{aligned}$$

The minimum factor of safety is:

$$\begin{aligned} \text{FS} &= \frac{1}{\text{I.R.}} \\ &= 1.8 > 1.0 \end{aligned}$$

The maximum interaction ratio for the bending load is therefore:

$$\begin{aligned} \text{I.R.} &= \left(\frac{S_{bb}}{\sigma_{ba}} \right)^2 \\ &= 0.00044 \end{aligned}$$

The minimum factor of safety is:

$$\text{FS} = \frac{1}{\text{I.R.}}$$

$$= 2279.9 > 1.0$$

The maximum stress intensity in the primary lid bolts under the combined loads S_{bi} is:

$$\begin{aligned} S_{bi} &= \sqrt{(S_{ba} + S_{bb})^2 + 4 \times (S_{bs} + S_{bt})^2} \\ &= 534.7 \text{ MPa} \end{aligned}$$

The primary lid closure bolts utilize a custom washer for the bolts with an outer diameter d_{ow} of 90 mm and a hole diameter d_{oh} of 40 mm. Therefore, the bearing stress under the bolt head S_{brg} is:

$$\begin{aligned} S_{brg} &= \frac{F_a}{A_{brg}} \\ &= 87.0 \text{ MPa} \end{aligned}$$

where,

$$\begin{aligned} A_{brg} &= \text{Bolt Bearing Area} \\ &= \frac{\pi}{4} \times (d_{ow}^2 - d_{oh}^2) \\ &= 0.0051 \text{ m}^2 \end{aligned}$$

The allowable normal condition bearing stress on the lid is taken to be the yield stress of the lid material at 250 °C. Thus, the maximum interaction ratio for the bearing load is:

$$\begin{aligned} \text{I.R.} &= \frac{S_{brg}}{S_{yl}} \\ &= 0.76 \end{aligned}$$

The minimum factor safety is:

$$\begin{aligned} \text{FS} &= \frac{1}{\text{I.R.}} \\ &= 1.31 > 1.0 \end{aligned}$$

Because the cask material is weaker than the bolting material, failure occurs at the root of the cask material threads. The minimum required thread engagement length to prevent cask material failure is determined in accordance with the "Machinery's Handbook" [Ref. 27]. Since the constants in the equation assume customary units, the metric units used for the RT-100 design are converted to English Units for determination of the required engagement length. Thus, the minimum engagement length L_e for the RT-100 is:

$$L_e = \frac{S_{ub} \times 2 \times A_b}{S_{ul} \times \pi \times n \times D_{s,min} \times \left[\frac{1}{2 \times n} + 0.57735 \times (D_{s,min} - E_{n,max}) \right]}$$

$$= 32.7 \text{ mm} < L_{ep} = 54.0 \text{ mm}$$

where,

A_b = Stress Area of Primary Bolt External Threads
= 1.27 in² (817 mm²) [Ref. 27]

P = Bolt Pitch
= 0.157 in (4.0 mm) [Ref. 27]

n = Number of Threads per Inch
= $\frac{1}{p} = 6.35$ threads/in

$D_{s,min}$ = Minimum Major Bolt Diameter
= 1.396 in (35.465 mm) [Ref. 44]

$E_{n,max}$ = Maximum Pitch Diameter of Internal Thread
= 1.270 in (32.270 mm) [Ref. 44]

L_{ep} = Provided Engagement Length
= 54.0 mm

Therefore, the secondary closure lid bolts are acceptable for the normal conditions of transport.

2.13.3.3 Primary Lid Closure Bolt Evaluation under Hypothetical Accident Conditions

The maximum tension, shear and bolt bearing loads in the primary lid bolts due to the combined HAC loads are evaluated in accordance with NUREG/CR-6007 [Ref. 10], with due consideration given to the prying effects on the fixed lid. An additional prying force is generated (NUREG/CR-6007 [Ref. 10]) due to the prying forces acting inward and normal to the cask lid. For HAC, the controlling load case is the summation of the bolt preload, the internal pressure load, and the end drop load. Since the internal pressure load acts counter to the drop load, the internal pressure load is considered as negative for determination of the maximum bolt tension load. The maximum bolt tension load F_t , shear load F_s , and torsional moment (M_t) for the primary lid bolts are (see Table 2.13.3-2):

$$F_t = F_p - F_{ap} + F_{atp}$$

$$= 130.6 - 20.7 + 628.9$$

$$= 738.8 \text{ kN/bolt}$$

$$F_s = F_{sp} + F_{st}$$

$$= 0.0 + 0.0$$

$$= 0.0 \text{ kN/bolt}$$

$$M_t = M_{pt} + M_{at} + M_{st}$$

$$= 0.5 + 0.0 + 0.0$$

$$= 0.5 \text{ kN-m/bolt}$$

Conservatively, the fixed-edge closure lid prying is taken from the end drop load case. The additional tensile bolt force per bolt F_{tp} caused by the prying action of the primary lid is (Table 2.1 of NUREG/CR-6007 [Ref. 10]):

$$F_{tp} = \left(\frac{\pi \times D_{lb}}{N_b} \right) \times \left[\frac{2 \times M_f - C1 \times (B - F_f) - C2 \times (B - P)}{C1 + C2} \right]$$

$$= 316.2 \text{ kN-m/m}$$

where,

$$F_f = \text{Fixed Edge Closure Force}$$

$$= 3336.4 \text{ kN/m} \quad (\text{Table 2.13.3-1})$$

$$M_f = \text{Fixed Edge closure Moment}$$

$$= 800.7 \text{ kN-m/m} \quad (\text{Table 2.13.3-1})$$

This bolt load is greater than the load generated by the minimum bolt preload ($130.6 \text{ kN} < 313.7 \text{ kN}$). However, the drop load is an inward load which presses the closure lid against the sealing gasket. Therefore, the prying force generated by the drop load does not result in the loss of lid closure seal. The outward load of the internal pressure has already been evaluated in Section 2.13.3.1 and found to be acceptable. All other accident loads are acceptable by comparison.

The total tension force F_a is:

$$F_a = F_t + F_{tp}$$

$$= 738.8 + 316.2$$

$$= 1055.1 \text{ kN/bolt}$$

The maximum bending moment generated by the applied loads M_{bb} is:

$$M_{bb} = \left(\frac{\pi \times D_{lb}}{N_b} \right) \times \left(\frac{Kb}{Kb + K1} \right) \times M_f$$

$$= 2.6 \text{ kN-m}$$

The average bolt stresses from the combined HAC loads are determined in accordance with Table 5.1 of NUREG/CR-6007 [Ref. 10]. The bolt stress diameter is as defined previously. The average tensile stress S_{ba} , average shear stress S_{bs} , maximum bending stress S_{bb} , and maximum torsional stress S_{bt} are:

$$\begin{aligned} S_{ba} &= \frac{1.2732 \times F_a}{D^2} \\ &= 716.2 \text{ MPa} \end{aligned}$$

$$\begin{aligned} S_{bs} &= \frac{1.2732 \times F_s}{D^2} \\ &= 0.0 \text{ MPa} \end{aligned}$$

$$\begin{aligned} S_{bb} &= \frac{10.186 \times M_{bb}}{D_b^3} \\ &= 242.5 \text{ MPa} \end{aligned}$$

$$\begin{aligned} S_{bt} &= \frac{5.093 \times M_t}{D_b^3} \\ &= 21.6 \text{ MPa} \end{aligned}$$

The allowable stresses for the bolts are as previously defined. Thus, the maximum interaction ratio for the combined shear and tension loads is:

$$\begin{aligned} \text{I.R.} &= \left(\frac{S_{ba}}{\sigma_{ta}} \right)^2 + \left(\frac{S_{bs}}{\sigma_{sa}} \right)^2 \\ &= 0.987 \end{aligned}$$

The minimum factor of safety is:

$$\begin{aligned} \text{FS} &= \frac{1}{\text{I.R.}} \\ &= 1.01 > 1.0 \end{aligned}$$

Therefore, the maximum interaction ratio for the bending load is:

$$\begin{aligned} \text{I.R.} &= \left(\frac{S_{bb}}{\sigma_{ba}} \right)^2 \\ &= 0.222 \end{aligned}$$

The minimum factor of safety is:

$$\begin{aligned} FS &= \frac{1}{I.R.} \\ &= 4.50 > 1.0 \end{aligned}$$

The primary lid closure bolts utilize a custom washer for the bolts with an outer diameter d_{ow} of 130 mm and a hole diameter d_{oh} of 52 mm. Therefore, the bearing stress under the bolt head S_{brg} is:

$$\begin{aligned} S_{brg} &= \frac{Fa}{A_{brg}} \\ &= 94.6 \text{ MPa} \end{aligned}$$

The allowable normal condition bearing stress on the lid is taken to be the yield stress of the lid material at 250 °C. Thus, the maximum interaction ratio for the bearing load is:

$$\begin{aligned} I.R. &= \frac{S_{brg}}{S_{yl}} \\ &= 0.83 \end{aligned}$$

The minimum factor of safety is:

$$\begin{aligned} FS &= \frac{1}{I.R.} \\ &= 1.21 > 1.0 \end{aligned}$$

Because the cask material is weaker than the bolting material, failure occurs at the root of the cask material threads. The minimum required thread engagement length to prevent cask material failure is determined in accordance with the “Machinery’s Handbook” [Ref. 27]. Since the constants in the equation assume customary units, the metric units used for the cask design are converted to English Units for determination of the required engagement length. Thus, the minimum engagement length L_e for the cask is:

$$\begin{aligned} L_e &= \frac{S_{ub} \times 2 \times A_b}{S_{ul} \times \pi \times n \times D_{s,min} \times \left[\frac{1}{2 \times n} + 0.57735 \times (D_{s,min} - E_{n,max}) \right]} \\ &= 43.5 \text{ mm} < L_{ep} = 72.0 \text{ mm} \end{aligned}$$

Where,

$$\begin{aligned}
 S_{ub} &= \text{Primary Bolt External Thread Tensile Strength} \\
 &\quad (\text{SA 354 Grade BD}) \\
 &= 149,389 \text{ psi (1,030 MPa) at } 20^{\circ}\text{C (Table 2.2.1-1)} \\
 S_{ul} &= \text{Cask Internal Thread Tensile Strength} \\
 &\quad (\text{SA 240 TYPE 304L}) \\
 &= 70,000 \text{ psi (483 MPa) at } 20^{\circ}\text{C (Table 2.2.1-1)} \\
 A_b &= \text{Stress Area of Primary Bolt External Threads} \\
 &= 2.28 \text{ in}^2 (1470 \text{ mm}^2) \quad [\text{Ref. 27}] \\
 p &= \text{Bolt Pitch} \\
 &= 0.197 \text{ in (5.0 mm)} \quad [\text{Ref. 27}] \\
 n &= \text{Number of Threads per Inch} \\
 &= \frac{1}{p} = 5.08 \text{ threads/in} \\
 D_{s,\min} &= \text{Minimum Major Bolt Diameter} \\
 &= 1.866 \text{ in (47.399 mm)} \quad [\text{Ref. 44}] \\
 L_{ep} &= \text{Provided Engagement Length} \\
 &= 72.0 \text{ mm}
 \end{aligned}$$

Therefore, the primary closure lid bolts are acceptable for the hypothetical accident conditions.

2.13.3.4 Secondary Lid Closure Bolt Evaluation under Hypothetical Accident Conditions

The maximum tension, shear and bolt bearing loads in the secondary lid bolts due to the combined HAC loads are evaluated in accordance with NUREG/CR-6007 [Ref. 10], with due consideration given to the prying effects on the fixed lid. An additional prying force is generated (NUREG/CR-6007 [Ref. 10]) due to the prying forces acting inward and normal to the cask lid. For HAC, the controlling load case is the summation of the bolt preload, the internal pressure load, and the end drop load. Since the internal pressure load acts counter to the drop load, the internal pressure load is considered as negative for determination of the maximum bolt tension load. The maximum bolt tension load F_t , shear load F_s , and torsional moment M_t for the primary lid bolts are (see Table 2.13.3-2):

$$\begin{aligned}
 F_t &= F_p - F_{ap} + F_{atp} \\
 &= 72.2 - 7.9 + 266.0 \\
 &= 330.4 \text{ kN/bolt} \\
 F_s &= F_{sp} + F_{st} \\
 &= 0.0 + 0.0 \\
 &= 0.0 \text{ kN/bolt}
 \end{aligned}$$

$$\begin{aligned} M_t &= M_{pt} + M_{at} + M_{st} \\ &= 0.2 + 0.0 + 0.0 \\ &= 0.2 \text{ kN-m/bolt} \end{aligned}$$

Conservatively, the fixed-edge closure lid prying is taken from the end drop load case. The additional tensile bolt force per bolt F_{tp} caused by the prying action of the primary lid is (Table 2.1 of NUREG/CR-6007 [Ref. 10]):

$$\begin{aligned} F_{tp} &= \left(\frac{\pi \times D_{lb}}{N_b} \right) \times \left[\frac{2 \times M_f - C1 \times (B - F_f) - C2 \times (B - P)}{C1 + C2} \right] \\ &= 173.5 \text{ kN-m/m} \end{aligned}$$

where,

$$\begin{aligned} F_f &= \text{Fixed Edge Closure Force} \\ &= 1646.1 \text{ kN/m} \quad (\text{Table 2.13.3-2}) \\ M_f &= \text{Fixed Edge Closure Moment} \\ &= 190.5 \text{ kN-m/m} \quad (\text{Table 2.13.3-2}) \end{aligned}$$

This bolt load is greater than the load generated by the minimum bolt preload ($130.6 \text{ kN} < 178.0 \text{ kN}$). However, the drop load is an inward load which presses the closure lid against the sealing gasket. Thus, the prying force generated by the drop load does not result in the loss of lid closure seal. The outward load of the internal pressure has already been evaluated in Section 2.13.3.2 and found to be acceptable. All other accident loads are acceptable by comparison.

The total tension force, F_a , is:

$$\begin{aligned} F_a &= F_t + F_{tp} \\ &= 330.4 + 173.5 \\ &= 503.8 \text{ kN/bolt} \end{aligned}$$

The maximum bending moment generated by the applied loads M_{bb} is:

$$\begin{aligned} M_{bb} &= \left(\frac{\pi \times D_{lb}}{N_b} \right) \times \left(\frac{K_b}{K_b + K_l} \right) \times M_f \\ &= 1.0 \text{ kN-m} \end{aligned}$$

The average bolt stresses from the combined HAC loads are determined in accordance with Table 5.1 of NUREG/CR-6007 [Ref. 10]. The bolt stress diameter is as defined previously. The average tensile stress S_{ba} , average shear stress S_{bs} , maximum bending stress S_{bb} , and maximum

torsional stress S_b , are:

$$\begin{aligned} S_{ba} &= \frac{1.2732 \times F_a}{D^2} \\ &= 616.8 \text{ MPa} \end{aligned}$$

$$\begin{aligned} S_{bs} &= \frac{1.2732 \times F_s}{D^2} \\ &= 0.0 \text{ MPa} \end{aligned}$$

$$\begin{aligned} S_{bb} &= \frac{10.186 \times M_{bb}}{D_b^3} \\ &= 218.9 \text{ MPa} \end{aligned}$$

$$\begin{aligned} S_{bt} &= \frac{5.093 \times M_t}{D_b^3} \\ &= 21.3 \text{ MPa} \end{aligned}$$

The allowable stresses for the bolts are as previously defined. Therefore, the maximum interaction ratio for the combined shear and tension loads is:

$$\begin{aligned} \text{I.R.} &= \left(\frac{S_{ba}}{\sigma_{ta}} \right)^2 + \left(\frac{S_{bs}}{\sigma_{sa}} \right)^2 \\ &= 0.732 \end{aligned}$$

The minimum factor of safety is:

$$\begin{aligned} \text{FS} &= \frac{1}{\text{I.R.}} \\ &= 1.37 > 1.0 \end{aligned}$$

The maximum interaction ratio for the bending load is:

$$\begin{aligned} \text{I.R.} &= \left(\frac{S_{bb}}{\sigma_{ba}} \right)^2 \\ &= 0.113 \end{aligned}$$

The minimum factor of safety is:

$$\begin{aligned} FS &= \frac{1}{I.R.} \\ &= 8.86 > 1.0 \end{aligned}$$

The primary lid closure bolts utilize a custom washer for the bolts with an outer diameter d_{ow} of 90 mm and a hole diameter d_{oh} of 40 mm. Therefore, the bearing stress under the bolt head S_{brg} is:

$$\begin{aligned} S_{brg} &= \frac{Fa}{A_{brg}} \\ &= 98.7 \text{ MPa} \end{aligned}$$

The allowable normal condition bearing stress on the lid is taken to be the yield stress of the lid material at 250 °C. The maximum interaction ratio for the bearing load is:

$$\begin{aligned} I.R. &= \frac{S_{brg}}{S_{yl}} \\ &= 0.86 \end{aligned}$$

The minimum factor of safety is:

$$\begin{aligned} FS &= \frac{1}{I.R.} \\ &= 1.16 > 1.0 \end{aligned}$$

Because the cask material is weaker than the bolting material, failure occurs at the root of the cask material threads. The minimum required thread engagement length to prevent cask material failure is determined in accordance with the “Machinery’s Handbook” [Ref. 27]. Since the constants in the equation assume customary units, the metric units used for the cask design are converted to English Units for determination of the required engagement length. Thus, the minimum engagement length L_e for the cask is:

$$\begin{aligned} L_e &= \frac{S_{ub} \times 2 \times A_b}{S_{ul} \times \pi \times n \times D_{s,min} \times \left[\frac{1}{2 \times n} + 0.57735 \times (D_{s,min} - E_{n,max}) \right]} \\ &= 32.7 \text{ mm} < L_{ep} = 54.0 \text{ mm} \end{aligned}$$

Therefore, the secondary closure lid bolts are acceptable for the hypothetical accident conditions.

2.13.4 Seal Integrity

The maximum stress analyses in the previous sections are based on criteria for the accident conditions intended to prevent failures by excessive plastic deformation or by the rupture of the bolt. Using the yield stress as the stress limit for average tensile bolt stress, as per NUREG/CR-6007 [Ref. 10], implies that a small amount (0.02%) of plastic deformation is permitted. The following calculations show that the O-rings will continue to provide positive sealing of the closure lids even with this small plastic deformation.

2.13.4.1 Primary Lid Seals

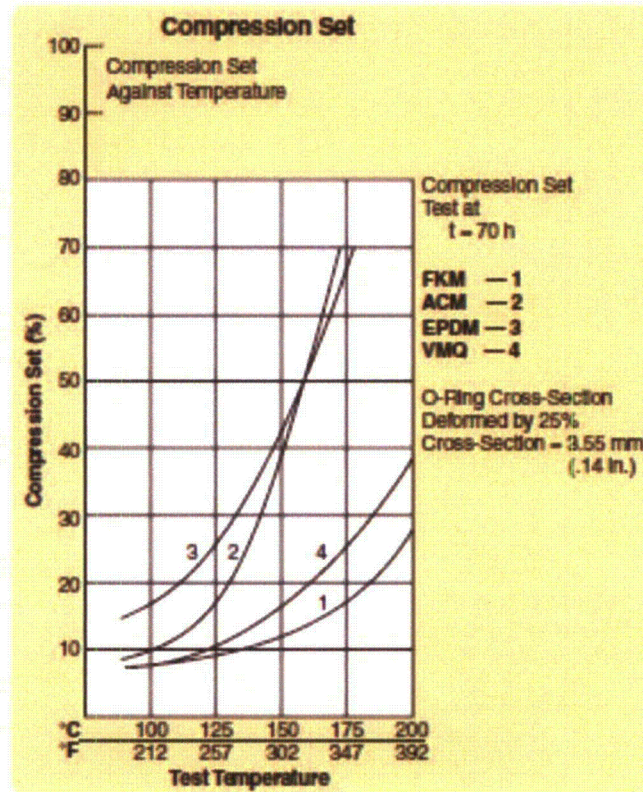
The 0.02% bolt plastic deformation permitted in NUREG/CR-6007 [Ref. 10] is distributed over the 67 mm bolt shank dimension shown in Detail 1 of Drawing RT-100 PE 1001-1 Rev. G (Chapter 1, Appendix 1.4, Attachment 1.4-2). This may result in a separation between the primary lid and cask flange mating surfaces of 0.0134 mm ($= 67\text{mm} \times 0.0002$). However, the primary lid seals are 12 +/-0.3 mm diameter EPDM rubber and the grooves for these seals are 9.4 +/- 0.15 mm deep (Drawing RT-100 PE 1001-1, Rev. G Appendix 1.4). Thus, the seal is minimally compressed 2.15 mm ($= (12 - 0.3) - (9.4 + 0.15)$). Considering that EPDM O-rings have a compression set of up to 45% at 150 °C (Figure 2.13.4-1), the minimum compression in the seal is 1.18 mm ($= 2.15 - 0.45 \times 2.15$). Since the minimum seal compression greatly exceeds the separation due to possible plastic deformation, the primary lid/cask flange containment boundary will remain sealed following an HAC drop event.

2.13.4.2 Secondary Lid Seals

The 0.02% bolt plastic deformation permitted in NUREG/CR-6007 [Ref.10] is distributed over the 43 mm bolt shank dimension shown in Detail 2 of Drawing RT-100 PE 1001-1 Rev G, (Chapter 1, Appendix 1.4, Attachment 1.4-2). This may result in a separation between the secondary and primary lid mating surfaces of 0.0086 mm ($= 43\text{mm} \times 0.0002$). However, the secondary seals are 12 +/-0.3 mm diameter EPDM rubber and the grooves for these seals are 9.4 +/- 0.15 mm deep (Drawing RT-100 PE 1001-1 Rev G (Chapter 1, Appendix 1.4, Attachment 1.4-2). Thus, the seal is minimally compressed 2.15 mm ($= (12 - 0.3) - (9.4 + 0.15)$). Considering that EPDM O-rings have a compression set of up to 45% (Figure 2.13.4-1) at 150 °C, the minimum compression in the seal is 1.18 mm ($= 2.15 - 0.45 \times 2.15$). Since the minimum seal compression greatly exceeds the separation due to possible plastic deformation, the primary to secondary lid containment boundary will remain sealed following an HAC drop event.

Figure 2.13.4-1 Compression Set vs. Temperature

(Figure 2-13 from Parker O-ring Handbook [Ref. 50])



2.13.5 Vent Port Cover Plate O-Ring and Bolt Evaluation

The RT-100 cask port cover utilizes a double polymer (EPDM) O-ring configuration face seal to protect the leak test port. For this evaluation the diameter of the outer O-ring is considered to maximize the seating force (Calculation Package RTL-001-CALC-ST-0203, Rev. 6 [Ref.60]). The port cover is sealed with six DIN912 M10 x 30-A4-70 bolts.

2.13.5.1 Vent Port Cover Plate O-Ring Evaluation

This section evaluates the vent port cover sealing force and calculates the preload to maintain a tight seal (Calculation Package RTL-001-CALC-ST-0203, Rev. 6 [Ref 60]).

2.13.5.1.1 O-ring Sealing Force

The O-ring requires a minimum 3.7 N/mm sealing force (Trelleborg, Appendix 1 [Ref. 58]). The force required to seat the polymer O-ring seal is:

$$F_s = Y_r \times C = 3.7 \times (\pi \times 136.6) = 1,587.8 \text{ N}$$

Where,

$$\begin{aligned} Y_f &= \text{Sealing force} \\ C &= \text{O-ring circumference} \end{aligned}$$

2.13.5.1.2 Vent Port Cover Plate Preload

The preload force available to maintain a tight seal that accounts for reduction in preload during HAC is:

$$P_L = F_c - P_{HAC} = 50,522 \text{ N}$$

Where,

$$\begin{aligned} F_c &= \text{Available closure force} \\ &= P_{\min} \times N_b \\ P_{\min} &= \text{Minimum preload per bolt} \\ &= T_{\min} / k / d \\ T_{\min} &= \text{Minimum torque (-10%, Chapter 7, Table 7.4.5-1)} \\ &= 24,300 \text{ N-mm} \\ k &= \text{Nut factor - non-lubricated condition} \\ &= 0.3 \\ d &= \text{Nominal bolt diameter} \\ &= 10 \text{ mm} \\ N_b &= \text{Number of bolts} \\ &= 6 \\ P_{HAC} &= \text{Loss of preload during HAC} \quad [\text{Ref. 10}] \\ &= 0.0002 \times E \times A_t \\ &= 8,910 \text{ N} \\ E &= \text{Modulus of elasticity} \\ &= 1.89 \times 10^{11} \text{ Pa @ } 100^\circ\text{C} \\ A_t &= \text{Tensile area of the bolt} \quad [\text{Ref. 27}] \\ &= 0.7854 \left(d - \frac{0.97431}{n} \right)^2 \\ &= 77.6386 \text{ mm}^2 \\ n &= \text{Number of threads per inch} \\ &= 16.93 \end{aligned}$$

2.13.5.1.3 Factor of Safety to Maintain a Tight Seal

Comparing the available preload force to the load required to maintain a tight seal, the factor of safety is:

$$FS = \frac{50,522}{1587.8} = 31.8$$

2.13.5.2 Bolt Evaluation

This section evaluates the vent port cover thread engagement and associate stress.

2.13.5.2.1 Thread Engagement

For the port cover, the mating internal and external threads are manufactured of materials of equal tensile strengths. To prevent stripping of the external threads, the minimum engagement length, L_e , is:

$$L_e = \frac{2 \times A_t}{\pi \times K_{n,max} \left[\frac{1}{2} + 0.57735 \times n \times (E_{s,min} - K_{n,max}) \right]}$$

$$= 2.46 \text{ mm}$$

Where,

$$K_{n,max} = 8.676 \text{ mm} \quad (\text{Machinery's Handbook [Ref. 27]})$$

$$E_{s,min} = 8.862 \text{ mm} \quad (\text{Machinery's Handbook [Ref. 27]})$$

The available thread length based on the drawings (RT-100 PE 1001-2 Rev G, Chapter 1, Appendix 1.4, Attachment 1.4-3) is 15.5 mm. Since 15.5 mm > 2.46 mm, there are sufficient threads to prevent stripping of the bolts.

2.13.5.2.2 Thread Shear Evaluation

The load necessary to shear the external threads due to the tensile force is:

$$P_s = 0.6 \times A_s \times S_y$$

$$= 121,044 \text{ N}$$

where,

$$A_s = \pi \times n \times L_e \times K_{n,max} \left[\frac{1}{2n} + 0.57735 (E_{s,min} - K_{n,max}) \right]$$

$$L_e = 15.5 \text{ mm}$$

$$S_y = 2.06 \times 10^8 \text{ Pa @ } 100^\circ\text{C}$$

The tensile force generated in the bolt is:

$$P_B = \frac{T}{\left(\frac{1}{2\pi} + \frac{d_2\mu}{2\cos\alpha} + \frac{(d+b)\mu}{4} \right)}$$

$$= 16,791 \text{ N}$$

where,

$$T = \text{Torque}$$

$$= 29700 \text{ N-mm}$$

$$\begin{aligned}d_2 &= \text{Min major diameter} && [\text{Ref. 27}] \\ &= d - 3/4H + EI \\ D &= 10 \text{ mm} \\ H &= \text{Thread height ignoring flats} \\ &= \frac{\sqrt{3}}{2} \times P = 1.299 \text{ mm} \\ EI &= \text{Fundamental deviation} && [\text{Ref.27}] \\ &= 0.032 \\ P &= \text{Thread pitch} \\ &= 1.5 \text{ mm} \\ \alpha &= \text{Half thread angle} \\ &= 30^\circ \\ \mu &= \text{Coefficient of friction} && [\text{Ref. 27}] \\ &= 0.15\end{aligned}$$

Comparing the load required to shear the external threads with the tensile force generated in the bolt, the factor of safety is:

$$\begin{aligned}FS &= \frac{121,044}{16,791} \\ &= 7.2\end{aligned}$$

2.13.5.2.3 Load to Break Bolt

The load necessary to break the bolt is:

$$\begin{aligned}P &= S_u \times A_t \\ &= 48,058 \text{ N}\end{aligned}$$

where,

$$S_u = 6.19 \times 10^8 \text{ Pa @ } 100^\circ\text{C}$$

Since the load required to break the bolt is less than the applied force ($48,058 \text{ N} > 16,791 \text{ N}$), the bolts will not fail.

2.14 Appendix – Fabrication Stress Evaluation

Manufacturing the RT-100 can introduce thermal stresses in the inner shell during the lead pouring process. These thermal stresses are evaluated in this section to provide assurance that the manufacturing process does not adversely affect the normal operation of the cask, or its ability to survive an accident.

According to Regulatory Position 7 of Regulatory Guide 7.6 [Ref. 4], any residual stresses in the containment vessel shell resulting from inelastic strain associated with the secondary local bending stresses (which are due to the lead pour thermal gradient) must be considered in the total stress range for normal and accident load conditions. Residual stresses in the containment vessel (inner shell) induced by shrinkage of the lead shielding after the lead pouring operation are relieved early in the life of the cask because of the low creep strength of lead.

The lead pour process is accomplished by first welding the inner and outer shells to the flange, which forms an annular region between the shells. Prior to the lead pour process; the initial temperature of the inner and outer shells is pre-heated to approximately 350°C. The lead is heated until the molten temperature is between 390°C and 440°C. Molten lead is then poured continuously through the open end of the cask until the entire annular region is filled. Solidification is allowed only when the entire cavity is completely filled. Water is then used to cool the cask below 327°C, where solidification occurs. Following the pouring process, the cask is allowed to cool to ambient conditions.

2.14.1 Lead Pour

This section evaluates the stresses generated during the lead pouring process.

2.14.1.1 Cask Shell Geometry

At 21°C, the cask inner and outer shell geometry dimensions are:

Inner Shell

Inside Diameter (d_{i-21})	=1.73 m
Outside Diameter (d_{o-21})	=1.79 m
Shell Thickness (t_i)	=.030 m

Outer Shell

Inside Diameter (D_{i-21})	=1.97 m
Outside Diameter (D_{o-21})	=2.04 m
Shell Thickness (T_o)	= .35 m

2.14.1.2 Stresses Resulting from Lead Pour

The hydrostatic pressure, Q, produced by the column of lead is:

$$Q = \rho \times h \times g = 224.8 \text{ kPa}$$

Where:

$$\rho = 11340 \text{ kg/m}^3 \text{ (lead density)}$$

$$h = 2.021 \text{ m (maximum height of lead column)}$$

$$g = 9.81 \text{ m/s}^2$$

For this analysis, it is assumed that the lead and shell reach an equilibrium temperature of 440°C based on a maximum temperature of 440°C for the lead and an initial shell temperature of 21°C. Key shell geometric dimensions are:

$$d_{o-400} = d_{o-21}(1 + \alpha\Delta T) = 1.80 \text{ m}$$

$$D_{i-400} = D_{i-21}(1 + \alpha\Delta T) = 1.99 \text{ m}$$

$$t_{i-400} = t_{i-21}(1 + \alpha\Delta T) = 0.0302 \text{ m}$$

Where:

$$\alpha = 1.824 \times 10^{-5} \text{ m/m/}^\circ\text{C at } 440^\circ\text{C (stainless steel)}$$
$$\Delta T = 400 - 21 = 419^\circ\text{C.}$$

The hydrostatic pressure of the molten lead subjects the inner shell to an external hydrostatic pressure. The hydrostatic pressure varies from a maximum of 224.8 kPa at the bottom of the inner shell to 0 psi at the top of the lead cylinder. Using Table 29, Case 6 of “Roark’s Formula for Stress and Strain” [Ref. 29], the deformation at the bottom of the inner shell y_B is found to be -3.567×10^{-5} m. The maximum circumferential membranes stress in the inner shell is:

$$S_{\theta_{\max}} = \frac{y_B E}{R} = -6.67 \text{ MPa}$$

Where:

$$E = 168.5 \text{ GPa at } 399^\circ\text{C}$$
$$R = 1.80/2 = 0.90 \text{ m}$$

This stress exists only as long as the lead is molten and produces no plastic deformation of the inner shell. When the lead solidifies and begins to cool, it shrinks and exerts a uniform external pressure on the inner shell due to the lead coefficient of expansion being larger than that of stainless steel.

2.14.2 Cool-down

This section evaluates the stresses that occur during the cool-down process.

2.14.2.1 Hoop (Circumferential) Stresses

Lead decreases in volume during solidification. As the lower region solidifies during the pour, the molten lead above fills the void created between the solidifying lead, inner shell, and form. Using the coefficients of expansion for stainless steel and lead, the outer diameter of the steel inner shell and the inner diameter of the lead cylinder (assuming it is free to shrink) is determined at 327°C (the melting point of lead) and at 21°C (ambient temperature). Because the lead has a higher coefficient of expansion than stainless steel, a shrinkage force develops between the steel shell outer surface and the lead inner surface. At 327°C , the outside diameter of the inner shell and the inside diameter of the lead (as it begins to solidify) is:

$$d_{\text{shell}327} = d_{\text{shell}21}(1 + \alpha\Delta T) = 1.79(1 + 1.78 \times 10^{-5}(327 - 21)) = 1.80 \text{ m}$$

Where:

$$d_{\text{oshell}21} = 1.79 \text{ m}$$
$$\alpha_{\text{shell}} = 1.78 \times 10^{-5} \text{ m/m/ } ^\circ\text{C (at } 327^\circ\text{C)}$$

If the lead cooled without restraint to 21°C, the inner diameter of the lead cylinder would shrink to:

$$d_{\text{ilead}21} = d_{\text{ilead}327} (1 - \alpha \Delta T) = 1.80 (1 - 2.90 \times 10^{-5} (327 - 21)) = 1.784 \text{ m}$$

Where:

$$d_{\text{ilead}327} = d_{\text{oshell}327} = 1.80 \text{ m}$$
$$\alpha_{\text{lead}} = 2.90 \times 10^{-5} \text{ m/m/ } ^\circ\text{C}$$

The interference between the lead cylinder and the inner shell is $(1.800 - 1.784)/2 = 0.008 \text{ m}$. To fully accommodate this interference, the lead must deform 0.008 m. For $\delta = 0.008 \text{ m}$, the maximum circumferential stress $S_{0\text{max}}$ in the inner shell is:

$$S_{0\text{max}} = \frac{\delta(E)}{R} = 149.4 \text{ MPa}$$

Where:

$$R = 1.784/2 = 0.892 \text{ m}$$
$$E = E_{\text{lead}70} = 16.7 \text{ GPa}$$

The stress in the inner shell exists until the lead creeps and relieves the residual stress. The inner shell responds elastically since the stress is less than the yield strength of steel.

2.14.2.2 Axial Stress

Axial stresses develop in the lead shell and inner shell during fabrication as a result of the unequal shrinkage of the lead and steel shells. Assuming that the lead bonds to the inner shell during the cool-down process after completion of lead pouring, the stress in the lead when cooled to 21°C is:

$$S_{\text{lead}} = \epsilon E = 3.44 \times 10^{-3} \times 16.7 \times 10^9 = 57.4 \text{ MPa}$$

Where:

$$\begin{aligned} \epsilon_{\text{lead}} &= (\alpha_{\text{lead}} - \alpha_{\text{shell}}) \Delta T = 3.44 \times 10^{-3} \text{ m/m} \\ \alpha_{\text{lead}} &= 2.90 \times 10^{-5} \text{ m/m/}^\circ\text{C} \\ \alpha_{\text{shell}} &= 1.78 \times 10^{-5} \text{ m/m/}^\circ\text{C} \\ \Delta T &= 327 - 21 = 327^\circ\text{C} \\ E &= E_{\text{lead70}} = 16.7 \text{ GPa} \end{aligned}$$

The calculated stress is above the yield point of lead (ranging between 5 and 19 MPa at 21°C). The axial load placed on the steel inner shell by shrinkage of the lead is therefore limited by the yield strength of lead. The maximum load imposed by the lead is:

$$P_{\text{lead}} = 19 \times \pi (0.985^2 - 0.895^2) = 1.010 \times 10^7 \text{ N}$$

The corresponding compression stress in the inner shell to maintain equilibrium is:

$$S_{\text{shell}} = \frac{P}{A} = \frac{-1.010 \times 10^7}{\pi((0.985)^2 - (0.895)^2)} = -60.9 \text{ MPa}$$

This value is conservative because the yield strength of lead is very low at elevated temperatures (approximately 3 MPa) and therefore, the creep rate is high. Also, complete bonding of the lead to the stainless steel inner shell is not expected to occur. This case bounds others axial loading configurations since the calculation is based on the yield strength of lead at 21°C

2.14.2.3 Effects of Temperature Differential during Cool-down

The preceding analyses assume that the inner shell and lead are always at the same temperature at any time during the cool-down process. This assumption may not be true under actual conditions. Because of the high thermal conductivity of the stainless steel and the lead, the temperature differential between the lead and steel inner shell is kept to a minimum. If the inner shell is cooler than the lead, the interference and the corresponding interface pressure and resulting hoop stresses are less than the equal temperatures case. Hence, the preceding analysis is conservative. An analysis is required if the inner shell is hotter than the lead shield. Assuming the temperature of the inner shell is 59°C and the lead is 21°C, the inner radius of the stress-free lead shell at 21°C is 0.892 m; the outer radius of the inner shell at 59°C is:

$$r_o = 0.892 [1 + (1.53 \times 10^{-5})(38)] = 0.893 \text{ m}$$

The interference between the inner shell and the lead is $0.893 - 0.892 = 0.001 \text{ m}$. To accommodate this interference, the lead must deform 0.001 m. For $\delta = 0.001 \text{ m}$, the maximum circumferential stress $S_{\theta\text{max}}$ in the inner shell is:

$$S_{\theta\text{max}} = \frac{\delta(E)}{R} = 9.7 \text{ MPa}$$

where

$$R = 1.784/2 = 0.892 \text{ m}$$

$$E = E_{\text{lead70}} = 16.7 \text{ GPa}$$

2.14.3 Lead Creep

As discussed previously, cooling of the lead shell and inner shell introduces acceptably low hoop and axial stresses in the inner shell. These stresses are relieved early in the life of the cask since lead demonstrates a significant creep rate at both room and elevated temperatures.

2.15 Appendix – Seal Region Stress Evaluation

To provide assurance that the primary and secondary cask seals meet the linear elastic requirements of Regulatory Guide 7.6 [Ref. 4] the contact stresses that represent the maximum nodal stresses on the sealing surfaces and the linearized nodal stresses in the solid elements that comprise the seal regions are evaluated and compared to the yield strength of the material at the maximum NCT temperature. The evaluation shows that the RT-100 seal region does not undergo inelastic deformation.

2.15.1 Seal Region Post-Processing Methodology

The cask body calculation reports the primary membrane and membrane plus bending stress intensities averages across linearized sections. To evaluate the stresses in the lid gasket region, the lid component is first selected as shown in Figure 2.15.4-1. As shown in Figure 2.15.4-2, the elements comprising the lid gasket region are then selected to evaluate the stresses specific to the primary gasket location. Visual inspection of the model shows the location of the peak stress in the gasket region and the nodes are identified to calculate the average stress. The ANSYS finite element program [Ref. 28] calculates the average stress across a section by identifying the nodal points using the ANSYS APDL commands PATH, PDEF and PPATH. Figure 2.15.4-2 provides an example of where 2 points are defined across the gasket region. Once the points and path are defined, the ANSYS APDL command PRSECT reports the average stresses.

2.15.2 Stress Concentration Factors

Trapezoidal grooves are cut into the primary and secondary lids to allow the gaskets to properly seat during the closure process. Figure 2.15.4-3 shows the lid/gasket geometry. Under load, the grooves can cause a stress riser at the radius, r , where the groove transitions from horizontal to vertical (“Standard Handbook for Mechanical Engineers” [Ref. 55]). For this evaluation, the load is in the form of a bending moment. Using the dimensions provided in Figure 2.15.4-3 and Table 2.15.4-1, the resulting stress concentration factors are calculated in terms of the ratios of D/d and r/d . For the primary and secondary lids, the stress concentration factors are 2.6 and 2.2, respectively.

